



Subsurface Characterization of the Edmonton-Area Acid-Gas Injection Operations

©Her Majesty the Queen in Right of Alberta, 2008

ISBN 978-0-7785-6949-7

The Energy Resources Conservation Board/Alberta Geological Survey (ERCB/AGS) and its employees and contractors make no warranty, guarantee or representation, express or implied, or assume any legal liability regarding the correctness, accuracy, completeness or reliability of this publication. Any digital data and software supplied with this publication are subject to the licence conditions. The data are supplied on the understanding that they are for the sole use of the licensee, and will not be redistributed in any form, in whole or in part, to third parties. Any references to proprietary software in the documentation, and/or any use of proprietary data formats in this release, do not constitute endorsement by the ERCB/AGS of any manufacturer's product.

If this product is an ERCB/AGS Special Report, the information is provided as received from the author and has not been edited for conformity to ERCB/AGS standards.

When using information from this publication in other publications or presentations, due acknowledgment should be given to the ERCB/AGS. The following reference format is recommended:

Bachu, S., Buschkuehle, M., Haug, K. and Michael, K. (2008): Subsurface characterization of the Edmonton-area acid-gas injection operations; Energy Resources Conservation Board, ERCB/AGS Special Report 092, 134 p.

Published March 2008 by:

Energy Resources Conservation Board
Alberta Geological Survey
4th Floor, Twin Atria Building
4999 – 98th Avenue
Edmonton, Alberta
T6B 2X3
Canada

Tel: (780) 422-1927
Fax: (780) 422-1918
E-mail: AGS-Info@ercb.ca
Website: www.ags.gov.ab.ca

This report is the AGS release of a 2004 client report prepared for the Acid Gas Management Committee, a consortium of provincial and federal agencies and industry partners.

Financial support to conduct this study was received from Environment Canada, Alberta Environment, Climate Change Central, Alberta Energy Research Institute, Western Economic Development, British Columbia Ministry of Energy, Mines and Petroleum Resources, Saskatchewan Industry and Resources, Keyspan Energy, and Total.

Executive Summary

Injection of acid gas in the Edmonton region takes place at five sites into three different stratigraphic intervals. Acid gas dissolved in water in the Redwater oil field, and the resulting weak acidic solution (“sour” water) is injected into the depleted Leduc Formation Redwater reef trough 47 alternating wells. Dry acid gas is injected at four other sites. At Golden Spike and Watelet, the acid gas is injected into deep Devonian carbonate aquifers (Beaverhill Lake Group and Cooking Lake Formation, respectively). At Acheson and Strathfield the acid gas is injected into depleted gas reservoirs in the Cretaceous Lower Mannville Group. Acheson, operating since 1990, is actually the oldest acid-gas injection operation in Canada and the world. At the end of 2003, more than 200 kt of acid gas had been injected into deep geological formations in the Edmonton region.

If only the natural setting is considered, including geology and flow of formation waters, the basin- and local-scale hydrogeological analyses indicate that injecting acid gas into these deep geological units in the Edmonton region is basically a safe operation with no potential for acid gas migration to shallower strata, potable groundwater and the surface. At Redwater the acid gas is already dissolved in water and it will dissolve further in the formation water, with no possibility for migration or leakage, being contained in the Redwater reef. At Golden Spike, the acid gas injected into an isolated, confined reefal carbonate in the Beaverhill Lake Group is contained by the surrounding and overlying low-permeability argillaceous limestone at the top of the Beaverhill Lake Group. At Watelet, upward migration is impeded by the overlying thick and tight shales of the Ireton Formation. While the acid gas plume may migrate updip, it will dissolve in formation water long before it may reach the sub-Cretaceous unconformity. Even there, thick overlying Cretaceous shales will impede any upward migration. At Strathfield and Acheson, the acid gas will be contained within the gas reservoir that is the respective injection target. Upward migration is not possible as a result of thick and tight overlying shales of the Clearwater Formation and its equivalents. Lateral migration within the gas reservoir has been recorded in 2003 at Acheson, where, after 13 years of injection, CO₂ has been detected at an offset producing well at 3,625 m distance in the same gas pool. However, migration within the same unit, particularly in a gas reservoir, is expected and its occurrence should not come as a surprise.

The entire stratigraphic interval from the Beaverhill Lake Group to the Lower Mannville Group is overlain by thick shales of the Colorado Group and Lea Park Formation. There are many barriers to acid gas migration from an injection zone into other strata, and the flow process, if it will ever happen, would take an extremely long time on a geological time scale. Any acid gas plume would disperse and dissolve in formation water during flow on such large time and spatial scales.

There is no potential for acid gas leakage through fractures. However, the possibility for upward leakage of acid gas exists along wells that were improperly completed and/or abandoned, or along wells whose cement and/or tubing has degraded or may degrade in the future as a result of chemical reactions with formation brine and/or acid gas. A review of the status and age of wells that penetrate the respective injection unit at each site shows that most wells were drilled in the 1950's and 1960's, and that the majority of wells are abandoned. Although no leakage has been detected and reported to date, the potential for this occurring in the future should be considered.

Contents

Executive Summary	ii
1 Introduction.....	1
2 Selection of an Acid-Gas Injection Site.....	3
2.1 Acid Gas Properties	3
2.2 Criteria for Site Selection	4
2.3 Issues	6
3 Basin-Scale Setting of the Edmonton-Area Acid-Gas Injection Sites	7
3.1 Basin Geology and Hydrostratigraphy.....	7
3.2 Basin-Scale Flow of Formation Water	15
4 Regional-Scale Setting of the Edmonton Cluster of Acid-Gas Injection Sites	19
4.1 Geology of the Beaverhill Lake to Lower Mannville Groups	19
4.1.1 Devonian Beaverhill Lake Group.....	19
4.1.2 Devonian Woodbend Group.....	20
4.1.3 Cretaceous Mannville Group	26
4.2 Hydrogeology of the Beaverhill Lake to Lower Mannville Groups	30
4.2.1 Hydrostratigraphy.....	30
4.2.2 Hydrogeological Observations	32
4.2.3 Flow Interpretation.....	41
4.3 Stress Regime and Rock Geomechanical Properties	43
5 Local-Scale Setting of the Edmonton Cluster of Acid-Gas Injection Sites.....	48
5.1 Golden Spike-Beaverhill Lake	49
5.1.1 Geology	49
5.1.2 Hydrogeological Characteristics and Rock Properties.....	51
5.2 Watelet-Cooking Lake.....	54
5.2.1 Geology	54
5.2.2 Hydrogeological Characteristics and Rock Properties.....	55
5.3 Redwater-Leduc	62
5.3.1 Geology	62
5.3.2 Hydrogeological Characteristics and Rock Properties.....	63
5.4 Acheson-Basal Quartz.....	69
5.4.1 Geology	69
5.4.2 Hydrogeological Characteristics and Rock Properties.....	72
5.5 Strathfield-Ellerslie.....	75
5.5.1 Geology	75
5.5.2 Hydrogeological Characteristics and Rock Properties.....	77
5.6 Summary of the Local-Scale Hydrogeological Analysis	81
5.7 Site Specific Characteristics of the Acid Gas Operations	84
6 Discussion.....	84
6.1 Acid Gas Migration.....	86
6.2 Acid Gas Leakage	94
7 Conclusions	99
8 References	106
9 Appendices.....	114

Figures

Figure 1	Location of the Edmonton cluster of acid-gas injection sites in western Canada at the end of 2003	2
Figure 2	Phase diagrams for methane (CH_4), carbon dioxide (CO_2), hydrogen sulphide (H_2S) and a 50%-50% acid gas mixture; hydrate conditions for CO_2 and H_2S	3
Figure 3	Solubility of water in acid gas as a function of pressure for: a) different acid gas composition (CO_2 and H_2S) at 30°C, and b) different temperatures for an acid gas with a composition of 49% CO_2 , 49% H_2S and 2% CH_4	5
Figure 4	Basin-scale stratigraphic and hydrostratigraphic delineation and nomenclature for the southern and central parts of the Alberta Basin.....	9
Figure 5	Paleogeography and lithofacies distribution during Beaverhill Lake Group time	10
Figure 6	Depositional and erosional boundaries of the Woodbend Group, and outlines of Cooking Lake platform carbonates, Leduc Formation reefs and Grosmont Formation platform carbonates	12
Figure 7	Paleogeography of the Alberta Basin during Cretaceous Lower Mannville time	14
Figure 8	Diagrammatic representation of flow systems in the Alberta Basin: a) in plan view, and b) in cross-section.....	16
Figure 9	Location of acid-gas injection sites, major oil fields, and local-scale study areas in the Edmonton regional-scale study area	20
Figure 10	Stratigraphic and hydrostratigraphic delineation and nomenclature for the strata in the Beaverhill Lake-Mannville sedimentary succession in the Edmonton regional-scale study area	21
Figure 11	Dip cross-section through the Beaverhill Lake-Mannville sedimentary succession in the Edmonton regional-scale study area showing the position of the acid-gas injection sites	22
Figure 12	Main geological features of the Beaverhill Lake Group in the regional-scale study area: a) depth to top, and b) top structure elevation	23
Figure 13	Location of the western boundary of the Cooking Lake Formation carbonate platform and of Leduc Formation reefs in the regional-scale study area	24
Figure 14	Main geological features of the Cooking Lake Formation in the regional-scale study area: a) depth to top, and b) top structure elevation	25
Figure 15	Erosional boundaries of Devonian and Mississippian strata that subcrop underneath Lower Mannville Group sediments in the regional-scale study area.....	27
Figure 16	Schematic cross-section through the Edmonton valley showing the distribution of channel sands versus surrounding shales.....	28
Figure 17	Main geological features of the Ellerslie Member in the regional-scale study area: a) depth to top, and b) top structure elevation.....	29
Figure 18	Facies distribution and lithology of Mannville Group strata in the regional-scale study area: a) Lower Mannville, and b) Upper Mannville.....	31
Figure 19	Salinity of formation water in aquifers in the regional-scale study area: a) Cooking Lake, and b) Winterburn	34
Figure 20	Salinity of formation water in aquifers in the regional-scale study area: a) Wabamun, and b) Mississippian	35
Figure 21	Salinity of formation water in aquifers in the regional-scale study area: a) Lower Mannville, and b) Upper Mannville	36
Figure 22	Distribution of hydraulic heads in aquifers in the regional-scale study area: a) Cooking Lake, and b) Winterburn	37

Figure 23	Distribution of hydraulic heads in aquifers in the regional-scale study area: a) Wabamun, and b) Mississippian.....	39
Figure 24	Distribution of hydraulic heads in aquifers in the regional-scale study area: a) Lower Mannville, and b) Upper Mannville	40
Figure 25	Generalized flow patterns in the Edmonton regional-scale study area.....	41
Figure 26	Diagrammatic representation in cross-section of the flow systems in the Beaverhill Lake-Mannville sedimentary succession in the regional-scale study area	42
Figure 27	Location of wells in the Edmonton regional-scale study area with data for determination of: a) the gradient of the minimum horizontal stress, and b) orientation of horizontal stresses	45
Figure 28	Rock and thin-section photographs of the Beaverhill Lake Group limestones in the Golden Spike area.....	50
Figure 29	Schematic cross-section of the Leduc Formation Golden Spike reef, showing its location above the Beaverhill Lake Group limestone build-up (injection target) within the otherwise argillaceous Waterways Formation.....	51
Figure 30	Isopach map of the Ireton Formation in the Golden Spike local-scale study area.....	52
Figure 31	Stiff diagrams of Devonian formation waters in the local-scale study areas: a) Golden Spike, b) Watelet, and c) Redwater.....	53
Figure 32	Salinity distribution in the Beaverhill Lake Group in the Golden Spike local-scale study area	54
Figure 33	Distribution of pressure versus elevation in the injection stratum (Beaverhill Lake Group) and adjacent formations in the area of the Golden Spike reef complex	55
Figure 34	Isopach map of the Cooking Lake Formation in the Watelet local-scale study area	56
Figure 35	Core and thin-section photographs of the Cooking Lake Formation limestone-dolostone sequence in the Watelet area.....	57
Figure 36	Isopach map of the Ireton Formation above the Cooking Lake Formation	58
Figure 37	Distribution of a) salinity, and b) hydraulic heads in the Cooking Lake aquifer in the Watelet local-scale study area	59
Figure 38	Distribution of pressure versus elevation in the injection stratum (Cooking Lake Formation) and adjacent formations in the Watelet area	61
Figure 39	Isopach map of the Leduc Formation Redwater reef	62
Figure 40	Schematic stratigraphic cross-section of the Leduc Formation Redwater reef.....	63
Figure 41	Core and thin-section photographs of the Leduc Formation limestone-dolostone sequence at Redwater	64
Figure 42	Isopach map of the Ireton Formation in the Redwater local-scale study area	65
Figure 43	Isopach map of the Cooking Lake Formation in the Redwater local-scale study area	66
Figure 44	Distribution of a) salinity, and b) hydraulic heads in the Cooking Lake aquifer in the Redwater local-scale study area	67
Figure 45	Distribution of pressure versus elevation in the injection stratum (Leduc Formation) and adjacent formations in the Redwater local-scale study area.....	68
Figure 46	Distribution of pressure versus elevation in the injection stratum (Leduc Formation) and adjacent formations in Townships 57-58, Ranges 20-21 of the Redwater local-scale study area	69
Figure 47	Isopach map of the Basal Quartz Member in the Acheson local-scale study area	70
Figure 48	Core and thin-section photographs of the Ellerslie/Basal Quartz Member sandstone at the Acheson injection site	71
Figure 49	Stiff diagrams of Lower Mannville formation waters in the local-scale study areas: a) Acheson and b) Strathfield	72

Figure 50 Distribution of a) salinity, and b) hydraulic heads in the Lower Mannville aquifer in the Acheson local-scale study area	73
Figure 51 Distribution of pressure versus elevation in the injection stratum (Ellerslie Member) and adjacent formation in the Acheson area.....	74
Figure 52 Isopach map of the Ellerslie Member in the Strathfield local-scale study area	76
Figure 53 Core and thin-section photographs of the Ellerslie/Basal Quartz Member sandstone in the Strathfield area.....	77
Figure 54 Distribution of a) salinity, and b) hydraulic heads in the Lower Mannville aquifer in the Strathfield local-scale study area.....	78
Figure 55 Distribution of pressure versus elevation in the injection stratum (Ellerslie Member) and adjacent formation in the Strathfield area	80
Figure 56 Comparison of formation waters from the various local-scale study areas using salinity and the molal ratio of Na/Cl	82
Figure 57 History of reservoir pressure and annual volumes of hydrocarbon production at: a) Redwater (Leduc Formation), and b) Acheson (Basal Quartz Member)	83
Figure 58 Distribution and status of the injection wells and of other wells that penetrate the Leduc Formation Redwater reef.....	86
Figure 59 Location of oil and gas fields in the Cretaceous Basal Quartz/Ellerslie Member in the vicinity of the Strathfield and Acheson acid-gas injection sites	89
Figure 60 Inferred outline of the Golden Spike reefal carbonates, and distribution and status of wells that penetrate: a) the acid-gas injection unit (Beaverhill Lake Group), and b) the overlying Leduc Formation Golden Spike reef	91
Figure 61 Inferred migration path for a plume of acid gas injected in the Cooking Lake aquifer at Watelet, and distribution and status of wells along this path	94
Figure 62 Histograms for wells that penetrate the Leduc Formation Redwater reef showing: a) well status, b) time of drilling, and c) time of abandonment for abandoned wells	96
Figure 63 Histograms for wells that penetrate the Leduc Formation Golden Spike reef showing: a) well status, b) time of drilling, and c) time of abandonment for abandoned wells.....	98
Figure 64 Histograms for wells that penetrate the Cooking Lake Formation at Watelet along a potential migration path of the acid gas plume, showing: a) well status, b) time of drilling, and c) time of abandonment for abandoned wells	100
Figure 65 Distribution and status of wells that penetrate the St. Albert-Big Lake Ostracod A gas pool in the Acheson area.....	101
Figure 66 Histograms for wells that penetrate the St. Albert-Big Lake Ostracod A pool in the Acheson area, showing: a) well status, b) time of drilling, and c) time of abandonment for abandoned wells.....	102
Figure 67 Distribution and status of wells that penetrate the Ellerslie Member in the nine sections around the Strathfield acid-gas injection site	103
Figure 68 Histograms for wells that penetrate the Ellerslie Member in the nine sections around the Strathfield acid-gas injection site, showing: a) well status, b) time of drilling, and c) time of abandonment for abandoned wells	104

Tables

Table 1	Number of chemical analyses of formation water and drillstem test data that were used in the regional assessment of formation water flow in the Edmonton area	32
Table 2	Gradients of the minimum horizontal, stress $S_{H\min}$, determined from tests performed in wells in the Edmonton regional-scale study area.....	46
Table 3	Orientations of the minimum and maximum horizontal stresses determined from breakouts in wells in the Edmonton regional-scale study area	47
Table 4	Geomechanical properties of rocks of interest from the Alberta Basin	47
Table 5	Major ion chemistry of Beaverhill Lake brines in the Golden Spike area.....	52
Table 6	Major ion chemistry of Cooking Lake brines in the Watelet area	60
Table 7	Well-scale porosity and permeability values obtained from measurements in core plugs from the Leduc/Cooking Lake formations in the Watelet local-scale study area	61
Table 8	Summary of major ion chemistry of Leduc/Cooking Lake brines in the Redwater area.....	65
Table 9	Well-scale porosity and permeability values obtained from core-scale measurements in core plugs from Leduc/Cooking Lake formations in the Redwater local-scale study area	68
Table 10	Major ion chemistry of Lower Mannville brines in the Acheson area	72
Table 11	Well-scale porosity and permeability values obtained from measurements in core plugs from the Lower Mannville and Wabamun groups in the Acheson local-scale study area	75
Table 12	Major ion chemistry of Lower Mannville brines in the Strathfield area	79
Table 13	Well-scale porosity and permeability values obtained from core-scale measurements in core plugs from the Lower Mannville and Wabamun groups in the Strathfield local-scale study area.....	80
Table 14	Characteristics of the acid-gas injection operations in the Edmonton area	85
Table 15	Properties of native fluids and injected acid gas at initial in-situ conditions for four acid-gas injection sites in the Edmonton area where dry acid gas is injected	87

Appendices

Appendix 1

1-1	Downhole stratigraphic model for the Golden Spike injection site	115
1-2	Downhole stratigraphic model for the Watelet injection site.....	116
1-3	Downhole stratigraphic model for the Strathfield and Acheson injection sites	117

Appendix 2

Table 1	Major ion chemistry of formation water from the Leduc and Cooking Lake formations in the Redwater area	119
Table 2	Major ion chemistry of formation water from the Lower Mannville Group in the Acheson area	124
Table 3	Major ion chemistry of formation water from the Lower Mannville Group in the Strathfield area.....	126

1 Introduction

Over the past decade, oil and gas producers in western Canada (Alberta and British Columbia) have been faced with a growing challenge to reduce atmospheric emissions of hydrogen sulphide (H_2S), which is produced from “sour” hydrocarbon pools. Sour oil and gas are hydrocarbons that contain H_2S and carbon dioxide (CO_2), which have to be removed before the produced oil or gas is sent to markets. Since surface desulphurization through the Claus process is uneconomical, and the surface storage of the produced sulphur constitutes a liability, increasingly more operators are turning to acid gas disposal by injection into deep geological formations. Acid gas is a mixture of H_2S and CO_2 , with minor traces of hydrocarbons, that is the by-product of “sweetening” sour hydrocarbons. In addition to providing a cost-effective alternative to sulphur recovery, the deep injection of acid gas reduces emissions of noxious substances into the atmosphere and alleviates the public concern resulting from sour gas production and flaring.

The first acid-gas injection operation was started in 1990 in Alberta. To date, 42 injection operations have been approved in Alberta and British Columbia; their locations are shown in Figure 1. In Alberta, the Oil and Gas Conservation Act requires that operators apply for and obtain approval from the Alberta Energy and Utilities Board (EUB), the provincial regulatory agency, to dispose of acid gas. Before approving any operation, the EUB reviews the application to maximize conservation of hydrocarbon resources, minimize environmental impact and ensure public safety. To adequately address these matters, the EUB requires that the applicants submit information regarding surface facilities, injection well configurations, geological characteristics of the injection reservoir or aquifer, and operations. After approval for acid gas injection is granted, the operators have to submit to the regulatory agencies biannual progress reports on the operations.

Although the purpose of the acid-gas injection operations is to dispose of H_2S , significant quantities of CO_2 are being injected at the same time because it is costly to separate the two gases. Actually, more CO_2 than H_2S has been injected to date into deep geological formations in western Canada. In the context of current efforts to reduce anthropogenic emissions of CO_2 , these acid-gas injection operations represent an analogue to geological storage of CO_2 . The latter is an immediately-available and technologically-feasible way of reducing CO_2 emissions into the atmosphere that is particularly suited for land-locked regions located on sedimentary basins, such as the Alberta Basin in western Canada. Large-scale injection of CO_2 into depleted oil and gas reservoirs and into deep saline aquifers is one of the most promising methods of geological storage of CO_2 , and in this respect it is no different from acid-gas injection operations. However, before implementation of greenhouse gas geological storage, a series of questions needs addressing, the most important ones relating to the short- and long-term fate of the injected CO_2 . Thus, the study of the acid-gas injection operations in western Canada provides the opportunity to learn about the safety of these operations and about the fate of the injected gases, and represents a unique opportunity to investigate the feasibility of CO_2 geological storage.

Geographically, the acid-gas injection operations in western Canada can be grouped in several clusters (Figure 1). The operations located in the cluster situated in the Edmonton area inject acid gas in the Devonian Beaverhill Lake and Woodbend groups and in the Cretaceous Mannville Group. Previous work characterized the subsurface at the injection sites in the Brazeau-Pembina area of west-central Alberta (Bachu et al., 2003a, b). The subsurface characterization of the acid-gas injection operations in the Edmonton area will help in understanding various issues that relate to the disposal and/or sequestration of acid and greenhouse gases in geological media. The characterization is based on reservoir-scale data and information submitted by the operators to the EUB, on basin-scale work performed at the Alberta Geological Survey (AGS) during the last 15 years, and on local and reservoir-scale work performed by the AGS specifically for this report.

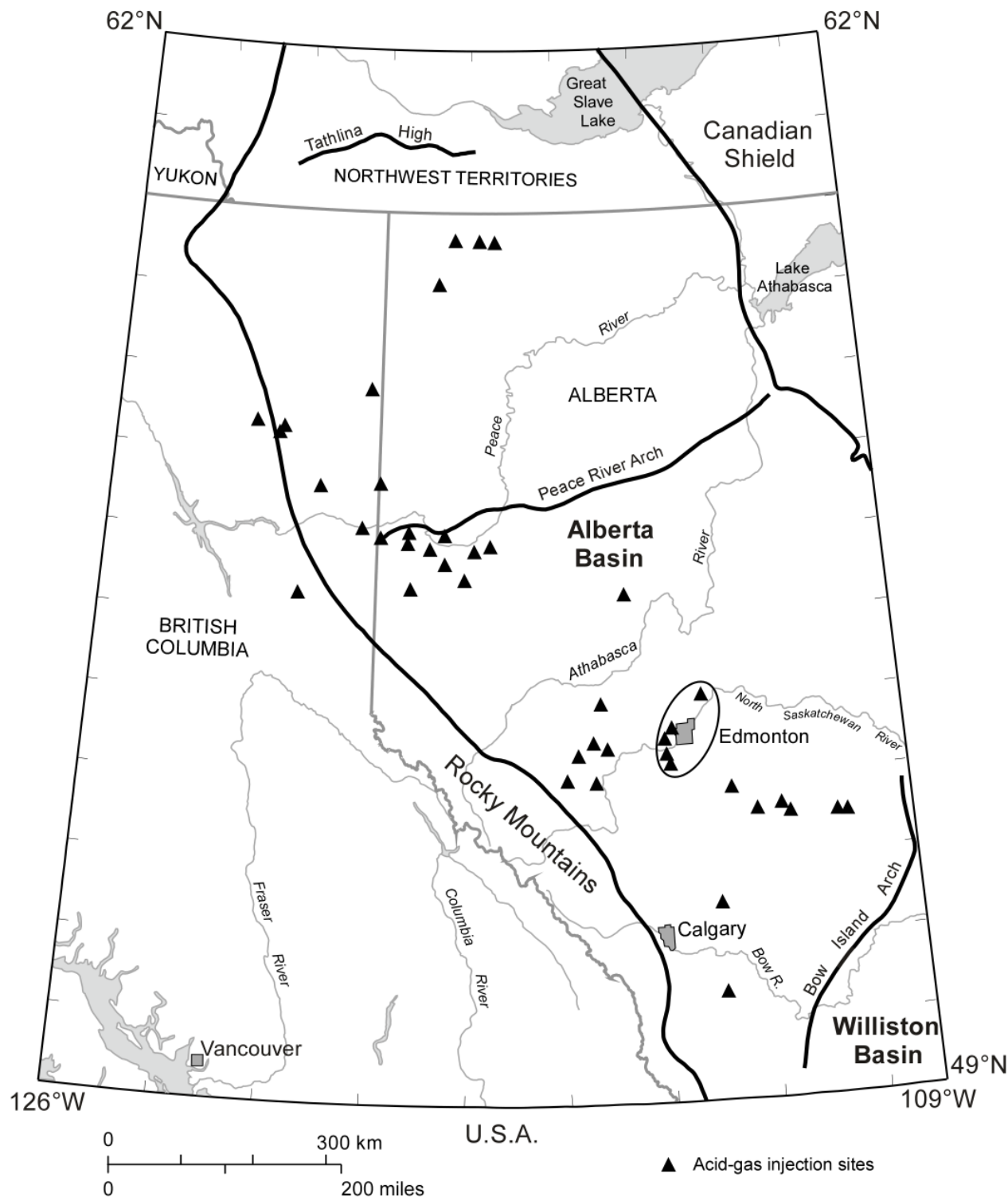


Figure 1. Location of the Edmonton cluster of acid-gas injection sites in western Canada at the end of 2003.

2 Selection of an Acid-Gas Injection Site

In Alberta, applications for acid gas disposal must conform to the specific requirements listed in Chapter 4.2 of Guide 65 that deals with applications for conventional oil and gas reservoirs (EUB, 2000). The selection of an acid-gas injection site needs to address various considerations that relate to: proximity to sour oil and gas production that is the source of acid gas; confinement of the injected gas; effect of acid gas on the rock matrix; protection of energy, mineral and groundwater resources; equity interests; wellbore integrity and public safety (Keushnig, 1995; Longworth et al., 1996). The surface operations and the subsurface aspects of acid gas injection depend on the properties of the H_2S and CO_2 mixture, which include, but are not limited to non-aqueous phase behaviour, water content, hydrate formation and the density and viscosity of the acid gas (Carroll & Lui, 1997; Ng et al., 1999).

2.1 Acid Gas Properties

The acid gas obtained after the removal of H_2S and CO_2 from the sour gas may also contain 1%-3% hydrocarbon gases, and is saturated with water vapor in the range of 2-6%. In their pure state, CO_2 and H_2S have similar phase equilibria, but at different pressures and temperatures (Carroll, 1998a). They exhibit the normal vapour/liquid behaviour with pressure and temperature (Figure 2), with CO_2 condensing at lower temperatures than H_2S . Methane (CH_4) also exhibits this behaviour, but at much lower temperatures. The phase behaviour of the acid-gas binary system is represented by a continuous series of two-phase envelopes (separating the liquid and gas phases) located between the unary bounding systems in the pressure-temperature space (Figure 2).

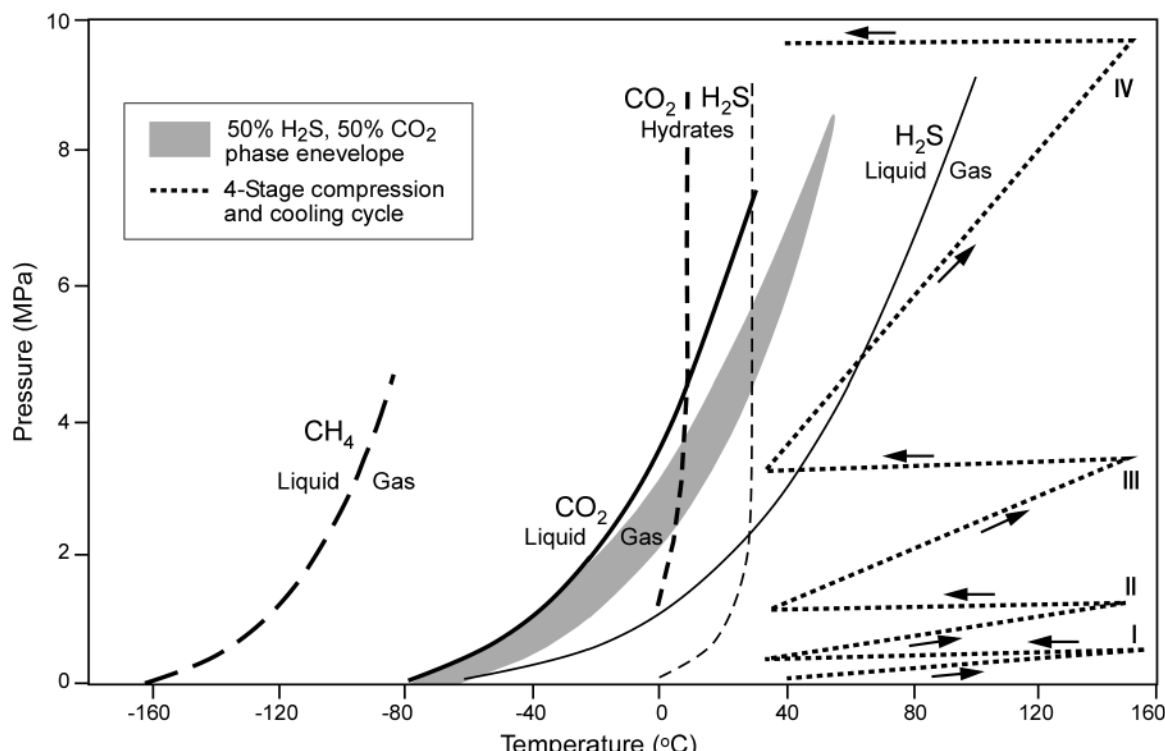


Figure 2. Phase diagrams for methane (CH_4), carbon dioxide (CO_2), hydrogen sulphide (H_2S) and a 50%-50% acid gas mixture; hydrate conditions for CO_2 and H_2S (after Wichert and Royan, 1996, 1997).

If water is present, both CO₂ and H₂S form hydrates at temperatures up to 10°C for CO₂ and more than 30°C for H₂S (Carroll and Lui, 1997). If there is too little water, the water is dissolved in the acid gas and hydrates will generally not form. However, phase diagrams show that hydrates can form without free water being present (Carroll, 1998a, b), thus, operating above the hydrate-forming temperature is desirable. Unlike the case of hydrocarbon gases, the solubility of water in both H₂S and CO₂, hence in acid gas, decreases as pressure increases up to 3-8 MPa, depending on temperature, after which it dramatically increases (Figure 3). The solubility minimum reflects the pressure at which the acid gas mixture passes into the dense liquid phase, where the solubility of water can increase substantially with increasing pressure due to the molecular attraction between these polar compounds (Wichert & Royan, 1996, 1997).

The properties of the acid gas mixture are important in facility design and operation because, to optimize storage and minimize risk, the acid gas needs to be injected: (1) in a dense-fluid phase, to increase storage capacity and decrease buoyancy; (2) at bottom-hole pressures greater than the formation pressure, for injectivity; (3) at temperatures generally greater than 35°C to avoid hydrate forming, which could plug the pipelines and well; and (4) with water content lower than the saturation limit, to avoid corrosion.

After separation, the water-saturated acid-gas stream leaves the regeneration unit at 35 to 70 kPa and must be cooled and then compressed for injection to pressures in excess of the subsurface storage formation pressure. Typically, four stages of compression are required to provide the required discharge pressure. By the fourth stage in a cycle, compression will tend to dewater the acid gas up to a maximum pressure between 3 and 5 MPa (Figure 3), if there are no hydrocarbon impurities present. Further compressing the acid gas to higher pressures increases the solubility of water in the acid gas, such that any residual excess water dissolves into the acid gas, and more than counteracts the decrease in solubility due to inter-stage cooling. To avoid pump cavitation, the acid gas must not enter the two-phase region during compression. Once the acid gas is compressed, it is transported through a pipeline to the injection wellhead usually a short distance from the gas plant. The high pressures after the fourth compression stage stabilize upon cooling, the high-density liquid-phase of the acid gas.

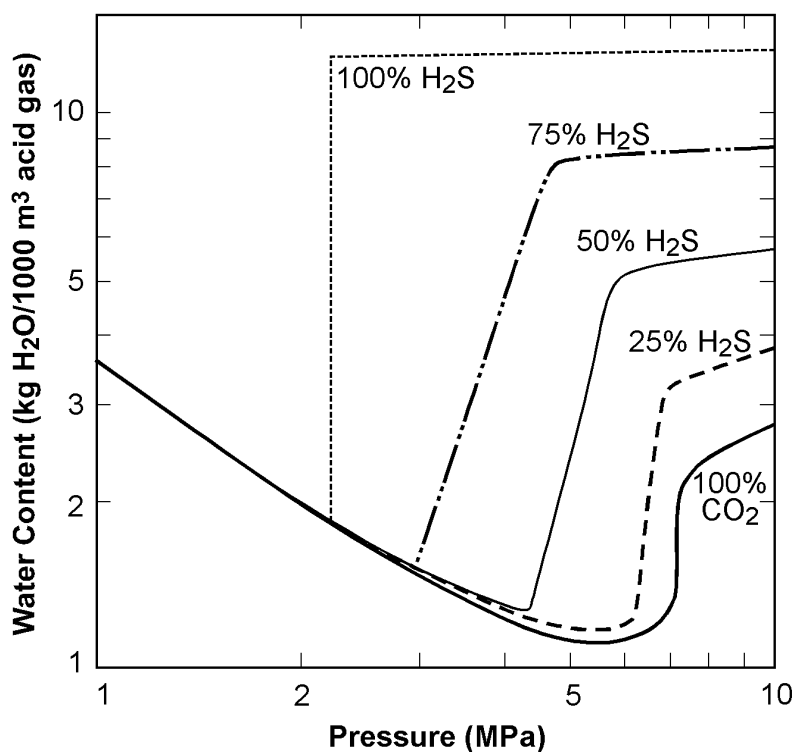
Although a number of safety valves are always installed, both in the well and in the surface facilities to be able to isolate the containment lines for the acid-gas injection system into small volumes, the release of even small volumes of acid gas can be harmful. Consequently, the operators are required to have a detailed emergency response plan (ERP) in case a leak occurs that may impact humans. An emergency planning zone, the EPZ (i.e., area of land which may be impacted by the release of H₂S), is defined around the sour gas facility.

2.2 Criteria for Site Selection

The general location for an acid-gas injection well is often influenced by the proximity to sour oil or gas production facilities that are the source of acid gas. The specific location is based on a general assessment of the regional geology and hydrogeology, which is designed to evaluate the potential for containment and avoidance of leakage (Longworth et al., 1996) and which includes

1. Size of the injection zone, to confirm that it is large enough to volumetrically hold all of the injected acid gas over the lifetime of the project;
2. Thickness and extent of the overlying confining layer (caprock), and any stratigraphic traps or fractures that may affect its ability to contain the acid gas;
3. Location and extent of the underlying or lateral bounding formations;
4. Folding or faulting in the area, and an assessment of seismic (neotectonic) risk;

a.



b.

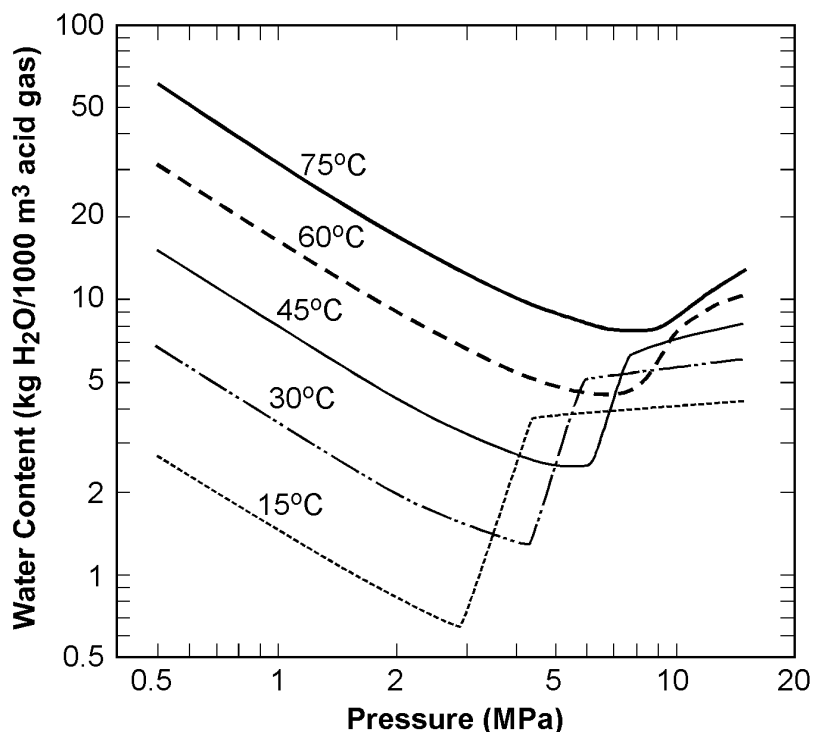


Figure 3. Solubility of water in acid gas as a function of pressure for: a) different acid gas composition (CO₂ and H₂S) at 30°C, and b) different temperatures for an acid gas with a composition of 49% CO₂, 49% H₂S and 2% CH₄ (see also Lock, 1997; Wichert and Royan, 1996, 1997).

5. Rate and direction of the natural flow system, to assess the potential for migration of the injected acid gas;
6. Permeability and heterogeneity of the injection zone;
7. Chemical composition of the formation fluids (water for aquifers, oil or gas for reservoirs);
8. Formation temperature and pressure;
9. Analyses of formation and caprock core (if available); and, finally,
10. A complete and accurate drilling history of offsetting wells within several kilometres of the injection well, to identify any wells or zones that may be impacted by the injected acid gas.

Knowledge of the geological setting and characteristics is critical to assess the integrity of the host formation or reservoir, and the short- and long-term fate of the injected acid gas. Of particular importance are potential migration pathways from the injection zone to other formations, shallow groundwater and/or the surface. These potential pathways are of three types: the caprock pore space (“membrane” type), natural and/or induced fractures (“cracks”) through the confining strata, and improperly completed and/or abandoned wells (“punctures”). To avoid diffuse gas migration through the caprock pore space, the difference between the pressure at the top of the injection aquifer or reservoir and the pressure in the confining layer must be less than the caprock threshold displacement pressure, which is the pressure needed for the acid gas to overcome the capillarity barrier and displace the water that saturates the caprock pore space. To avoid acid gas migration through fractures, the injection zone must be free of natural fractures, and the injection pressure must be below a certain threshold to ensure that fracturing is not induced. The maximum bottomhole injection pressure is set by regulatory agencies at less than 90% of the fracturing pressure of the reservoir rock. In the absence of site-specific tests, the pressures are limited by pressure-depth correlations, based on basin-wide statistical data for the Alberta Basin. If injection takes place into a depleted oil or gas reservoir, the maximum bottom-hole injection pressure is usually set at no more than the initial reservoir pressure. From this point of view, injection into a depleted oil or gas reservoir has the advantages of injection pressures being low and of wells and pipelines being already in place (Keushnig, 1995).

2.3 Issues

Critical issues are for the most part environmental and safety-related and they directly affect the economics of acid gas injection. Acid gas leaks can result in loss of life or contamination of the bio- and atmosphere. Surface safety is addressed through engineering, installation of safety valves and monitoring systems, and emergency procedures for the case of H₂S leaks. Subsurface issues are of two inter-related categories: the effect of the acid gas on the rock matrix and well cements, and plume containment.

When the acid gas contacts the subsurface formation, it will readily dissolve in the formation water in an aquifer, or connate water in a reservoir, and create weak carbonic and sulphuric acids. This leads to a significant reduction in pH that accelerates water-rock reactions. Depending on mineralogy, mineral dissolution or precipitation may occur, affecting the porosity and permeability of the host rock. The fact that both CO₂ and H₂S are dissolving in the formation water leads to some complex reaction paths where carbonates precipitate and dissolve, and pyrite/pyrrhotite precipitates (Gunter et al., 2000; Hitchon et al., 2001). Dissolution of some of the rock matrix in carbonate strata, or of the carbonates surrounding the sand grains in sandstone units results in lower injection pressures in the short term as a result of increased permeability. A major concern with the injection process is the potential for formation damage and reduced injectivity in the vicinity of the acid gas scheme. The reduction in injectivity could possibly be the result of fines migration, precipitation and scale potential, oil or condensate banking and plugging,

asphaltene and elemental sulphur deposition, and hydrate plugging (Bennion et al., 1996).

Cement compatibility with the acid gas, primarily in the injection well, but also in neighboring wells, is crucial for safety and containment. For example, a non-carbonate and calcium cement blend shattered when tested in an acid gas stream for several weeks (Whatley, 2000). Thus, the compatibility of the acid gas with the cement that bonds the casing to the formation must be tested at a minimum. While the cement for the newly implemented acid-gas operation can be tested and properly selected prior to drilling, the cements in nearby wells are already in place and their condition is largely unknown. Some of these wells could be quite old (several decades), with the cement already in some stage of degradation as a result of brine composition. The acid gas, when reaching these wells, may enhance and speed up the cement degradation, leading to possible leaks through the well annulus and/or along casing.

If the acid gas is injected into the originating or other oil or gas pool, the main concern is the impact on further hydrocarbon recovery from the pool and acid gas production at the wellhead, although the injection operation and enhanced oil recovery may prove successful, like in the case of the Zama X2X pool (Davison et al., 1999). If the gas mixture is injected into an aquifer, the degree to which it forms a plume and migrates from the injection well depends on various factors, including pressure and temperature, solubility, interplay between driving forces like buoyancy and aquifer hydrodynamics, and aquifer heterogeneity, which controls gravity override and viscous fingering.

The fate of the injected acid gas in the subsurface is not known, because subsurface monitoring is not currently required and is difficult and expensive. Only the wellhead gas composition, pressure, temperature and rate have to be reported to the EUB. Thus, a proper understanding of the geology and hydrogeology of the acid-gas injection unit (reservoir or aquifer) is critical in assessing the fate of the injected acid gas and the potential for migration and/or leakage into other units.

3 Basin-Scale Setting of the Edmonton-Area Acid-Gas Injection Sites

The geology, stratigraphy and hydrostratigraphy of the sedimentary succession are different in the northern part of the Alberta Basin (north of the Peace River Arch) from those in the area south of the Peace River Arch (see Figure 1), because of differences in the tectonostratigraphic evolution, with corresponding effects on the flow of formation waters (Bachu, 1999). In the following, the geology and hydrostratigraphy of area of the Alberta Basin south of the Peace River Arch, relevant to the Edmonton-area sites, will be presented. The geology described herein is based on Porter et al. (1982), Ricketts (1989) and Mossop & Shetsen (1994) (and references cited therein), and the hydrogeology on Bachu (1999). Of the five acid-gas injection operations in the Edmonton area (Figure 1), three inject into the Devonian Beaverhill Lake and Woodbend groups and two into the Cretaceous Mannville Group.

3.1 Basin Geology and Hydrostratigraphy

The Alberta Basin sits on a stable Precambrian platform and is bound by the Rocky Mountain Trench to the west and southwest, the Tethys High to the north and the Canadian Precambrian Shield to the northeast (Figure 1). The Bow Island Arch separates the Alberta Basin from the Williston Basin to the southeast. The basin was initiated during the late Proterozoic by rifting of the North American craton. It consists at the base of a Middle Cambrian to Middle Jurassic passive-margin succession dominated by shallow-water carbonates and evaporites with some intervening shales (Porter et al., 1982). From the Late Jurassic to Early Tertiary, accretion of allochthonous terranes to the western margin of the proto North American continent during the Columbian and Laramide orogenies pushed sedimentary strata eastward, resulting in the Rocky Mountains thrust and fold belt, and creating conditions for foreland-

basin development east of the deformation front. Because of lithospheric loading and isostatic flexure, the Precambrian basement tilted westward, with a gentle slope of <4 m/km in the east near the Canadian Shield, becoming steeper westward, up to >20 m/km near the deformation front. As a result of this tilting and significant pre-Cretaceous erosion, progressively older Jurassic to Middle Devonian strata subcrop from west to east at the sub-Cretaceous unconformity. Deposition during the foreland stage of basin development was dominated by synorogenic clastics, mainly muds and silts, derived from the evolving Cordillera. The basin fill attained maximum thickness and burial during the Laramide orogeny in the Paleocene. Tertiary-to-Recent erosion since then has removed an estimated 2000 to 3800 m of sediments in the southwest (Nurkowski, 1984, Bustin, 1991). As a result of these depositional and erosional processes, the undeformed part of the Alberta Basin comprises a wedge of sedimentary rocks that increases in thickness from zero at the Canadian Shield in the northeast to close to 6000 m in the southwest at the thrust and fold belt. The present-day topography of the undeformed part of the basin has a basin-scale trend of decreasing elevations from highs in the 1200 m range in the southwest to lows around 200 m in the north-northeast at Great Slave Lake, which is the lowest topographic point in the basin. The stratigraphic and hydrostratigraphic nomenclature and delineation for the entire sedimentary succession in the Alberta Basin south of the Peace River Arch are shown in Figure 4.

Hydrostratigraphically, the Precambrian crystalline basement constitutes an aquiclude, except possibly for fault and shear zones that may have served as conduits for fluid flow and may still be active today. Thin, diachronous basal sandstone units (Basal Sandstone in the south and Granite Wash in the area of the Peace River Arch) cover the Precambrian basement. As a result of pre-Middle Ordovician erosional beveling and of major pre-Middle Devonian erosion, Cambrian strata are eroded near the Peace River Arch. Ordovician strata are present only in the southeast along a narrow band along the basin edge, and Silurian strata are completely absent. The Cambrian Basal Sandstone unit forms the Basal Cambrian aquifer, while the shale-dominated Cambrian and Ordovician strata form the Cambrian aquitard system.

A Middle Devonian interbedded succession of low-permeability anhydritic red beds and carbonates, halite and argillaceous carbonates of the Lower Elk Point Group overlies the Cambrian units or Granite Wash detritus, and forms the Elk Point aquitard system. The overlying platformal and reefal carbonates of the Upper Elk Point Group Winnipegosis Formation form the Winnipegosis aquifer. This unit is overlain over most of the basin by the thick halite of the Prairie Formation, followed by the shales of the Watt Mountain Formation, which together form the Prairie aquiclude system. Because of variable lithology (mixed siliciclastics and evaporites) of the Prairie Formation in the western part of the basin, and salt dissolution along the eastern basin edge, this hydrostratigraphic system has aquiclude characteristics where the salt is present, and aquitard characteristics where the salt is absent, or present only in minor quantities.

The Elk Point Group is unconformably overlain by the Middle to Upper Devonian Beaverhill Lake Group. It has been subdivided into the Fort Vermilion, Slave Point, Swan Hills, and Waterways formations. Beaverhill Lake Group deposition was marked by the spread of marine seas from the north into the Western Canada Sedimentary Basin during Late Middle Devonian time. Topographic highs, like the Peace River Landmass (Figure 5), were progressively onlapped as the water level rose. Following the deposition of tight evaporites (anhydrite and carbonates) of the Fort Vermilion Formation in the northern part of the basin, marine carbonates of the Slave Point Formation formed large carbonate platforms (e.g., Hay River Bank) in shallow water environments. Reef growth occurred along the margins of the Slave Point platforms (e.g., fringing the Peace River Landmass). Farther south, large reefal complexes of the Swan Hills Formation (Swan Hills Complex) composed of a sequence of stacked carbonate cycles developed on the Slave Point platforms. Contemporaneous sedimentation in off-platform and off-reef areas of the Waterways Basin (Figure 5) resulted in the deposition of the calcareous shales and

Stratigraphic Nomenclature			Hydrostratigraphy	
Period	Group	Formation		
Quaternary	Preglacial and glacial drift			
Tertiary	Paskapoo Scollard Battle Whitemud Brazeau Horseshoe Canyon Bearpaw Belly River Lea Park Milk River Colorado Cardium Second White Speckled Sandstone Viking Mannville Clearwater			
Cretaceous	Upper	Brazeau	Scollard - Paskapoo aquifer	
		Horseshoe Canyon	Battle aquitard	
		Bearpaw	Horseshoe Canyon aquifer	
		Belly River	Bearpaw aquitard	
		Lea Park	Belly River aquifer system	
		Milk River	Lea Park aquitard	
		Colorado	Milk River aquifer	
		Cardium	Colorado aquitard system	
		Second White Speckled Sandstone	Upper Mannville aquifer	
		Viking	Clearwater aquitard	
Jurassic	Lower	Mannville	Lower Mannville aquifer	
		Clearwater	Jurassic aquitard	
		U		
Triassic	U	M		
		L		
Permian			Triassic aquitard system	
Pennsylvanian				
Mississippian	Stoddart Rundle Banff Exshaw Wabamun Winterburn		Mississippian - Jurassic aquifer system	
	Woodbend Ireton Grosmont Leduc Cooking Lk. Beaverhill Lake			
Devonian	Upper	Elk Point	Upper Devonian aquifer system	
		Upper	Woodbend aquitard	
		Lower	Middle - Upper Devonian aquifer system	
			Prairie aquiclude - aquitard system	
			Winnipegosis aquifer	
			Elk Point aquiclude system	
Silurian				
Ordovician				
Cambrian	U	Basal Sandstone	Cambrian aquitard system	
		Not deposited	Basal aquifer	
		Not deposited		
Precambrian				

Figure 4. Basin-scale stratigraphic and hydrostratigraphic delineation and nomenclature for the southern and central parts of the Alberta Basin (after Bachu, 1999).

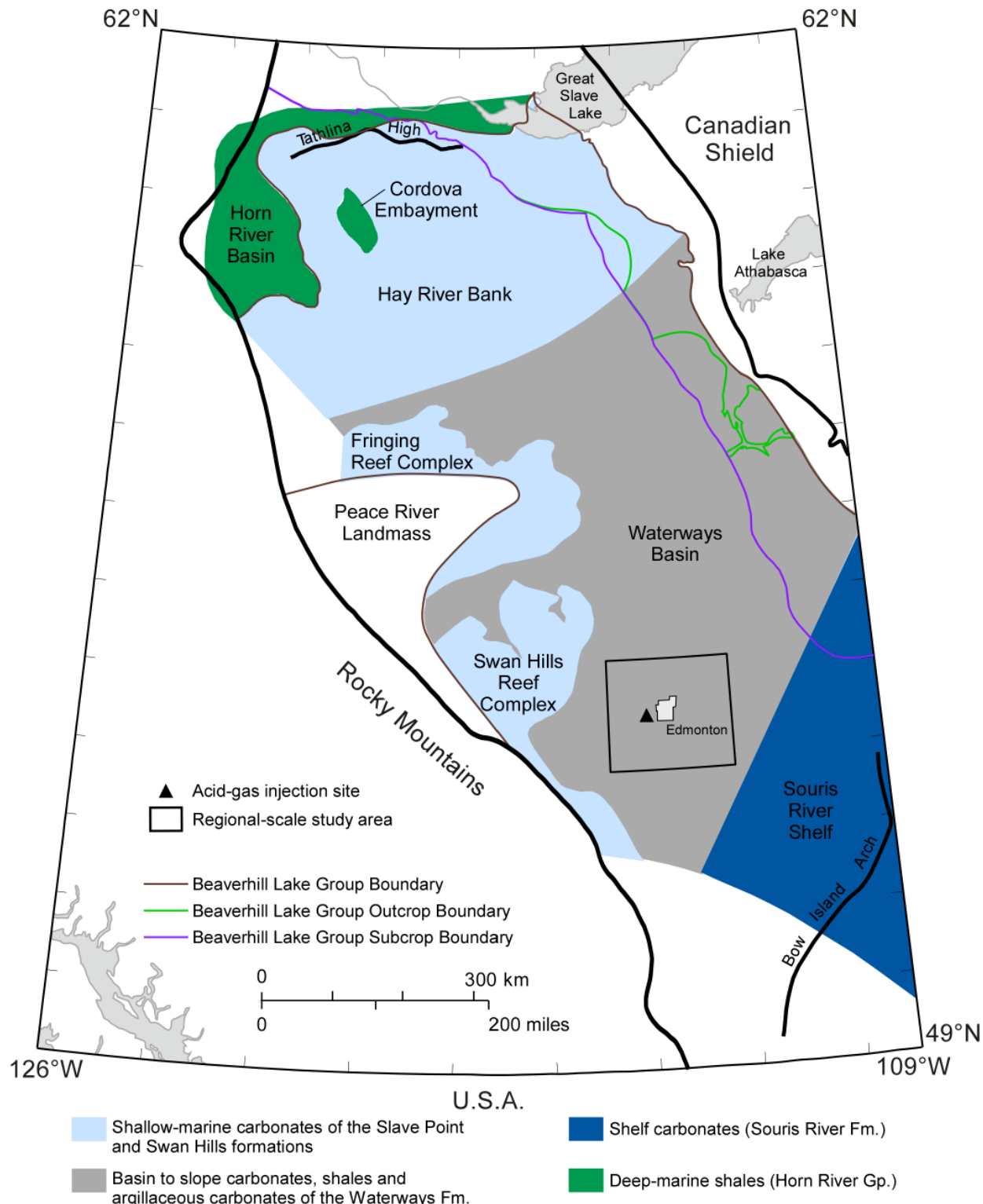


Figure 5. Paleogeography and lithofacies distribution during Beaverhill Lake Group time (modified after Oldale and Munday, 1994). Erosional boundaries of the Beaverhill Lake Group and the location of the Golden Spike acid-gas injection site are also shown.

argillaceous carbonates of the Waterways Formation. The platformal and reefal carbonates of the Slave Point and Swan Hills formations (Figure 5) together form the main aquifer unit within the Beaverhill Lake Group. The basinal deposits of the overlying Waterways Formation have, depending on location and dominant lithology, either aquifer or aquitard characteristics. The southeastern margin of the Waterways Basin is characterized by a transition to shelf carbonates and evaporites of the Souris River Formation, which extends eastward into the Williston Basin. The aquifers and aquitards of the Beaverhill Lake Group subcrop at the sub-Cretaceous unconformity, and crop out along the Athabasca River and its tributaries in northeastern Alberta (Figure 5).

The Upper Devonian Woodbend Group conformably overlies the Beaverhill Lake Group. Extensive platform carbonates and associated reefs of the Cooking Lake and Leduc formations developed in shallow water environments, while thick organic rich shales of the Majeau Lake Member (Cooking Lake Formation) and Duvernay Formation were deposited contemporaneously in deeper water settings (Figure 6). Calcareous shales and argillaceous limestones of the Ireton Formation progressively filled the basin from the northeast, thereby terminating Leduc reef growth. In northeastern Alberta, a large carbonate shelf platform, the Grosmont Formation, developed over the prograding Ireton Formation (Figure 6). Except for a small area in west-central Alberta, almost the entire basin had been filled in by the end of Woodbend Group deposition. In central Alberta, the basin-fill succession of the Woodbend Group differs significantly from that of the underlying Beaverhill Lake Group (Waterways Formation). Instead of being comprised of carbonate muds derived from coeval carbonate banks to the southeast and east, Woodbend Group basin-fill units have a considerably higher clay shale content. All the units of the Woodbend Group subcrop at the sub-Cretaceous unconformity. The Grosmont Formation crops out along the Peace River at an elevation of approximately 250 m (Figure 6).

Hydrostratigraphically, the Cooking Lake and Leduc carbonates form the Cooking Lake aquifer, which, together with the aquifers of the underlying Beaverhill Lake Group, form the Middle-Upper Devonian aquifer system (Figure 4). The Ireton, Duvernay and Majeau Lake formations form the Woodbend aquitard. The Grosmont Formation is an aquifer that is included in the overlying Upper Devonian aquifer system as a result of its hydraulic continuity with and influence on the Winterburn and Wabamun aquifers in the area of subcrop in the northeast (Anfort et al., 2001).

The Woodbend Group is conformably overlain by the Winterburn Group, which has been subdivided into the Nisku, Calmar and Graminia formations. The Nisku Formation at the base of the Winterburn Group is comprised of fossiliferous shelf and reef carbonates in southern and northeastern Alberta with a transition to more open-marine, deeper-water carbonates and shales in westcentral Alberta. It is followed by widespread dolomitic silts and shales of the Calmar Formation. The overlying Graminia Formation consists of the transgressive shallow shelf carbonates of the Blue Ridge Member and a northwestward thickening wedge of “Graminia Silt”, which marks the final infilling of the basin at the end of Winterburn time (Burrowes and Krause, 1987).

The Winterburn Group is conformably overlain by carbonates and evaporites of the Wabamun Group. Wabamun carbonates consist of dolomitic limestones and calcareous dolomites, with dolomites predominating in the lower and middle parts of the group and limestones in the upper part. In southeastern Alberta, these carbonates interfinger with peritidal evaporites (mainly anhydrite) of the Stettler Formation. Close to the end of Wabamun time, open marine limestones of the Big Valley Formation were deposited over most of Alberta.

The widespread platform carbonates interspersed with minor shales of the Winterburn and Wabamun groups subcrop at the sub-Cretaceous unconformity, and, at the basin-scale, form the Upper Devonian

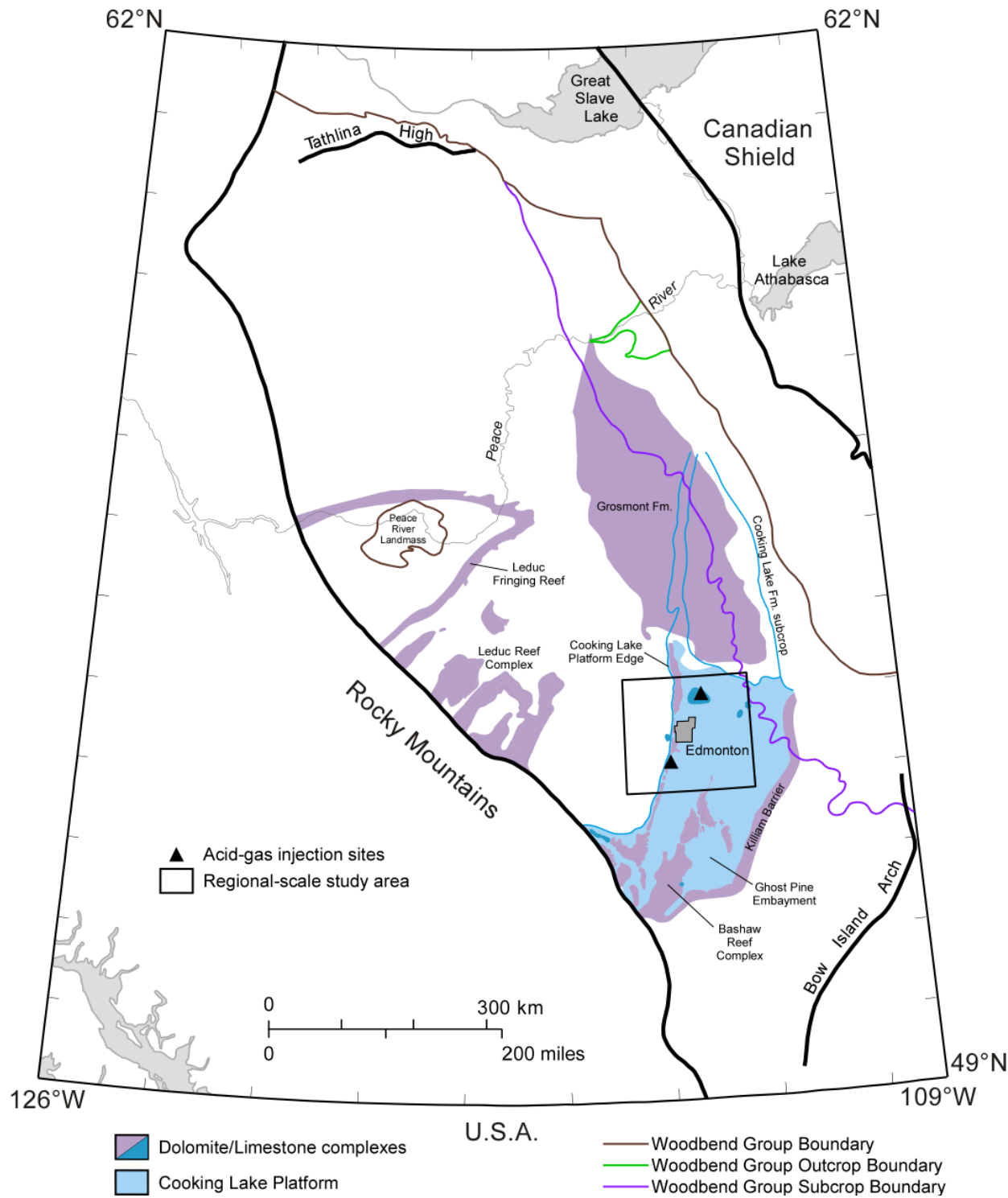


Figure 6. Depositional and erosional boundaries of the Woodbend Group, and outlines of Cooking Lake platform carbonates, Leduc Formation reefs and Grosmont Formation platform carbonates. The location of the Redwater and Watelet acid-gas injection sites is also shown.

aquifer system (Figure 4). Reefs of the Leduc Formation breach the Ireton aquitard in places, thus establishing local hydraulic communication between the Middle-Upper Devonian aquifer system and the overlying Upper Devonian aquifer system, including the Grosmont aquifer (Bachu & Underschultz, 1993; Rostron & Toth, 1996, 1997; Hearn & Rostron, 1997; Anfort et al., 2001).

The thin, organic rich, competent shales of the Exshaw Formation were conformably deposited on top of the Wabamun Group during the Late Devonian to Early Mississippian, followed by a succession of interbedded shales and carbonates of the Banff Formation, with an increase in the presence of carbonates toward the top. These are in turn overlain by thick carbonate successions of the Rundle and Stoddart groups. Permian, Triassic and early Jurassic strata are present only in the Peace River Arch area in the northwest near the eastern edge of the thrust and fold belt, and consist of interbedded sandstones, siltstones, carbonates, evaporites and shales. The shales of the Exshaw Formation and the shale-dominated lower part of the Banff Formation form the Exshaw-Banff aquitard (Figure 4). At the basin-scale, the entire Upper Banff to Lower Jurassic succession, except for the Triassic, forms the Carboniferous-Jurassic aquifer system in the southern and central parts of the basin. The shales and evaporites that dominate the Triassic succession, including intervening sandstone units form the Triassic aquitard system.

Late Jurassic siliciclastics were deposited along the western edge of the basin at the beginning of the foreland-stage of basin evolution. They are variably dominated by either sandstones or shales, which form aquifers or weak aquitards, depending on location.

The overlying Cretaceous strata are divided into several depositional successions. The Mannville Group and age-equivalent strata are the oldest Cretaceous rocks over most of the Western Canada Sedimentary Basin and represent a major period of subsidence and sedimentation following a long time of uplift, exposure, and erosion of older strata (Figure 4). The Mannville Group strata, the depositional response to the Columbian orogeny (Porter et al., 1982), consist of fluvial and estuarine valley-fill sediments as well as sheet sands and shales deposited by repeated marine transgressive-regressive events (Figure 7). The Lower Mannville Group was deposited over a broad unconformity surface cut by big valley systems (Figure 7). In the eastern part of the basin, northward flowing rivers occupied a network of incised valley systems, including the Spirit River and Edmonton valleys in Alberta and the Assiniboia Valley in Saskatchewan. These rivers drained the remainder of the foreland basin and discharged into the northern sea. The Ellerslie Member, which is an injection target within the Lower Mannville, and its equivalents (Basal Quartz), were accumulated within these valleys, whereas the intervening highlands remained emergent (Figure 7). The sandstones in the western part of the basin throughout the Mannville interval are rich in quartz and chert and poor in igneous detritus, suggesting that they derived from older, upthrust sedimentary rocks in the Cordilleran source area or more distant source areas. In the southern part of the basin, the Mannville Group forms at the basin-scale a single sandstone-dominated aquifer, while in the central-to-northern part, the Lower and Upper Mannville aquifers are separated by the intervening shale-dominated Clearwater aquitard (Figure 4). At a local scale, the lithology and, therefore, the hydrostratigraphy of the Mannville Group are much more complex, with lateral and vertical discontinuities caused by siliciclastic deposition in a fluvio-deltaic environment. The stratigraphy of the Mannville Group is described in more detail in the subsequent regional geology chapter.

The overlying Colorado Group was deposited during a lull in tectonic plate convergence when the basin was subject to a widespread marine transgression. Colorado strata consist predominantly of thick shales that form aquitards, within which there are isolated, thin, sandy units that form aquifers. Some of the sandstones, like the Viking and Cardium formations, are laterally extensive. Others are more restricted areally, like the Second White Speckled Sandstone, which is present only in the southern part of the Alberta Basin.

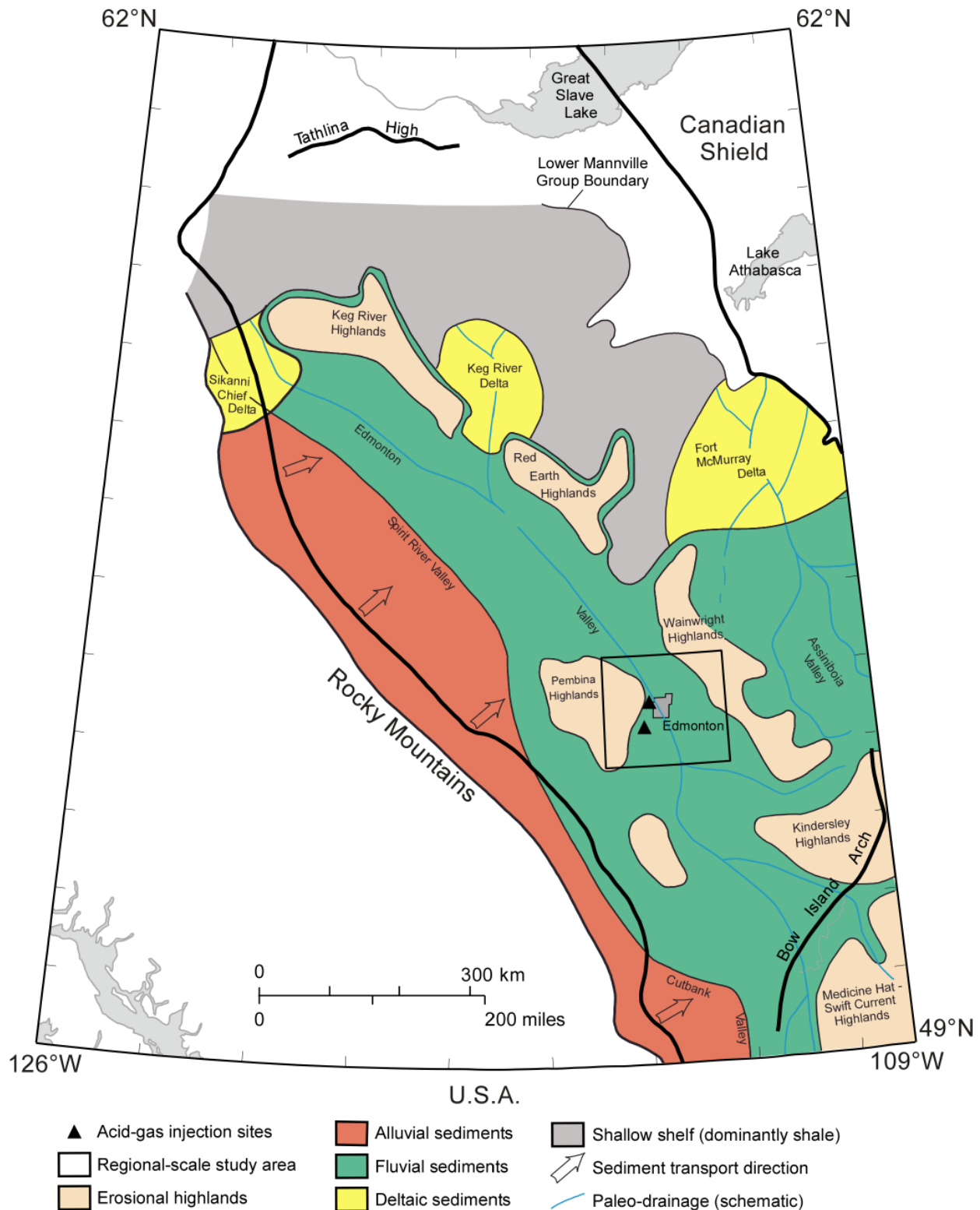


Figure 7. Paleogeography of the Alberta Basin during Cretaceous Lower Mannville time (after Smith, 1994). The location of the Strathfield and Acheson acid-gas injection sites is also shown.

Post-Colorado Cretaceous and Tertiary strata were deposited during the Laramide orogeny and the subsequent period of tectonic relaxation, and consist of eastward-thinning nonmarine clastic wedges intercalated with argillaceous sediments. This cyclicity is developed best in the southern and southwestern parts of the basin, where the Milk River, Belly River, Horseshoe Canyon and Scollard-Paskapoo formations form the clastic wedges, and the Lea Park, Bearpaw, Whitemud and Battle formations comprise the intervening shales. In the central and northern parts of the basin many of these cycles are absent due to either non-deposition or erosion. The clastic wedges form aquifers, while the intervening shales form aquitards. A variety of pre-glacial, glacial and post-glacial surficial deposits of Quaternary age overlie the bedrock over the entire basin.

3.2 Basin-Scale Flow of Formation Water

The flow of formation water in the Alberta Basin is quite well understood at the basin-scale as a result of work performed over the last three decades by various researchers, starting with the pioneering work of Hitchon (1969a, b) and ending with a comprehensive summary and synthesis of previous work by Bachu (1999). Publications since then (i.e., Anfort et al., 2001; Michael & Bachu, 2001, 2002; Michael et al., 2003; and Bachu & Michael, 2003) confirm and detail the broad understanding of the flow of formation water in the basin. The flow in the deformed part of the basin (the Rocky Mountains and the thrust and fold belt) seems to be driven by topography in local-scale systems. Recharge takes place at the surface throughout the entire system, with discharge as springs, in lakes and along river valleys. In most cases, fresh groundwater of meteoric origin discharges along various faults and thrust sheets, such as the Brazeau, Burnt Timber and McConnell, that separate the flow systems in the Rocky Mountain thrust and fold belt from the flow systems in the undisturbed part of the basin (Wilkinson, 1995; Grasby & Hutcheon, 2001). The flow in the undeformed part of the Alberta Basin (from the eastern edge of the deformation front in the southwest to the edge of the exposed Precambrian Shield in the northeast) (Figure 8) is extremely complex due to basin evolution, geology, lithology and hydrostratigraphy.

Topography-Driven Flow

The flow of formation water is driven by topography in local, intermediate, regional and basin-scale systems, from regions of recharge at high elevations to regions of discharge at low elevations. A basin-scale flow system in the southern and central parts of the basin is recharged with fresh meteoric water in the south where Devonian, Carboniferous and Cretaceous aquifers crop out at high elevation in Montana. Water flows northward and discharges at outcrop of the Grosmont aquifer along the Peace River (Figure 8). The aquifers in this flow system are the Upper Devonian and Carboniferous-Jurassic in the region of respective subcrop at the sub-Cretaceous unconformity, the Grosmont, and the Lower Mannville. They all are in hydraulic contact in southeastern and central Alberta due to the absence of intervening aquitards as a result of pre-Cretaceous erosion (Figures 4 and 8). In this basin-scale flow system, low hydraulic heads corresponding to discharge areas propagate far upstream, inducing widespread sub-hydrostatic pressures, as a result of high aquifer permeability downstream (Anfort et al., 2001).

An intermediate-scale flow system driven by topography is present in the Athabasca region, where meteoric water recharges at relatively high elevations in the Birch and Pelican mountains, penetrates down to the Slave Point (Beaverhill Lake Group) aquifer and discharges at low-elevation outcrop along the Athabasca, Peace and Hay rivers (Bachu & Underschultz, 1993; Bachu, 1999). All aquifers and aquitards in the Upper Devonian to Jurassic succession are absent in this area due to pre-Cretaceous erosion (Figures 4 and 8). The Slave Point and Winnipegosis aquifers in northeastern Alberta are in an intermediate position between regional-scale flow in the western part of the basin, and local-scale flow systems close to the basin's eastern edge (Hitchon et al., 1990; Bachu & Underschultz, 1993).

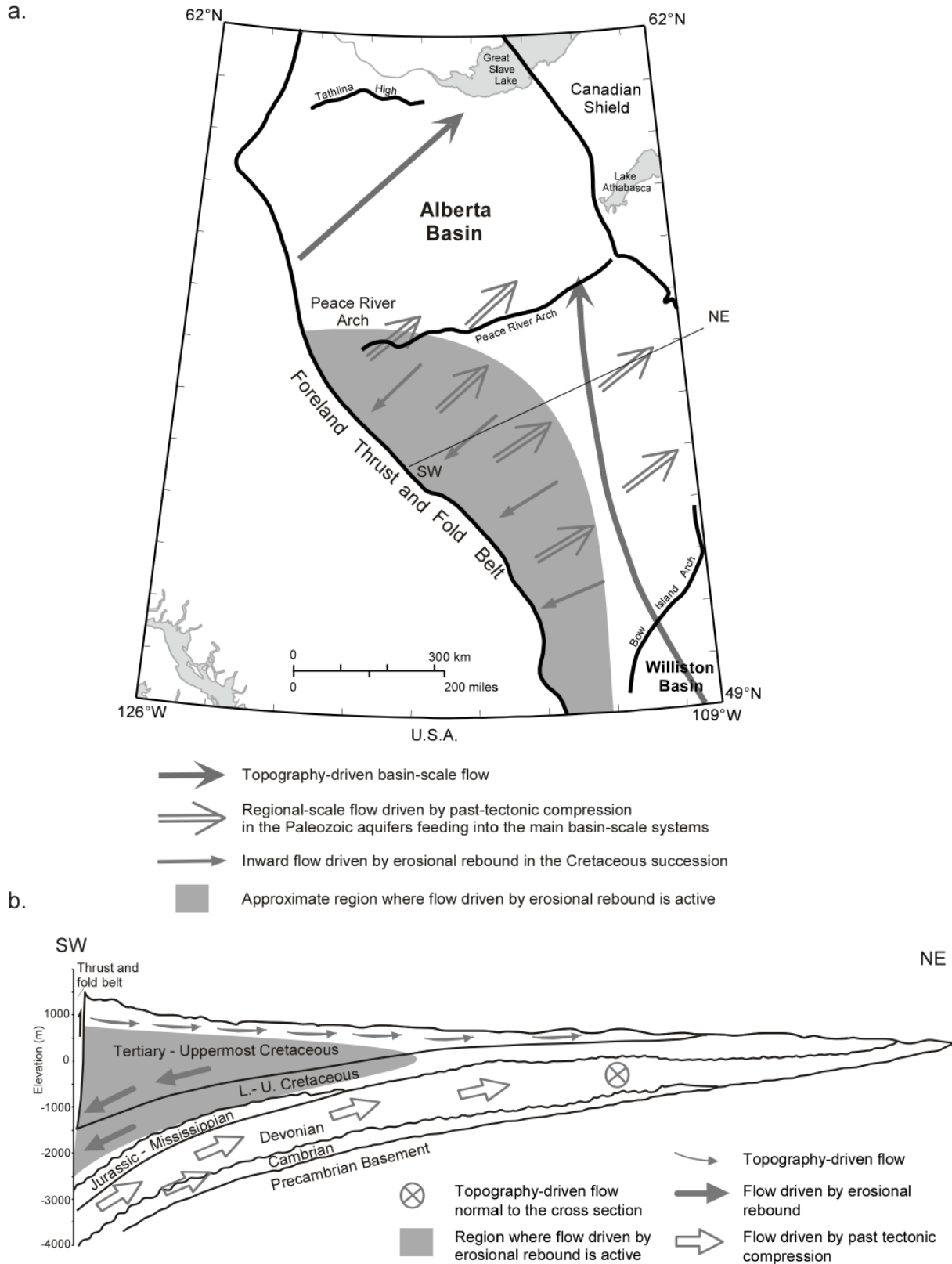


Figure 8. Diagrammatic representation of flow systems in the Alberta Basin: a) in plan view, and b) in cross-section (after Bachu, 1999).

Local-scale flow systems are present throughout the entire basin in the shallower strata. Fresh meteoric water is driven from local topographic highs, such as Swan Hills, Cypress Hills and Pelican Mountains, to the nearest topographic lows, usually a river valley. Such local flow systems were identified in the Upper Cretaceous-Tertiary strata in the south, southwest and west (Toth & Corbet, 1986; Michael & Bachu, 2001; Bachu & Michael, 2003), and in the Red Earth and Athabasca regions (Toth, 1978; Bachu & Undershultz, 1993).

Flow Driven by Erosional and/or Post-Glacial Rebound

During sediment loading, water flows vertically in compacting sand-shale successions, out of overpressured shaly aquitards into the adjacent sandstone aquifers (expulsion), then laterally in the sandstones, outward toward the basin edges. Directions of water movement are reversed during erosional unloading, with transient effects lasting for long periods of time in rocks characterized by very low hydraulic diffusivity. Significant underpressuring in shales drives the flow of formation waters in the intervening aquifers laterally inward from the permeable basin edges, and vertically into the rebounding shaly aquitards (“suction”). This type of flow is present at both local and large scales in the southern and southwestern part of the Alberta Basin in the siliciclastic Mannville, Viking, Second White Speckled Sandstone, Belly River and Horseshoe Canyon aquifers in the Cretaceous succession (Figures 4 and 8) (Toth & Corbet, 1986; Parks & Toth, 1993; Bachu & Undershultz, 1995; Anfort et al., 2001; Michael & Bachu, 2001). The flow is driven by erosional and post-glacial rebound in the thick intervening shales of the Colorado Group, and Lea Park, Bearpaw and Battle formations, as a result of up to 3800 m of sediments having been eroded in the area since the peak of the Laramide orogeny some 60 MyBP (Nurkowski, 1984; Bustin, 1991) and since the retreat of 2 km thick Laurentide ice sheets since the Pleistocene. The flow in these Cretaceous aquifers is in a transient state, driven inward from the aquifers' eastern boundary to the west-southwest, downdip toward the thrust and fold belt. The aquifers are severely underpressured in places, with corresponding hydraulic heads being less than 200 m close to the thrust and fold belt (Bachu et al., 2002; Bachu & Michael, 2003). These hydraulic heads are lower than the lowest topographic elevation in the basin at Great Slave Lake more than 1500 km away in the northeast.

Tectonic Compression

Unlike compaction and erosion, which create vertical stresses in the fluid-saturated sedimentary succession, tectonic compression during orogenic events creates lateral stresses and pressure pulses that lead to water expulsion from the overridden and thrusted rocks into the foreland basin. These pressure pulses dissipate over several million years, depending on the hydraulic diffusivity of the sedimentary succession (Deming and Nunn, 1991). In the deep part of the Alberta Basin in the southwest, the flow of formation waters in the Devonian and Mississippian-Jurassic aquifer systems is northeastward updip until it reaches the sub-Cretaceous unconformity, where it joins the northward basin-scale gravity-driven flow system (Figure 8) (Hitchon et al., 1990; Bachu & Undershultz, 1993, 1995; Rostron & Toth, 1997; Anfort et al., 2001). In the deeper Basal Cambrian and Winnipegosis aquifers the flow of formation waters is also northeastward updip to their respective northeastern boundary (Hitchon et al., 1990; Bachu & Undershultz, 1993). The salinity of formation waters in these aquifers generally increases southwestward downdip. (Hitchon et al., 1990; Bachu & Undershultz, 1993, 1995; Rostron & Toth, 1997; Anfort et al., 2001; Michael & Bachu, 2001, 2002; Michael et al., 2003). Up to their respective eastern erosional or depositional boundary, all of these aquifers are separated by intervening strong aquitards or aquiclude. Direct freshwater meteoric recharge from the surface of these aquifers in either the deformed or the undeformed parts of the basin in the southwest is not possible or is very unlikely for a variety of reasons (Bachu, 1999; Michael & Bachu, 2001, 2002; Bachu et al., 2002; Michael et al., 2003). Based on

the high salinity of formation waters in the deep Paleozoic aquifers in the southwestern part of the basin, and because of the lack of an identified recharge source and mechanism, Bachu (1995) postulated that the flow in these aquifers is driven by past tectonic compression (Figure 8). This hypothesis is supported by isotopic analyses of formation waters and late-stage cements in both the deformed and undeformed parts of the basin (Nesbitt & Muehlenbachs, 1993; Machel et al., 1996; Buschkuehle & Machel, 2002).

Hydrocarbon Generation

During the process of hydrocarbon generation, the phase change of solid kerogen that fills the pore space into fluid hydrocarbons leads to volumetric expansion and generation of internal stresses that create overpressures capable of driving flow. However, the overpressures caused by active hydrocarbon generation can be maintained only if the respective reservoirs are well sealed by very low permeability rocks. Overpressured reservoirs are present in Cretaceous strata in the deep parts of the Alberta Basin (e.g., Masters, 1984). Most of the overpressuring attributed to hydrocarbon generation occurs in the southwest, in the deep basin near the thrust and fold belt in the Cretaceous Mannville, Viking and Cardium strata associated with low-permeability (tight) rocks and seals (Bachu & Underschultz, 1995; Anfort et al., 2001; Michael & Bachu, 2001). The high pressures are caused by present-day or recent (last few million years) hydrocarbon generation in strata that still contain organic matter capable of yielding thermally generated hydrocarbons, but which have very low permeability that impedes pressure dissipation. The rock succession in the Cretaceous deep basin is generally gas or oil saturated, and discrete hydrocarbon-water contacts generally are not present. In the absence of contact between the overpressured reservoirs and formation water in aquifers, hydrocarbon generation is not an effective flow-driving mechanism.

Buoyancy

The flow of formation water is driven in the gravitational field by hydraulic gradients and by density differences (buoyancy). Generally, Paleozoic waters are more saline than Mesozoic waters (Hitchon, 1969a, b; Bachu, 1999; Anfort et al., 2001; Michael & Bachu, 2001, 2002; Michael et al., 2003). The increase in salinity is mild in Cretaceous strata, rather abrupt at the sub-Cretaceous unconformity, and steep in Paleozoic strata, particularly in the vicinity of evaporitic beds (Bachu, 1999). In southern Alberta, water salinity in Upper Devonian and Carboniferous aquifers is lower than in the central and northern parts of the basin and comparable with water salinity in Mesozoic aquifers, as a result of meteoric water recharge at outcrop in Montana (Anfort et al., 2001). The existence of high-salinity connate waters in the Paleozoic strata shows that the basin has not been flushed yet of the original waters existing in the basin at the time of deposition. Thus, buoyancy, rather than generating or enhancing the flow of formation waters in the Alberta Basin, retards it, to the point of stagnation or sluggishness in some places. A zone of mixing between high-salinity Paleozoic connate waters and freshwater of meteoric origin is present in the Lower Mannville aquifer in the south-central part of the basin, in the region where Devonian aquifers subcrop at the sub-Cretaceous unconformity (Bachu, 1995; Rostron & Toth, 1997; Anfort et al., 2001).

Cross-Formational Flow

Generally there is little cross-formational flow in the Alberta Basin because of its “layer-cake” structure, where strong aquitards and aquiclude separate the major aquifers and aquifer systems in the sedimentary succession. Cross-formational flow takes place over large areas only where aquitards are weak. Such cases are the Clearwater and Watt Mountain aquitards in the northeast in the Athabasca area (Bachu & Underschultz, 1993), and the Calmar aquitard in the Upper Devonian aquifer system (Rostron & Toth,

1997; Anfort et al., 2001). Localized, direct cross-formational “pipe” flow between aquifers takes place across Devonian aquitards and aquiclude only in places where Winnipegosis and Leduc reefs breach through the intervening shaly aquitards. Such “pipes” were identified between the carbonate platforms of the Woodbend Group and the Winterburn Group in the Cheddarville and Bashaw areas, and along the Rimley-Meadowbrook reef trend (Bachu & Underschultz, 1993; Wilkinson, 1995; Rostron & Toth, 1996, 1997; Anfort et al., 2001). Reefs of the Leduc Formation create a path for direct hydraulic communication across the Ireton aquitard between the underlying and overlying Cooking Lake-Leduc and Upper Devonian aquifer systems. Otherwise, mixing of formation waters from different aquifers, and consequently of fresh meteoric and connate waters, takes place at the sub-Cretaceous unconformity in the area where various Devonian-to-Carboniferous strata subcrop (Figure 4) (Hitchon et al., 1990; Bachu & Underschultz, 1993, 1995; Rostron & Toth, 1997; Anfort et al., 2001).

4 Regional-Scale Setting of the Edmonton Cluster of Acid-Gas Injection Sites

To better understand the geology, hydrogeology, formation water flow at the acid-gas injection sites in the Edmonton area, and the containment of the injected acid gas, a regional-scale study area was defined between 52.8°N 112.15°W and 54.2°N 114.75°W (approximately T59 R5W5 to T46 R17W4) (Figure 9). The following description is subdivided into the two major stratigraphic packages that correspond to the two main injection intervals: the Devonian Beaverhill Lake and Woodbend groups, and the Cretaceous Mannville Group (Figure 10). The stratigraphic and structural relationships between various injection units are shown along an updip cross-section in Figure 11.

4.1 Geology of the Beaverhill Lake to Lower Mannville Groups

The Devonian carbonates of the Beaverhill Lake Group and of the overlying Cooking Lake and Leduc formations of the Woodbend Group constitute the main Paleozoic acid-gas injection interval in the Edmonton area.

4.1.1 Devonian Beaverhill Lake Group

The regional-scale study area is located within the Waterways Basin (Figure 5), which, during the Middle to Early Upper Devonian was the site of deposition of deeper water carbonates and calcareous shales of the Waterways Formation. These argillaceous carbonates and calcareous shales generally exhibit low porosity and permeability. However, isolated carbonate horizons, similar in facies to the Swan Hills reefs to the northwest (Figure 5), occur within the upper part of the Waterways Formation in the regional-scale study area (Figure 11). These isolated carbonate horizons have sufficient porosity and permeability to allow injection, as is the case at the Golden Spike injection site. The surrounding and overlying argillaceous limestones and shales are sealing these build-ups laterally and vertically, preventing outflow.

The depth to the top of the Beaverhill Lake Group in the regional-scale study area ranges between more than 2600 m in the southwest close to the deformation front, to less than 1100 m in the northeast (Figure 12a). The Beaverhill Lake Group succession has an average thickness of 200 m in most of the area. The top surface of the Beaverhill Lake Group dips southwestward from elevations of -500 m in the northeast to -1900 m in the southwest with a slope of about 10 m/km in the northeast and 12 m/km near the deformation front (Figure 12b).

Within the regional-scale study area, the Beaverhill Lake Group is conformably overlain by Cooking Lake shelf platform carbonates and equivalent basinal shales (Majeau Lake Member) of the Cooking

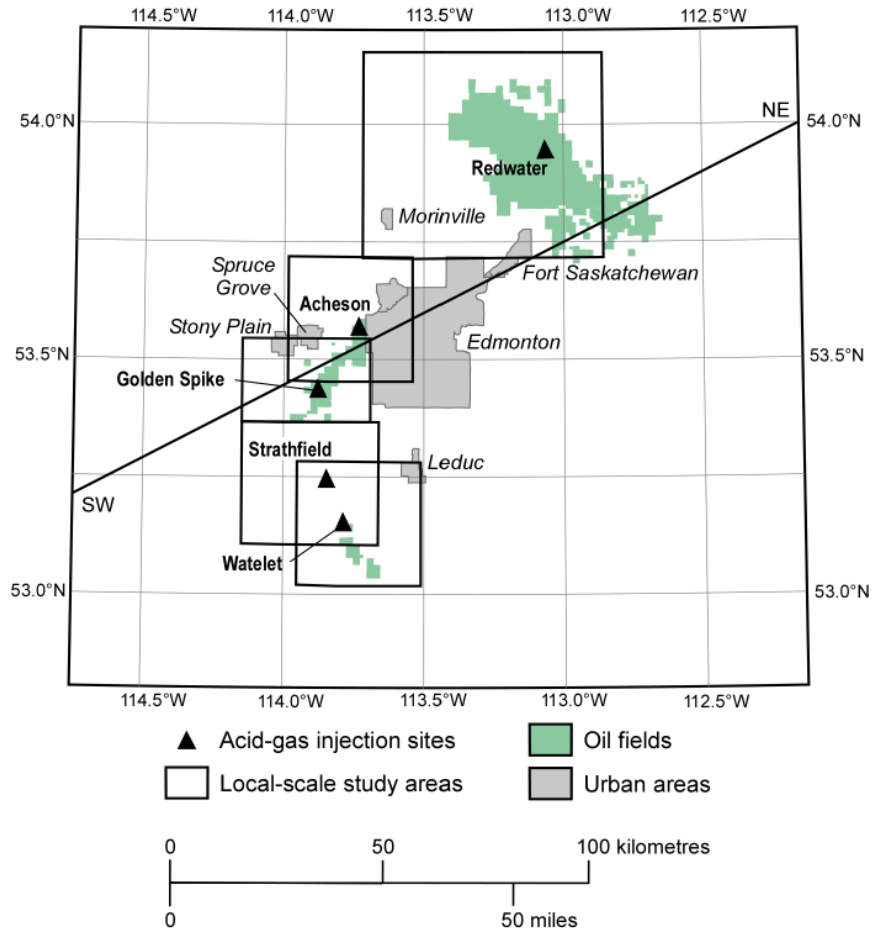


Figure 9. Location of acid-gas injection sites, major oil fields, and local-scale study areas in the Edmonton regional-scale study area. Line of cross-section refers to Figure 11.

Lake Formation (Woodbend Group; see below) (Figure 10). However, the Beaverhill Lake Group in the Golden Spike injection area is directly overlain by a Leduc Formation reef, which itself is a porous carbonate build-up. The Beaverhill Lake Group is underlain by shales and siltstones of the Watt Mountain Formation (Elk Point Group).

4.1.2 Devonian Woodbend Group

The Upper Devonian Woodbend Group consists of shallow-water carbonates of the Cooking Lake, Leduc and Grosmont formations, as well as deeper-water carbonates and shales of the Majeau Lake Member (Cooking Lake Formation), and Duvernay and Ireton formations (Figure 10).

The shallow-water shelf carbonates of the Cooking Lake Formation are present in the eastern part of the regional-scale study area (Figure 13), and, except for a dolomitized area along the north/south-trending shelf platform edge, consist predominantly of limestone. West of the platform edge, a transition to basinal shales of the time-equivalent Majeau Lake Member occurs. Various lithologies, including grayish brown nodular mudstones (with scattered crinoids and brachiopods), light to medium brown mudstones and wackestones with gastropods and ostracodes - some with stromatolitic laminations, non-skeletal grainstones with pellets, intraclasts and coated grains, and light to medium brown stromatoporoid rudstones and floatstones occur across the platform resulting in a high variability in porosity and

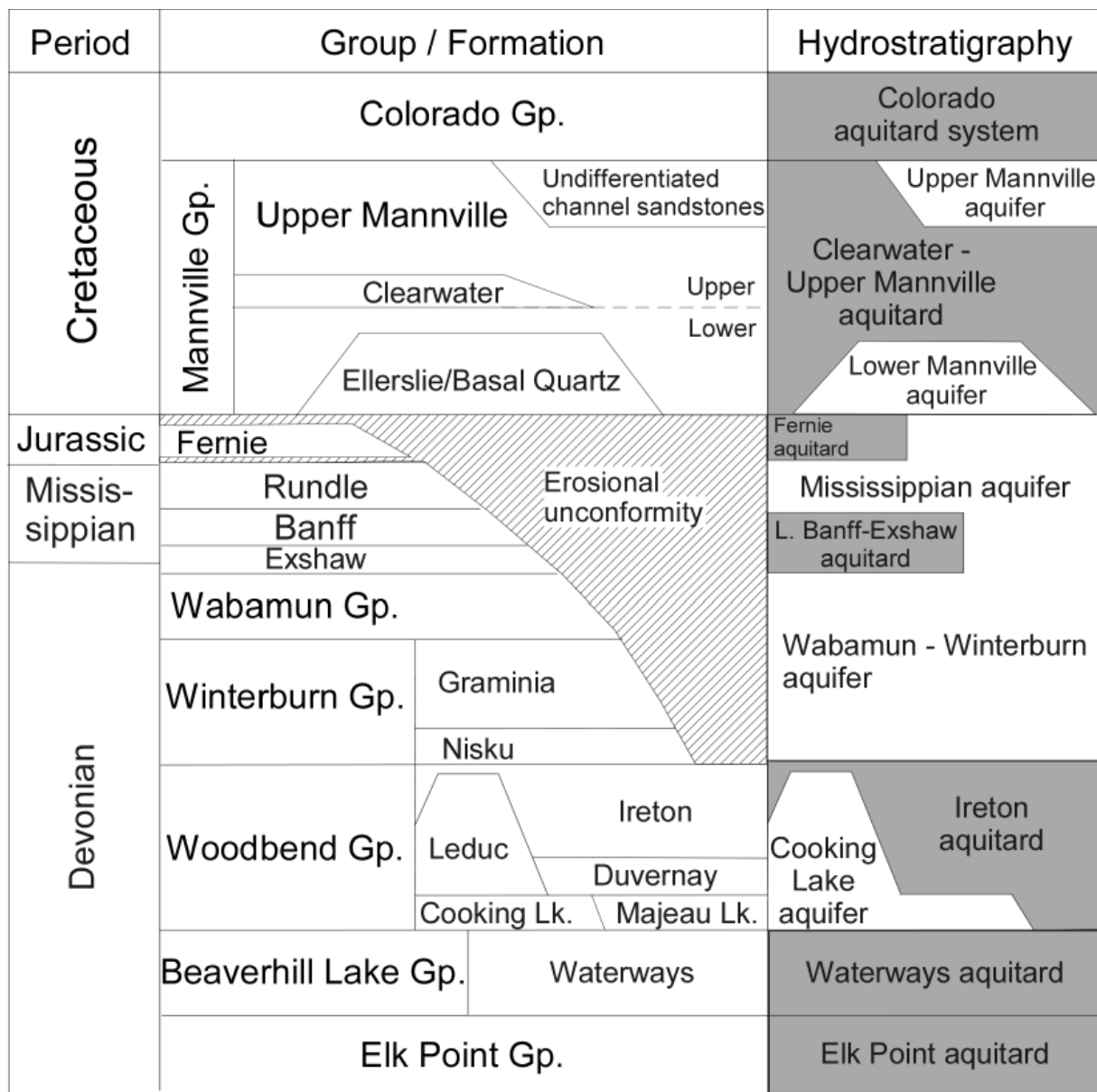


Figure 10. Stratigraphic and hydrostratigraphic delineation and nomenclature for the strata in the Beaverhill Lake - Mannville sedimentary succession in the Edmonton regional-scale study area.

Aquifer Aquitard

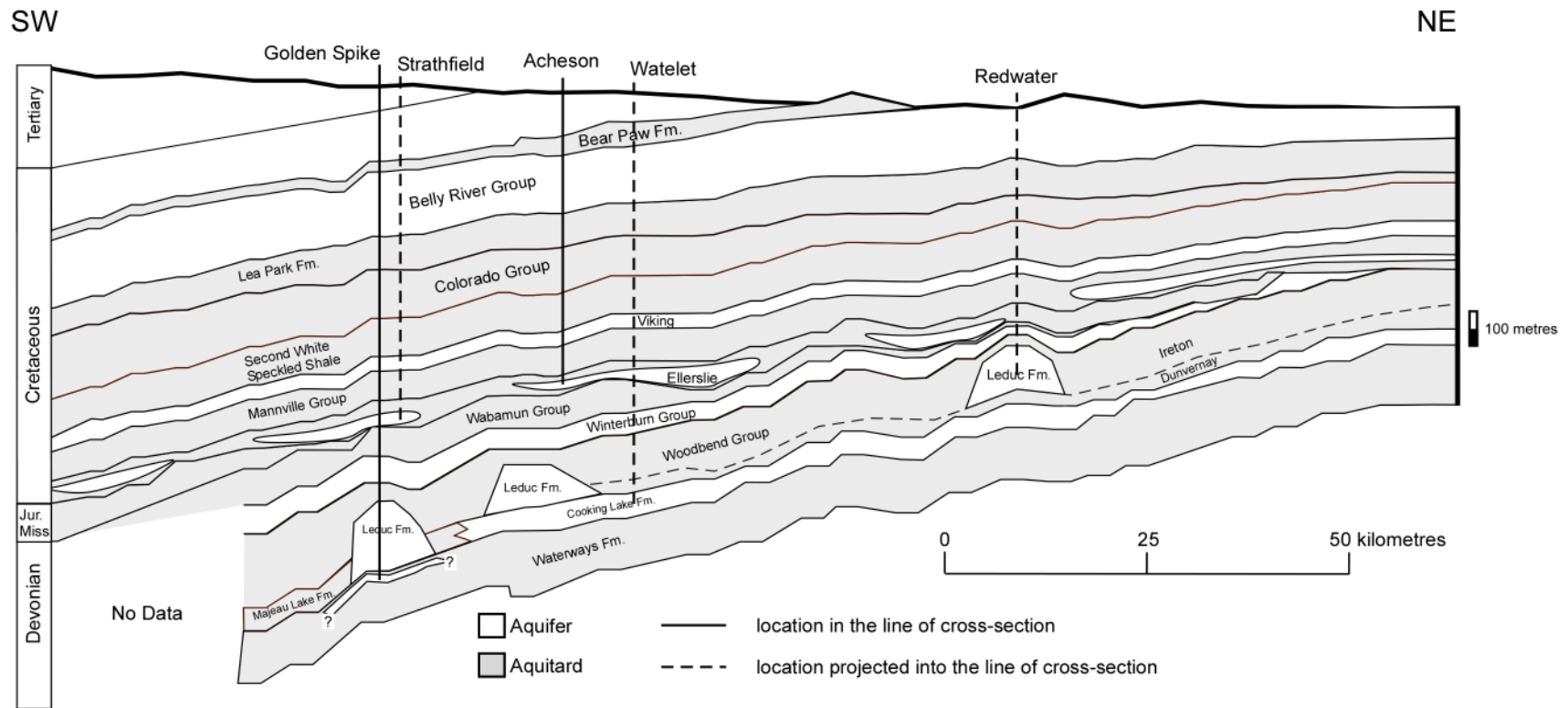


Figure 11. Dip cross-section through the Beaverhill Lake - Mannville sedimentary succession in the Edmonton regional-scale study area showing the position of the acid-gas injection sites. See Figure 9 for the location of the line of cross-section.

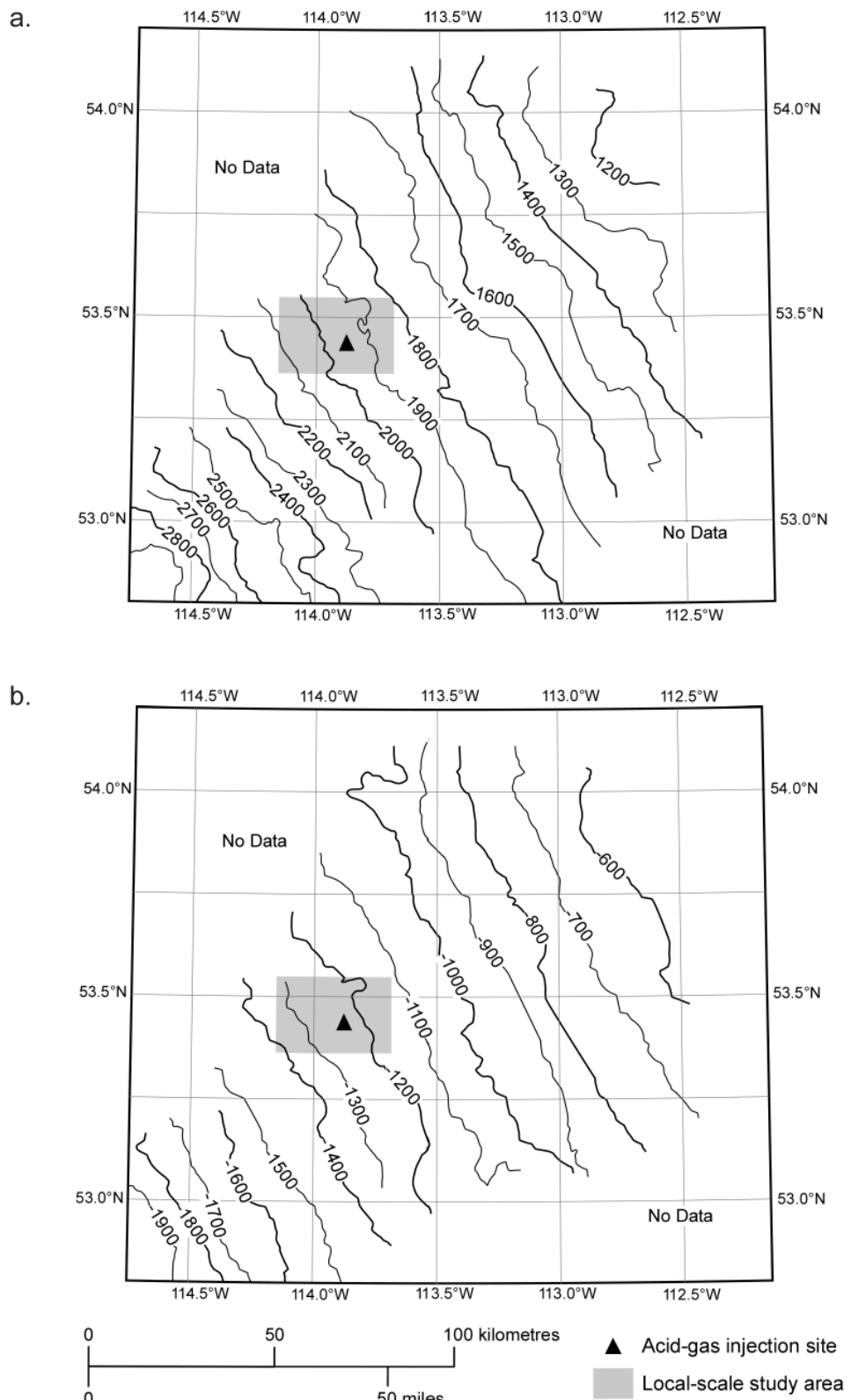


Figure 12. Main geological features of the Beaverhill Lake Group in the regional-scale study area: a) depth to top, and b) top structure elevation. The location of the Golden Spike acid-gas injection site and local-scale study area is also shown. Contours in metres.

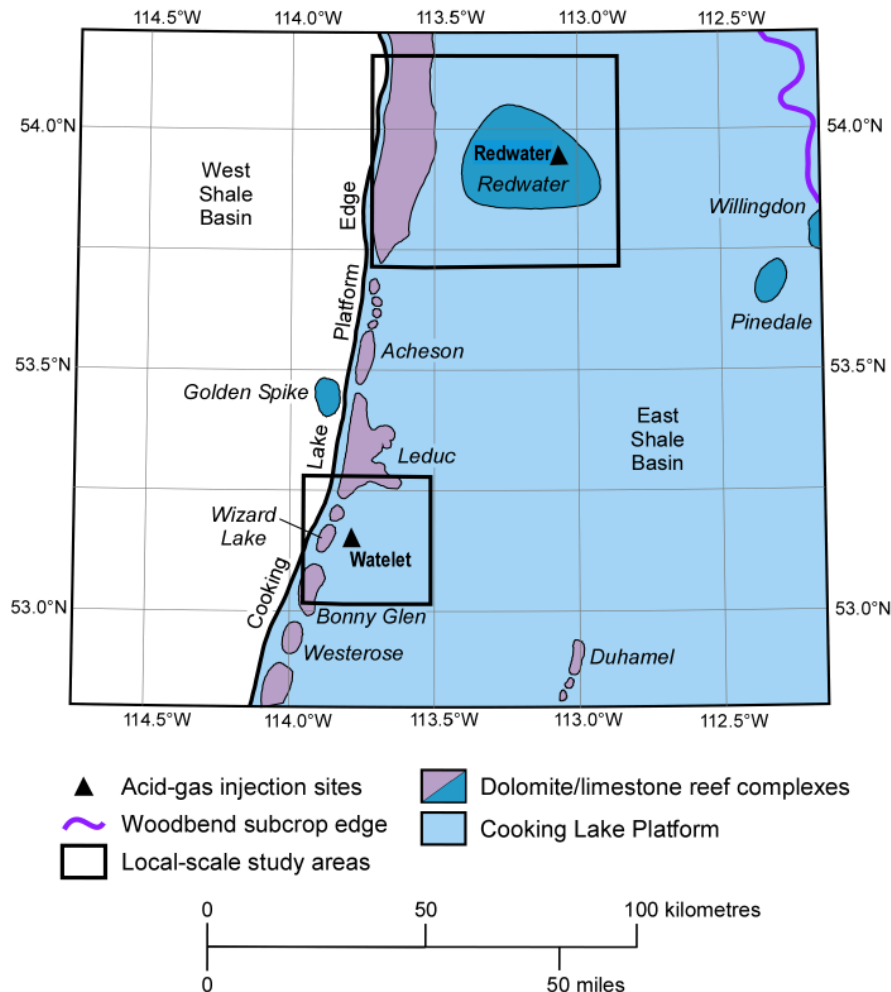


Figure 13. Location of the western boundary of the Cooking Lake Formation carbonate platform and of Leduc Formation reefs in the regional-scale study area.

permeability. Areas where stromatoporoid-bearing platform carbonates of the Cooking Lake Formation attain their greatest thickness (predominantly, but not exclusively, along the platform edge) often coincide with the location of overlying reefs of the Leduc Formation.

The depth to the top of the Cooking Lake Formation in the regional-scale study area ranges between more than 2600 m in the southwest closer to the deformation front to less than 1100 m in the northeast (Figure 14a). The top of the Cooking Lake Formation dips southwestward with a slope of about 10 m/km in the northeast and 12 m/km near the deformation front, from above-400 m in the northeast to -1600 m in the southwest (Figure 14b). The average thickness of the Cooking Lake Formation is about 80 m, however, in places where it is directly overlain by reefal carbonates of the overlying Leduc Formation, its thickness is difficult to determine.

The lithology of the Leduc Formation is highly variable as a result of facies variations inherent to shallow-water reef systems (see also Whalen et al., 2000) and of post-sedimentary (diagenetic) processes, such as dolomitization. Most of the reefs in the regional-scale study area are pervasively dolomitized, and the original facies patterns are largely destroyed. Although the reefs are commonly dolomitized, some undolomitized occurrences are known (Golden Spike, Redwater, Willingdon and Pinedale reef complexes and the uppermost part of the Duhamel reef). The reefs may reach thicknesses of up to 250 m. Leduc

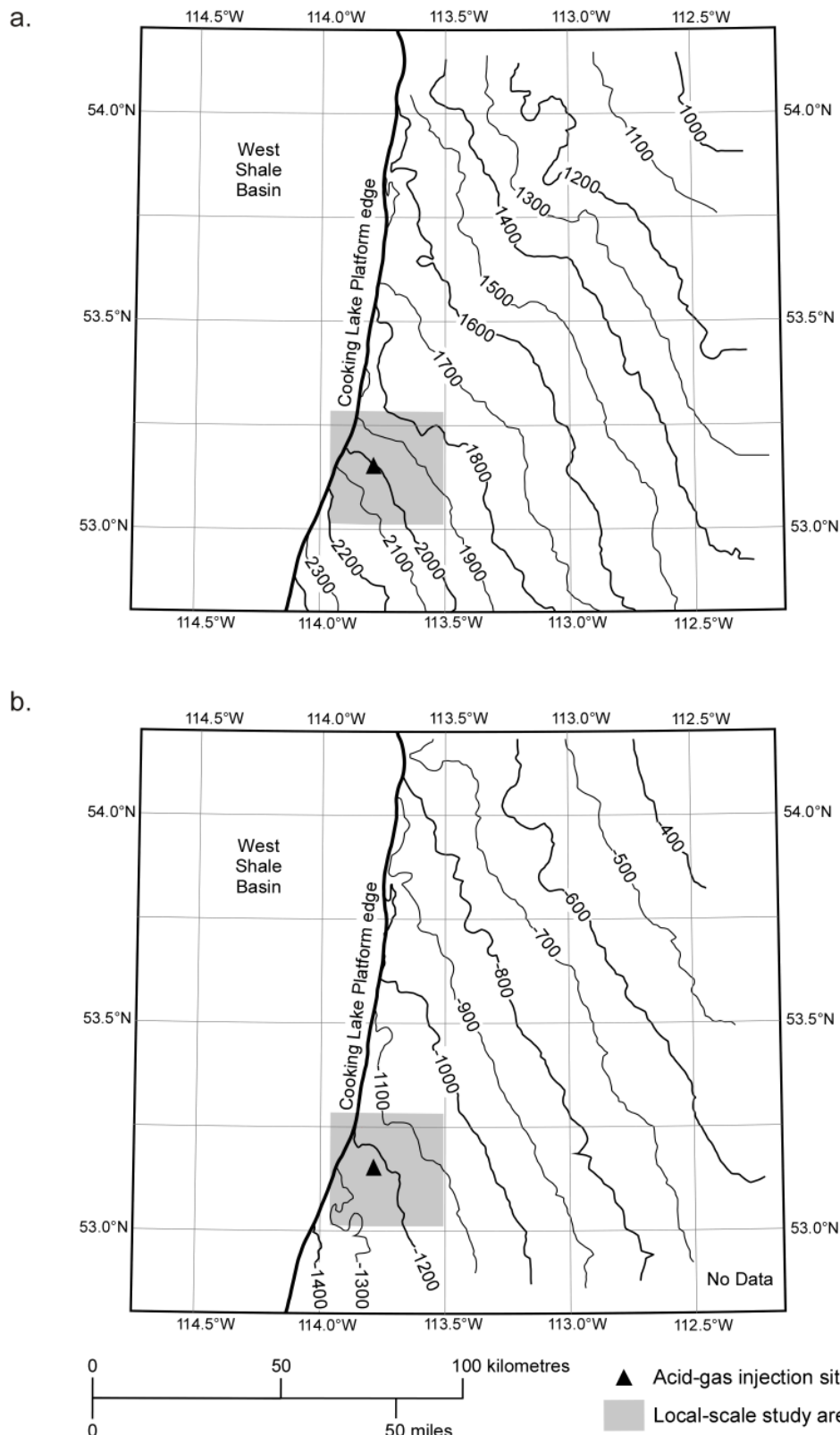


Figure 14. Main geological features of the Cooking Lake Formation in the regional-scale study area: a)depth to top, and b) top structure elevation. The location of the Watelet acid-gas injection site and local-scale study area is also shown. Contours in metres.

reef growth within the regional-scale study area preferentially took place along the shelf-platform edge of the underlying Cooking Lake Formation, resulting in a chain of reefs that is commonly known as the Rimbev-Meadowbrook Reef Trend (Figure 13). Areas of deeper-water conditions to the west and east of this reef trend were the site of deposition of basinal limestones and shales of the Duvernay and Ireton formations and have been aptly named the West Shale Basin and East Shale Basin, respectively (Figure 13).

Contemporaneous with the early phases of Leduc reef development, interbedded dark brown, organic-rich shales, dark brown calcareous shales and dense argillaceous limestones of the Duvernay Formation (Imperial Oil, 1950) were deposited in the basinal areas surrounding the reefs. Within the regional-scale study area the thickness of the Duvernay Formation decreases from about 70 m in the northeastern part to about 30 m in the west.

The Duvernay Formation is overlain by calcareous shales and argillaceous carbonates of the Ireton Formation. In the East Shale Basin the unit has an average thickness of 150 m, thickening westwards as the underlying Duvernay Formation thins. In the West Shale Basin it thickens to over 250 m in the southwestern part of the regional-scale study area. The Ireton Formation thins to about 3 m on top of the reefal carbonates of the Leduc Formation.

The depth to the top of the Leduc Formation in the regional-scale study area ranges between more than 2400 m in the southwest closer to the deformation front to less than 1100 m in the northeast. The top of the Woodbend Group (Ireton Formation) dips southwestward with a slope of about 10 m/km, from above-300m in the northeast to -1700 m in the southwest.

The Woodbend Group conformably overlies the calcareous shales and argillaceous limestones of the Beaverhill Lake Group (Waterways Formation). The Woodbend Group is conformably overlain by carbonates of the Winterburn Group (Switzer et al., 1994).

4.1.3 Cretaceous Mannville Group

Sandstones of the Cretaceous Mannville Group are the second acid-gas injection interval in the Edmonton area. The Mannville Group was deposited over a broad unconformity surface that truncates strata ranging from lowermost Cretaceous in the foothills to lower Paleozoic at the eastern margin of the basin. In the regional-scale study area the Mannville sandstones are successively underlain from west to east by Mississippian carbonates and shales of the Banff and Exshaw formations, and Upper Devonian carbonates of the Wabamun and Winterburn Groups, with shales of the Woodbend Group Ireton Formation present in the northeast corner of the study area (Figures 10 and 15). In addition to tectonic factors, differential erosion of dipping Paleozoic carbonates likely influenced the development of relief on the unconformity surface (Hayes et al., 1994).

The Mannville Group is subdivided into Lower and Upper Mannville (Figure 10). The Ellerslie injection interval lies within the Lower Mannville Group and the following description emphasizes its origin and development within the regional-scale study area.

Deposition of the Lower Mannville Group sediments in the regional-scale study area was limited to the Edmonton Valley, which was bordered by the Pembina Highlands to the west and the Wainright Highlands to the east (Figures 7 and 16). Predominantly fluvial sandstones and conglomerates of the Ellerslie Member grade upwards into brackish sandstones, siltstones, shales and limestones of the Ostracod Beds (Cant and Stockmal, 1989). Deltaic and shoreline sandstones of the Glauconitic Sandstone

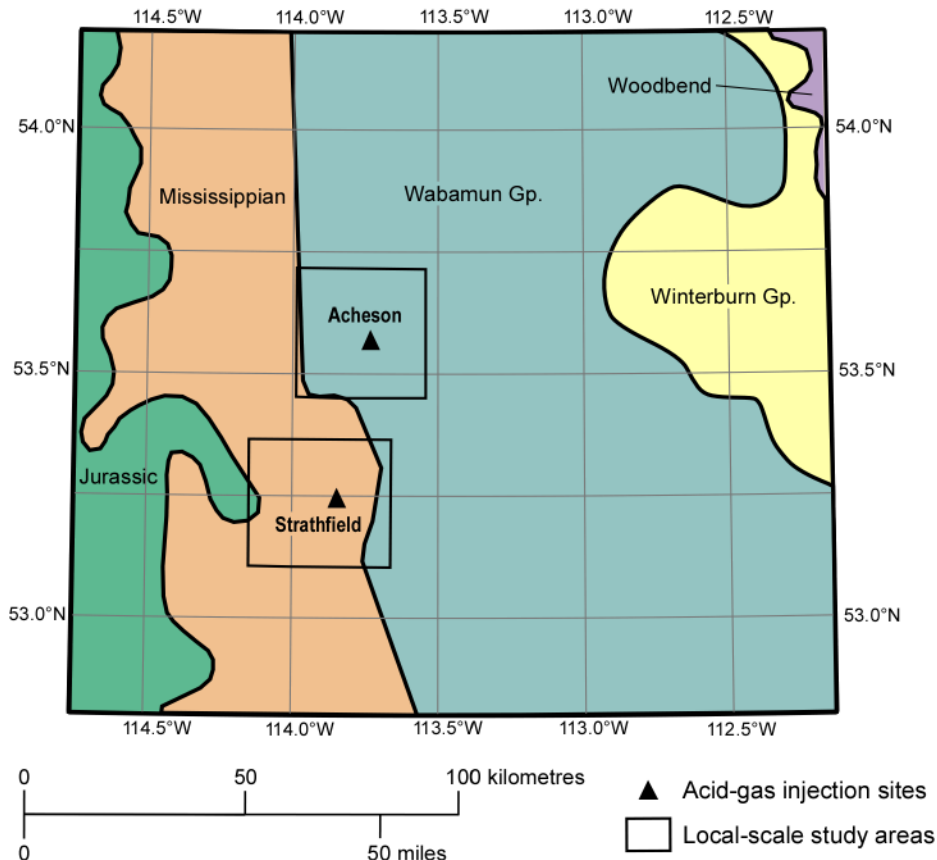


Figure 15. Erosional boundaries of Devonian and Mississippian strata that subcrop underneath Lower Mannville Group sediments in the regional-scale study area.

Formation interfingering with and incising into Clearwater equivalent shales and siltstones define the boundary between the Lower and the Upper Mannville groups. The remainder of Upper Mannville Group strata in the regional-scale study area consists mainly of undifferentiated non-marine to marginal marine sandstone to shale units (Cant and Stockmal, 1989).

The sandstones of the Lower Ellerslie are generally siliceous. The Upper Ellerslie and the overlying Ostracod Beds consist mainly of dark calcareous shales, siltstones and lenticular sandstones coupled in thin coarsening-upward sequences (Hayes et al., 1994). The sandstones are generally siliceous, as in the underlying lower Ellerslie interval. Thin micritic limestone beds and pelecypod/gastropod/ostracod coquinas are widespread and gave the zone its name. The deposition of the Ostracod Beds was linked to the early stages of transgression of the Clearwater Sea from the north. Brackish bays advanced southward along the Spirit River and Edmonton valley systems (Figure 7), but the major highlands still remained emergent. Tides had a significant effect on sedimentation within the brackish bay setting.

The depth to the top of the Ellerslie Member in the regional-study area ranges between more than 1800 m in the southwest to less than 700 m in the northeast (Figure 17a). The average thickness is 70 m in most of the area. The top of the Ellerslie Member dips southwestward from elevations of above-100 m in the northeast to -1000 m in the southwest with a slope of about 7-8 m/km (Figure 17b). The structural dip of the Ostracod Zone is in the same order as the Ellerslie Member, since its general thickness in the regional-scale study area is rarely more than 7 m.

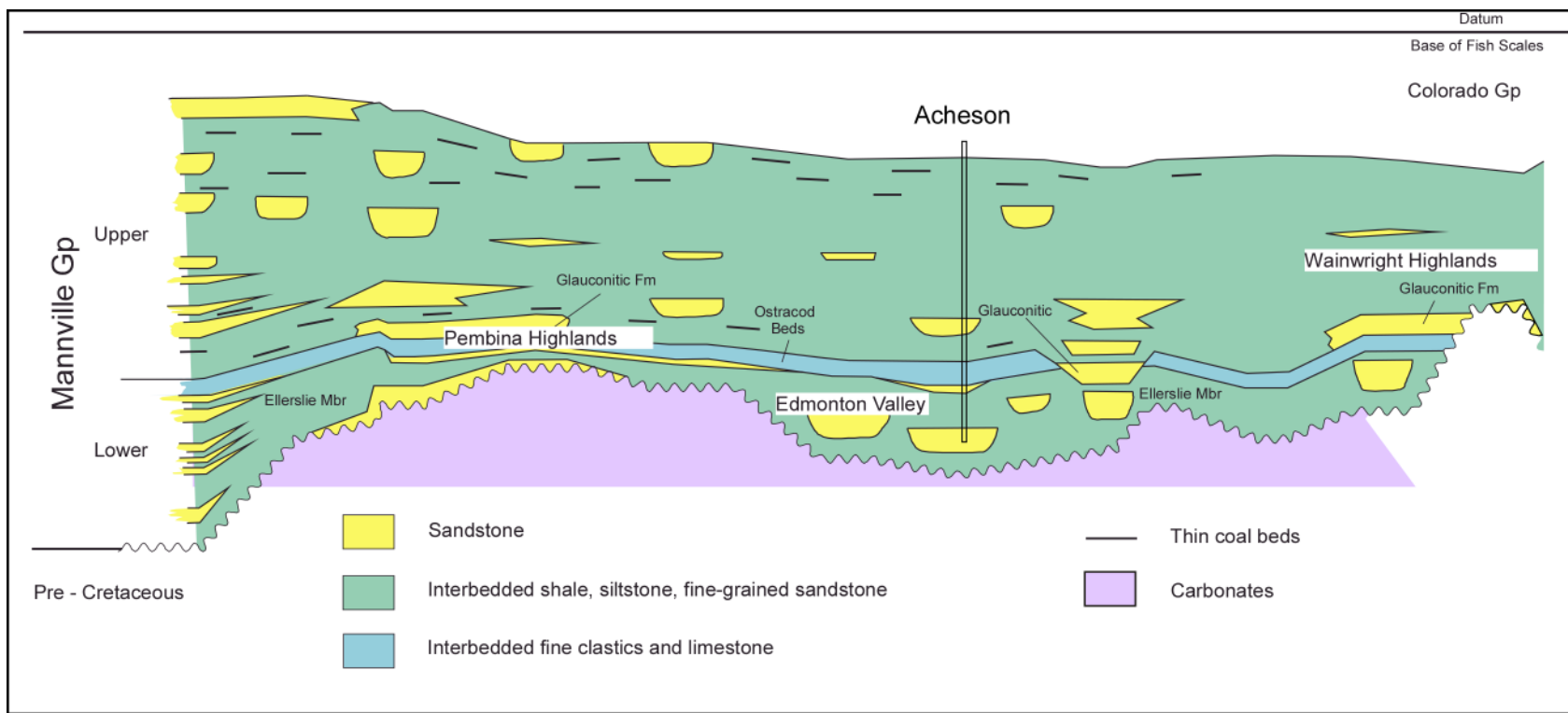


Figure 16. Schematic cross-section through the Edmonton valley showing the distribution of channel sands versus surrounding shales. Acid gas injection takes place into the channel sands of the Ellerslie/Basal Quartz Member in the Edmonton valley, which are surrounded and sealed by shales and siltstones (modified after Hayes et al., 1994).

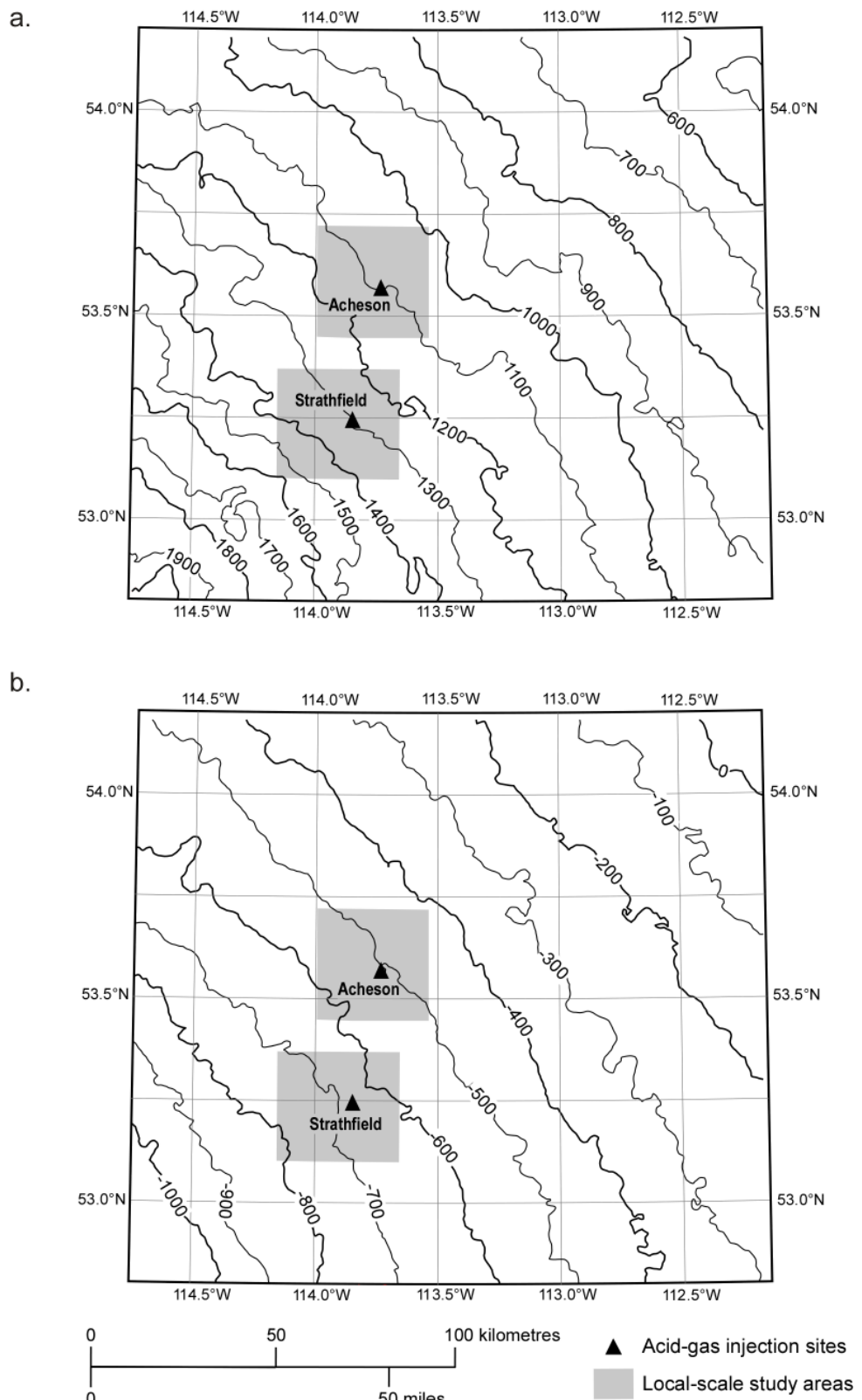


Figure 17. Main geological features of the Ellerslie Member in the regional-scale study area: a) depth to top, and b) top structure elevation. The location of the Acheson and Strathfield acid-gas injection sites and local-scale study areas is also shown. Contours in metres.

The continued, but highly episodic transgression of the Clearwater Sea from the north resulted in the deposition of marine shales of the Clearwater Formation as far south as Edmonton. The shales consist of soft black and greenish grey shales, with some interbedded grey and green sands, as well as ironstone concretions. The Clearwater zero depositional edge runs through the southeastern part of the regional-scale study area, where unnamed Clearwater equivalent shales and siltstones are present.

The generalized lithofacies distribution of the Lower Mannville shows sandstones in the central part of the regional-scale study area (approximately Edmonton Valley), which change laterally to interbedded shales and siltstones (Figure 18a). In contrast, the lithofacies distribution in the Upper Mannville is dominated by shales and siltstones (Figure 18b).

The Mannville Group is unconformably overlain by the thick, shale-dominated Late Cretaceous Colorado Group.

4.2 Hydrogeology of the Beaverhill Lake to Lower Mannville Groups

The Devonian Beaverhill Lake and Woodbend groups, and the Cretaceous Lower Mannville Group are the focus of the regional hydrogeological assessment because these stratigraphic units contain the targets for the five acid-gas injection operations in the Edmonton region. However, a short discussion is included on the hydrogeology of the intervening Devonian Winterburn and Wabamun groups and Mississippian strata, because they lie above the Woodbend Group and successively subcrop underneath the Lower Mannville Group along the sub-Cretaceous unconformity (Figures 10 and 15).

4.2.1 Hydrostratigraphy

The Beaverhill Lake Group in the regional-scale study area is underlain by the Elk Point aquitard system (Bachu, 1999) and consists predominantly of Waterways Formation shales, therefore forming an aquitard system over most of the area (Figure 10). However, some porous and permeable shallow marine carbonate horizons occur within the upper part of the Waterways Formation (Figure 11), e.g. in the Golden Spike area where they are the acid-gas injection target. These carbonates are surrounded and overlain by tight deeper-water limestones, which provide a lateral and vertical permeability barrier. In the western third of the study area, including the Golden Spike region, the shales of the Majeau Lake Member, Duvernay and Ireton formations, all forming the thick Ireton aquitard, directly overlie the Waterways aquitard. The platform carbonates (Cooking Lake Formation) and associated reef complexes (Leduc Formation) of the Woodbend Group that overlie the Waterways Formation in the eastern two thirds of the study area form a regional aquifer (Figure 13). These carbonates are encased in and capped by the shales of the Majeau Lake Member, and Duvernay and Ireton formations, which form a thick aquitard at the top of the Woodbend Group. Exceptions are places where the Ireton shales locally thin above Leduc reefs. In the northeast corner of the regional-scale study area the shales of the Ireton Formation subcrop beneath the Cretaceous Lower Mannville Group. In these cases, direct hydraulic communication is possible between Leduc reefs and the Nisku Formation in the overlying Winterburn Group, and between the carbonate Cooking Lake aquifer and the Lower Mannville sandstone aquifer, respectively. Hydraulic communication between Leduc reefs and the Nisku Formation has been documented in the Bashaw area (Rostrom and Toth, 1997) and in the Cooking Lake area (Bachu and Underschultz, 1995) to the south and to the north of the study area, respectively.

Other intervening regional-scale carbonate aquifers that are in contact with the Lower Mannville aquifer along the unconformity are, from west to east and with increasing stratigraphic age, the Mississippian, Winterburn and Wabamun aquifers (Figures 10, 11 and 15). The sandstones of the Lower Mannville

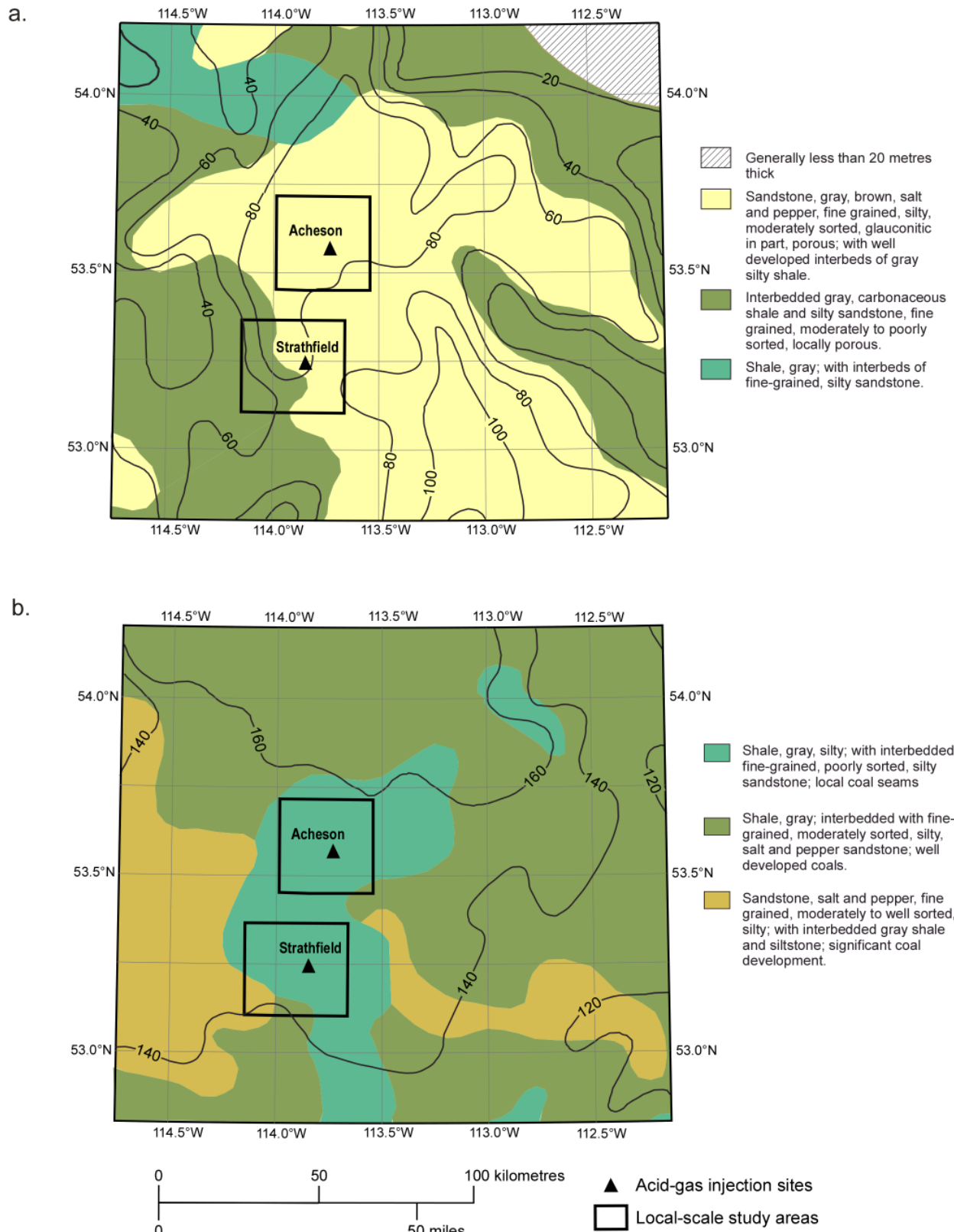


Figure 18. Facies distribution and lithology of Mannville Group strata in the regional-scale study area: a) Lower Mannville, and b) Upper Mannville.

aquifer are restricted largely to the north-south trending Edmonton Valley, which takes up the central part of the regional-scale study area (Figure 18a). These sandstones are encased in and overlain by Lower and Upper Mannville shales and siltstones, which form the Clearwater-Upper Mannville aquitard, and are confined laterally by relatively tighter carbonates of the Wabamun and Winterburn groups (Figure 16). Major sandstone bodies exist in the Upper Mannville Group only in the northeastern and southwestern corners of the study area, while the remainder of the strata, consisting of siltstones and shales (Figure 18b), has aquitard characteristics. A “deep basin” type, dominantly gas-saturated region is present in the downdip portion of the Mannville Group in the southwest corner of the study area. The Mannville Group is overlain by the thick, basin-scale Colorado aquitard system (Bachu, 1999).

4.2.2 Hydrogeological Observations

Hydrochemical analyses of formation waters and drillstem tests were used to interpret the flow of formation waters in the various aquifers in the regional-scale study area. The data used in this study (Table 1) are in the public domain and are available from the Alberta Energy and Utilities Board (EUB). The data were culled for erroneous analyses and tests, including production influence, and processed according to the methods presented by Hitchon and Brulotte (1994), Hitchon (1996) and Michael and Bachu (2002). The formation water density was calculated using regression expressions from measured data in the Alberta Basin and scaling to in-situ conditions after Rowe and Chou (1979) (Adams and Bachu, 2003).

Table 1. Number of chemical analyses of formation water and drillstem test (DST) data that were used in the regional assessment of formation water flow in the Edmonton area, and estimates of formation water density.

	Number of Chemical Analyses	Number of DSTs	Average Density
Beaverhill Lake	7	9	1102 kg/m ³
Woodbend	282	100	
Winterburn	326	140	1081 kg/m ³
Wabamun	157	174	
Mississippian	123	65	1060 kg/m ³
Lower Mannville	528	599	
Upper Mannville	64	162	

Chemistry of Formation Waters

The Devonian formation waters in west-central Alberta are of Na-Cl and Na-Ca-Cl types in the shallow and deep parts, respectively (Spencer, 1987; Adams and Bachu, 2002; Michael et al., 2003). Because of its aquitard-type nature, hydrogeological data are limited in the Beaverhill Lake Group and this group is not discussed on a regional scale. In the regional-scale study area, salinity distributions in the Cooking Lake, Winterburn and Wabamun aquifers are generally very similar, varying between less than 60 g/l in the northeast where the Devonian units subcrop underneath the Mannville Group, and greater than 180 g/l in the southwest (Figures 19a, 19b and 20a). Differences in distribution patterns of salinity are associated with the respective subcrop areas of the Devonian aquifers where they come in contact and mix with Lower Mannville formation waters (see also Anfort et al., 2001). Most of the Woodbend aquifer is separated from the Mannville aquifer by the Ireton shales and other intervening stratigraphic units, and the high saline water extends farther towards the northeast than in the Winterburn and Wabamun aquifers. Also, relatively less saline water (< 80 g/l) in the Winterburn aquifer extends farther to the southeast in the vicinity of its subcrop edge (Figure 19b). In the subcrop area, the salinity distribution in

the Wabamun aquifer is very similar to that in the overlying Lower Mannville aquifer (Figures 20a and 21a).

Formation waters are of a Na-Cl type in the overlying Mississippian aquifer. In the regional-scale study area the Mississippian is present only in the western part of the study area and is generally in direct contact with the Lower Mannville aquifer. The salinity ranges from less than 60 g/l to 120 g/l (Figure 20b). These values are significantly lower than the salinity range in the underlying Devonian aquifers, indicating that the intervening Exshaw-Lower Banff aquitard at the base of the Mississippian succession is an effective barrier to cross-formational flow between Devonian and Mississippian aquifers, as shown in many other studies in the Alberta Basin (Bachu, 1999, and references therein).

The salinity of formation water (Na-Cl type) in the Lower Mannville aquifer ranges from 50 g/l in the northeast to 120 g/l in the southwest (Figure 21a). A tongue of high saline brine extends northwestward in the centre of the study area, with salinity decreasing from > 120 g/l in the south-southeast to < 80 g/l in the northwest, and running east of and sub-parallel to the Devonian subcrop edge. This tongue of high salinity water corresponds to the subcrop of the Devonian Wabamun aquifer underneath the Lower Mannville aquifer, and follows approximately the extent of the Edmonton Valley (Ellerslie/Basal Quartz), whereas the surrounding off-channel sediments are filled with less-saline formation water. The high salinity of formation water in the Lower Mannville aquifer in this region is due to the discharge of and mixing with higher-salinity Devonian water from the Wabamun aquifer into the Lower Mannville aquifer, with some spill-over and backflow downdip into the Lower Mannville and Mississippian aquifers (Figures 20a, 20b and 21a) (Anfert et al., 2001).

In the Upper Mannville aquifer, which is restricted to the northeastern part of the study area, the salinity distribution and range (45 to 80 g/l, Figure 21b) are very similar to those in the Lower Mannville aquifer in this area.

Flow of Formation Waters

The analysis of the flow of formation waters is based on distributions of hydraulic heads in the Woodbend to Mannville groups. The hydraulic heads were calculated with a reference density of 1080 kg/m³ in order to minimize the errors in representing and interpreting the flow of variable density water in the vicinity of the acid-gas injection sites (Bachu and Michael, 2002). The reference density corresponds to the average brine density at conditions characteristic for the Mannville - Beaverhill Lake succession in the regional-scale study area (Table 1). Hydraulic heads were calculated according to

$$H = \frac{P}{\rho_0 g} + z \quad (1)$$

where z (m) is the elevation of the pressure recorder, p (Pa) is pressure, ρ_0 (kg/m³) is the reference density and g is the gravitational constant (9.81 m/s²).

Formation water flow inferred from hydraulic head distributions in the Cooking Lake aquifer is channelled generally in a northwestward direction, from areas with hydraulic heads > 400 m in the south and northeast to an area with hydraulic head elevations < 300 m in the northwest (Figure 22a). The hydraulic head distribution in the overlying Winterburn aquifer shows a similar northwestward flow direction (Figure 22b). However, lower hydraulic head values than those in the Cooking Lake aquifer in the south and east, and slightly higher values in the north indicate that: 1) these aquifers are not in hydraulic continuity (i.e., the Ireton aquitard is strong), and 2) there is potential for upward or

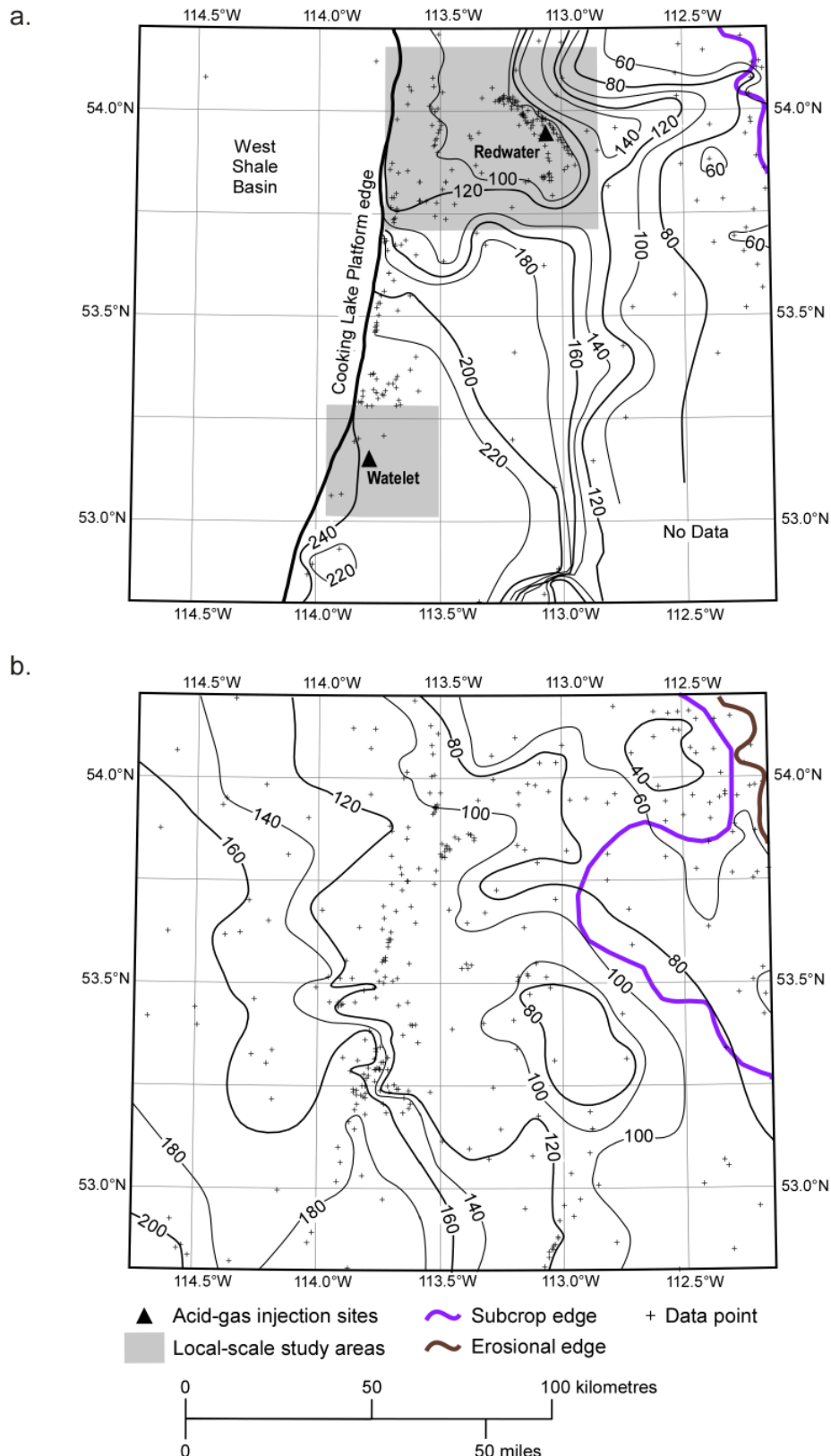


Figure 19. Salinity of formation water in aquifers in the regional-scale study area: a) Cooking Lake, and b) Winterburn. The acid-gas injection sites and local-scale study areas are shown for the Cooking Lake aquifer. Contour lines in g/l.

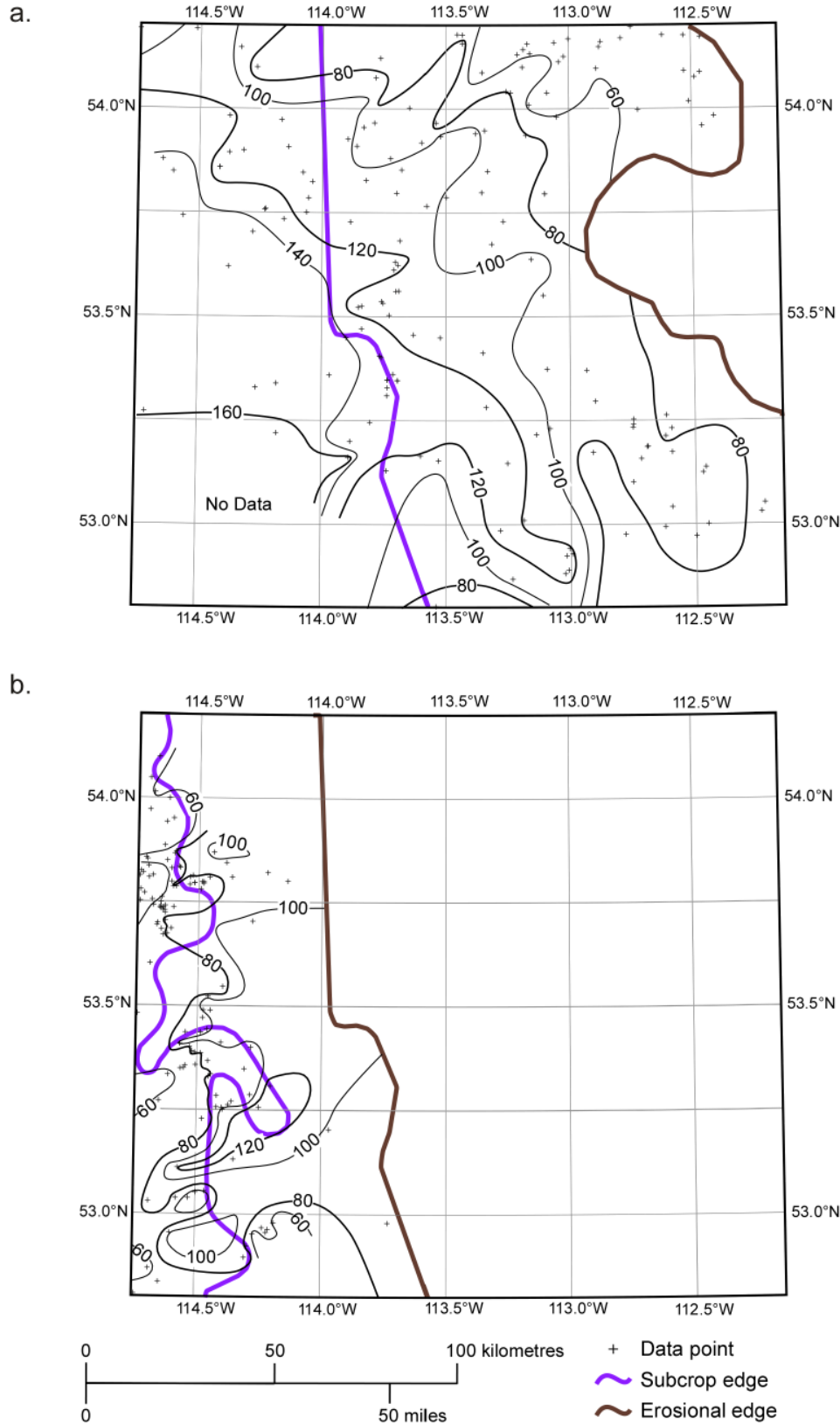


Figure 20. Salinity of formation water in aquifers in the regional-scale study area: a) Wabamun, and b) Mississippian. Contour lines in g/l.

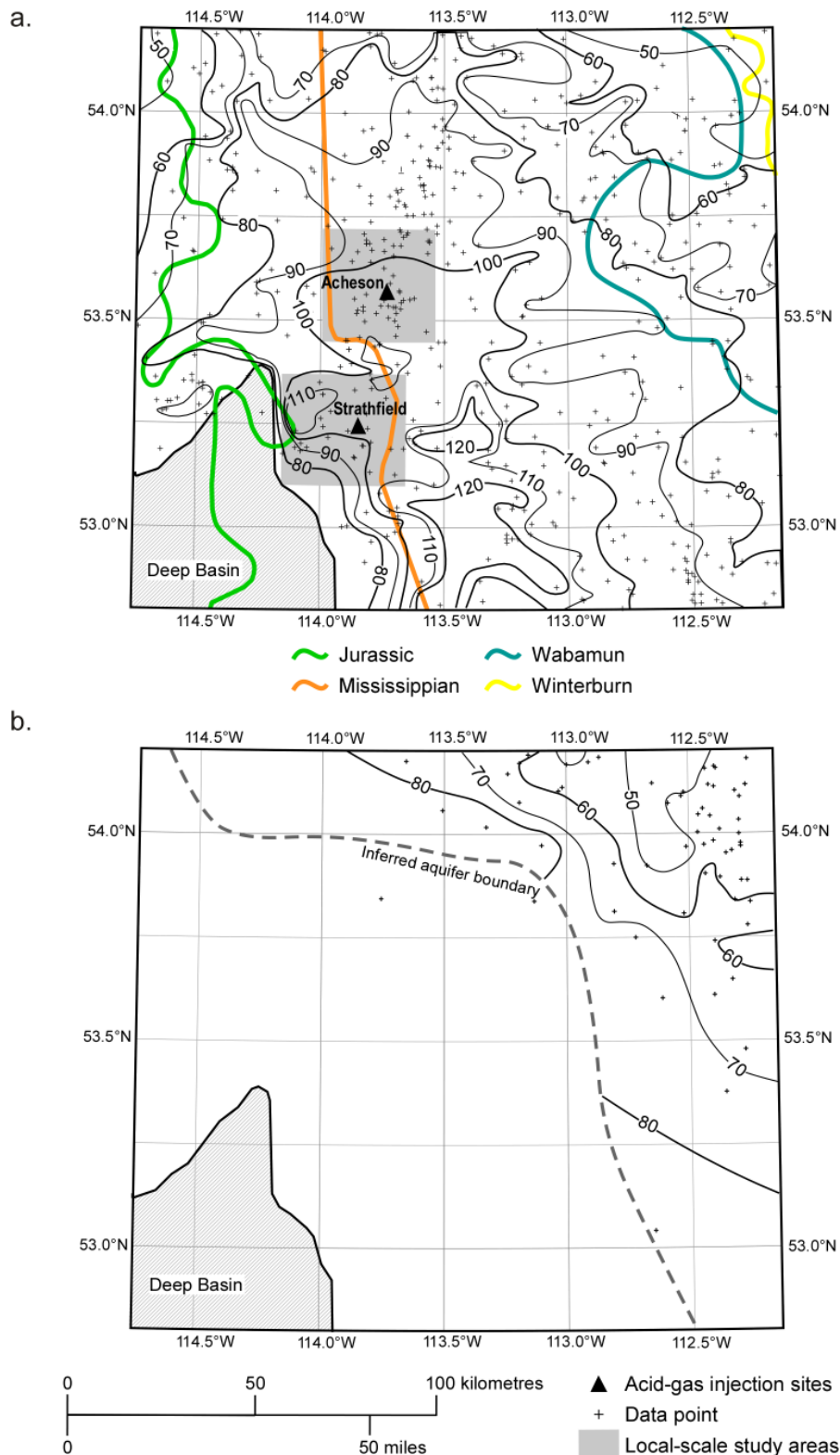


Figure 21. Salinity of formation water in aquifers in the regional-scale study area: a) Lower Mannville, and b) Upper Mannville. Shown on the Lower Mannville map are the subcrop edges of the Jurassic, Mississippian, Wabamun and Winterburn strata. The acid-gas injection sites and local-scale study areas are shown for the Lower Mannville aquifer. Contour lines in g/l.

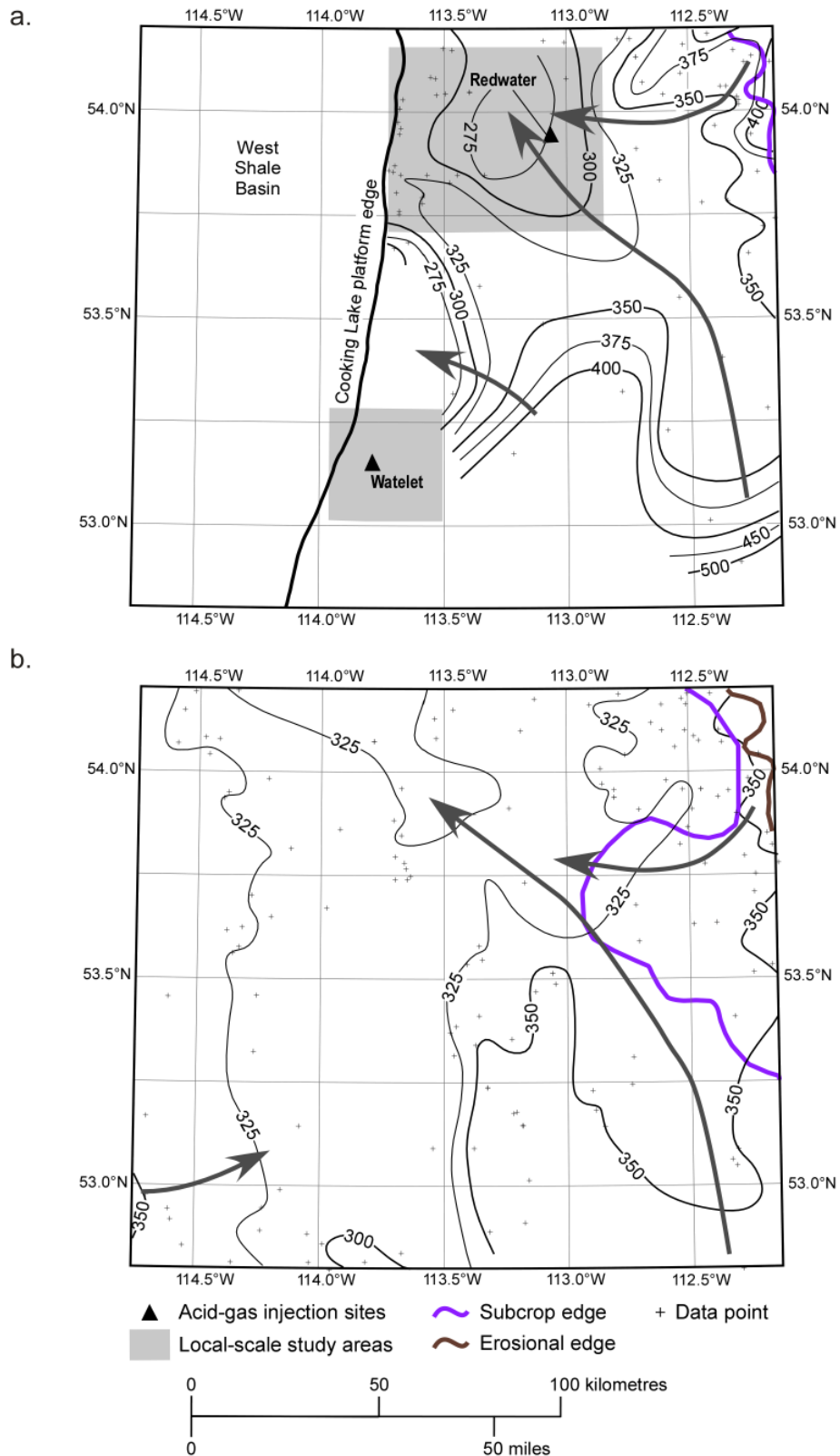


Figure 22. Distribution of hydraulic heads in aquifers in the regional-scale study area: a) Cooking Lake, and b) Winterburn. Hydraulic heads were calculated with a reference water density of 1080 kg/m^3 . Arrows indicate main flow direction. The acid-gas injection sites and local-scale study areas for the Cooking Lake aquifer are shown. Contours in metres.

downward flow, depending on location, if hydraulic communication is established. Flow in the overlying Wabamun aquifer is also towards the northwest (Figure 23a), hydraulic head values being in the same range as in the underlying Winterburn aquifer, which indicates that these two aquifers are in hydraulic communication, particularly along their subcrop areas, as generally shown at the basin-scale by various other studies (Bachu, 1999, and references therein; Anfort et al., 2001). Only in the southwest are hydraulic head values > 600 m significantly higher than values observed in the underlying Devonian aquifers in the study area. Hydraulic heads in the Mississippian aquifer range from > 600 m in the west to approximately 350 m in the northeast along the subcrop edge (Figure 23b), indicating northeastward, updip flow of formation waters.

The hydraulic head distribution in the Lower Mannville aquifer (Figure 24a) mirrors the hydraulic head distributions in the respective subcropping aquifers along the pre-Cretaceous unconformity, where the Paleozoic aquifers are in hydraulic communication with the Lower Mannville aquifer. In the area of Mississippian subcrop, hydraulic heads decrease rather rapidly eastward from 600 m to 350 m suggesting updip flow in that direction. However, the steep hydraulic gradient indicates relatively low permeability in the Lower Mannville aquifer in this part of the study area, which can be inferred also from the lithofacies distribution (Figure 18a). Hydraulic heads above the subcrop of the Devonian aquifers have a comparatively narrow range of 300 to 400 m and hydraulic gradients are relatively low, suggesting a homogeneous permeability distribution and lower flow velocities. The flow of formation waters converges in the north central part of the study area. In this region there is the potential for downward flow into the Devonian aquifers, which have lower hydraulic head values in this area as opposed to higher values in the Upper Mannville aquifer.

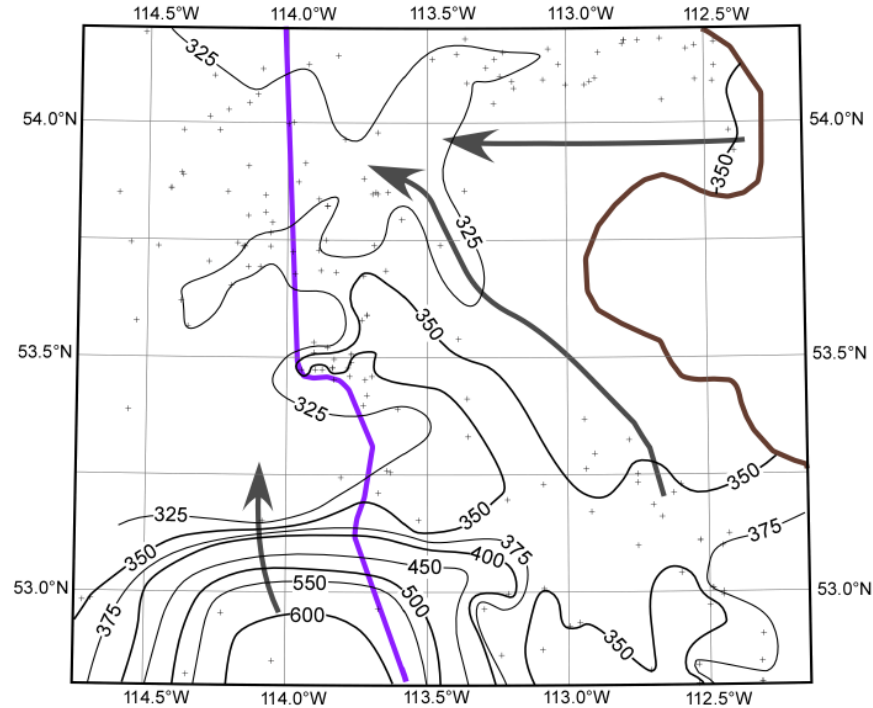
Hydraulic heads are generally 100 m higher in the Upper Mannville aquifer (Figure 24b) than in the Lower Mannville aquifer, indicating that the intervening Clearwater-Upper Mannville aquitard forms a barrier to potentially downward flow of formation water. The exceptions are low hydraulic heads in the southwest corner of the study area, along the boundary of the gas-saturated deep basin, where flow appears to be directed downdip towards the southwest. In addition to the lithofacies distribution map of the Upper Mannville (Figure 18b), low permeability characteristics of the Upper Mannville aquifer in the central part of the study area are inferred from the low number of available drillstem test data in this area.

All aquifers from the Cooking Lake to the Lower Mannville show a similar generalized flow pattern: updip flow from the southwest and down dip flow of fresher water from the northeast converging into generally northwestwardly channelled flow in the center of the study area. Converging flow in the northern part of the Lower Mannville aquifer coincides with successively lower hydraulic heads from the Wabamun to the Cooking Lake aquifer and the presence of Leduc reefs, suggesting hydraulic communication and downward flow from the Lower Mannville aquifer into the Cooking Lake aquifer (Figures 25 and 26).

Combining the analysis of formation water flow and salinity distribution in the various aquifers, the hydrogeology and flow pattern in the regional-scale study area can be summarized as follows:

- The shales and argillaceous limestones of the Waterways Formation (Beaverhill Lake Group), the Majeau Lake, Duvernay and Ireton formations (Woodbend Group), and large parts of the Upper Mannville Group form the regionally extensive Waterways, Ireton and Clearwater-Upper Mannville aquitards, respectively. The shales of the Mississippian Exshaw and Lower Banff formations form the competent Exshaw aquitard in the western part of the regional-scale study area where Mississippian strata are present.

a.



b.

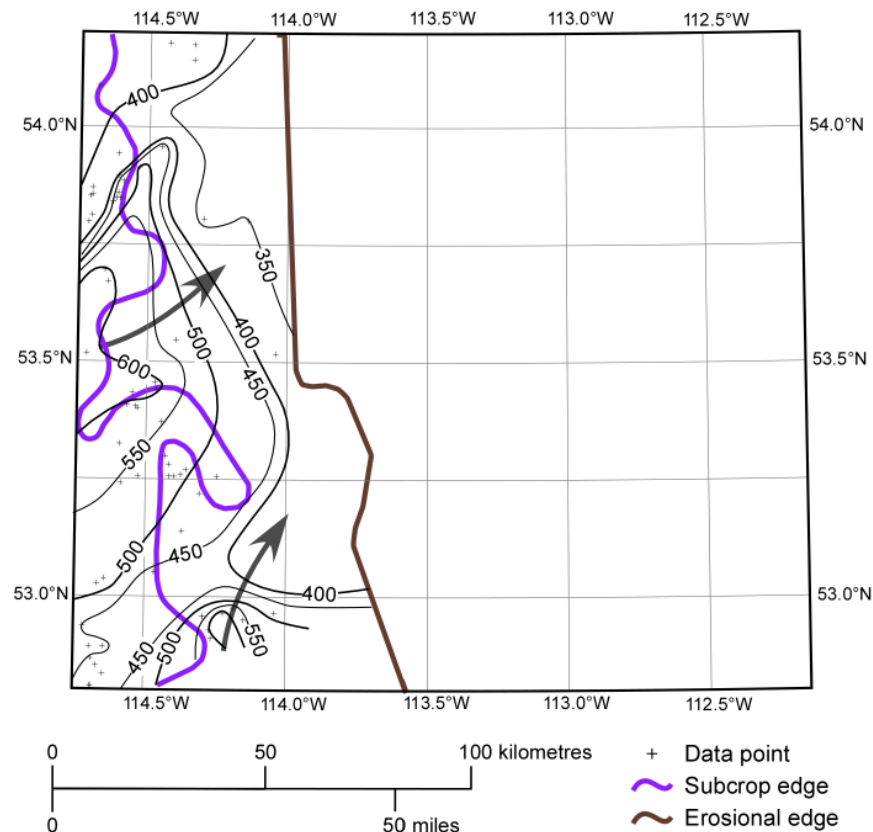


Figure 23. Distribution of hydraulic heads in aquifers in the regional-scale study area: a) Wabamun, and b) Mississippian. Hydraulic heads were calculated with a reference water density of 1080 kg/m^3 . Arrows indicate main flow direction. Contours in metres.

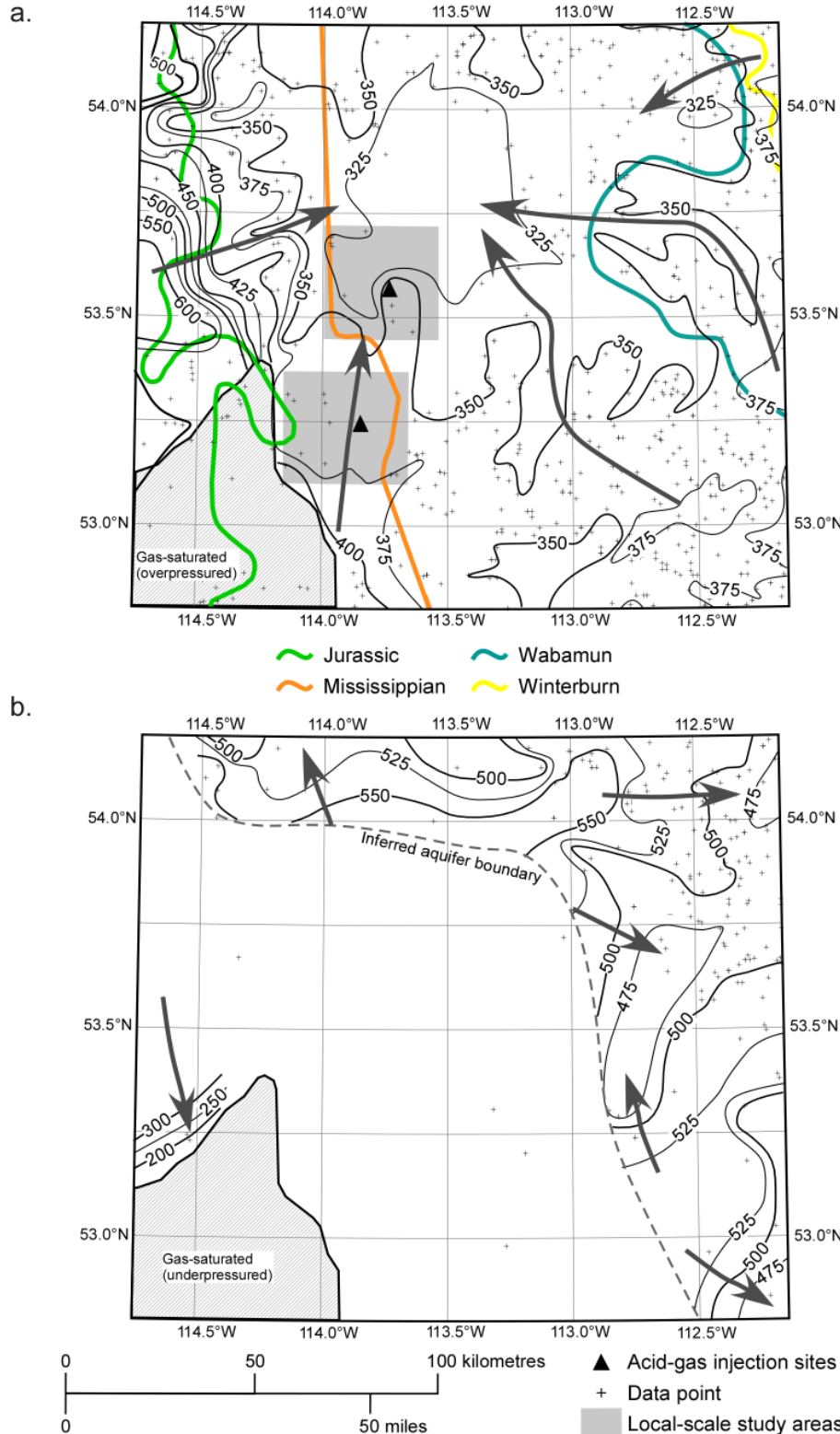


Figure 24. Distribution of hydraulic heads in aquifers in the regional-scale study area: a) Lower Mannville, and b) Upper Mannville. Hydraulic heads were calculated with a reference water density of 1080 kg/m^3 . Shown on the Lower Mannville map are the subcrop edges of the Jurassic, Mississippian, Wabamun and Winterburn strata. The acid-gas injection sites and local-scale study areas are shown for the Lower Mannville aquifer. Contours in metres.

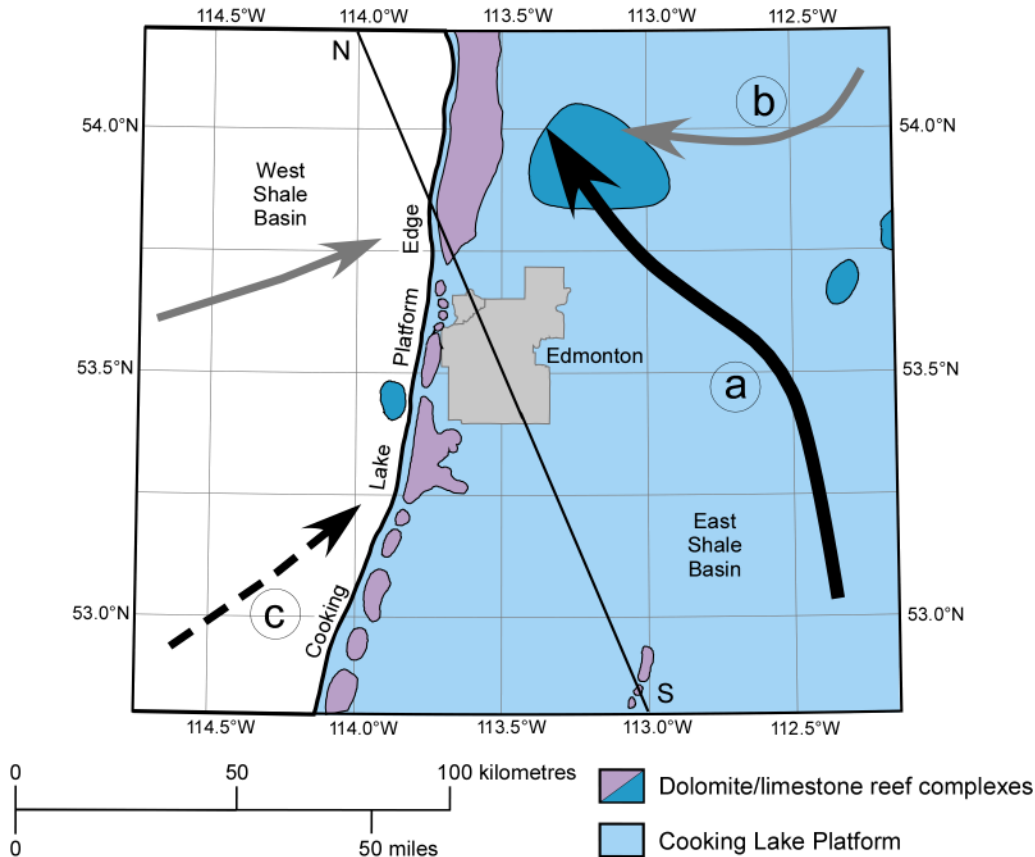


Figure 25. Generalized flow patterns in the Edmonton regional-scale study area: a) part of the basin-scale gravity-driven flow from recharge in Montana to discharge at the Peace River (Cooking Lake to Lower Mannville aquifers), b) regional - to local-scale gravity-driven flow (Mississippian and Lower Mannville aquifers, and the Devonian aquifers in the northeast), and c) tectonically-driven flow (Devonian aquifers). Line of cross-section refers to Figure 26.

- The salinity of formation waters varies over an extremely wide range from approximately < 50 g/l in the shallowest aquifer in the northeast to > 240 g/l in the deepest aquifer in the southwest.
- Brines from the various Paleozoic aquifers (from west to east: Mississippian, Wabamun, Winterburn and Cooking Lake) discharge(d) into the Lower Mannville aquifer in areas of their respective subcrops, forming a high-salinity plume in the latter (see also Bachu and Underschultz, 1995; Rostron and Toth, 1997; Bachu, 1999; Anfort et al., 2002).
- The plume of high-salinity brine preferentially occupies high-permeability Lower Mannville fluvial sediments deposited in the Edmonton Valley.
- Relatively fresher formation water enters the various aquifers from the northeast corner of the study area and flows downdip.
- The general lateral regional flow direction is southeast-northwest, subparallel to the Devonian subcrop edge, except for divergent flow in the Upper Mannville.

4.2.3 Flow Interpretation

Present-day formation water flow in the regional-scale study area is mainly driven by gravity, through a long-range, basin-scale flow system originating at topographic highs in Montana to the south (Bachu, 1999). North of the study area, formation water flow continues and is channelled northward through the

S

N

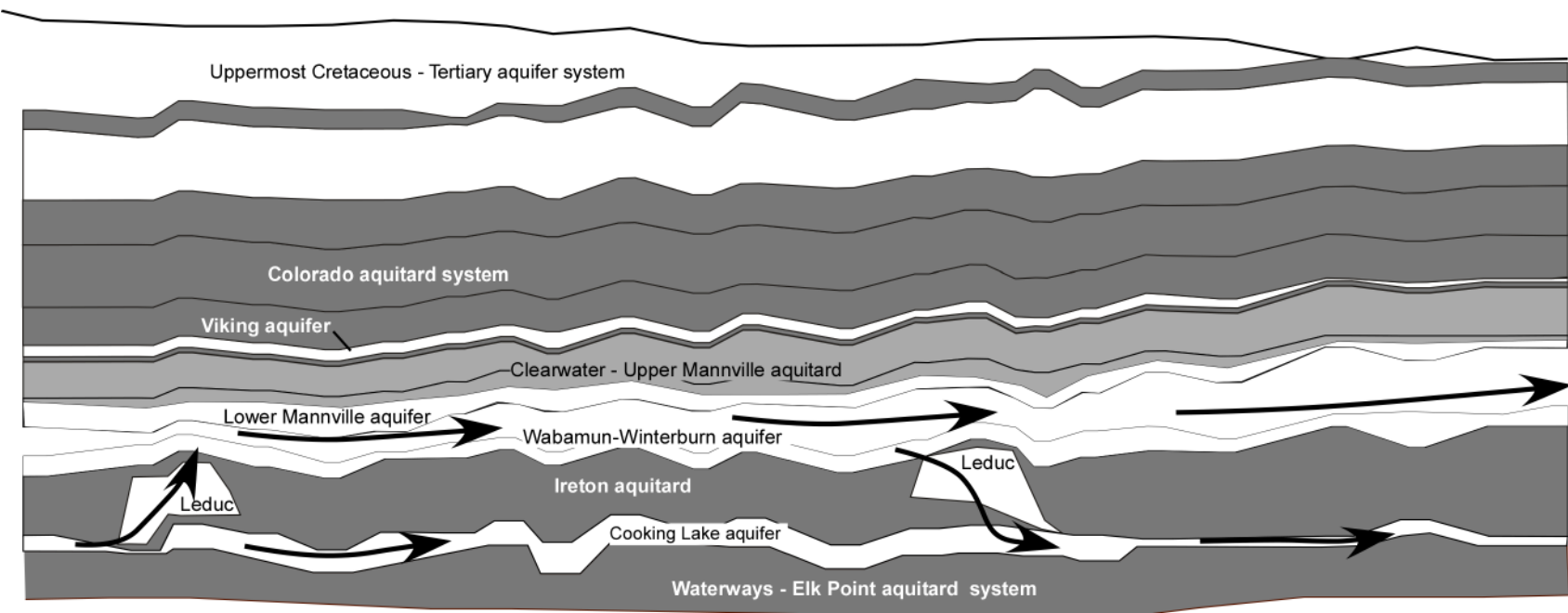


Figure 26. Diagrammatic representation in cross-section of the flow systems in the Beaverhill Lake - Mannville sedimentary succession in the regional-scale study area. The location of the cross-section is shown in Figure 25.

Grosmont carbonate platform of the Woodbend Group, discharging along the Peace River where these carbonates and their equivalents crop out (Bachu, 1999; Anfort et al., 2002). This north-northwestwardly directed basin-scale flow system is joined by two flow systems from the southwest and northeast, respectively (Figure 25). Based on the relatively high salinity of formation waters, and because of the lack of an identified recharge source and flow-driving mechanism for meteoric water, Bachu (1995) postulated that the updip northeastward flow component in the Paleozoic aquifers originates from past tectonic compression. This hypothesis is supported by isotopic and fluid inclusion analyses of formation waters and late-stage diagenetic products in both the deformed and undeformed parts of the basin (Nesbitt & Muehlenbachs, 1993; Machel et al., 1996; Buschkuhle & Machel, 2002; Buschkuhle, 2003). The downward, southwestward flow component of fresher water in the northeast of the study area and flow in most of the Upper Mannville aquifer is probably due to more local-scale topography (Barson et al., 2001). The Waterways, Ireton, Lower Banff-Exshaw, and Clearwater-Upper Mannville formations form effective aquitards on a regional scale, but the erosional surface of the pre-Cretaceous unconformity facilitates cross-formational hydraulic communication (Figure 26). Cross-formational flow takes place also in places where the Ireton shales thin over Leduc reefs (Figure 26). Although the origins are different, the common ‘sink’ for updip flow in the Paleozoic aquifers and downward flow in the Cretaceous aquifers is the ‘Grosmont drain’ to the north (Bachu, 1999; Barson et al., 2001; Anfort et al., 2001). When looking at the present-day flow patterns in the Lower Mannville aquifer, only the high-salinity plume indicates that updip-flowing Paleozoic brines have entered the Lower Mannville aquifer across pre-Cretaceous unconformity in the past. However, hydraulic head distributions show that the driving force behind this flow from the Paleozoic has weakened or almost ceased, and penetration of meteoric water from above and negative buoyancy effects of the dense brine caused a reversal of flow directions from the Lower Mannville aquifer into the Paleozoic aquifers in some areas. Only marginally affecting flow in the study area, the downdip flow component in the southeastern corner of the Upper Mannville aquifer is attributed to the re-imbibement of formerly gas-saturated areas by formation water (Michael and Bachu, 2001), and underpressuring created by the erosional rebound of overlying shales (Bachu, 1995).

With respect to the regional hydrostratigraphy and hydrogeology, the acid-gas injection targets in the Edmonton area are in ascending stratigraphic order in: a) an isolated reef structure within the Waterways aquitard (Golden Spike), b) the Cooking Lake platform (Watelet) and a Leduc reef (Redwater) in the Cooking Lake aquifer, and c) fluvial channel sandstones in the Lower Mannville aquifer (Strathfield and Acheson).

4.3. Stress Regime and Rock Geomechanical Properties

Knowledge of the stress regime at any injection site is important for establishing the potential for hydraulic rock fracturing as a result of injection, and for setting limits for operational parameters. Given its tensorial nature, the stress regime in any structure, including the Earth, is defined by the magnitude and orientation of the three principal stresses, which are orthogonal to each other. In the case of consolidated rocks, the fracturing threshold is greater than the smallest principal stress, σ_3 , but less than the other two principal stresses, σ_1 and σ_2 . If fracturing is induced, fractures will develop in a plane and direction perpendicular to the trajectory of the smallest principal stress. Basin-scale studies of the stress regime in the Alberta basin suggest that, in most of the basin, the smallest principal stress, σ_3 , is horizontal (Bell and Babcock, 1986; Bell et al., 1994; Bell and Bachu, 2003). Due to the orthogonality of the stress tensor, this means that the smallest stress is the minimum horizontal stress ($\sigma_3 = S_{H\min}$). Rock fracturing occurs at pressures P_b that are greater than the minimum horizontal stress and that can be estimated using the equation:

$$P_b = 3S_{H\min} - S_{H\max} + P_0 + T_0 \quad (2)$$

where $S_{H\max}$ is the maximum horizontal principal stress, P_0 is the pressure of the fluid in the pore space, and T_0 is tectonic stress. In the case of injection, the fluid pressure at the well is the bottom hole injection pressure. This equation demonstrates that the fracturing pressure is related to the effective stress (stress less fluid pressure), beside the tensile strength of the rock.

The minimum horizontal stress, $S_{H\min}$, can be evaluated using a variety of tests. The most accurate method for estimating the magnitude of the $S_{H\min}$ is through micro-fracture testing, but mini-fracturing, leak-off tests and Fracture Breakdown Pressure tests are also used (Bell, 2003; Bell & Bachu, 2003). The maximum horizontal stress cannot be directly measured, but it can be calculated according to the relation:

$$S_{H\max} = \frac{\nu}{1-\nu} (S_v - P_0) \quad (3)$$

where S_v is the vertical stress and ν is Poisson's ratio, which is determined through laboratory tests on rock samples. The magnitude of the vertical stress S_v at any depth coincides with the pressure exerted by the rocks above that point (weight of the overburden), and can be calculated by integrating the values recorded in density logs. Unfortunately there are no methods for estimating the tectonic stress, T_0 , hence it is not possible to estimate the rock fracturing pressure. However, previous studies have shown that in the regional-scale study area the $S_{H\max}$ is less than S_v (Bell and Babcock, 1986; Bell et al., 1994). Thus, estimation of $S_{H\min}$ and S_v in a well provides loose lower and upper bounds for the fracturing pressure in that well.

If fractures occur, they will develop in a direction perpendicular to the plane of the minimum horizontal stress, hence the need to know the principal directions of the stress field. Horizontal stress orientations can be determined from breakouts, which are spalled cavities that occur on opposite walls of a borehole (Bell, 2003). They form because the well distorts and locally amplifies the far-field stresses, producing shear fracturing on the borehole wall. If the horizontal principal stresses are not equal, the wall rock of a quasi-vertical well is anisotropically squeezed. Caving occurs preferentially aligned with the axis of the smaller $S_{H\min}$. More detailed description of the methods used for estimating stress magnitude, gradient and orientation are found in Bell (2003).

No records of stress and/or geomechanical testing in the acid-gas injection wells in the Edmonton area exist in the public domain (i.e., operator applications to EUB). Micro-frac, mini-frac, leak-off and hydraulic fracturing tests from wells in the regional-scale study area were used to estimate the gradient of the minimum horizontal stress, $\nabla S_{H\min}$. These gradients were then used to infer the value of the minimum horizontal gradient at the acid-gas injection sites on the basis of stress gradient and depth (Bell, 2003; Bell and Bachu, 2003). Table 2 presents the location, formation, depth, and gradient of the minimum horizontal stress determined from tests in Devonian and Lower Mannville strata in the regional-scale study area. Figure 27a shows the location of these tests.

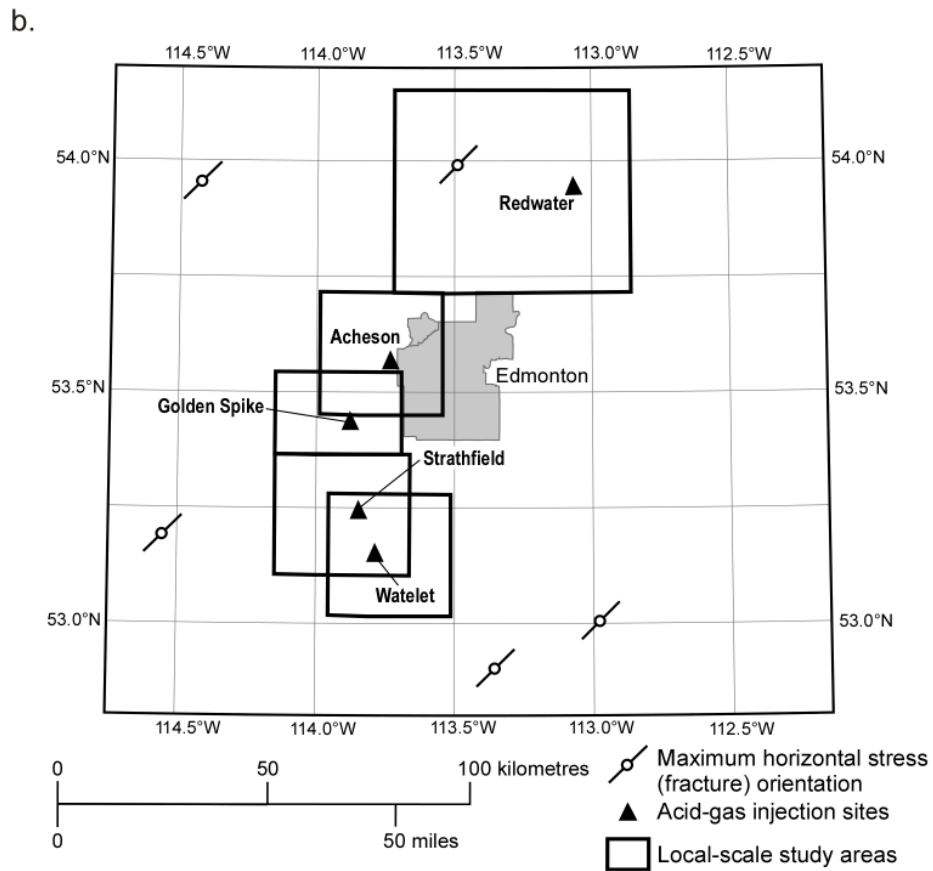
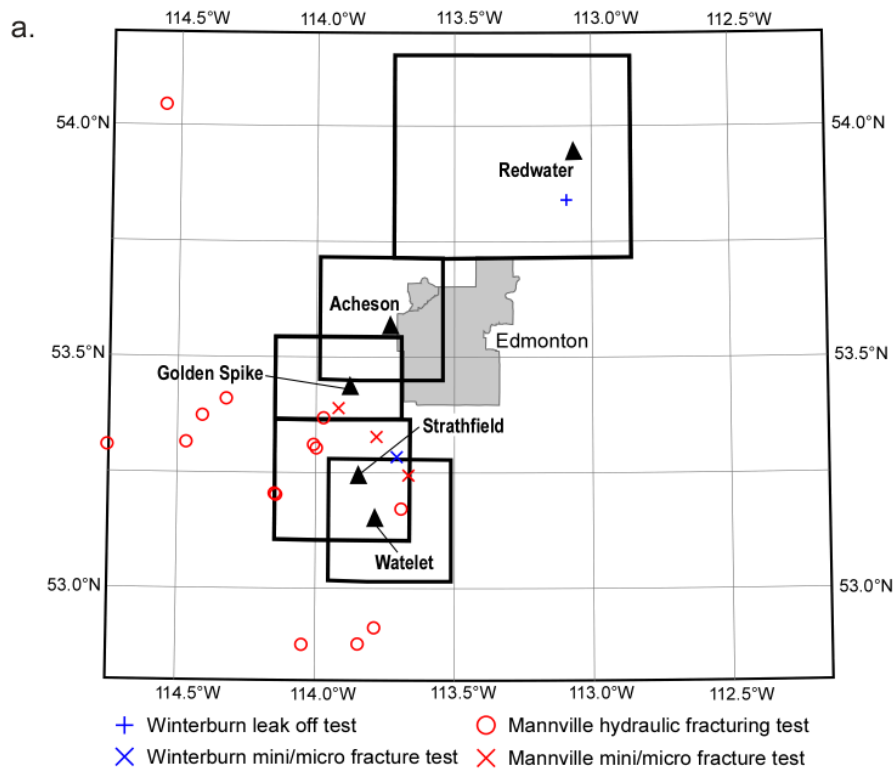


Figure 27. Location of wells in the Edmonton regional-scale study area with data for determination of: a) the gradient of the minimum horizontal stress, and b) orientation of horizontal stresses.

Table 2. Gradients of the minimum horizontal stress S_{Hmin} determined from tests performed in wells in the Edmonton regional-scale study area.

Well Location	Formation	Group	Test Type	Depth (m)	Grad(S)(kPa/m)
00/04-02-050-26W4/0	Nisku	Winterburn	Mini-frac	1581.00	14.00
00/06-17-056-21W4/0	Calmar	Winterburn	Leak-off	919.00	17.20
00/08-24-049-26W4/0	Ellerslie	Mannville	Mini-frac	1337.00	15.00
00/04-20-050-26W4/0	Glauconitic Ss	Mannville	Mini-frac	1581.00	14.00
00/08-09-051-27W4/0	Glauconitic Ss	Mannville	Mini-frac	1300.00	14.00
00/06-05-051-03W5/0	Ellerslie	Mannville	Hydro-frac	1462.00	21.20
00/10-25-045-27W4/0	Glauconitic Ss	Mannville	Hydro-frac	1522.00	23.52
00/08-29-058-04W5/0	Glauconitic Ss	Mannville	Hydro-frac	1144.50	16.25
00/12-06-049-01W5/0	Glauconitic Ss	Mannville	Hydro-frac	1548.50	18.73
00/16-14-051-03W5/0	Ostracod Beds	Mannville	Hydro-frac	1420.25	19.71
00/08-14-050-04W5/0	Ellerslie	Mannville	Hydro-frac	1557.50	20.42
00/05-11-050-28W4/0	Glauconitic Ss	Mannville	Hydro-frac	1369.25	25.42
00/14-12-050-06W5/0	Glauconitic Ss	Mannville	Hydro-frac	1622.25	15.41
00/16-12-050-01W5/0	Glauconitic Ss	Mannville	Hydro-frac	1381.90	15.20
00/11-06-049-01W5/0	Glauconitic Ss	Mannville	Hydro-frac	1536.75	17.24
00/04-14-045-01W5/0	Glauconitic Ss	Mannville	Hydro-frac	1695.25	12.45
00/05-15-045-27W4/0	Glauconitic Ss	Mannville	Hydro-frac	1548.50	15.95
00/02-06-051-27W4/0	Glauconitic Ss	Mannville	Hydro-frac	1372.25	18.15
00/08-26-048-26W4/0	Ostracod Beds	Mannville	Hydro-frac	1396.00	13.61

The mini-frac tests in the Lower Mannville Group strata indicate a gradient of the minimum horizontal stress of 14 to 15 kPa/m (Table 2), while the hydraulic fracturing tests suggest an average gradient for the breakdown pressure of 18.1 kPa/m. However, hydraulic fracturing pressures are always higher than the pressures needed for initiating a fracture (Bell, 2003), and the gradient of 14 kPa/m is considered as being representative for the minimum horizontal stress in the sandstones of the Lower Mannville Group in the Edmonton area.

Carbonate rocks usually are stronger than sandstones, and one would expect that gradients of the minimum horizontal stress for rocks in the Beaverhill Lake and Woodbend groups are higher than for the sandstones of the Lower Mannville Group. In the regional-scale study area there are only two tests for carbonate rocks from the overlying Winterburn Group (Table 2 and Figure 27a). Estimates of gradients of the minimum horizontal stress in carbonates of the Wabamun Group at four acid-gas injection sites in the Pembina area to the west-southwest of the Edmonton area vary between 15.7 and 17.6 kPa/m (Bachu et al., 2003b). On the basis of these gradients and of the two tests in the Edmonton regional-scale study area, the gradient of the minimum horizontal stress for Devonian rocks at acid-gas injection sites near Edmonton is estimated to be 16.7 kPa/m.

Orientations of the minimum horizontal stress S_{Hmin} were determined from breakouts in five wells in the regional-scale study area (Table 3 and Figure 27b). The direction of the minimum horizontal stress varies between 120.0° and 150.5° (average 138.6°), in a general southeast-northwest direction. This means that fractures will form and propagate in a vertical plane in a southwest-northeast direction (30° - 60.5° ;

average 48.6°), basically perpendicular to the Rocky Mountain deformation front and along the direction of the tectonic stress induced by the Laramide orogeny and by the collision of the Pacific and Juan de Fuca tectonic plates with the North American continent (Figure 27b). This preferential fracturing direction was observed previously in coal mines in Alberta (Campbell, 1979), and was similarly determined for overlying Cretaceous rocks in southern and central Alberta (Bell and Bachu, 2003).

Table 3. Orientations of the minimum and maximum horizontal stresses determined from breakouts in wells in the Edmonton regional-scale study area

Well Location	Stratigraphic Age	S _{Hmin} Azimuth	S _{Hmax} Azimuth
00/10-24-045-24W4/0	Upper Cretaceous	150.5	60.5
00/10-24-045-24W4/0	Lower Cretaceous	149.1	59.1
00/11-27-046-21W4/0	Upper Cretaceous	138.5	48.5
00/11-27-046-21W4/0	Lower Cretaceous	138.2	48.2
00/11-27-046-21W4/0	Paleozoic	130.0	40.0
00/11-27-046-21W4/0	Upper Devonian	130.0	40.0
00/14-09-058-24W4/0	Paleozoic	148.0	58.0
00/14-09-058-24W4/0	Upper Devonian	148.3	58.3
00/10-32-048-04W5/0	Upper Cretaceous	120.0	30.0
00/04-29-057-03W5/0	Carboniferous	130.7	40.7
00/04-29-057-03W5/0	Upper Devonian	141.0	51.0

Knowledge of the geomechanical properties of rocks in formations affected by acid gas injection is an essential part of the subsurface characterization of any injection site, including the acid-gas injection operations in the Edmonton area. These properties, in combination with the stress regime, play an important role in evaluating the safety of the operation and avoiding rock fracturing and acid gas leakage into overlying formations. Two parameters are essential to understanding the rock mechanics of an injection site: Young's modulus and Poisson's ratio. A literature review of geomechanical properties provided general values for Poisson's ratio and Young's modulus from rock samples outside of the regional-scale study area. Measurements in each case cover a number of samples and a range of values. The value closest to the average of that particular set of measurements was considered as representative and is provided in Table 4. Four of the values given represent Mannville Group parameters, three sandstones and one clay-siltstone. Shale caprock values are represented by a measurement taken in the underlying Jurassic Fernie Group. The carbonate injection interval is characterized by an Upper Devonian dolomite parameter and the shale caprock is represented by a value from the Calmar Formation (Table 4).

Table 4. Geomechanical properties of rocks of interest from the Alberta Basin (derived based on data from McLennan et al., (1982), Miller and Stewart (1990) and Penson et al., (1993)).

Formation	Group	Rock Type	Well Location	Depth (m)	Poisson's Ratio	Young's Modulus (GPa)
Basal Quartz	Mannville	sandstone	1-12-035-7-W5	2984	0.19	45.4
Basal Quartz	Mannville	sandstone	9-5-39-3W5	2149	0.18	50.6
Basal Quartz	Mannville	clay-siltstone	1-12-035-7W5	2998	0.16	50.2
Glauconitic	Mannville	sandstone	15-18-39-3W5	2185	0.16	42.2
	Fernie	shale	9-13-039-4W5	2183	0.30	29.2
Calmar	Winterburn	shale	4-014-16W4	-	0.34	51.8
Nisku	Winterburn	dolomite	4-014-16W4	1392	0.32	38.8

Young's modulus, E, is defined as the amount of strain (deformation) caused by a given stress, and is a function of the stiffness of the material. Young's modulus is used as an indication of the possible width of fractures. A high Young's modulus correlates to a narrower fracture width. In general, typical Young's modulus values for rocks range from 20 to 82.5 GPa (Jumikis, 1983; Haas, 1989). The Young's modulus values for Mannville sandstone range from 27 GPa to 59 GPa, compared with a value of 30 GPa to 65 GPa for the Mannville siltstone (McLennan et al., 1982). For the Basal Quartz Formation, the Young's modulus was calculated using the following equation:

$$E=2G(1+v) \quad (4)$$

where the Poisson's ratio, v, and the shear modulus, G, were measured from static triaxial tests (McLennan et al., 1982). The Glauconitic Formation and Fernie Group values for Young's modulus and Poisson's ratio were both derived from P-wave (Vp) and S-wave (Vs) velocities from sonic logs (Miller and Stewart, 1990). The Young's modulus provided for the Calmar Formation was estimated static Young's modulus and the values in the literature range from 51.8 GPa to 53.3 GPa (Penson et al., 1993). The Upper Devonian carbonate values for Young's modulus were determined from static triaxial bench tests and range from 30 GPa to 67 GPa (Penson et al., 1993).

Poisson's ratio, v, is defined as the ratio of the strain perpendicular to an applied stress, to the strain along the direction of that stress. It is a measure of the deformation perpendicular to and along the stress being applied to the rock, and indicates the plasticity of the rock. The rock plasticity, expressed by Poisson's ratio, and $S_{H\min}$, have a significant effect in determining the rock fracture threshold (see equations 2 and 3). A formation with high S_{\min} and Poisson's ratio would likely be an effective barrier to fracture propagation. In general, values for Poisson's ratio for carbonates range from 0.15 to 0.35, for sandstones 0.1 to 0.3, and for shales from 0.1 to 0.4 (Jumikis, 1983; Lambe and Whitman, 1951; Haas, 1989). The Poisson's ratio for Mannville sandstone ranges from 0.13 to 0.2, compared with a value of 0.12 to 0.32 for the Mannville clay siltstone. The three Basal Quartz values were measured from core samples subjected to representative temperatures and loading conditions (McLennan et al., 1982). The static Poisson's ratio values for the Upper Devonian shale range from 0.3 to 0.35 and for carbonate, range from 0.19 to 0.43 (Penson et al., 1993).

5 Local-Scale Setting of the Edmonton Cluster of Acid-Gas Injection Sites

Because the acid-gas injection sites in the Edmonton region are distributed over a large stratigraphic interval of variable characteristics and over a wide area, the geological and hydrogeological characteristics of the these injection sites are described at a local scale in individual specific areas (each defined broadly by the respective oil or gas field they are located in), rather than a single, all-encompassing local-scale study area. The five injection sites are located within the boundaries of the Golden Spike, Redwater, Watelet, Strathfield and the Acheson fields (Figure 9). The geology in these specific areas is moderately well known and understood. Core, albeit in restricted numbers, is available as a result of exploration for and production of hydrocarbons from both Devonian and Cretaceous strata. Maps showing the depth to and the structure top of the injection unit are not presented at the local scale. This information is readily available from corresponding regional-scale maps (Figures 12, 14 and 17). In turn, isopach maps are presented, since information about the thickness of the injection unit is relevant at the local scale.

The set of high-quality DSTs used in the regional-scale interpretation had to be augmented in some local-scale study areas with lower-quality DST data. Final shut-in pressures from these tests have not been extrapolated to formation pressure (Horner plot), and therefore have to be considered with caution. Still,

tests supposedly influenced by production from nearby wells were culled from the data set, by comparing DST pressures and dates to initial pool pressures and discovery dates (Alberta's Reserves; EUB, 1998), respectively. Production from the Lower Mannville and Woodbend pools in the Edmonton area started in the early 1950's. Therefore, pressure data not influenced by production that can be used to interpret virgin formation water flow are generally also from the 1950's and data quality from older testing technology is definitely an issue that should be kept in mind. The actual in-situ formation water density in the local-scale study areas is generally higher 1080 kg/m^3 . However, for the calculation of hydraulic head values at the regional scale, a reference density of 1080 kg/m^3 was used (see Section 4.2.2) and this value will be used at the local scale as well. This allows for the comparison between contour maps of hydraulic heads on the regional and local scales, but won't significantly affect the accuracy of the flow analysis (Bachu & Michael, 2002).

Rock properties relevant to the flow of formation fluids and injected acid gas that were used in the local-scale characterization are porosity and permeability. The core-scale porosity values were up-scaled to the well scale using the weighted arithmetic average. Permeability values were up-scaled to the well scale using a power-law average with a power of $\omega=0.8$ (Desbarats and Bachu, 1994). Representative values presented in tables in the following sections present the statistics of the well-scale averaged porosity and permeability values.

5.1 Golden Spike-Beaverhill Lake

5.1.1 Geology

The local-scale study area is defined around the Golden Spike oil field just west-southwest of Edmonton and includes Townships 51 to 52 and Range 26W4 to Range 1W5 (Figure 9). Acid gas injection takes place into reefal carbonates in the Moberly Member within the upper part of the Waterways Formation of the Beaverhill Lake Group (Figure 28, Appendix 1). The Moberly Member is overlain by 10-15 m of open marine limestones of the Mildred Member, which are tight and seal the Moberly carbonates from the overlying strata. The Beaverhill Lake carbonates lie at depths of about 1900 m (-1200 m elevation) and have a thickness of 10 to 20 m in the injection area. The lateral extent of the reefal horizon cannot be determined because of a lack of data, however it is assumed that it laterally mimicks the outline of the overlying Leduc reef ($\sim 30 \text{ km}^2$). The inception of reef growth in this area during Leduc time was probably the result of slight relief on the ocean floor caused by the development of localized reefal areas in the underlying Moberly Member of the Waterways Formation (Wendte, 1992).

In the local-scale study area, the Upper Waterways Formation consists of two portions: an upper open marine, dense limestone (Mildred Member) and a lower shallow marine fossiliferous limestone (Moberly Member). The Moberly Member even exhibits a reefal facies in places and can have sufficient porosity for injection. The medium-grey reefal carbonates are embedded in cyclical beds of limy shales and argillaceous limestones. The reefal carbonates are composed mainly of limestone (93%), with sparry calcite cements and bioclasts in a micritic matrix, which is intermixed with minor (5%) amounts of secondary, patchy replacement dolomite. In addition, there are traces of iron minerals (fracture infills and stylolites), chalcedony and an unidentified opaque material (Figure 29). The reefal carbonates have high vuggy and moldic, as well as intercrystalline porosity.

In the Golden Spike field area, a prominent isolated Leduc reef overlies the limestones of the Beaverhill Lake Group (Figures 9 and 28). This reef (the Golden Spike reef) is up to 300 m thick and is encased laterally in Woodbend Group shales of the Majeau Lake Member, and Ireton and Duvernay formations. The Golden Spike reef differs from many Leduc reefs in the basin, because it is not located on the

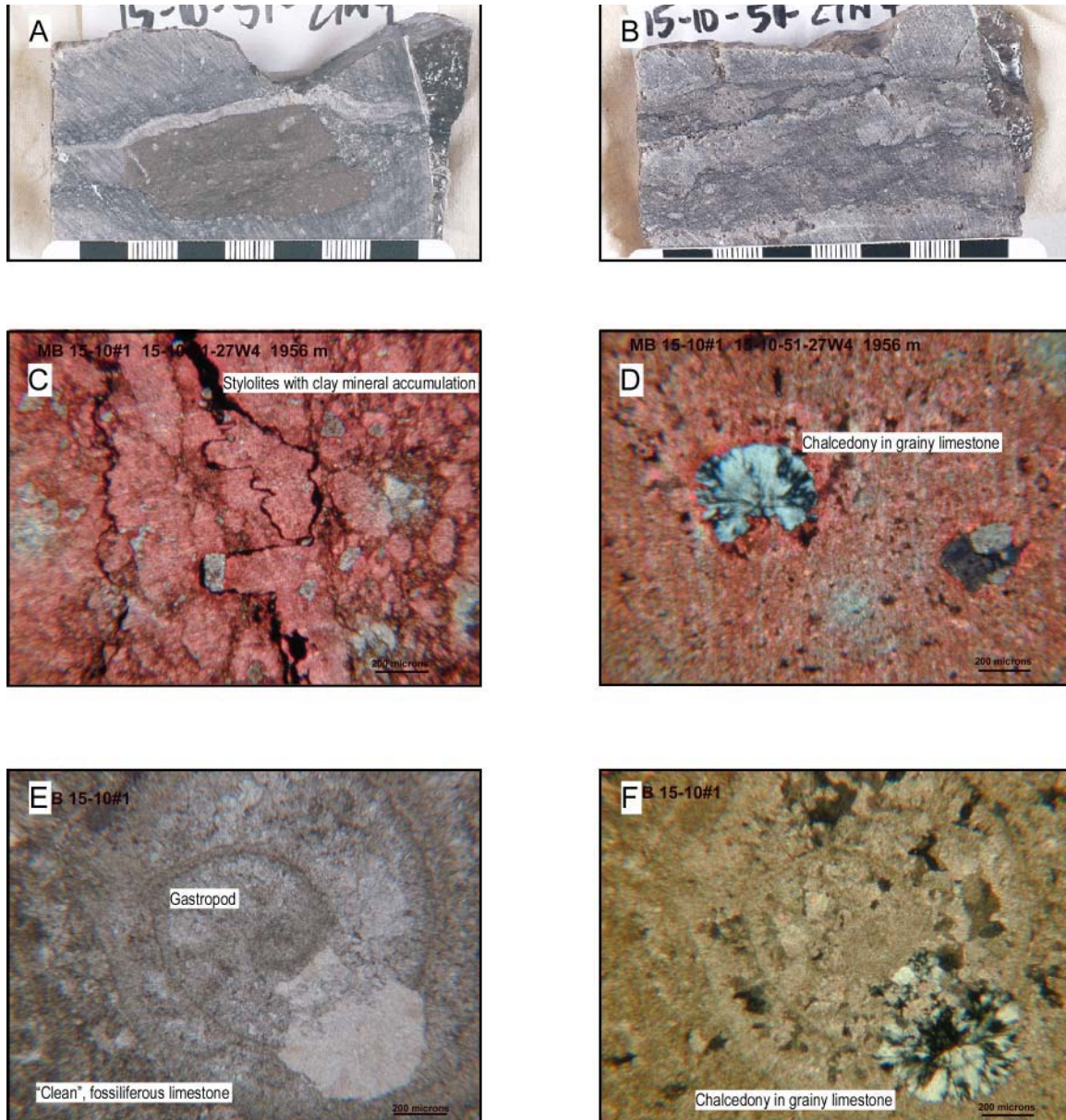


Figure 28. Rock and thin-section photographs of the Beaverhill Lake Group limestones in the Golden Spike area. The lithology varies between clean and porous limestones and argillaceous tighter limestones to marlstones. Photo A shows a crinoid-rich intraclast floating in reefal limestone indicating the proximity of a shallow marine environment next to a deeper marine setting, resulting in local facies and porosity changes. Photo B depicts a more porous, "cleaner" carbonate. Photo C shows a limestone with stylolites along which are dark-brown, clay accumulations. Chalcedony occurs occasionally as a diagenetic mineral within the limestone as seen in Photos D, E and F. Photos D and F also show the recrystallization and cementation of a gastropod shell with the finer crystalline shell which is filled with a coarser grained cement.

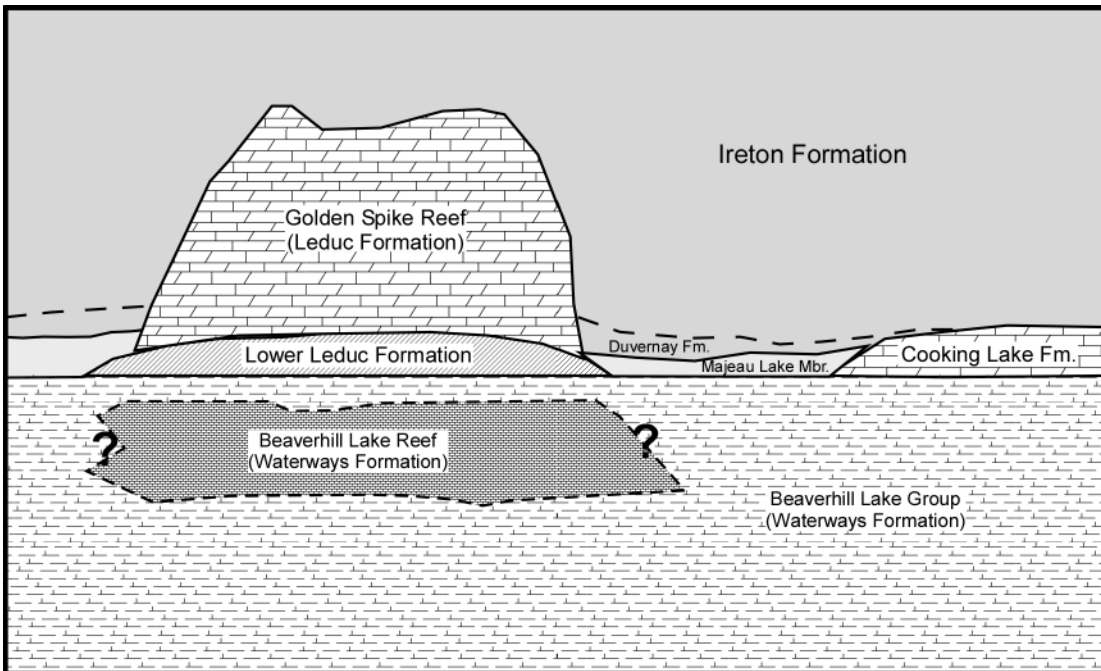


Figure 29. Schematic cross-section of the Leduc Formation Golden Spike reef showing its location above the Beaverhill Lake Group limestone build-up (injection target) within the otherwise argillaceous Waterways Formation (modified after Walls et al., 1979). See also the downhole model for the Golden Spike in Appendix 1.

Cooking Lake platform to the east, but merely grew isolated on undulations of the seafloor created by underlying Beaverhill Lake build-ups within the West Shale basin. It is overlain by a succession of Ireton Formation shale, which has a thickness of 50 m above the reef and thickens to almost 200 m away from the build-up (Figure 30). The Woodbend Group shales provide the seal for the reef carbonates of the Leduc Formation and the Cooking Lake Formation platform carbonates in the eastern part of the study area (East Shale Basin), as well as to the underlying Beaverhill Lake Group strata (Figure 30) in the Golden Spike reef area and further to the west (West Shale basin). Due to their position west of the boundary of the Cooking Lake carbonate platform, both the Leduc Formation Golden Spike reef and the reefal carbonates in the underlying Beaverhill Lake Group (the injection target) are offset and in no hydraulic communication, direct or potential, with the Cooking Lake aquifer. Shales and evaporites of the Middle Devonian Fort Vermilion, Watt Mountain and Muskeg formations, which have a combined thickness of 50 m in the injection area, underlie the Beaverhill Lake Group.

There was never hydrocarbon production from the Beaverhill Lake Group in the Golden Spike field. Currently there is production from the Leduc Formation (Woodbend Group), from the Wabamun Group in the Upper Devonian, and from several Cretaceous horizons, all overlying the Beaverhill Lake Group. Production from the Nisku Formation (Winterburn Group) has ceased. The Beaverhill Lake Group reefal carbonates seem to be hydraulically isolated from the overlying Leduc Formation through the relatively tight, open marine limestone sequence (see further discussion in the hydrogeology section below).

5.1.2 Hydrogeological Characteristics and Rock Properties

Chemistry of Formation Waters

Only 3 chemical analyses of Beaverhill Lake formation water exist in the local-study area. The major constituents are sodium (~65 g/l) and chloride (~150 g/l), making up 87% of the total dissolved solids,

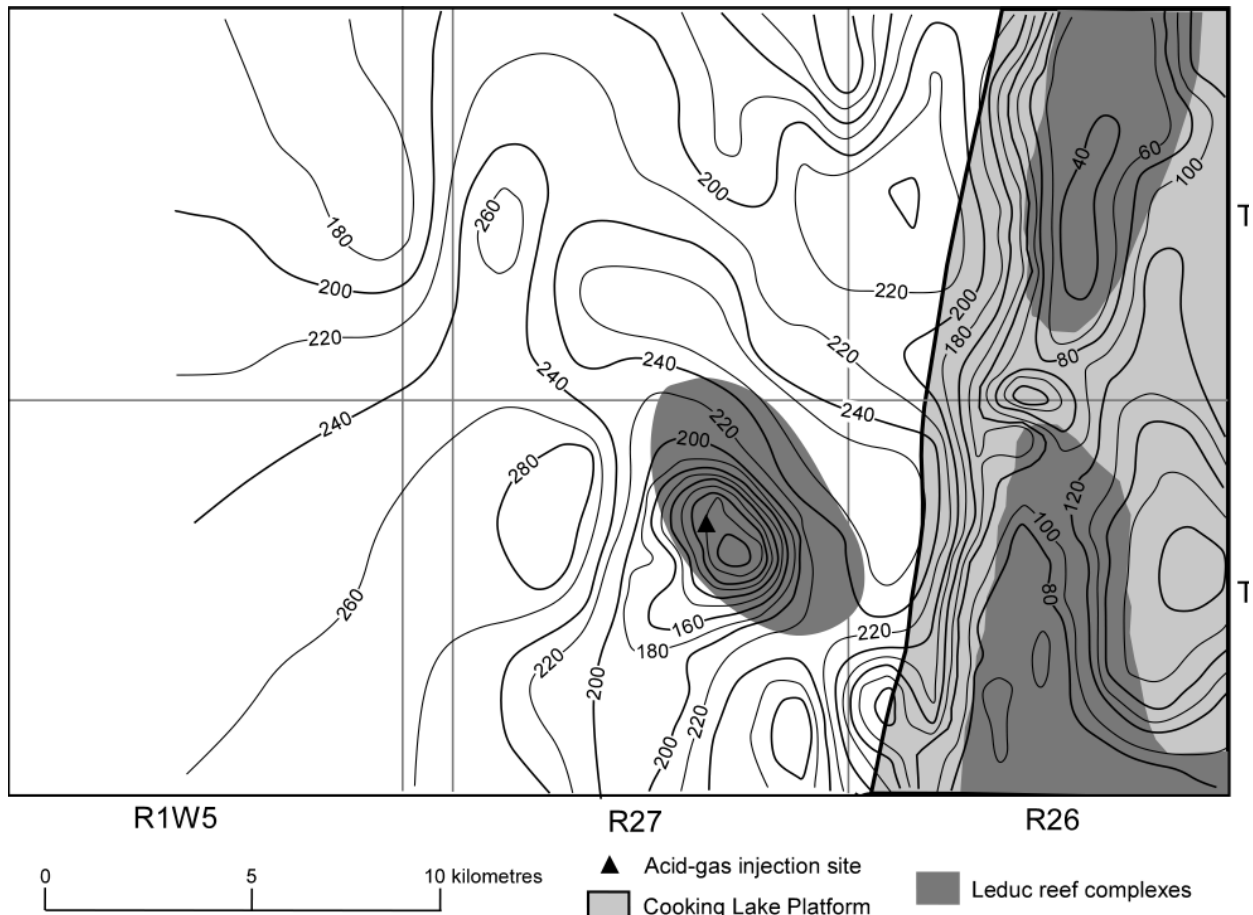


Figure 30. Isopach map of the Ireton Formation in the Golden Spike local-scale study area. Note the thinning of the shale above the Leduc reefs. The Cooking Lake platform is continuous towards the east. Contours in metres.

and calcium ($\sim 25 \text{ g/l}$) (Table 5). The average molal ratio of Na/Cl is 0.4. The brine contains in lesser concentrations magnesium, bicarbonate and sulfate (Figure 31a). The salinity has a narrow range between 230 and 245 g/l (Figure 32). Both the bicarbonate and sulfate concentrations are low, ranging between 0.24 to 0.45 g/l, and between 0.13 to 0.20 g/l, respectively (Table 5). The average in-situ density of formation water in the Beaverhill Lake Group in the local-scale study area was estimated to be 1185 kg/m^3 using the methods presented in Adams and Bachu (2002).

Table 5. Major ion chemistry of Beaverhill Lake brines in the Golden Spike area (concentrations in g/l).

DLS	Na	Ca	Mg	Cl	SO_4	HCO_3	TDS
12-24-51-27W4	62.0	24.0	4.5	151.0	0.24	0.16	241.8
11-09-52-26W4	53.6	25.7	5.1	142.5	0.45	0.20	227.4
05-29-52-27W4	68.2	21.6	3.1	152.0	0.32	0.13	245.2
Average	61.3	23.8	4.2	148.5	0.33	0.16	238.2

Due to its aquitard characteristics in the Edmonton area, there is no hydrocarbon production from the Beaverhill Lake Group, and only one DST and no core analyses data exist for this succession. Hence, no assessment of the lateral flow regime and rock properties could be made. The pressure at injection elevation in the Beaverhill Lake Group plots along the same trend as the pressure in the overlying

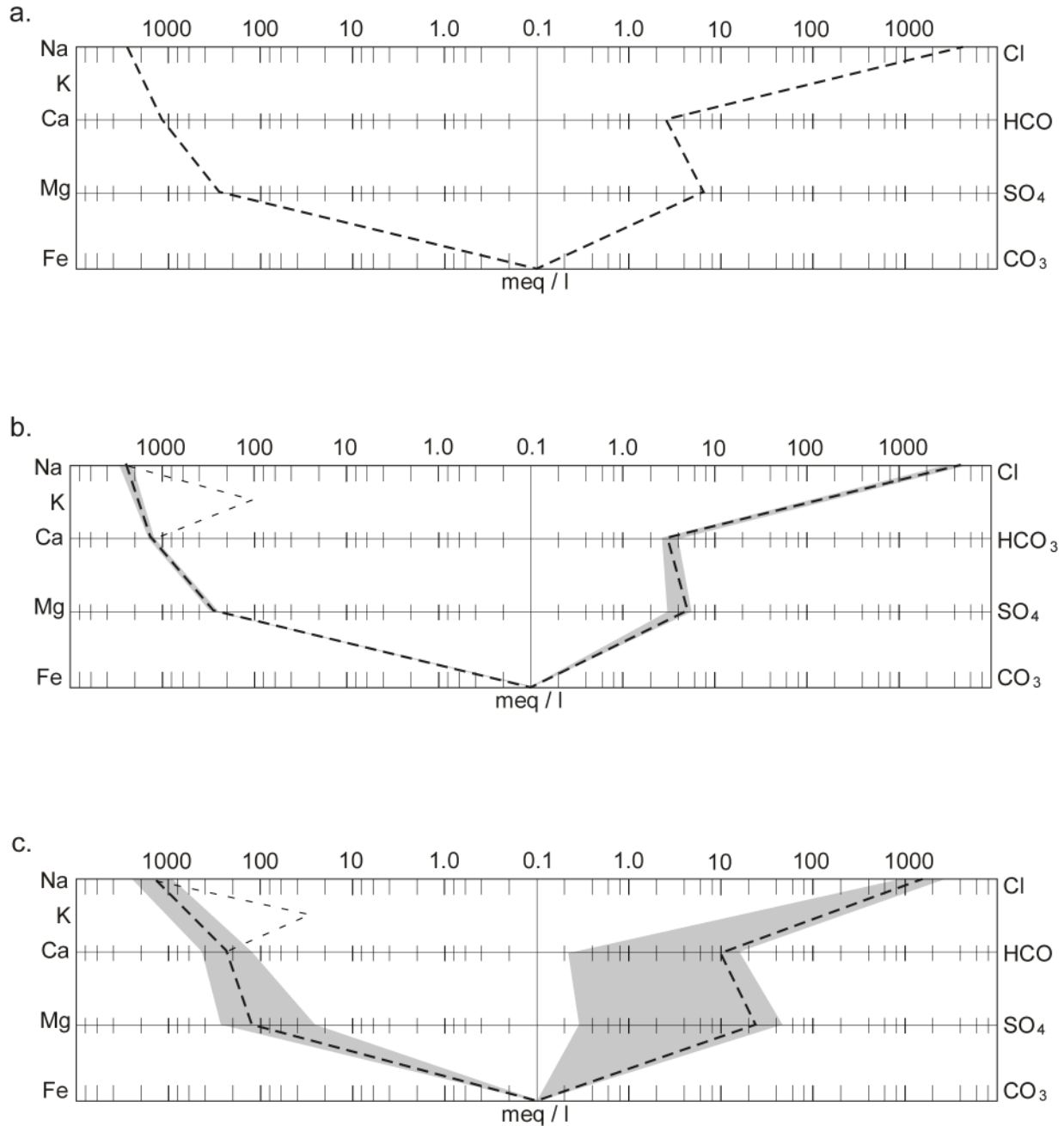


Figure 31. Stiff diagrams of Devonian formation waters in the local-scale study areas: a) Golden Spike (4 analyses), b) Watelet (4 analyses), and c) Redwater (191 analyses). The grey-shaded area shows the range and the bold dashed line represents the average concentrations in meq/l. The thin dashed line represents potassium.

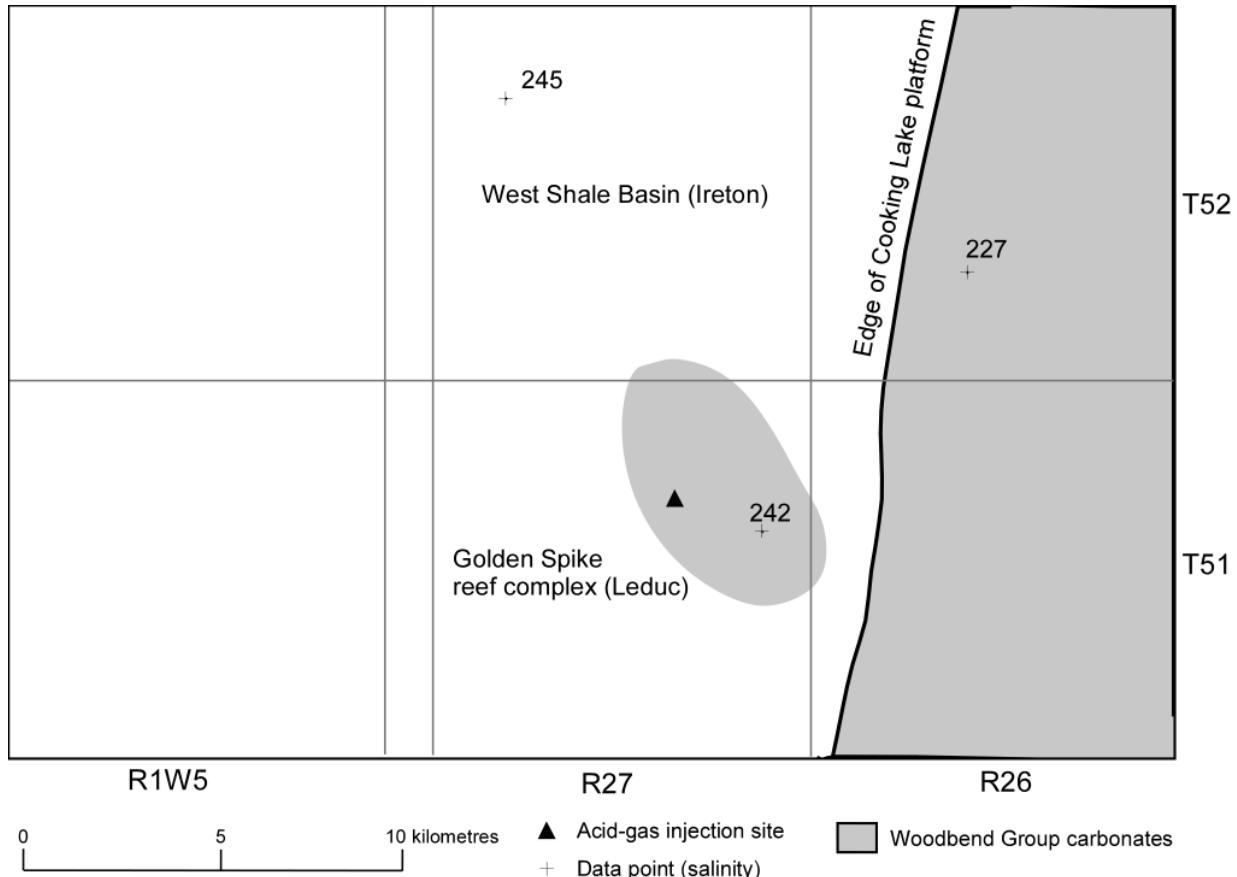


Figure 32. Salinity distribution in the Beaverhill Lake Group in the Golden Spike local-scale study area. Also shown are the extent of the Leduc reefs and the Cooking Lake platform in the overlying Woodbend Group.

Leduc reef (Figure 33), indicating that they are part of the same initial pressure regime. In contrast, the pressure-elevation trend in the overlying Nisku aquifer is offset towards higher pressures, indicating that the intervening Ireton aquitard effectively impedes vertical cross-formational hydraulic communication in the area of the Golden Spike reef complex.

5.2 Watelet-Cooking Lake

5.2.1 Geology

The local-scale study area is defined around the Watelet oil field just south-southwest of Edmonton and includes Townships 47 to 49 and Ranges 25 to 27W4 (Figure 9). The Watelet-Cooking Lake injection site is located about 50 km south-southwest of Edmonton (Figure 9). Acid gas injection takes place in the Upper Devonian Cooking Lake Formation of the Woodbend Group, which is water saturated and underlies a series of thick shale sequences of the Duvernay and Ireton formations (Appendix 1). In the Watelet area the Cooking Lake carbonates lie at depths of about 1800 m to 2100 m (-1060 m to -1350 m elevation) in the Watelet area and have a thickness of 40 m (Figure 34).

The Cooking Lake Formation consists predominantly of limestone and dolostone. Limestones and their dolomitized equivalents consist of varied facies types, including greyish brown nodular mudstones with scattered crinoids and brachiopods, light to medium brown mudstones, and wackestones with gastropods and ostracodes - some with stromatolitic laminations, non-skeletal grainstones with pellets, intraclasts

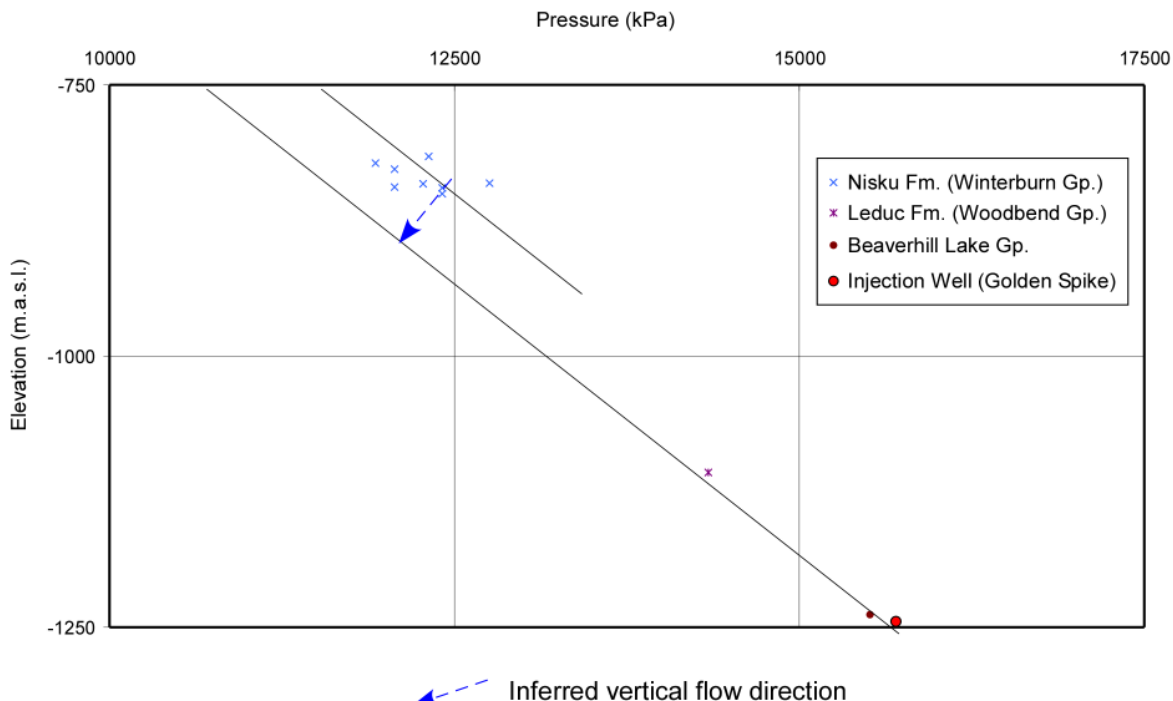


Figure 33. Distribution of pressure versus elevation in the injection stratum (Beaverhill Lake Group) and adjacent formations in the area of the Golden Spike reef complex (Townships 51 - 52, Range 27).

and coated grains, and light to medium brown stromatoporoid rudstones and floatstones (Figure 35). The main porosity types are intercrystalline and vuggy, with minor fracture and moldic porosity. The stromatoporoid-bearing carbonates are thickest beneath and in direct vicinity of the overlying Leduc reef complexes.

Shales of the Duvernay/Ireton Formation overlie the Cooking Lake carbonates with a thickness of more than 100 m (Figure 36). They are interbedded dark brown bituminous shales, dark brown, black and occasionally grey-green calcareous shales and dense argillaceous limestones. Shaly and nodular limestones of the Mildred Member of the Waterways Formation, Beaverhill Lake Group, underlie the Cooking Lake carbonates with a total thickness of about 40 m.

5.2.2 Hydrogeological Characteristics and Rock Properties

Chemistry of Formation Waters

Only 7 chemical analyses of Cooking Lake formation water exist in the local-scale study area. The major constituents are sodium (~50 g/l) and chloride (~150 g/l), making up 83% of the total dissolved solids, and calcium (~30 g/l) (Table 6). The average molal ratio of Na/Cl is 0.5. The brine contains in lesser concentrations potassium, magnesium, bicarbonate and sulfate (Figure 31b). Formation water analyses exist only along the Cooking Lake platform edge in the east and north of the local study area, and there are no analyses in the near vicinity of the Watelet injection site. Salinity decreases from 260 g/l in the southeast to 220 g/l in the northeast (Figure 37a). Both the bicarbonate and sulfate concentrations have a narrow range between 0.16 to 0.4 g/l (Table 6). The average in-situ density of formation water in the Cooking Lake aquifer in the local-scale study area was estimated to be 1180 kg/m³ using the methods presented in Adams and Bachu (2002).

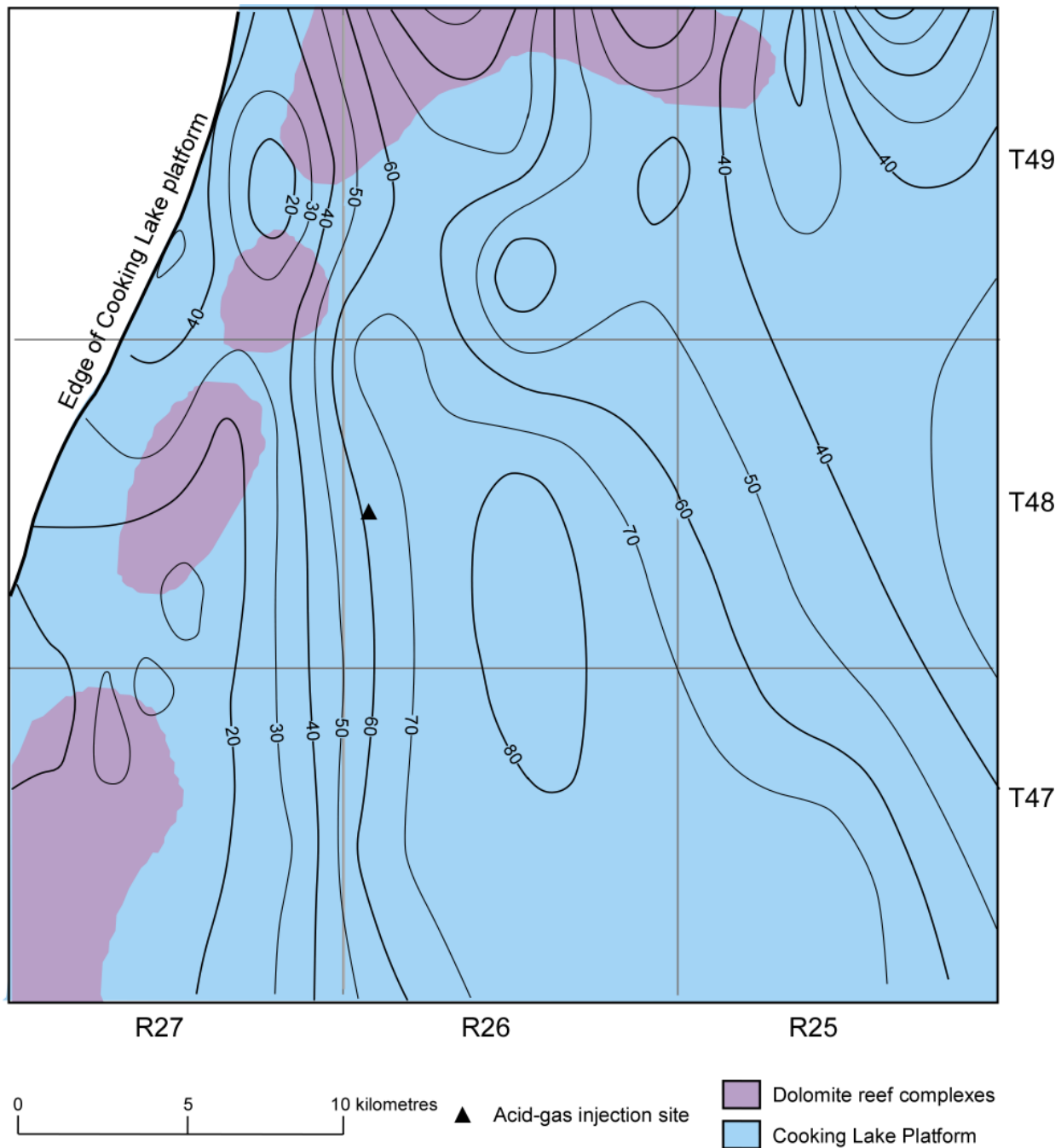


Figure 34. Isopach map of the Cooking Lake Formation in the Watelet local-scale study area. Contours in metres.

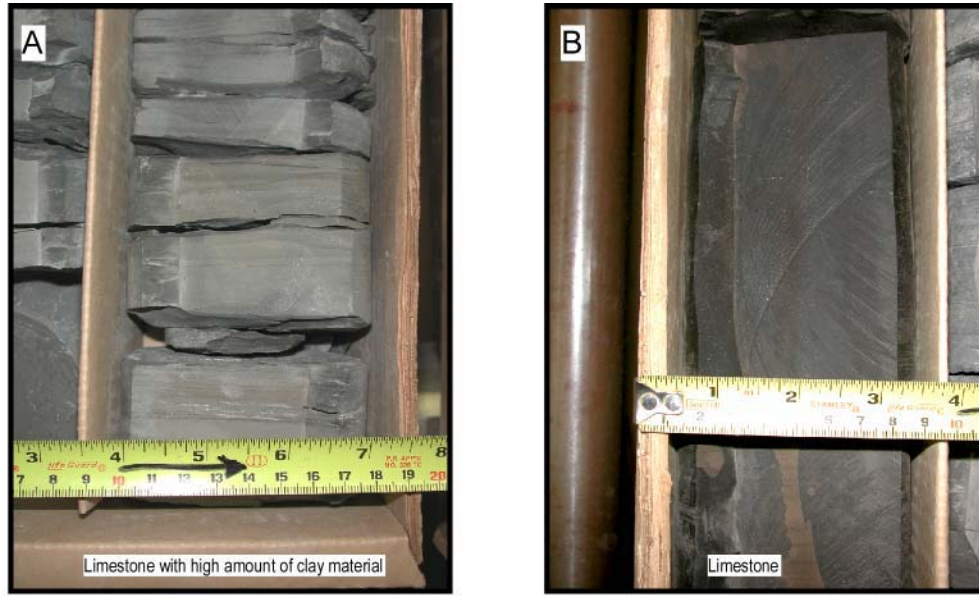


Figure 35. Core and thin-section photographs of the Cooking Lake Formation limestone-dolostone sequence in the Watelet area. Photos A and B show a shaler and a cleaner unit, respectively, indicating facies changes within the Cooking Lake Formation. The thin-section photographs (Photos C and D) show the vuggy micro-porosity as well as “floating” subhedral dolomite crystals in the red-stained limestone. Dolomitization usually enhances reservoir quality.

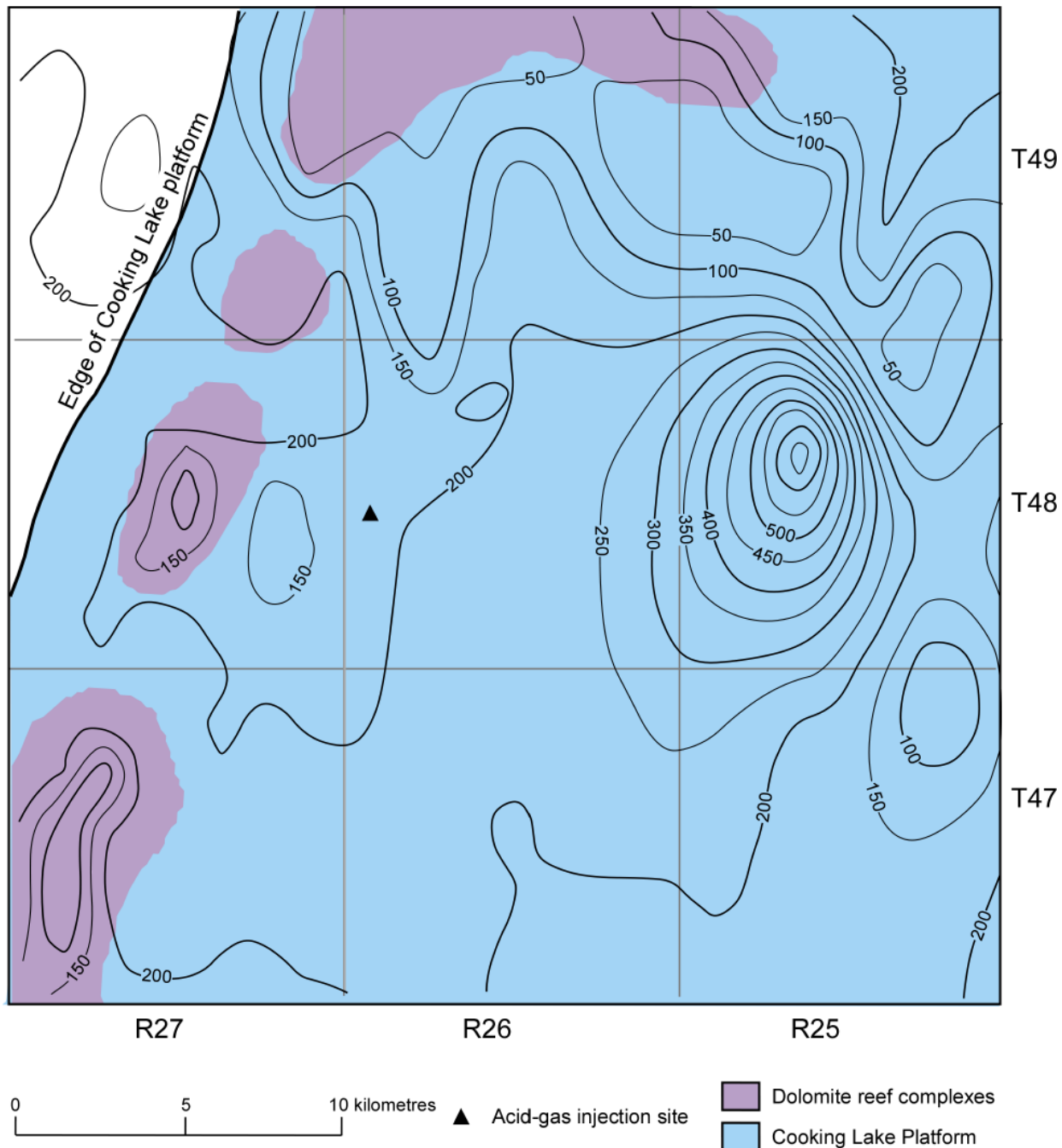


Figure 36. Isopach map of the Ireton Formation above the Cooking Lake Formation showing an average thickness of 200 m of shale on top of the Cooking Lake carbonates. Contours in metres.

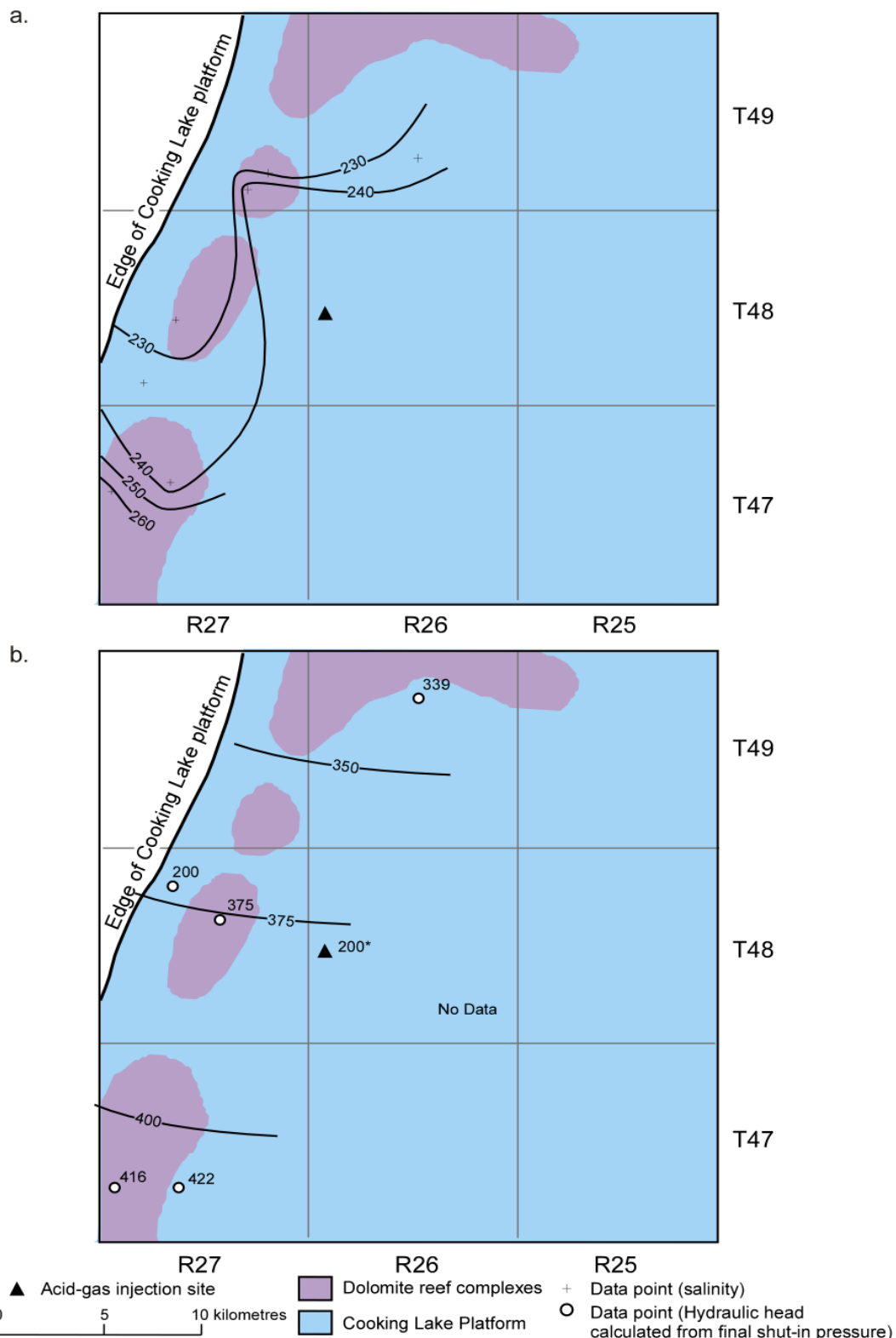


Figure 37. Distribution of a) salinity (g/l), and b) hydraulic heads (m) in the Cooking Lake aquifer in the Watelet local-scale study area. The 200 m hydraulic head values were deemed to be influenced by production and were excluded from the contouring of hydraulic-heads.

Table 6. Major ion chemistry of Cooking Lake brines in the Watelet area (concentrations in g/l).

DLS	Na	K	Ca	Mg	Cl	SO ₄	HCO ₃	TDS
05-21-47-27W4	49.0	4.0	31.6	3.9	149.0	0.234	0.216	239.6
03-19-47-27W4	53.1	4.4	32.0	4.0	162.0	0.256	0.230	260.5
01-16-48-27W4	48.9	n/a	30.9	3.2	139.2	0.204	0.166	222.7
16-05-48-27W4	52.0	n/a	32.0	3.1	145.5	0.164	0.234	233.0
04-10-49-26W4	66.8	n/a	16.4	4.5	145.0	0.375	0.352	233.5
03-02-49-27W4	50.4	n/a	30.0	5.6	144.6	0.346	0.220	244.2
09-02-49-27W4	54.6	n/a	19.5	9.1	139.2	0.164	0.177	260.5
Average	53.5	4.2	27.5	4.8	148.4	0.28	0.23	237.4

Pressure Regime

No high-quality DSTs with Horner-plot extrapolated pressures are available in the Cooking Lake aquifer in the local-scale study area. Therefore, DSTs were used that are of lower quality, only reporting non-Horner-extrapolated, final shut-in pressures. Corresponding hydraulic heads, calculated with a reference density of 1080 kg/m³, vary between 422 m in the southwest to 339 m in the northwest (Figure 37b), indicating northward flow along the Cooking Lake platform edge. The two values of 200 m north of the Wizard Lake reef complex and at the Watelet injection site are abnormally low, and might be affected by production from the nearby Wizard Lake field or of bad quality, and are therefore questionable. They have not been culled from the data set, because they represent, aside from the 422 m value in the southwest, the only measurements that are actually from the Cooking Lake platform, while the other pressure measurements are from overlying Leduc reefs. Also, 200 m is the hydraulic head value that was calculated from the initial reservoir pressure reported by the operator for the Watelet injection interval and was included on the map for reasons of completeness and lack of other, more representative measurements of formation pressures in the Cooking Lake.

The recorded pressures are plotted versus elevation in Figure 38 and compared to pressures in over- and underlying formations. Pressures in the Cooking Lake platform plot along a linear trend representative of the pressure distribution in an underpressured static column of brine. Pressure trends in the overlying Leduc reefs and Winterburn aquifer are shifted towards higher pressures by approximately 2500 kPa and 500 kPa, respectively. This pressure distribution indicates both the potential for upward flow from the Leduc reefs into the Winterburn aquifer and downward flow into the Cooking Lake platform. There is no apparent natural physical explanation for the underpressures and for the existence of a fluid sink in this part of the Cooking Lake aquifer. The hydraulic head value of 200 m at the injection site reflects a reservoir pressure of 15,500 kPa at a depth of 2050 m given by the operator in the original application. Initial reservoir pressures in the neighboring Wizard Lake (Year 1951) and Bonny Glen (Year 1952) Leduc reef complexes are reported as 15,700 kPa at 1940 m depth and 17,300 kPa at 2140 m depth, respectively (EUB, 1998). These reservoir pressures translate into hydraulic head values between 325 m and 365 m, which are in good agreement with the other values in the Watelet area. Therefore, it is very likely that the pressure measured in the Cooking Lake Formation at the Watelet injection site and west of the Wizard Lake reef complex in 1954, were influenced by production from the overlying Leduc reefs in the Wizard Lake complex, and the very low value of 200 m will not be used subsequently.

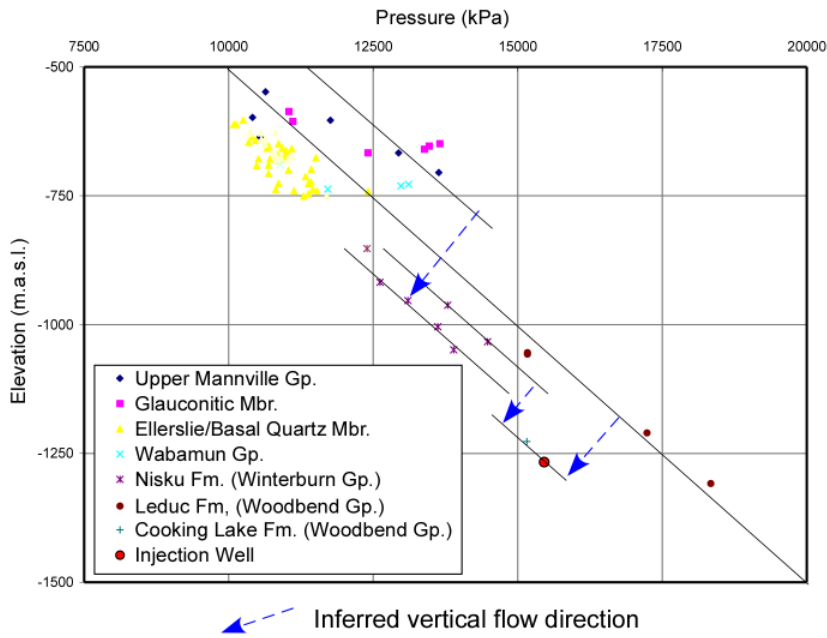


Figure 38. Distribution of pressure versus elevation in the injection stratum (Cooking Lake Formation) and adjacent formations in the Watelet area.

Rock Properties

The well-scale porosity and permeability values for the Cooking Lake/Leduc formations are shown in Table 7. Most measurements in the Cooking Lake-Leduc interval are actually from the Leduc reefs. Porosity values range from 3 to 12%. The horizontal and vertical permeability values are between 3 and 3700 mD, and 0.1 and 850 mD, respectively.

Table 7. Well-scale porosity and permeability values obtained from measurements in core plugs from the Leduc/Cooking Lake formations (9 wells) in the Watelet local-scale study area.

Porosity (%)			Horizontal Permeability (mD)			Vertical Permeability (mD)		
Min	Max	Average	Min	Max	Average	Min	Max	Average
3	12	8	3	3710	976	0.1	854	643

Flow of Formation Water

The pressure regime and hydraulic head distribution in the Cooking Lake aquifer (including data from the Leduc Formation) suggest that the flow of formation water is northward along the platform edge towards the Grosmont platform, as shown in the regional flow interpretation. The low pressures measured in the Cooking Lake platform were probably influenced by production-induced drawdown originating in the overlying Leduc reefs, and therefore do not represent virgin formation pressures. The Watelet acid-gas injection occurs in an area where the Cooking Lake platform is not overlain by any Leduc reefs. Still, the bottom hole pressure measured in 2000, before the start-up of injection, is low and the corresponding hydraulic head of 200 m again suggests that the pressures in the Cooking Lake platform were influenced by production from the Wizard Lake Leduc reef complex, approximately 10 km away. Similar effects of production from the Leduc Formation on pressures in the Cooking Lake and neighbouring Leduc reefs were reported for the Westerose Leduc pool (Hnatuk and Martinelli, 1967; Randall, 1975) just south of the Watelet area. The high salinity of brines (>200 g/l) shows that these waters have not been diluted with

fresher formation waters from the Lower Mannville aquifer, as it is observed farther east of the Watelet area.

5.3 Redwater-Leduc

5.3.1 Geology

The local-scale study area is defined around the Redwater oil field just northeast of Edmonton and includes Townships 55 to 59 and Ranges 20 to 25W4 (Figures 9 and 39). Injection takes place in the Leduc Formation Redwater reef, a previously producing oil reservoir. This large, depleted oil reservoir is currently used for water disposal. Acid gas dissolved in water, forming a weak acidic solution (“sour water”), is injected in this reef through 49 alternating wells. The Leduc Formation carbonates lie at depths of about 1000 m (-400 m elevation) in the Redwater field and have a thickness of 160 to 200 m in the injection area (Figure 39).

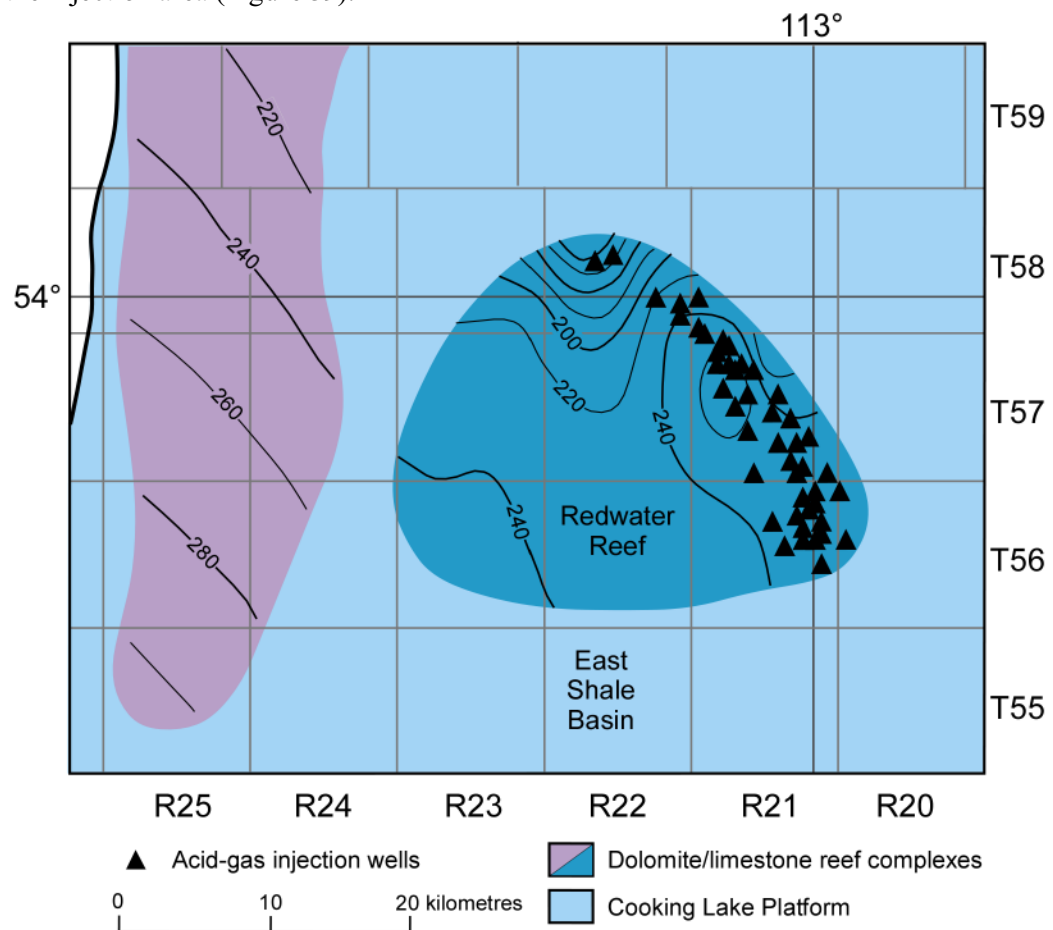


Figure 39. Isopach map of the Leduc Formation Redwater reef. Contours in metres.

The Leduc Formation carbonates in the Redwater field form a large reefal build-up (Figures 40 and 38; Appendix 1). The build-up consists mainly of medium to light-gray fossiliferous limestone (84%), with minor (15%) amounts of secondary, patchy replacement dolomite. In addition, there are traces of iron minerals (fracture infills and stylolites) and anhydrite, as well as other unidentified opaque materials (Figure 41). Porosity consists mainly of intercrystalline and moldic porosity, as well as fractures.

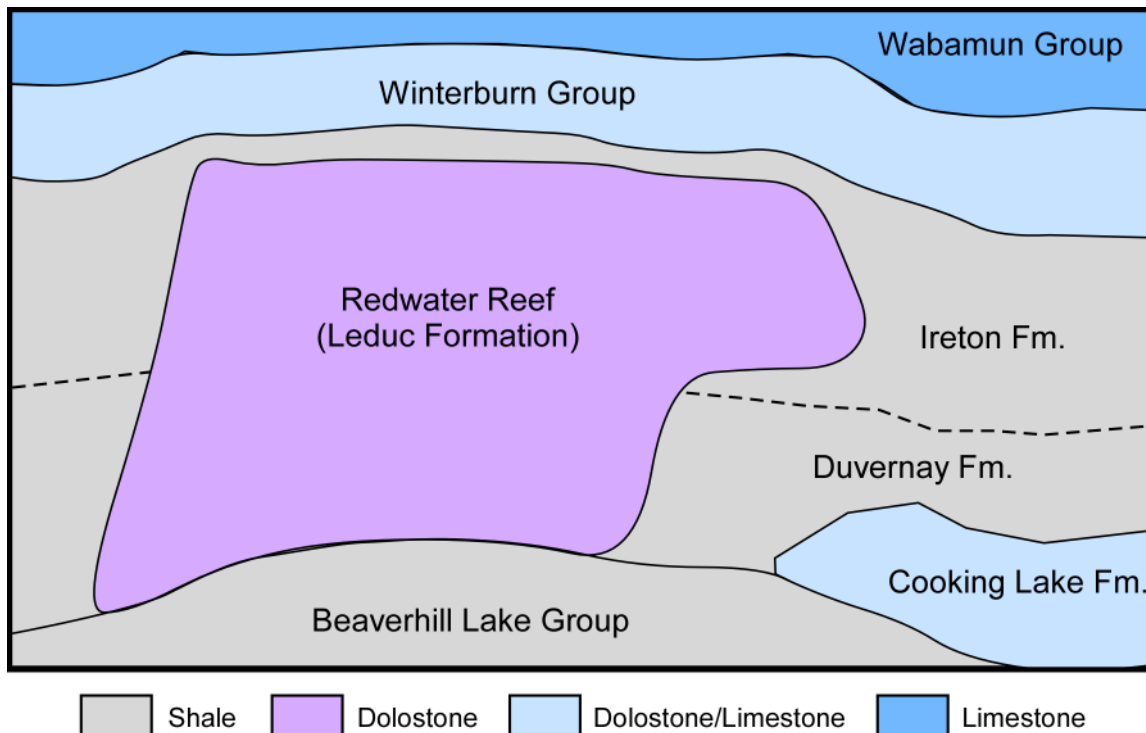


Figure 40. Schematic stratigraphic cross-section of the Leduc Formation Redwater reef from west to east, showing thinning and termination by shales towards the east.

The Redwater reef is capped by shales of the Ireton Formation, which are 10-50 m thick immediately above the reef and thicken to approximately 120 m in the East-Shale basin (Figure 42). The reef developed directly on platform carbonates of the Cooking Lake Formation (Figure 43) (rock features as described above). The Cooking Lake Formation is in turn underlain by shales and nodular limestones of the Waterways Formation, which are generally thicker than 50 m and have very low porosity.

5.3.2 Hydrogeological Characteristics and Rock Properties

Chemistry of Formation Water

Almost 200 analyses of Leduc formation waters are available in the local-scale study area and the concentration ranges and averages of dissolved solids are shown in Table 8. The major constituents of the Leduc formation water are sodium (33 g/l) and chloride (63 g/l), making up 92% of the total dissolved solids, and in lesser concentrations calcium, potassium, magnesium, bicarbonate and sulfate (Figure 31c). The average molal ratio of Na/Cl is 0.8. Salinity in the Redwater area ranges from 85 to 140 g/l. The lowest values of 90 g/l or less are observed in the northeast and southeast corner of the study area (Figure 44a). There is a southeast - northwest trend of less saline formation water (< 100 g/l), centered on the Redwater reef outline, whereas the off-reef areas are filled with more saline brine (up to 140 g/l). The in-situ density of formation water in the Cooking Lake aquifer in the local-scale study area was estimated to be 1083 kg/m³ using the methods presented in Adams and Bachu (2002).

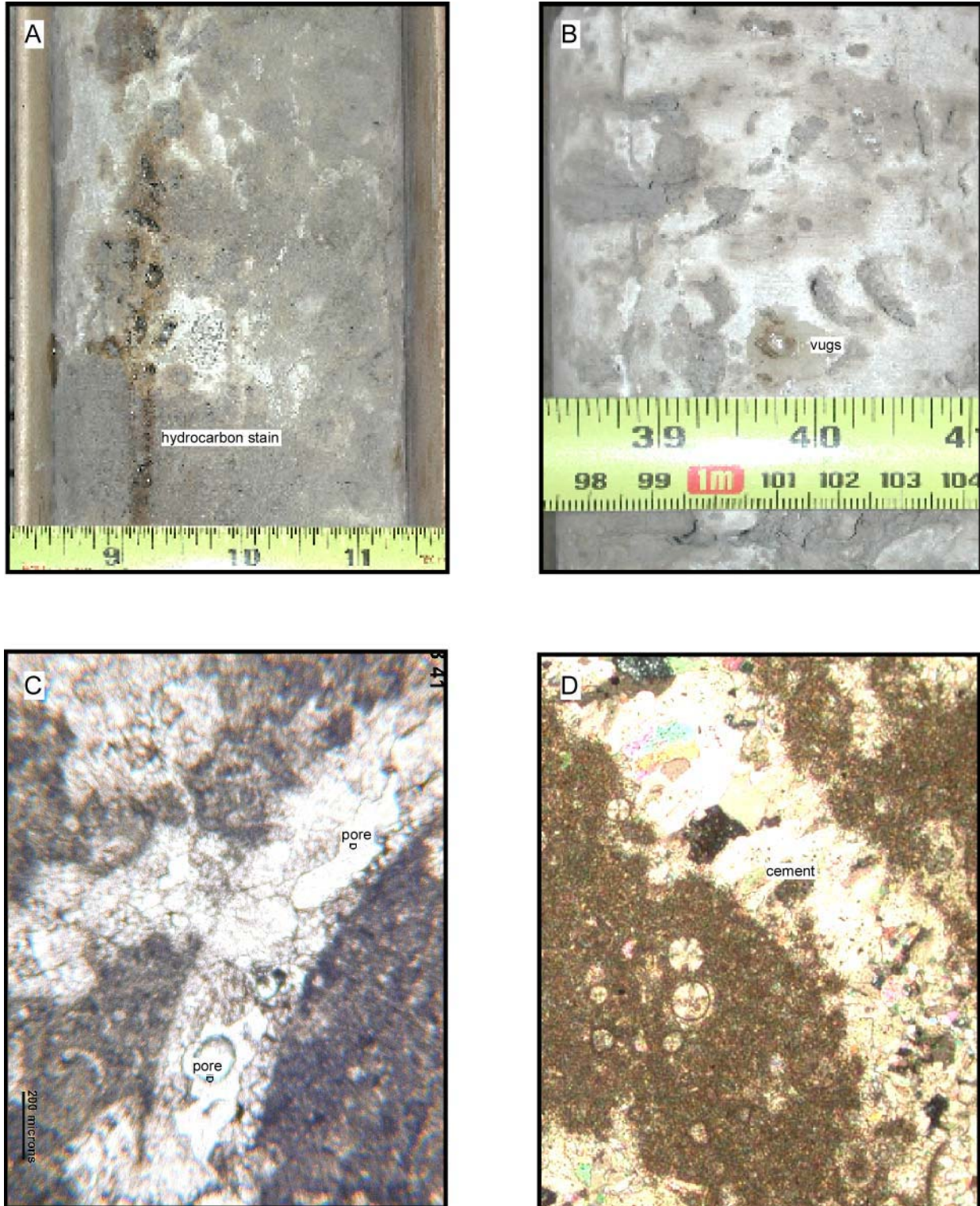


Figure 41. Core and thin-section photographs of the Leduc Formation limestone-dolostone sequence at Redwater. Photos A and B show the vuggy and very high porosity of the reefal dolostones, whereas Photos C and D depict the smaller sized moldic porosity in thin-section where fossil shells were dissolved and stayed open (Photo C) or were later filled with cement (Photo D).

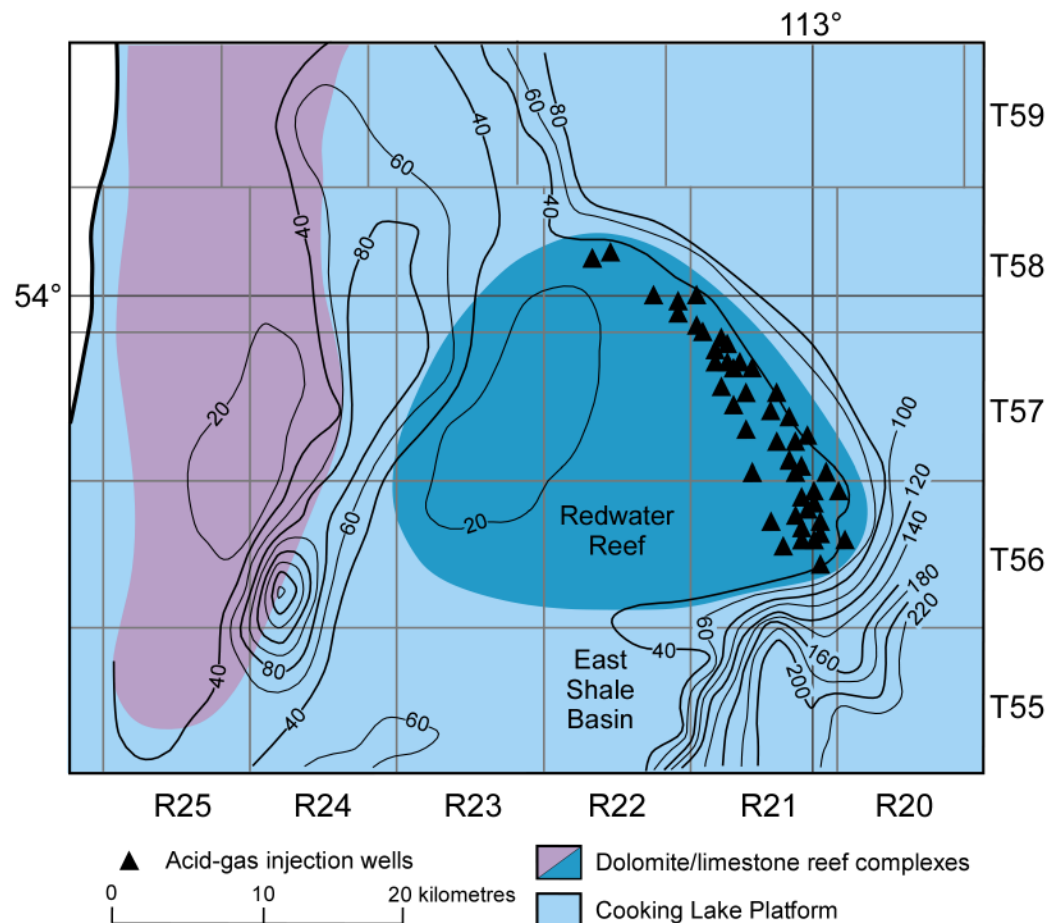


Figure 42. Isopach map of the Ireton Formation in the Redwater local-scale study area. Note the thinning of the Ireton shales above the Leduc reefs and the thickening towards the shale basin. Contours in metres.

Table 8. Summary of major ion chemistry of Leduc/Cooking Lake brines based on 191 analyses (see Appendix 2) in the Redwater area (concentrations in g/l).

	Na	K	Ca	Mg	Cl	SO ₄	HCO ₃	TDS
min	19.2	0.5	2.4	0.3	34.4	0.01	0.007	58.6
max	56.2	2.3	10.7	4.3	100.4	2.45	1.091	164.7
average	32.6	1.4	5.2	1.6	63.0	1.24	0.613	104.1

Pressure Regime

High-quality DST data from the Cooking Lake aquifer exist in the western half of the study area and they are from the Leduc reefs along the Cooking Lake platform margin. This set of pressure measurements was augmented with presumably lower-quality DST data from the Redwater reef complex in the east, for which only final shut-in pressures are available (not extrapolated to formation pressure).

Corresponding hydraulic heads, calculated with a reference density of 1080 kg/m³, decrease from approximately 320 m along the southern, western and eastern boundaries of the study area to 270 m in the center and in the north (Figure 44b). The inferred flow direction from the hydraulic head distribution is northward, and flow appears to be channelled towards the Leduc Formation Redwater reef complex and out of it.

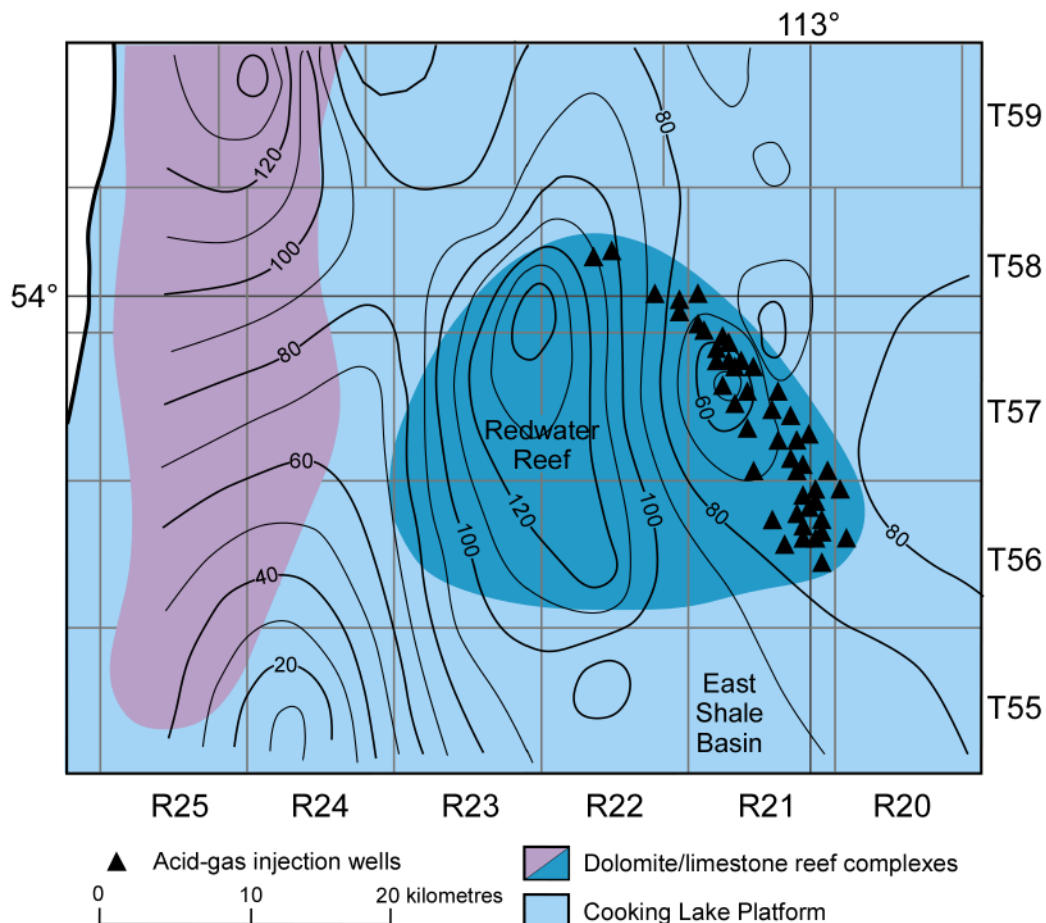


Figure 43. Isopach map of the Cooking Lake Formation in the Redwater local-scale study area. Note the thickening of the platform carbonates underneath the Leduc reefs and thinning towards the basin. Contours in metres.

The recorded pressures are plotted versus elevation in Figure 45 and compared to pressures in the over- and underlying formations. Pressures in the Cooking Lake aquifer plot approximately along a linear trend representative of the pressure distribution in a static column of brine with a density of 1080 kg/m^3 . Pressure measurements from the overlying Winterburn to Lower Mannville aquifer plot along the same trend, suggesting possible hydraulic continuity between these aquifers. In contrast, pressure measurements from the Upper Mannville aquifer and the underlying Beaverhill Lake Group follow a parallel trend with higher pressures, which suggests that the intervening Clearwater-Upper Mannville aquitard at the top of the succession, and the underlying Waterways aquitard are effective barriers to cross-formational flow. The fact that hydraulic-heads and pressures are lower in the intervening Cooking Lake to Lower Mannville aquifers than in the Upper Mannville and Beaverhill Lake indicates potential for downward and upward vertical flow from these aquifers, respectively.

Rock Properties

The well-scale porosity and permeability values for the Cooking Lake/Leduc formations are shown in Table 9. Most measurements in the Cooking Lake-Leduc interval are actually from the Leduc reefs. Porosity ranges between 1 and 17%, being on average 7%. The horizontal and vertical permeability values in the Cooking Lake-Leduc interval span several orders of magnitude, from 0.01 to 4000 mD and 0.01 to 670 mD, respectively.

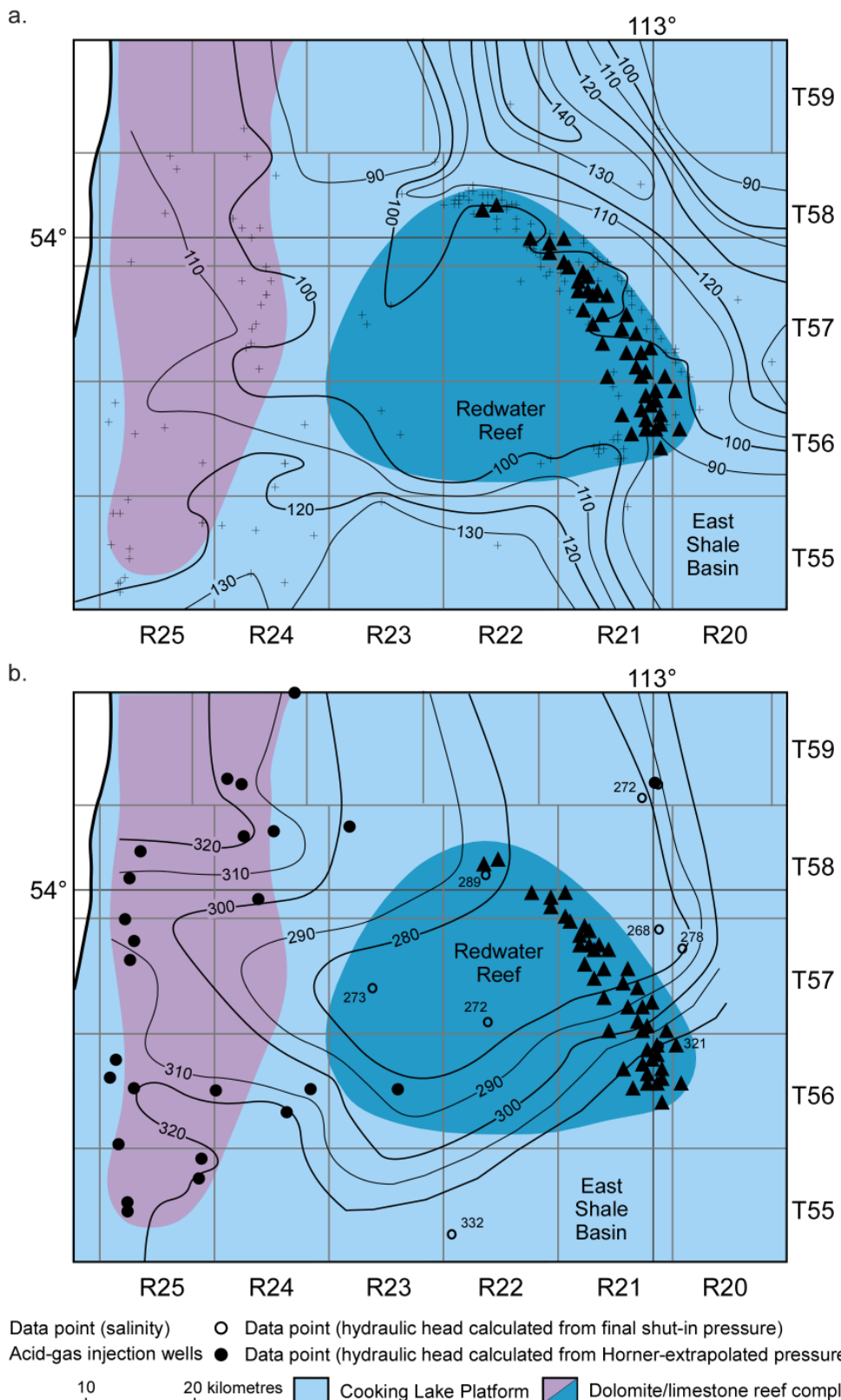


Figure 44. Distribution of a) salinity (g/l), and b) hydraulic heads (m) in the Cooking Lake aquifer in the Redwater local-scale study area.

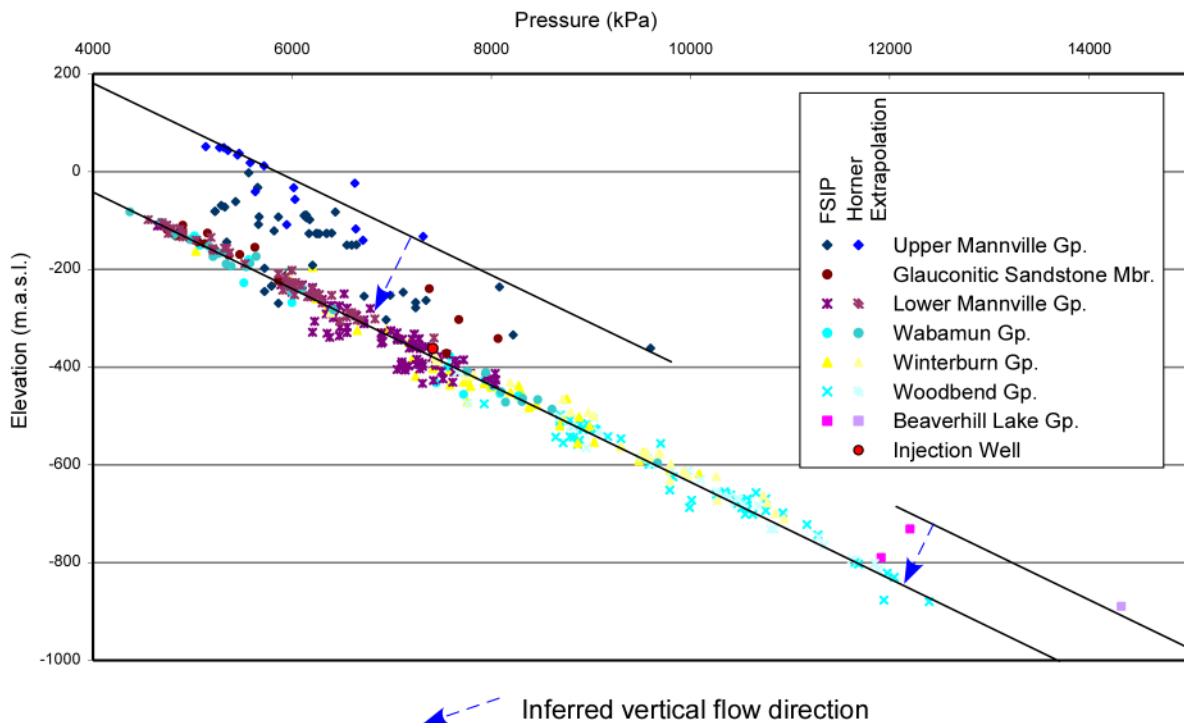


Figure 45. Distribution of pressure versus elevation in the injection stratum (Leduc Formation) and adjacent formations in the Redwater local-scale study area.

Table 9. Well-scale porosity and permeability values obtained from measurements in core plugs from the Leduc/Cooking Lake formations (239 wells) in the Redwater local-scale study area.

Porosity (%)			Horizontal Permeability (mD)			Vertical Permeability (mD)		
Min	Max	Average	Min	Max	Average	Min	Max	Average
1	17	7	0.01	3940	330	0.01	670	30

Flow of Formation Water

The pressure regime and hydraulic head distribution in the Cooking Lake aquifer suggest that flow of formation water is northward towards the Grosmont platform as shown in the regional flow interpretation. Furthermore, there is potential hydraulic communication between the Cooking Lake, Winterburn, Wabamun and Lower Mannville aquifers, as indicated by a similar pressure-versus-elevation trend (Figure 45) and comparable hydraulic head values. This can be explained by the fact that, in the Redwater area, the Wabamun-Winterburn aquifer system is in direct contact with the Lower Mannville aquifer and the Ireton aquitard thins to less than 15 m above the western part of the Redwater reef complex. The Lower Mannville sandstones shale out in the Redwater area (Figure 18a), the ensuing decrease in permeability favouring formation water flow downwards into the slightly-higher permeable, yet discontinuous Wabamun-Winterburn strata, and further down into the highly permeable Cooking Lake-Leduc aquifer. The Cooking Lake aquifer connects with the Grosmont reef complex to the north, forming a preferential flow path and effective drainage system for regional flow in central Alberta. A detailed pressure-versus-elevation plot (Figure 46) in Townships 57-58 Ranges 20-21 shows the potential for downward flow from the Mannville into the Cooking Lake aquifer. Another indication for possible

downward-penetrating Mannville formation waters into the Cooking Lake aquifer is the “plume” of diluted brine (<100 g/l) in the area of the Redwater reef complex (Figure 44a). Also, Leduc formation waters in the Redwater area are of a Na-Cl type, as opposed to the typical Na-Ca-Cl type for undiluted Devonian brines in central Alberta (Michael et al., 2003), which suggests mixing of Devonian and Cretaceous Mannville waters at Redwater.

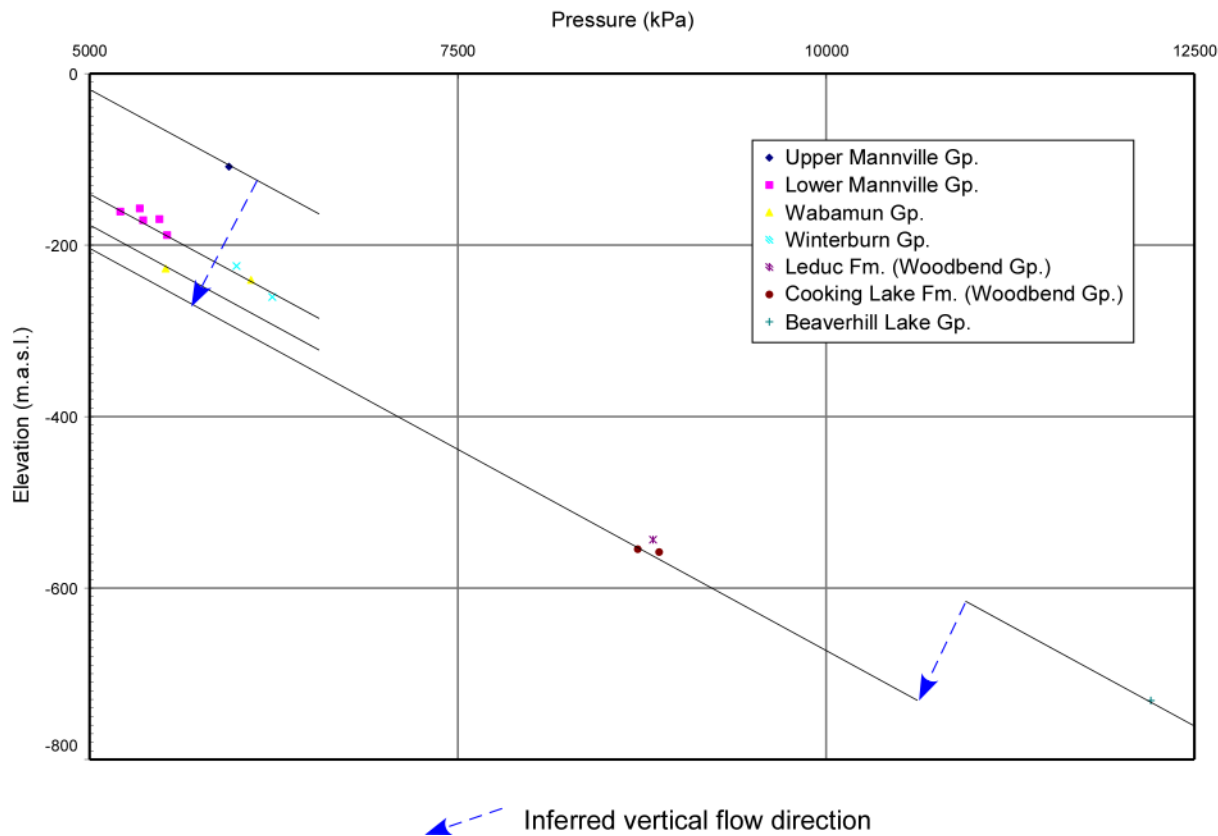


Figure 46. Distribution of pressure versus elevation in the injection stratum (Leduc Formation) and adjacent formations in Townships 57-58, Ranges 20-21 in the Redwater local-scale study area.

5.4 Acheson-Basal Quartz

Acheson is the oldest acid-gas injection operation anywhere in the world. Initially, approval was granted to inject the acid gas in the Blairmore T gas pool in the Acheson field. This Basal Quartz gas pool was located in the vicinity of St.Albert — Big Lake Ostracod. In 2003, CO₂ broke through at one producing well in the St. Albert — Big Lake Ostracod A gas pool (see Section 6.1). This led to a reevaluation by EUB of pool boundaries on the basis of pressure data and new stratigraphic interpretation, and inclusion in September 2003 of the Blairmore T gas pool in the larger St. Albert — Big Lake Ostracod A pool.

5.4.1 Geology

The local-scale study area is defined around the Acheson oil field just west of Edmonton and includes Townships 52 to 54 and Ranges 25 to 27W4 (Figures 9 and 47). The injection zone in the Acheson field lies within the Cretaceous Ellerslie Member, which is equivalent to the Basal Quartz. The Basal Quartz sandstones lie at depths of about 1200 m (-500 m elevation) in the Acheson field and have a thickness of 75 to 90 m in the injection area (Figure 47; Appendix 1), however the net pay zone may be smaller.

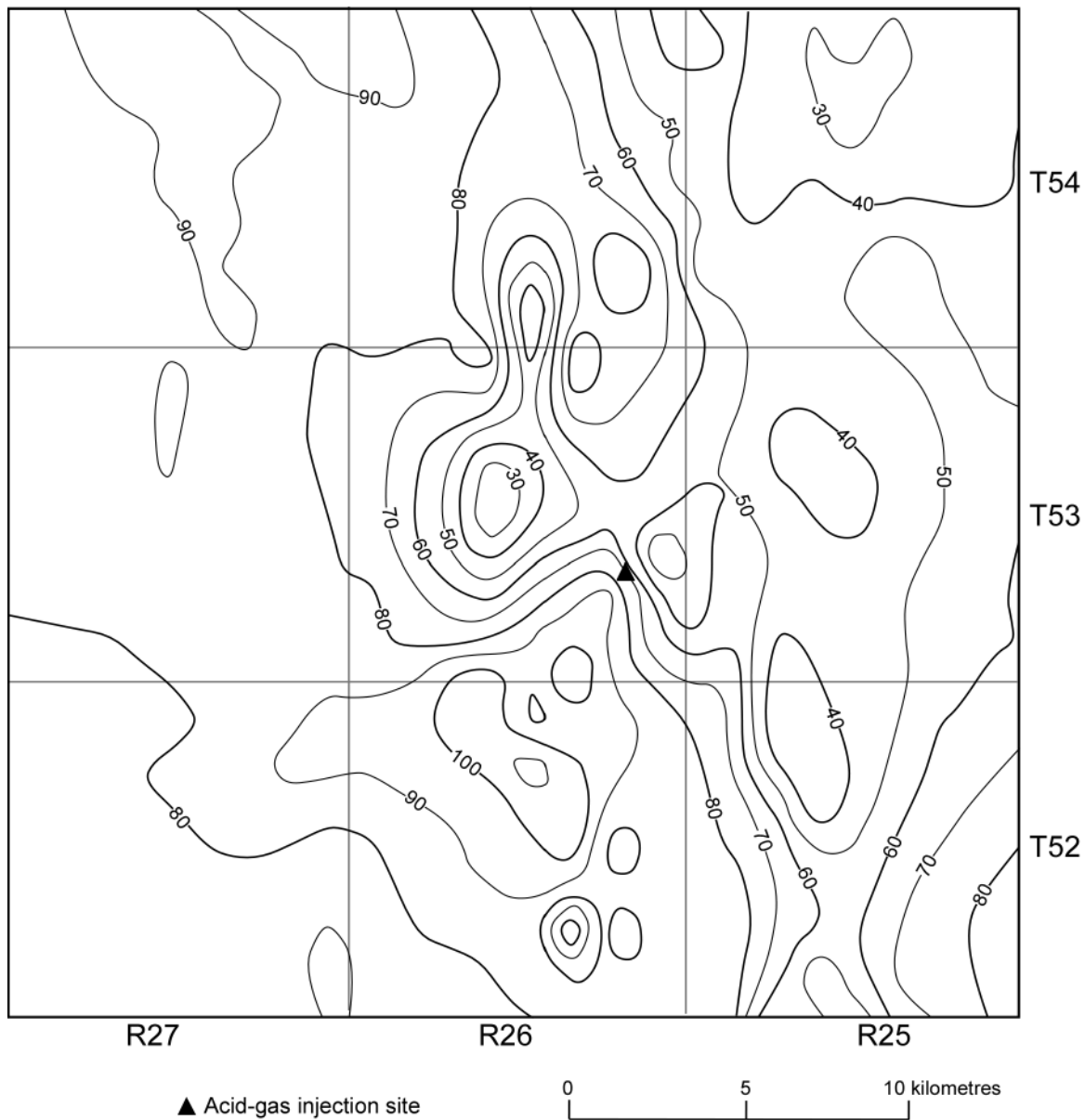


Figure 47. Isopach map of the Basal Quartz Member in the Acheson local-scale study area. Contours in metres.

The Basal Quartz sandstones are gray to brown, often have a “salt & pepper” appearance, and are fine grained, silty, moderately sorted, porous with well-developed interbeds of gray silty shale (Figure 48). The porosity type is mainly intergranular and the grain and pore sizes are in the 10 µm to 50 µm scale.

The injection units are part of the Lower Mannville Group and are overlain by thick (100 m) shale/sand/silt packages of the Upper Mannville Group, which are not subdivided, but can be considered equivalents to the Clearwater Formation. The Ellerslie Member is underlain by the Upper Devonian Wabamun Group, which consists of mostly tight limestones more than 150 m in thickness.

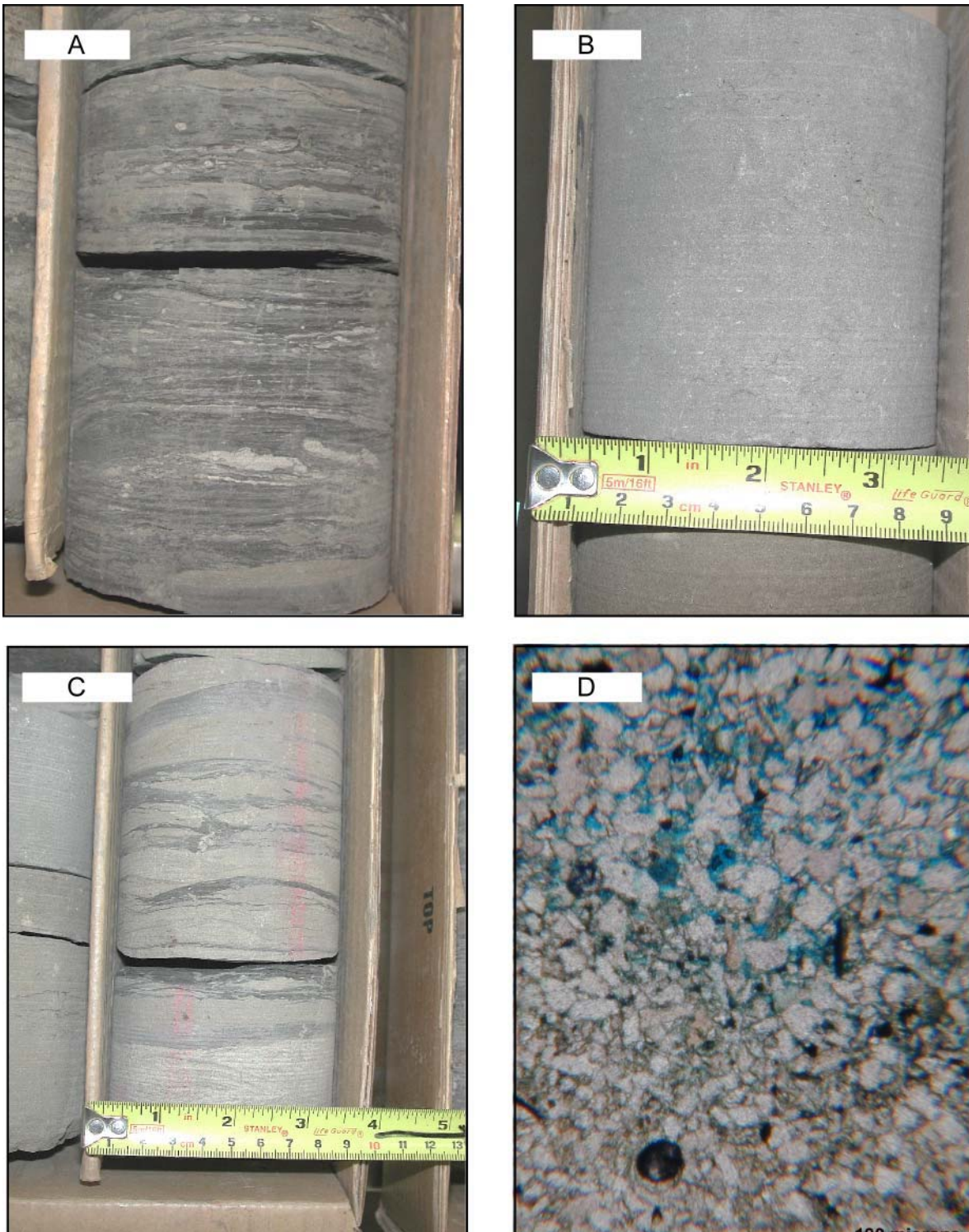


Figure 48. Core and thin-section photographs of the Ellerslie/Basal Quartz Member sandstone at the Acheson injection site. Banded silt to sandstones (Photo A) change to porous, grainy sandstone (Photo B), which consist mainly of quartz, with minor clay layers (Photo C). The intergranular porosity can best be seen on the blue stained parts of the thin-section photo in the upper half of the picture (Photo D).

5.4.2 Hydrogeological Characteristics and Rock Properties

Chemistry of Formation Water

Seventy-one analyses of Lower Mannville formation water exist in the local-scale study area (Table 10). The major constituents are sodium and chloride, making up 93% of the total dissolved solids, and in lesser concentrations calcium, magnesium, potassium, bicarbonate and sulfate (Figure 49a). The average molal ratio of Na/Cl is 0.8. Generally, the salinity in the Acheson area is relatively constant around 110 g/l (Figure 50a). Only in Range 25, between Townships 52 and 53, a tongue of slightly less saline formation water of less than 90 g/l extends into the study area from the east (see also Figure 21a). The in-situ density of formation water in the Lower Mannville aquifer in the local-scale study area was estimated to be 1088 kg/m³ using the methods presented in Adams and Bachu (2002).

Table 10. Major ion chemistry of Lower Mannville brines based on 71 analyses (see Appendix 2) in the Acheson area (concentrations in g/l).

	Na	K	Ca	Mg	Cl	SO ₄	HCO ₃	TDS
Minimum	25.2	0.1	2.2	0.6	47.9	0.03	0.1	78..
Maximum	43.2	1.7	6.9	1.6	76.0	0.8	0.9	124.6
Average	33.2	0.8	4.84	1.1	62.8	0.3	0.4	102.6

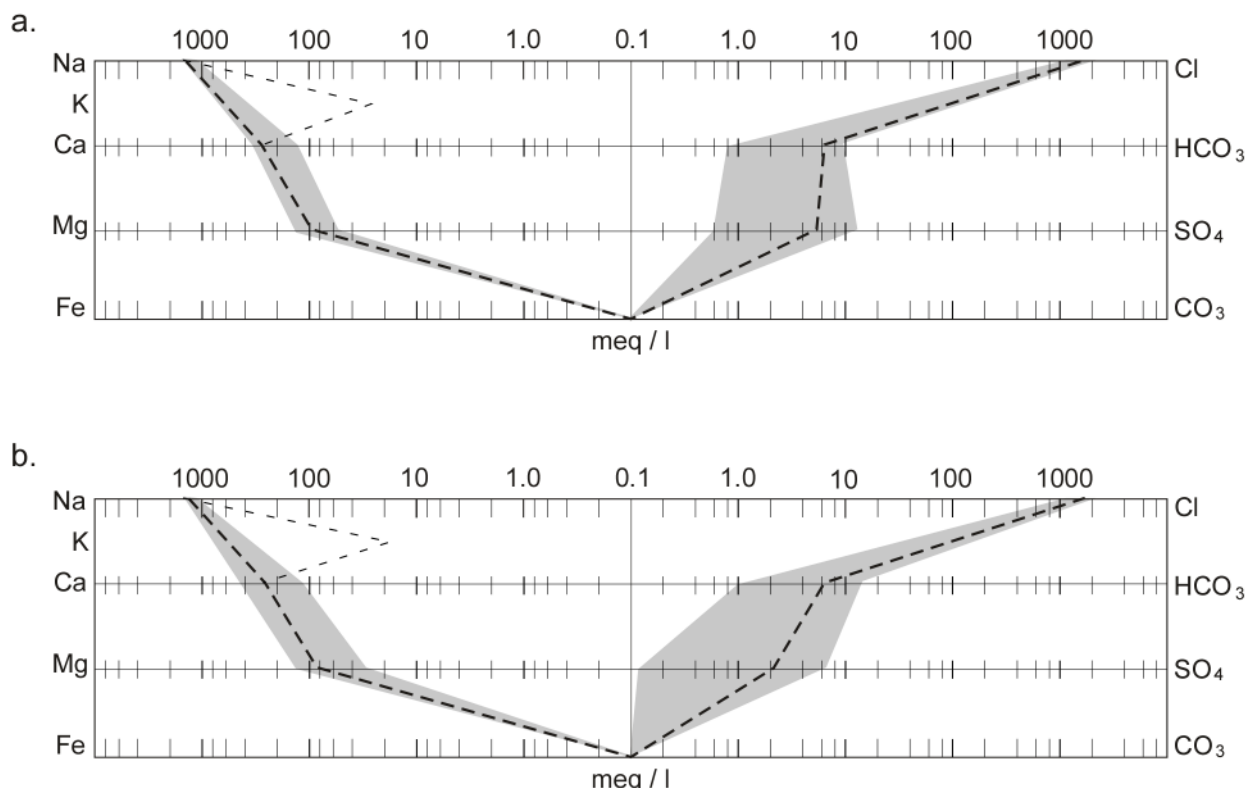


Figure 49. Stiff diagrams of Lower Mannville formation waters in the local-scale study areas: a) Acheson (42 analyses) and b) Strathfield (35 analyses). The grey-shaded area shows the range and the bold dashed line represents the average concentrations in meq/l. The thin dashed line represents potassium.

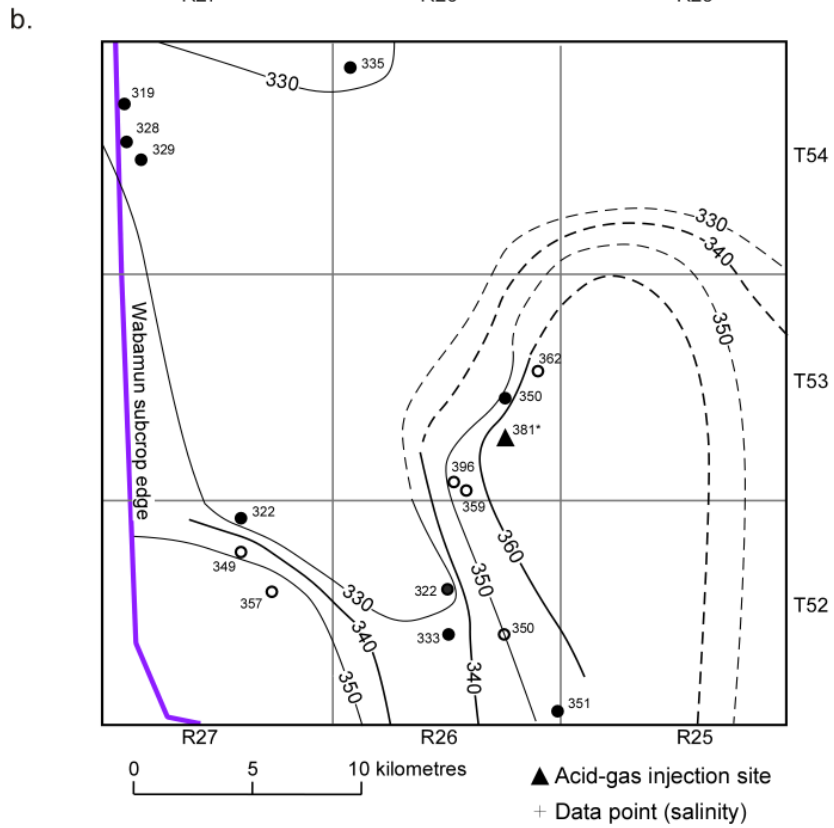
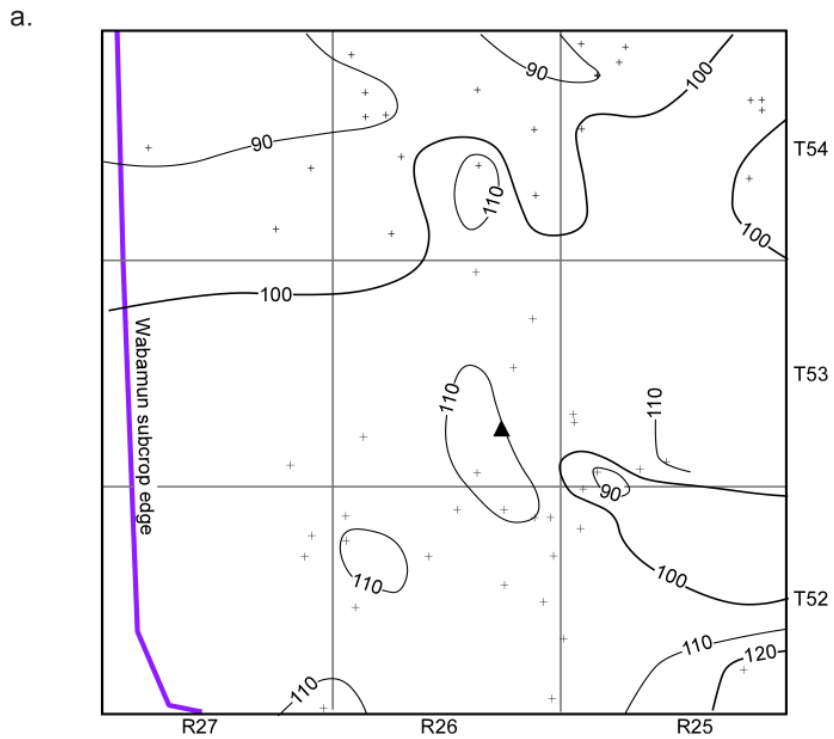


Figure 50. Distribution of a) salinity (g/l), and b) hydraulic heads (m) in the Lower Mannville aquifer in the Acheson local-scale study area. Dashed contour lines are extrapolated from regional-scale map (Figure 24a).

Pressure Regime

Only nine high-quality DSTs exist for the Lower Mannville aquifer in the Acheson area. This set of pressure measurements was augmented with presumably lower-quality DST data, for which only non-Horner extrapolated, final shut-in pressures are available.

Corresponding hydraulic heads, calculated with a representative density of 1080 kg/m³ (Bachu and Michael, 2002), decrease from above 360 m in the southeast to less than 330 m in the center of the study area (Figure 50b). Flow inferred from the hydraulic head distribution appears to be channelled northwestward following the regional flow pattern (Figure 24a).

The recorded pressures are plotted versus elevation in Figure 51 and compared to pressures in the over- and underlying formations. Pressures in the Lower Mannville aquifer spread along a linear trend that is representative of the pressure gradient in a static column of brine with a density of 1088 kg/m³. Pressures measurements from the underlying Wabamun, Winterburn and Cooking Lake aquifers plot along the same trend, suggesting possible hydraulic continuity between these aquifers. The spreading of data points between the upper and lower line implies a downward gradient of flow from the Lower Mannville into the Cooking Lake aquifer. In contrast, pressure measurements from the Upper Mannville aquifer follow a parallel trend that is offset distinctively towards higher pressures, which suggests that the intervening Clearwater-Upper Mannville aquitard is an effective barrier to cross-formational flow.

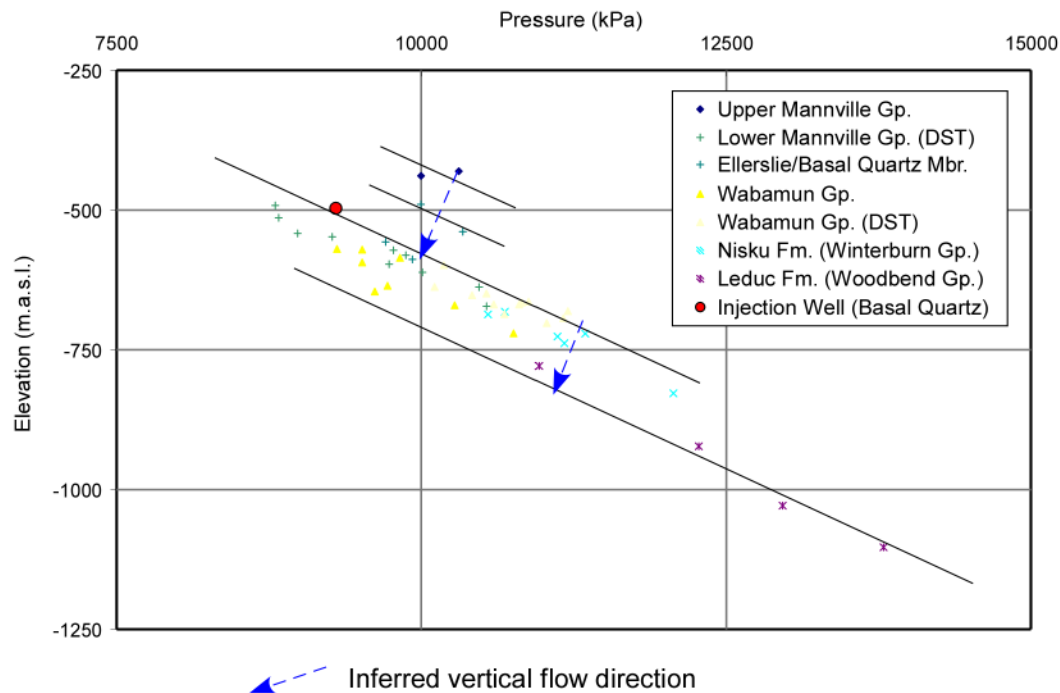


Figure 51. Distribution of pressure versus elevation in the injection stratum (Ellerslie Member) and adjacent formations in the Acheson area.

Rock Properties

The well-scale porosity and permeability values for the Ellerslie/Basal Quartz Member, the overlying Glauconitic Sandstone and the underlying Wabamun strata are shown in Table 11. Average porosity (16%) and permeability ($k_H = 150$ mD, $k_V = 50$ mD) in the injection strata, the Ellerslie/Basal Quartz, are noticeably higher than the respective values in the over- and underlying strata. In comparison, the average porosity values in the Glauconitic Sandstone and Wabamun Group are 13% and 8%, respectively. Average horizontal and vertical permeability values are 36 mD and 24 mD (Glauconitic Ss) and 32 mD and 7 mD (Wabamun Group), respectively. The porosity and permeability measured from core in the confining strata (Glauconitic Sandstone and Wabamun Group) probably are biased towards higher values than would be expected for these units generally characterized as aquitards, because core is preferably taken from potentially high-permeability productive zones.

Table 11. Well-scale porosity and permeability values obtained from measurements in core plugs from the Lower Mannville (67 wells) and Wabamun (13 wells) groups in the Acheson local-scale study area.

Formation/Group	Porosity (%)			Horiz. Permeability (mD)			Vert. Permeability (mD)		
	Min	Max	Average	Min	Max	Average	Min	Max	Average
Glauconitic	9	17	13	0.2	250	36	0.04	133	24
Ellerslie/BQTZ	9	28	16	0.5	1600	150	0.1	225	50
Wabamun	4	10	8	10	58	32	1.1	22	7

Flow of Formation Water at Acheson

The pressure regime and hydraulic head distribution in the Lower Mannville aquifer at Acheson suggest that the flow of formation water generally is northwestward as shown in the regional flow interpretation. The Acheson area is located east of the Mississippian subcrop, therefore the Upper Devonian (Wabamun-Winterburn) aquifer system is in direct contact with the Lower Mannville aquifer. The underlying Ireton aquitard thins to less than 40 m above the Acheson Leduc reef complex. There is potential for downward flow from the Lower Mannville aquifer into the underlying Wabamun, Winterburn, and Cooking Lake aquifers, as indicated by a continuous offset in pressure-versus-elevation trends (Figure 51) and slightly decreasing hydraulic head values from approximately 325 m in the Lower Mannville aquifer and Wabamun-Winterburn aquifer system to less than 300 m in the Cooking Lake aquifer. (Figures 22 and 23a). This apparent sink for formation water in the Cooking Lake aquifer appears not to be connected to the northwestwardly channelled flow towards the “Grosmont drain”. Due to the lack of a natural mechanism that could explain these underpressures, it is very likely that the pressure measurements were affected by hydrocarbon production from the Lower Mannville in the Acheson and/or Acheson East pools and/or are the result of poor-quality test data

5.5 Strathfield-Ellerslie

5.5.1 Geology

The local-scale study area for the Strathfield injection site is located south-southwest of Edmonton and includes Townships 48 to 50 and Range 26W4 to Range 1W5 (Figures 9 and 52). Acid gas injection in the Strathfield area takes place in the Cretaceous Ellerslie Member (Basal Quartz equivalent) of the Lower Mannville Group (Appendix 1). There is not much information available for this site, most likely because of its sparse well control and lack of core. The Ellerslie Member sandstones lie at depths of about 1200 m

in the Strathfield area and have a thickness of 40 to 110 m in the local-scale study area (Figure 52), however the net pay zone may be thinner.

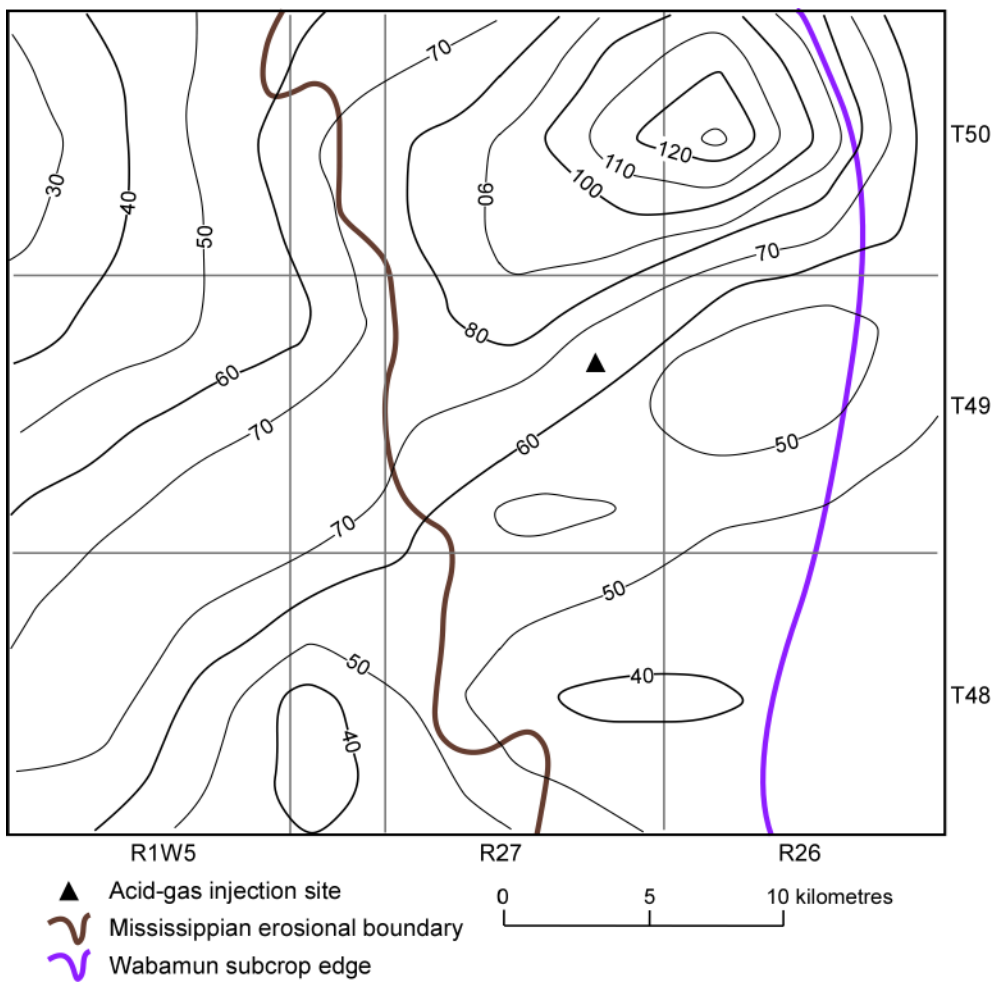


Figure 52. Isopach map of the Ellerslie Member in the Strathfield local-scale study area. Contours in metres.

The Ellerslie Member sandstones are gray to brown, often have a “salt & pepper” appearance, and are fine grained, silty, moderately sorted, porous with well-developed interbeds of gray silty shale (Figure 53). The porosity type is mainly intergranular and the grain and pore sizes are in the 10 μm to 50 μm scale.

The unit is part of the Lower Mannville Group and is overlain by thick shale and siltstone packages of the Upper Mannville Group (Clearwater equivalents). The Ellerslie Member is underlain by the Mississippian Banff and Exshaw formations in the west and by the Devonian Wabamun Group in the east (Figure 52). The Exshaw-Banff interval consists of a lower succession of shale and marlstone grading upward into chert and carbonates with a thickness of about 0 to 20 m. The Wabamun Group is a thick sequence of grey to dark grey, shallow marine, massive to burrow mottled, platform carbonates of 150 m thickness. The sediments usually consist of limestone with minor amounts of dolomite and they are generally tight.

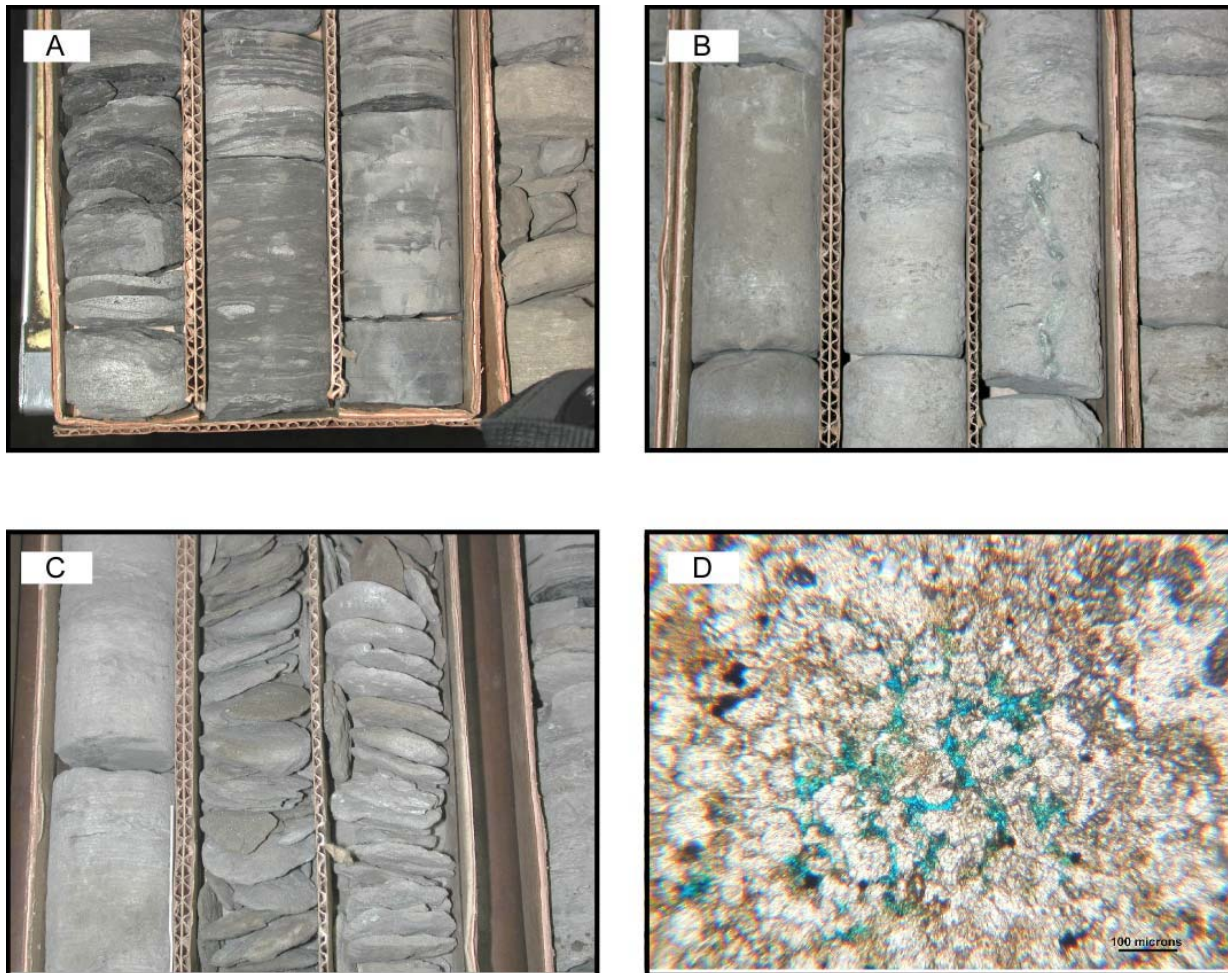


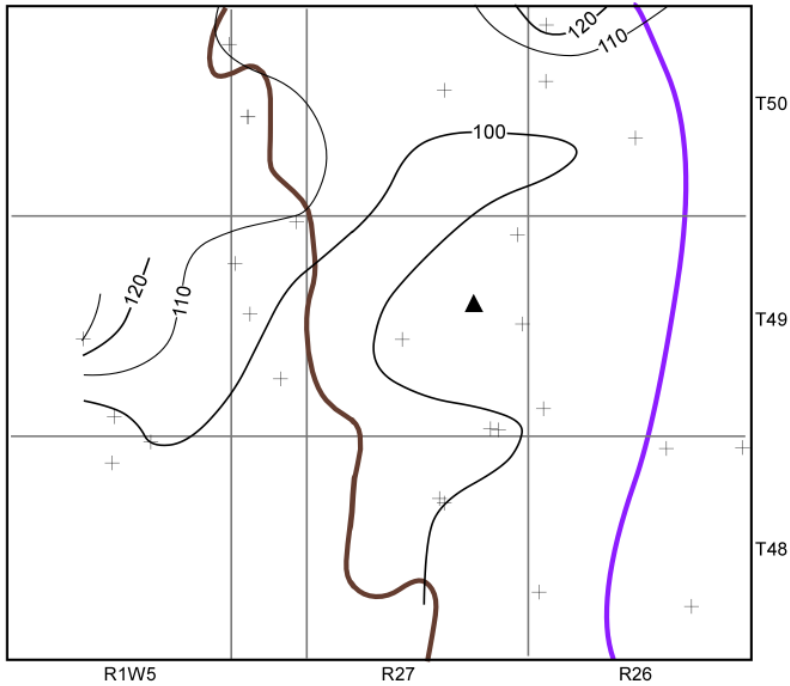
Figure 53. Core and thin-section photographs of the Ellerslie/Basal Quartz Member sandstone in the Strathfield area. Banded silt to sandstones (Photo A) change to porous, grainy sandstone (Photo B), which consist mainly of quartz, with minor clay layers (Photo C). The intergranular porosity can best be seen on the blue stained pores in the center of the thin-section photo (Photo D).

5.5.2 Hydrogeological Characteristics and Rock Properties

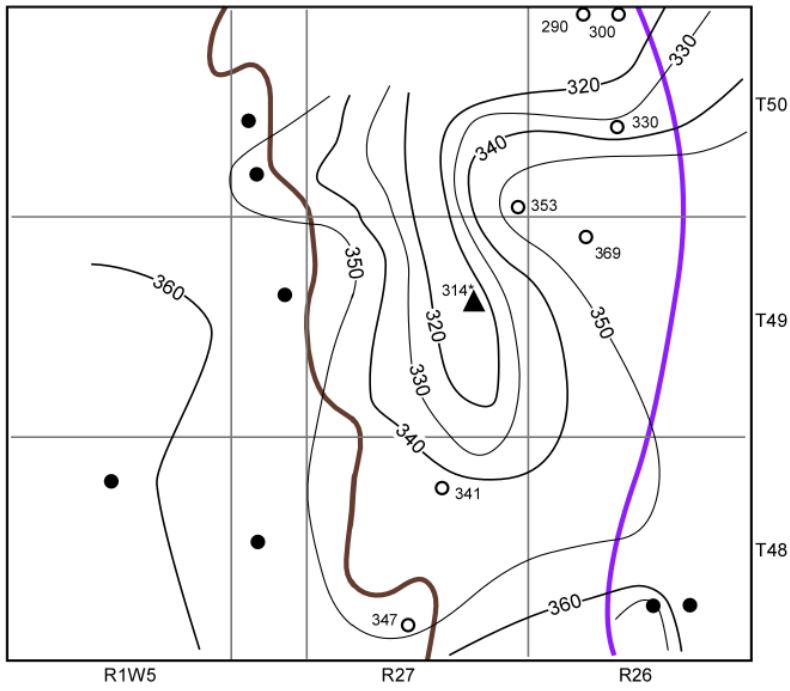
Chemistry of Formation Water

Thirty five chemical analyses of Lower Mannville formation water in the local-scale study area indicate that the major constituents are sodium (34 g/l) and chloride (65 g/l), making up 93% of the total dissolved solids (Table 12). The average molal ratio of Na/Cl is 0.8. Present in lesser concentrations are calcium, potassium, magnesium, bicarbonate and sulfate (Figure 49b). The salinity of formation water in the Ellerslie Member in the Strathfield area ranges from 90 to 130 g/l (Figure 54a), being highest in the northeast (T50, R26W4) and at the western boundary (T49, R1W5). A tongue of slightly less saline formation water of less than 100 g/l extends into the central part of the study area from the southwest (see also Figure 21a). The in-situ density of formation water in the Lower Mannville aquifer in the local-scale study area was estimated to be 1085 kg/m³ using the methods presented in Adams and Bachu (2002). For the calculation of hydraulic head values, a slightly lower reference density of 1080 kg/m³ was used, so that the resulting contour maps of hydraulic head could be compared to the regional maps and to the other local study areas.

a.



b.



▲ Acid-gas injection site
0 5 10 kilometres

○ Data point (Hydraulic head calculated from final shut-in pressure)
● Data point (Hydraulic head calculated from Horner-extrapolated pressure)

✓ Mississippian erosional boundary
Wabamun subcrop edge
+ Data point (salinity)

Figure 54. Distribution of a) salinity (g/l), and b) hydraulic heads (m) in the Lower Mannville aquifer in the Strathfield local-scale study area.

Table 12. Major ion chemistry of Lower Mannville brines based on 35 analyses (see Appendix 2) in the Strathfield area (concentrations in g/l).

	Na	K	Ca	Mg	Cl	SO ₄	HCO ₃	TDS
Minimum	28.7	0.3	2.1	0.5	54.5	0.001	0.1	89.8
Maximum	41.2	2.3	9.8	1.8	81.5	0.33	1.0	131.7
Average	34.2	0.7	5.1	1.0	64.9	0.12	0.4	105.8

Pressure Regime

Only seven high-quality DSTs exist in the Lower Mannville aquifer in the Strathfield area. This set of pressure measurements was augmented with eight presumably lower-quality DST data, for which only non-Horner extrapolated, final shut-in pressures are readily available.

Corresponding hydraulic heads, calculated with a representative density of 1080 kg/m³ (Bachu and Michael, 2002), decrease from above 360 m in the south and west to less than 320 m in the center of the study area (Figure 54b). Flow inferred from the hydraulic head distribution appears to be channelled northward into an area that corresponds to the closed 325 m contour line on the regional-scale map (Figure 24a), where there appears to exist a sink for regional flow in the Lower Mannville aquifer.

The recorded pressures are plotted versus elevation in Figure 55 and compared to pressures in the over- and underlying formations. The pattern looks very similar to the pressure versus elevation distribution at the Acheson injection site just north of the Strathfield local-scale study area. Pressures in the Lower Mannville aquifer plot between two lines, with a linear trend that is representative of the pressure distribution in a static column of brine with a density of 1085 kg/m³. Pressure measurements from the underlying Wabamun, Winterburn and Cooking Lake aquifers plot along the same trend, shifted slightly downwards, suggesting hydraulic continuity between these aquifers. The spreading of data points between the upper and lower lines implies a downward gradient of flow from the Lower Mannville into the Cooking Lake aquifer. In contrast, pressure measurements from the Upper Mannville aquifer are offset distinctively towards higher pressures, indicating that the intervening Upper Mannville-Clearwater aquitard is an effective barrier to cross-formational flow.

Rock Properties

The well-scale porosity and permeability values for the Ellerslie/Basal Quartz, the overlying Glauconitic Sandstone and the underlying Wabamun strata are shown in Table 13. Average porosity (15%) and permeability ($k_H = 125$ mD, $k_V = 45$ mD) in the injection strata, the Ellerslie/Basal Quartz, are noticeably higher than the respective values in the over, and underlying strata. In comparison, the average porosity values in the Glauconitic Sandstone and Wabamun Group are 10% and 8%, respectively. Average horizontal and vertical permeability values are 34 mD and 28 mD (Glauconitic Sandstone) and 32 mD and 4 mD (Wabamun Group), respectively. The porosity and permeability measured from core in the confining strata (Glauconitic Sandstone and Wabamun Group) probably are biased towards higher values than would be expected for these units generally characterized as aquitards, because core is preferably taken from potentially high-permeability, productive zones.

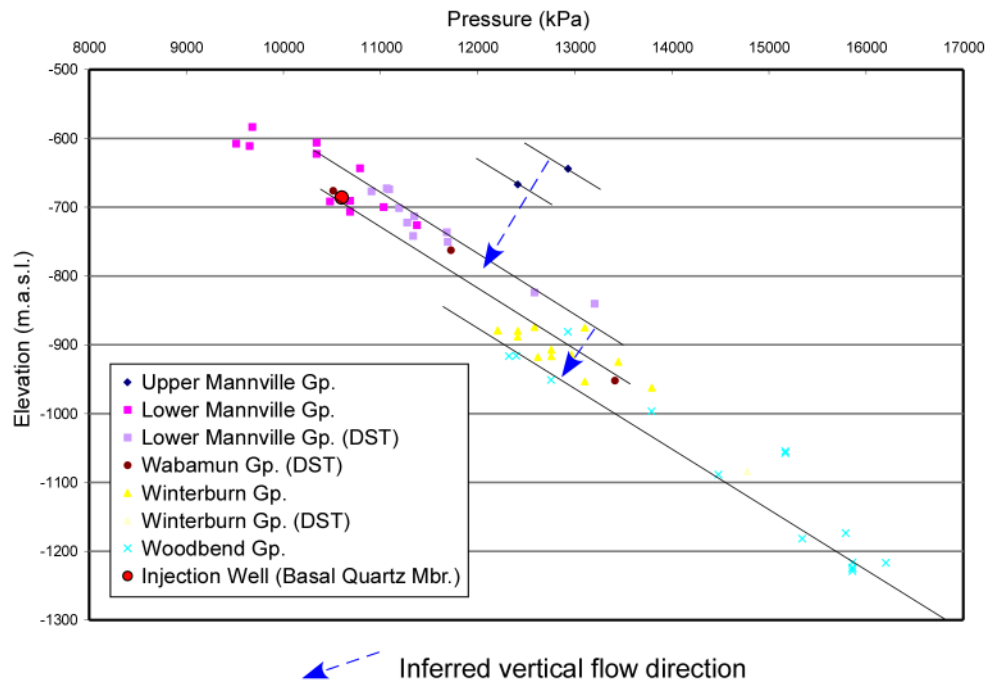


Figure 55. Distribution of pressure versus elevation in the injection stratum (Ellerslie Member) and adjacent formations in the Strathfield area.

Table 13. Well-scale porosity and permeability values obtained from measurements in core plugs from the Lower Mannville (31 wells) and Wabamun (13 wells) groups in the Strathfield local-scale study area.

Formation/ Group	Porosity (%)			Horiz. Permeability (mD)			Vert. Permeability (mD)		
	Min	Max	Average	Min	Max	Average	Min	Max	Average
Glauconitic	5	14	10	0.01	126	34	0.01	88	28
Ellerslie/BQTZ	7	24	15	0.12	594	125	0.03	105	45
Wabamun	3	14	8	2	111	32	0.2	13	4

Flow of Formation Water

The pressure regime and hydraulic head distribution in the Lower Mannville aquifer suggest that the flow of formation water is channelled northward and this flow pattern continues into the Acheson area (Figure 54b). The combined low of hydraulic heads from both local-scale study area lies within the closed 325 m contour line on the regional-scale hydraulic-head map of the Lower Mannville (Figure 24a). The Mississippian subcrop edge runs parallel to the western boundary through Range 26 (Figure 52). Therefore, the Lower Mannville aquifer is separated from the Wabamun-Winterburn aquifer system by the Lower Banff-Exshaw aquitard over most parts of the area. Still, the hydraulic head distribution and the pressure-elevation analysis (Figure 55) indicate that there is potential downward flow from the Lower Mannville aquifer into the underlying Wabamun, Winterburn, and Cooking Lake aquifers (Figures 22, 23 and 24).

5.6 Summary of the Local-Scale Hydrogeological Analysis

The acid-gas injection sites in the Edmonton area target Cretaceous Lower Mannville sandstone deposits (Acheson and Strathfield) and Devonian carbonate units in Leduc reefs (Redwater), Cooking Lake platform (Watelet) and Beaverhill Lake Group (Golden Spike). Although efforts have been made to use only “virgin” formation pressures in this study, the high density of producing hydrocarbon pools and old age since production start-up in the Edmonton area made it difficult to obtain a sufficiently large set of high-quality drillstem test data that represent original formation pressures. Instead, the data presented in this report probably represent the quasi-mid-to-late 1950s pressure distribution in the Edmonton area. Furthermore, the different production histories from the various pools in the area make it difficult to assess and represent the pressure regime at any given time, and only very small data sets exist for a certain time interval. The present-day pressure regime, after more than 50 years of production, would probably show even higher underpressures over larger areas in the Cooking Lake and Lower Mannville aquifers. However, in areas where primary production has ceased (i.e., Redwater), reservoir pressures have recovered or are in the progress of re-equilibrating to original formation pressures, because most of the Lower Mannville and Woodbend reservoirs have good aquifer support.

Overall, the general vertical hydraulic gradient is downwards; however, the flow is controlled by permeability distribution and does not necessarily occur if permeability barriers exist. The local-scale hydrogeological analysis in the Edmonton area shows that the Clearwater-Upper Mannville aquitard is an effective barrier to cross-formational flow, hydraulically separating the Upper Mannville aquifer and younger overlying formations from the underlying Lower Mannville and Devonian aquifers. On the other hand, both salinity and pressure distributions indicate the possibility of hydraulic communication between the Lower Mannville aquifer and the various underlying Devonian aquifers. This potential for downward cross-formational flow is facilitated by the sub-Cretaceous unconformity, along which different Devonian aquifers come in direct contact with the Lower Mannville aquifer. Also, cross-formational flow may occur in areas where the Ireton aquitard thins above Leduc reef complexes (i.e., Redwater, Acheson, Wizard Lake). The potential flow paths are not necessarily directly vertical (i.e., the Watelet injection site in the Cooking Lake platform is laterally offset from the Wizard Lake reef complex, and flow would be initially lateral, confined by the overlying Ireton aquitard). When the flow path encounters an overlying Leduc reef, downward vertical fluid migration becomes possible. The result is a network of tortuous flow paths, whereby the Leduc reef complexes represent the vertical conduit for flow.

Typical undiluted Devonian brines in west-central Alberta are of a Na-Ca-Cl type and have a very high salinity (Michael et al., 2003), like the formation waters from the Cooking Lake Formation at Watelet and from the Beaverhill Lake Group at Golden Spike ($\text{TDS} > 200 \text{ g/l}$, $\text{Na}/\text{Cl} < 0.6$). In contrast, Lower Mannville formation waters are generally Na-Cl type waters with salinity below 100 g/l and relatively low calcium concentrations. Lower Mannville formation waters at Acheson and Strathfield, and Leduc brines at Redwater have similar hydrochemical characteristics (TDS between 75 and 175 g/l, $\text{Na}/\text{Cl} > 0.65$). These formation waters are of a Na-Cl type, but have salinity values higher than the typical Lower Mannville formation water and lower than the typical Devonian brine (Figure 56), which suggests mixing of these brines in the areas.

Another evidence for the tortuous interconnection between and within the Lower Mannville and the Devonian aquifers are the underpressures observed in the Cooking Lake platform and equivalent expressions in the Lower Mannville aquifer. These underpressures are most probably due to pressure drawdowns induced by production from the neighbouring Leduc Formation reef complexes and the Lower Mannville Group. The Lower Mannville and Woodbend pools in the Edmonton area have been produced since the early 1950's, resulting in large pressure drawdowns. Similar effects of production

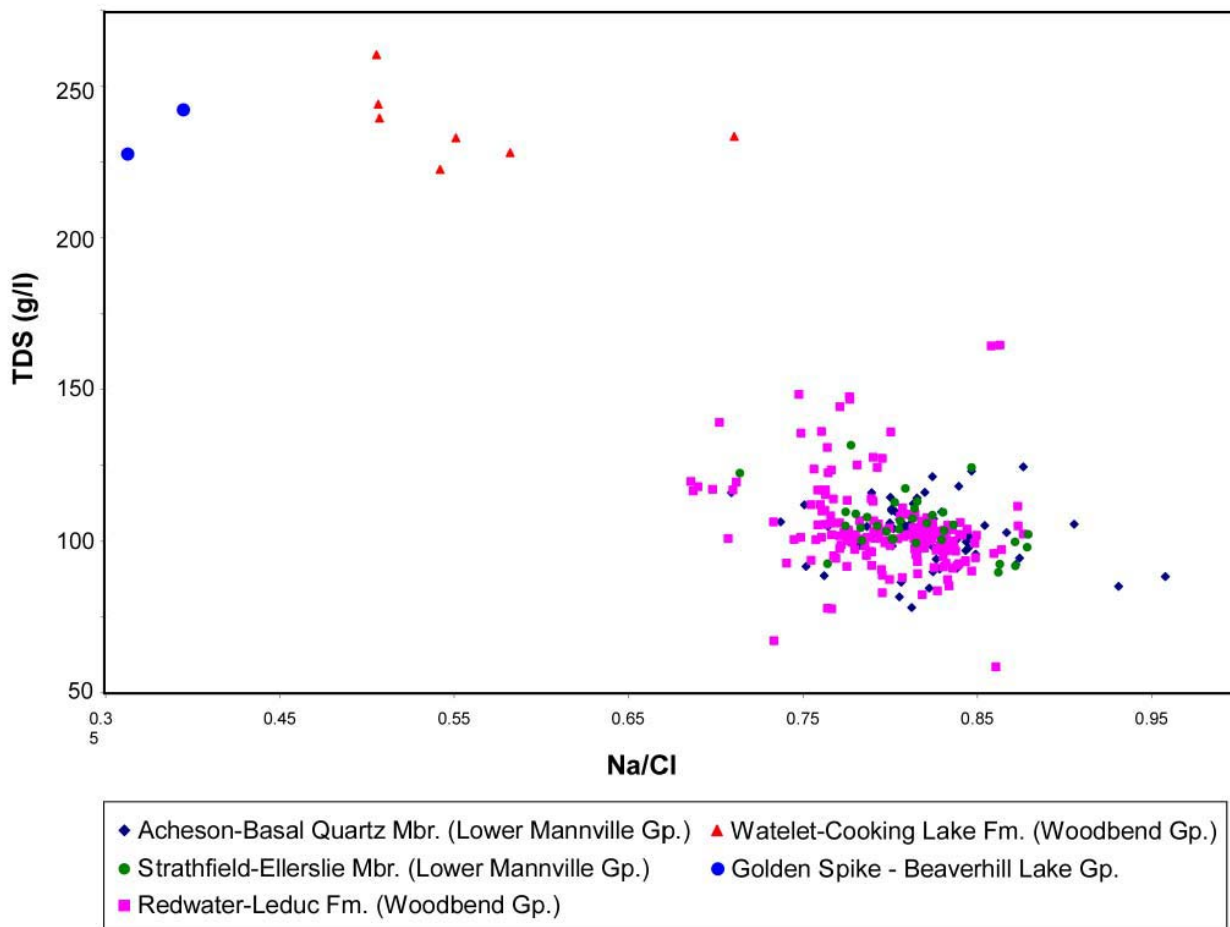


Figure 56. Comparison of formation waters from the various local-scale study areas using salinity and the molal ratio of Na/Cl.

from the Leduc Formation on pressures in the Cooking Lake and neighboring Leduc reefs were reported earlier on for the Westerose Leduc pool (Hnatiuk and Martinelli, 1967; Randall, 1975) just south of the Watelet area. Examples of pressure histories in relationship to hydrocarbon production from the Redwater pool and Acheson injection sites are shown in Figure 57.

At Redwater, initial pool pressures of 7400 kPa were depleted by a maximum of 4000 kPa at the peak of hydrocarbon production in the mid-seventies (Figure 57a). However, pressures appear to have recovered to initial reservoir pressures after production from the Leduc Formation has significantly decreased, as a result of hydraulic continuity between the reefs and the underlying Cooking Lake aquifer that is known to have generally high permeability and a strong hydrodynamic drive. In addition, water for secondary oil recovery has been injected into the Redwater pool since 1973. More recently, the Redwater reef has been used for disposal of oilfield produced water.

The Acheson acid-gas injection site is located at the southern edge of the St. Albert-Big Lake Ostracod A gas reservoir and it neighbours the Acheson oil field. As a result, pressure at the site is affected by production from both. Oil and gas production from the Lower Mannville in the Acheson area started in 1951. Oil production from the Acheson field peaked in 1985, while gas production from the St. Albert-Big Lake Ostracod A reservoir declined between 1961 and 1994, with a large spike in production since

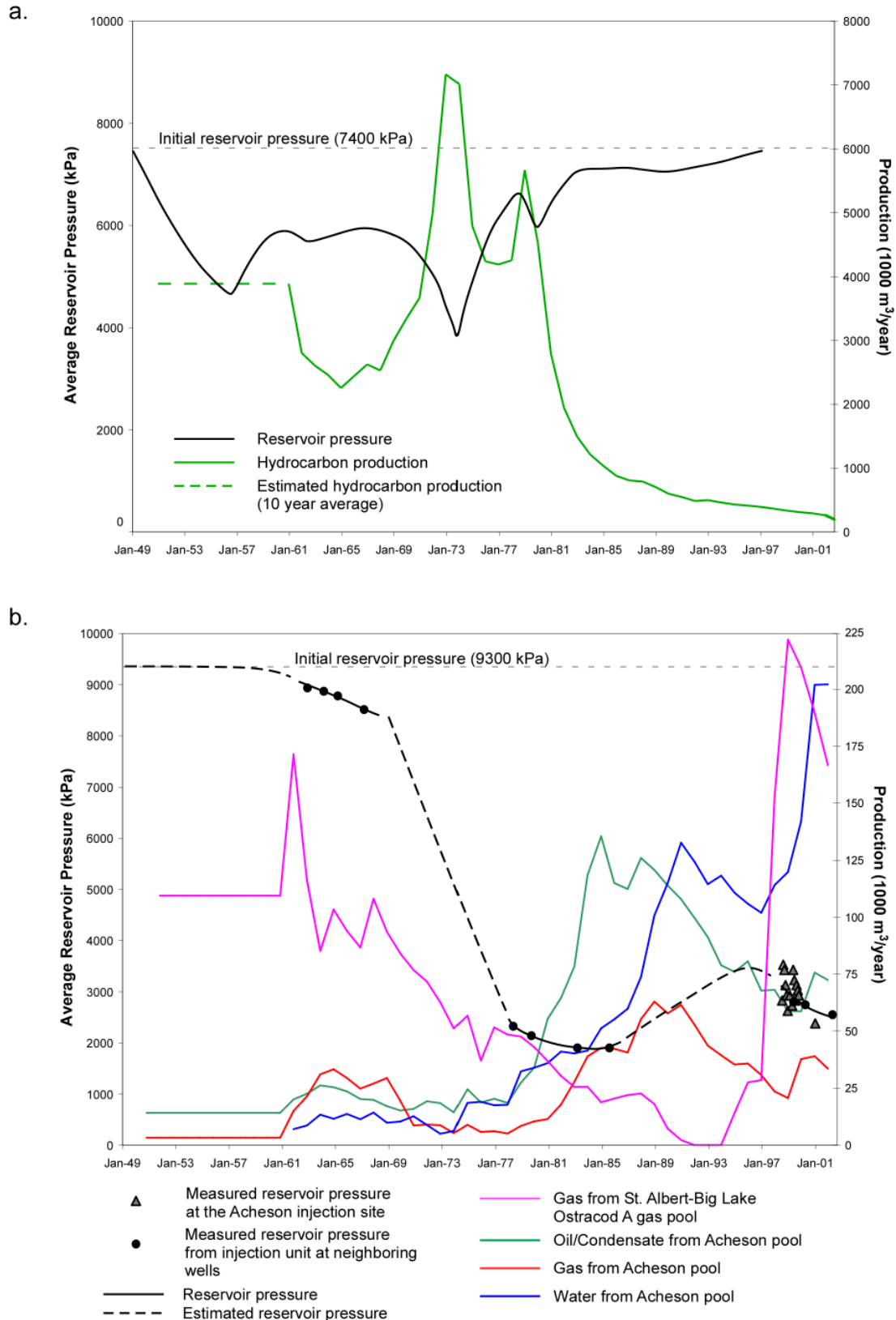


Figure 57. History of reservoir pressure and hydrocarbon production at: a) Redwater (Leduc Formation), and b) Acheson (Basal Quartz Member).

then (Figure 57b). Although hydrocarbon production is on decline, water production is on the rise (Figure 57b), thus maintaining the pressure drawdown. Initial reservoir pressures of approximately 9300 kPa were depleted to less than 2000 kPa and the Acheson acid-gas injection operation currently injects gas at bottom hole pressures between 2000 and 3000 kPa. In the case of the Acheson site, pressures have not recovered to initial pressures as in the case of the Redwater site because the underlying Wabamun aquifer has lower permeability and is a weaker aquifer than the Cooking Lake aquifer that underlies the Redwater reef, and because reservoir fluids are still being produced.

5.7 Site Specific Characteristics of the Acid Gas Operations

The site specific characteristics of the acid-gas injection operations in the Edmonton area are summarized in Table 14. The information contained therein has been compiled from the applications submitted by operators to the EUB in the process of obtaining approval for these operations, and from other sources. It is worth noting that the operators indicate site-specific porosity and permeability values that, except for the Acheson site, are lower than the local-scale averages (Tables 7, 9, 11, 13 and 14). According to EUB regulations, acid-gas injection operators must submit annual or bi-annual progress reports that contain operating information, such as injection rate, volume and gas composition, and wellhead pressure and temperature.

Vertical stresses, S_v , at the top of the various injection intervals vary between 21.8 MPa and 47.9 MPa and reflect the depth and density of the strata that overlie the injection interval (Table 14). The gradient of the vertical stress was determined from density logs of the injection well, or, where this was incomplete or not available, combined with wells in the vicinity of the injection well. The gradient varies between 21.3 kPa/m and 23.8 kPa/m, reflecting variations in rock density. Minimum horizontal stresses, S_{Hmin} , in the five injection intervals vary between 16.3 MPa and 33.5 MPa (Table 14) and corresponding gradients between 13.6 kPa/m to 16.7 kPa/m, reflecting variations in the rock properties, injection depth and stress distribution. The implication of these results is that the rock fracturing threshold in each well is between S_{Hmin} and S_v , but generally closer to S_{Hmin} . If the bottom hole injection pressure (BHIP) reaches the S_{Hmin} value, pre-existing fractures, if present, may open up. If no fractures are present, and there is no indication that there are any (except maybe around the well bore), the pressure has to increase beyond S_{Hmin} to overcome the compressive strength of the rocks, at which time the rocks will fracture. However, fractures may be limited to reservoir rocks only and may not propagate into the caprock. In order to avoid reservoir fracturing, EUB regulations require that the maximum BHIP be less than 90% of the fracturing threshold.

Because the injected acid gas may react with the formation rocks and fluids, it is important to know what is the geochemical composition of the rocks at each site. The results of mineralogical analyses and modeling of potential geochemical reaction between the injected acid gas and formation water and rocks are presented in a companion report (Perkins et al., 2004).

6 Discussion

Based on the hydrogeological analysis of the acid-gas injection sites at local-, regional-, and basin- scales presented in the preceding chapters, the potential for acid gas migration and/or leakage from the injection sites in the Edmonton area can be qualitatively assessed. Migration is defined here as flow along bedding within the same formation (reservoir or aquifer), and leakage is defined as upward flow to overlying formations and possibly to the surface. Both will be considered in the context of the natural hydrogeological setting and of man-made features, such as pressure drawdown, wells and induced fractures.

Table 14. Characteristics of the acid-gas injection operations in the Edmonton area.

	Operation Description	Acheson	Golden Spike-Beaverhill Lake	Redwater	Strathfield Leduc	Watelet Cooking Lake
Injection Operations	Gas Plant	Acheson Gas Plant	Golden Spike Gas Plant	Redwater Gas Plant	Calmar Sour Gas Plant	Wizard Lake Gas Plant
	Current Operator	Enerpro Midstream Inc.	Atco Midstream Ltd.	Redwater Water Disposal Co. Ltd.	Enbridge Inc.	ATCO Midstream
	Approval Date	29-Jun-89	23-Apr-99	10-Oct-97	04-Nov-97	10-Feb-97
	Status	active	active	active	active	active
	Location (DLS)	05-02-053-26W4	08-27-051-27W4	01-29-057-21W4	02/07-23-049-27W4	08-18-048-26W4
	Latitude (N)	53.547	53.430	53.949	53.242	53.140
	Longitude (W)	-113.735	-113.888	-113.075	-113.837	-113.785
	KB Elevation (m AMSL)	702.0	712.8	618.3	735.9	783.2
	Depth of Injection Interval (m)	1182-1286	1957.5-2300	945-1005	1422-1439	2010-2090
	Average Injection Depth (m)	1234	2128.75	975	1430.5	2050
Reservoir Geology	Injection Formation Name	Ostracod-Basal Qtz Mbr	Beaverhill Lake Gp	Leduc Fm	Ellerslie Mbr	Cooking Lake Fm
	Injection Formation Lithology	Sandstone	Dolomitic Limestone	Carbonates	Sandstone	Limestone
	Injection Formation Thickness (m)	104.0	342.5	60.0	17.0	80.0
	Net Pay (m)	3	10	35	17	40
	Caprock Formation	Glauconitic/Clearwater	Lower Leduc	Ireton Fm	Glauconitic/Clearwater	Duvernay Fm
	Caprock Formation Lithology	Sandstone and Shale	Lime mudstone	Shale	Sandstone and Shale	Shale
	Caprock Thickness (m)	150	150	40	12	42
	Underlying Formation	Wabamun Gp	Muskeg Fm	Beaverhill Lake Gp	Ellerslie Mbr	Mildred Mbr
	Underlying Formation Lithology	Limestone	Evaporites	Shale and Limestone	Shale	Limestone
	Underlying Thickness (m)	102	50	200	14	51
Rock Properties	Porosity (fraction)	0.16	0.07	0.07	0.15	0.05
	Permeability (md)	260.00	16.00	204.51	50.00	26.90
	S_v (MPa)	21.8	46.1	22.5	31.4	47.9
	S_{HMIN} (MPa)	14.1	28.2	15.8	19.7	33.5
Reservoir Properties	Original Formation Pressure (kPa)	9300	15700	7413	10600	15459
	Formation Temperature (°C)	50.6	70.5	34.0	60.0	70.0
	Reservoir Volume (1000 m³)	Not Available	671	Not Applicable - sour water injection	539	480.9
Formation Water	TDS Calculated (mg/L)	152813	241914	106618	69400	222663
	Na (mg/L)	41530	61972	32600	23200	48930
	Ca (mg/L)	9830	24000	4510	2880	30968
	HCO ₃ (mg/L)	481	160	552	397	166
Licensed Injection Operations	Injected Gas - CO ₂ (mole fraction)	0.87	0.76	NA	0.72	0.84
	Injected Gas - H ₂ S (mole fraction)	0.11	0.19	NA	0.26	0.10
	Maximum Approved H ₂ S (mole fraction)	0.15	0.50	Not Applicable - sour water injection	0.26	0.25
	Maximun Approved WHIP (kPa)	6000	11700	8273	9000	10000
	Maximum Approved Injection Rate (1000 m ³ /d)	6	40	Not Applicable - sour water injection	58	25
	Total Approved Injection Volume (10 ⁶ m ³)	30000	185100	Not Applicable - sour water injection	213000	115000
	EPZ (km)	0.45	2.85	Not Applicable - sour water injection	Not Available	1.90

6.1 Acid Gas Migration

Because sour water rather than acid gas is injected at Redwater, this case will be treated separately from the other four injection sites in the Edmonton area. Initially, oilfield produced water was injected (disposed of) at Redwater. Subsequently the operator was granted permission to co-dispose of acid gas by dissolving it into the produced water prior to injection. Dissolution of acid gas leads to an increase in water density by 2-4% (see Bachu and Adams, 2003, for the case of pure CO₂). Although the produced water is generally from the Redwater reef itself, its density is not necessarily equal to that of in-situ formation water because the produced water loses dissolved gases as it is brought to the surface. If the density of the injected water is less than the density of formation water, then the injected sour water will rise to the top of the water leg in the reef and will be confined within the reef, with no possible migration except within the reef itself. Since injection takes place in the top region of the reef along its eastern, updip part (Figure 58), no real water migration would be expected. Mixing with and diffusion within the formation water in the Redwater reef will occur over time. On the other hand, if the injected sour water is heavier than the formation water, then it will drop to the bottom of the reef and then to the bottom of the underlying Cooking Lake aquifer, generating convective flow. There, the sour water will be subjected to hydrodynamic forces in the natural flow system of the Cooking Lake aquifer and to negative buoyancy that will drive the water downdip to the southwest. Because the two forces are likely comparable in magnitude, the resultant flow direction will be to the west-northwest. In any case, the flow magnitude will be on the order of ~1 cm/year, estimated on the basis of a hydraulic gradient of 1.5 m/km and permeability of 300 mD, and ignoring buoyancy effects that most likely are negligible. At this extremely low velocity, the sour water will mix with and diffuse further within the formation water, such that the plume of injected water will ultimately disappear.

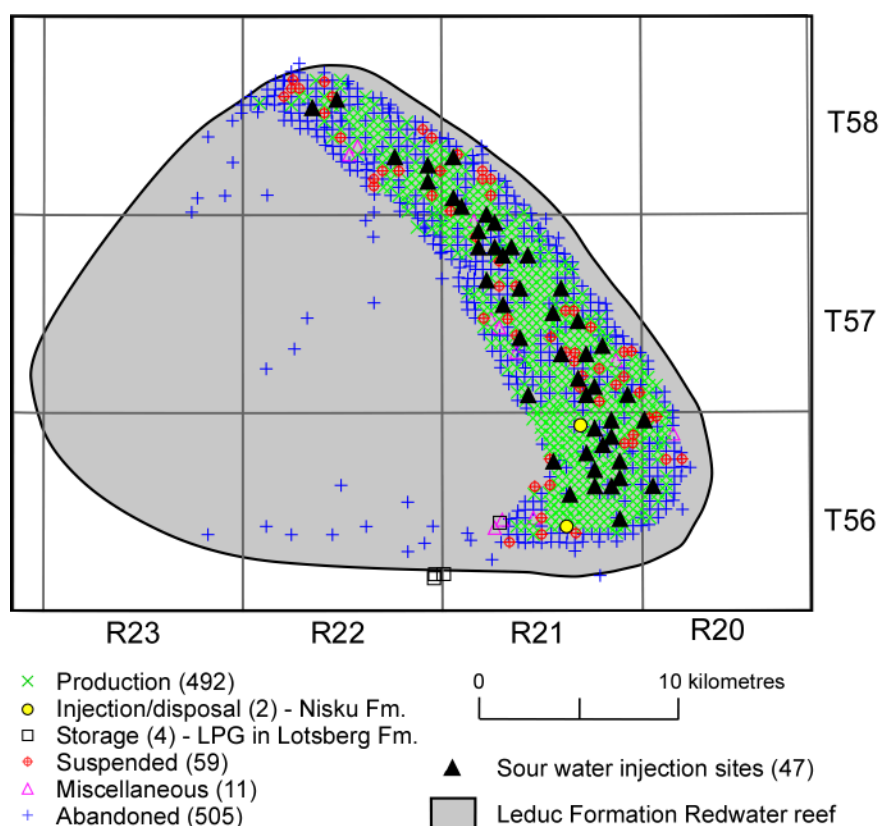


Figure 58. distribution and status of the injection wells and of other wells that penetrate the Leduc Formation Redwater reef.

The fate of the injected acid gas in the case of the other four injection sites in the Edmonton area where dry acid gas is injected is different from the Redwater case. These four cases can be also split into two categories:

- injection into depleted gas reservoirs at Acheson in the Ostracod A pool in the Basal Quartz sandstone, and at Strathfield into an undefined pool in the Ellerslie Member, both of them in the Lower Mannville Group, and
- injection into a deep saline aquifer at Golden Spike and Watelet, both in Devonian carbonates.

The fate of the injected acid gas in all four cases is controlled by the in-situ properties of the gas and native fluid (reservoir gas or formation water). Table 15 below presents the density and viscosity of the injected acid gas and native reservoir gas or formation water calculated for the initial in-situ conditions given in Table 14 (Adams and Bachu, 2003; Bachu and Carroll, 2004).

Table 15. Properties of native fluids and injected acid gas at initial in-situ conditions for four acid-gas injection sites in the Edmonton area where dry acid gas is injected.

Fluid Property	Acheson	Golden Spike	Strathfield	Watelet
Native fluid	Gas	Water	Gas	Water
Density (kg/m ³)	77.2	1175.4	90.1	1160.7
Viscosity (mPa·s)	0.014	0.64	0.015	0.63
Acid gas density (kg/m ³)	308.5	478.6	361.7	446.7
Acid gas viscosity (mPa·s)	0.024	0.037	0.028	0.034

In the case of the two gas reservoirs, Acheson and Strathfield, since the pressure at injection start-up was, and the current pressure is still below the initial reservoir pressure, the actual density and viscosity of the native gas and injected acid gas are lower than the values presented in Table 15. For both gases they will continue to increase towards the values presented in Table 15 as the reservoir is pressured up through injection. However, both gases compress directionally in the same way (although not proportionally), such that the values presented in Table 15 are a good indication of the large density and viscosity contrast between the two. The injected acid gas is approximately four times heavier and twice more viscous than the reservoir gas. If the acid gas is injected at the bottom of the reservoir, it will stay there and will gradually fill up the reservoir, chasing the residual natural gas to the top of the reservoir. Since both gases are non-wetting fluids, there are no capillary forces to play a role in the flow of the two gases. This method can be actually used to produce additional gas (enhanced gas recovery), but some acid gas will be recovered at the producing well and it will have to be stripped out. If the acid gas is injected at a level higher than the bottom of the reservoir, the acid gas will flow to the bottom of the reservoir, with a similar effect. There will be some gas dissolution in the underlying formation water at the gas-water contact, but the amount of acid gas that will dissolve is going to be small since the formation water has already a very high salinity.

In terms of migration, the acid gas will be confined to the injection reservoir by the same stratigraphic trap that initially trapped the natural gas. Lateral, updip migration will be impeded by the overlying shales that confine the Edmonton channel within the paleo-highs at the sub-Cretaceous unconformity (Figures 7, 16 and 18). Upward flow will be similarly impeded by the overlying shales (caprock) of the Glauconitic and Clearwater formations. If there is still production from these reservoirs, or if these reservoirs are connected in any way with other producing reservoirs, then acid gas may migrate toward the producing wells as a result of the hydrodynamic drive created between an injecting well (high pressure) and producing wells (low pressure).

Figure 59 shows the extent of the Acheson original Blairmore T and subsequent St. Albert-Big Lake Ostracod A pools, and of the Strathfield (undefined) gas reservoir in the context of lithofacies changes in the Lower Mannville Basal Quartz and Ellerslie formations. When approval was granted for acid gas injection at Acheson, the regulatory agency required the operator to file annually with EUB and each other operator in the Acheson Blairmore T and St. Albert-Big Lake Ostracod A pools progress reports that “shall include the impact of acid gas injection on the performance of offsetting producing wells”. In March 2004 the operator at Acheson reported that CO₂ was detected in 2003 in well 10-22-53-26W4 in the St. Albert-Big Lake Ostracod A pool, located at 3,625 m north from the acid-gas injection well. No H₂S has been detected in the produced gas. Since at Acheson the average composition of the acid gas is 87% CO₂ and 11% H₂S (Table 14), with H₂S being denser and more viscous than CO₂, it is expected that CO₂ would show first at a producing well. In addition, diagenetic processes within the reservoir could have reduced the H₂S concentration in the injected acid gas as a result of pyrite precipitation, if an iron source was available. The issue was brought to EUB’s attention and was heading to a hearing, but the operator at Acheson has indicated to the regulatory agency that it has initiated an Appropriate Dispute Resolution process with the operator of the offset producing well to address the issue of CO₂ breakthrough, and that this situation “will be addressed pursuant to the terms of the Mediated Settlement Agreement”. This case shows that, after 13 years of injection, CO₂ has migrated northward a distance of >3.5 km mostly under the combined drive of injection and production. The drive into the St. Albert-Big Lake Ostracod A gas pool has increased lately with the large spike in gas production from this pool (Figure 57b). There are five producing wells much closer to the acid-gas injection well (Figure 59) that did not report CO₂ breakthrough, but these wells are owned by the same operator that operated until recently the Acheson acid-gas injection site. If acid gas broke through at any of these wells, it is most likely that the operator just stripped the acid gas from the sour reservoir gas and re-injected it, as the produced gas in this area is sour to begin with. Understanding the migration path and fate of the injected acid gas at Acheson requires a separate study that is beyond the scope of this report.

The situation is different in the case of injection in the two carbonate aquifers at Golden Spike and Watelet. In the near-field (injection well and its vicinity), pressures are actually higher than the initial aquifer pressure. Since water is only very slightly compressible, and its density is affected mostly by temperature and salinity and very little by pressure (Adams and Bachu, 2003), the density values presented in Table 15 for formation water are valid even if pressure increases as a result of injection. However, for acid gas, whose properties are strongly dependent on pressure, the density is higher at the well and decreases away from the well as pressure drops, towards the values presented in Table 15. The bottom hole injection pressure is not measured, but can be estimated based on the hydrostatic weight of the acid gas column in the well assuming average gas density. As an upper limit, pressures have to be always below 90% of the fracturing pressure. Using this upper limit for pressure, the maximum acid gas density at the injection well would be 723 kg/m³ at Golden Spike and 744 kg/m³ at Watelet. Thus, in both cases the density contrast between the injected acid gas and formation water will likely vary between approximately 1:2 at the injection well to 1:2.5 at the boundary of the area of influence, and the viscosity contrast will vary correspondingly between 1:12 to 1:18, but in any case the contrast will be greater than 1:1.6 for density and 1:9 for viscosity.

During injection of a non-aqueous fluid into an aquifer, the flow of the injected fluid is driven by injection hydrodynamics and by the density contrast between the two fluids (buoyancy), and is controlled by the viscosity contrast (mobility) between the two fluids. The following dimensionless parameter:

$$\Gamma = \frac{2\pi\varphi\Delta\rho g k k_{rb} B^2}{\mu_b Q} \quad (5)$$

represents the ratio of buoyant versus viscous and pressure forces, and is an indication of the importance of buoyancy (density differences) in driving the flow of the injected acid gas (Nordbotten et al., 2004a). In the above expression, porosity ϕ , permeability k (m^2) and thickness B (m) are aquifer characteristics, k_{rb} and μ_b ($Pa \cdot s$) are, respectively, the relative permeability and viscosity of the formation water (brine) and express mobility (including viscous forces), Q (m^3/s) is the injection rate and expresses injection forces, and $\Delta\rho$ (kg/m^3) is the density contrast between the injected acid gas and formation water, expressing buoyant forces.

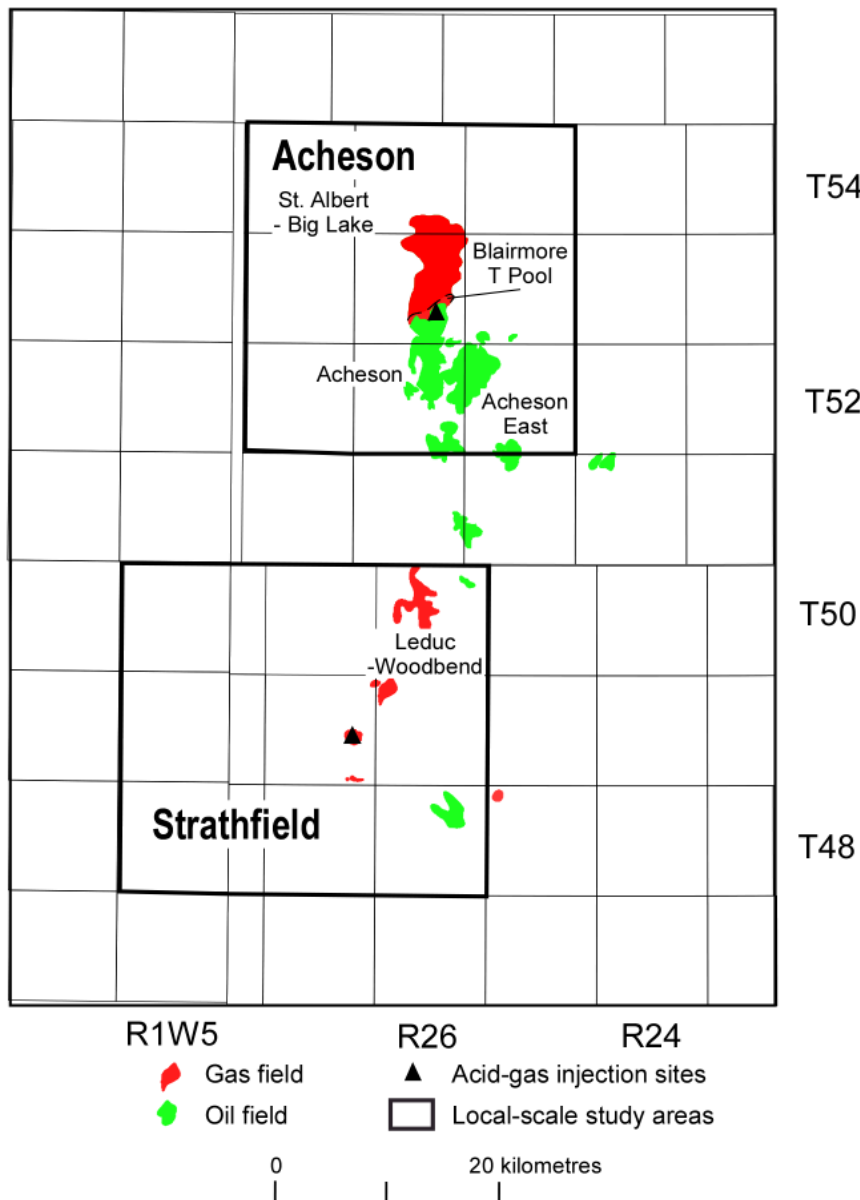


Figure 59. Location of oil and gas fields in the Basal Quartz/Ellerslie Member in the vicinity of the Strathfield and Acheson acid-gas injection sites.

For $\Gamma < 0.5$ hydrodynamic and viscous forces dominate and buoyancy can be neglected in the near field (Nordbotten et al., 2004a). This situation will happen for: 1) high injection rate (strong hydrodynamic force); 2) small density difference between the injected gas and formation water (low buoyancy); and 3) injection into a thin and/or low porosity and permeability aquifer. At the other end of the spectrum,

buoyancy totally dominates for $\Gamma > 10$. Such cases will occur for a combination of the following factors: 1) large density differences between the injected fluid and formation water; 2) injection into a thick aquifer characterized by high porosity and permeability; and 3) low injection rate (small hydrodynamic force). For $0.5 < \Gamma < 10$, buoyancy, hydrodynamic and viscous forces are comparably important (Nordbotten et al., 2004a). The change from one flow regime to another is not sharp, but rather gradual. These results are quite intuitive, because the injected acid gas will rise to the top of the aquifer (gravity override) if the aquifer has large enough permeability, porosity and thickness, and if the density difference is large enough; otherwise the plume will spread mostly laterally as a result of the strong hydrodynamic drive, being controlled by the mobility contrast between the two fluids.

Considering full saturation in the regions occupied respectively by the injected gas and formation water (i.e., $k_{rb} = k_{rag} = 1$), the average injection rates to date of $\sim 16,700 \text{ m}^3/\text{day}$ at Golden Spike and $\sim 11,630 \text{ m}^3/\text{day}$ at Watelet lead to values of $\Gamma = 0.01$ and $\Gamma = 0.29$, respectively. The injection reefal carbonate is relatively thin at Golden Spike (10 m) and the injected acid gas will flow mostly laterally. However, once in the far field where the hydrodynamic forces decrease significantly, buoyancy will become dominant and the acid gas will rise to the top of the Beaverhill Lake reef. Further upward migration will be stopped by the tight argillaceous limestone at the top of the Waterways Formation. In addition, capillary forces will impede acid gas flow through the caprock. After cessation of injection and rise to the top, the plume of injected acid gas will spread laterally and updip within the reef. However, large-scale migration is not possible because the reef that is the injection target is confined laterally by the tight argillaceous carbonates of the Waterways Formation. Thus, the acid gas injected at Golden Spike will likely remain confined within the injection reef, whose tentative outline is presented in Figure 60a. Lack of data precludes a precise delineation of this reef.

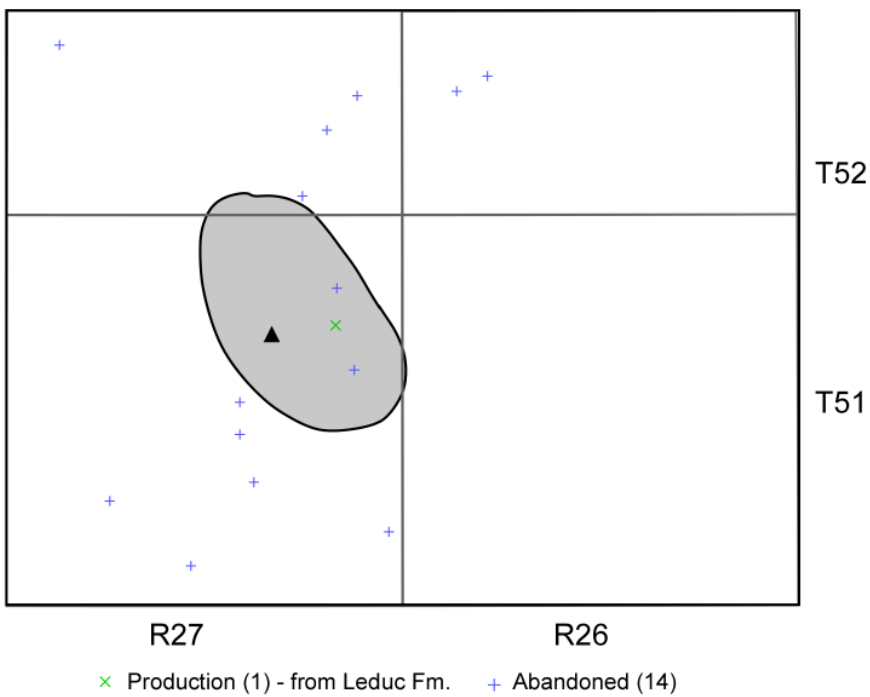
The likely fate of acid gas injected at Watelet in the Cooking Lake aquifer is quite different because this is an aquifer with very large areal extent (defined in reservoir engineering as an infinite aquifer) and there are no lateral physical constraints to the flow of the injected acid gas. The larger value of the parameter Γ at Watelet ($\Gamma = 0.29$) is due to larger thickness, higher permeability and smaller injection rate at Watelet than at Golden Spike (Table 15). The injected acid gas will rise to the top of the aquifer where it will spread laterally as a result of buoyancy and large mobility contrast. Further upward migration is stopped by the tight and thick shales of the overlying Ireton aquitard.

Acid gas flows as a result of the interplay between the hydrodynamic drive imposed by injection, the natural hydrodynamic drive in the Cooking Lake aquifer and buoyancy. The specific discharge, q , (or Darcy velocity) of the flow of acid gas in a sloping aquifer can be written with respect to a reference density ρ_0 as (Bachu, 1995):

$$q = -\frac{k k_{rag} \rho_0 g}{\mu_{ag}} (\nabla H_0 + \frac{\Delta \rho}{\rho_0} \nabla E) \quad (6)$$

where g is the gravitational constant, μ_{ag} is acid gas viscosity, k_{rag} is the relative permeability of the acid gas, ρ_0 is the reference density (that of formation water), $\Delta \rho$ is the density difference between the acid gas and formation water, ∇H_0 is the hydrodynamic drive, and ∇E is the slope of the aquifer. The first term in brackets in relation (6), ∇H_0 , represents the hydrodynamic drive, and the second term represents buoyancy. The relative importance of the two driving forces is expressed by the driving force ratio, DFR (Bachu, 1995):

a.



b.

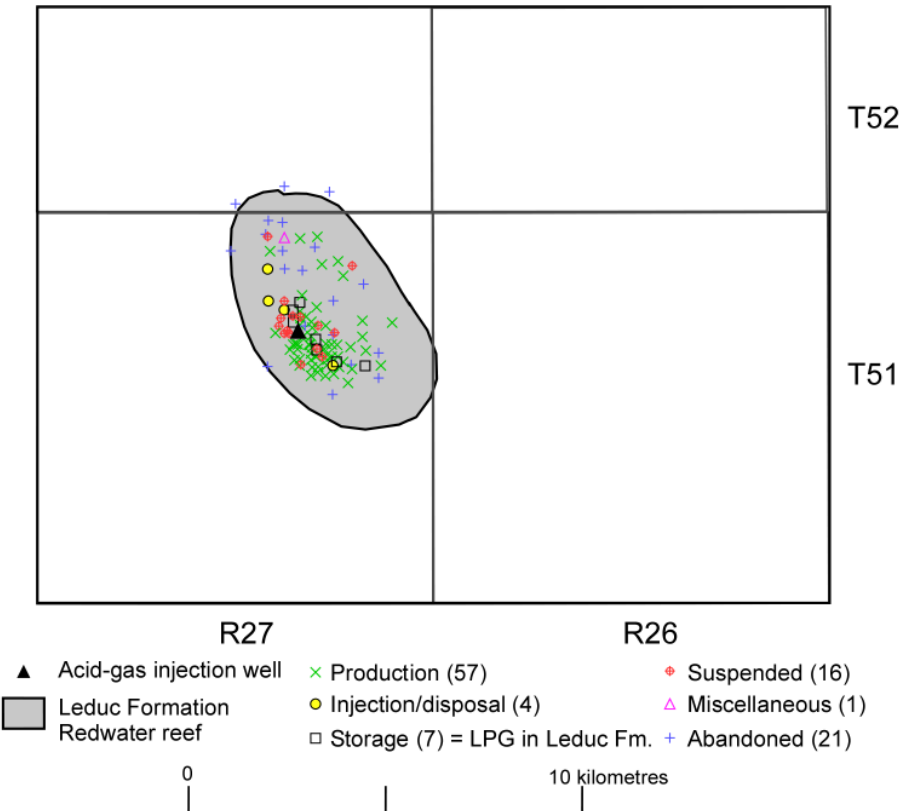


Figure 60. Inferred outline of the Golden Spike reefal carbonates, and distribution and status of wells that penetrate: a) the acid-gas injection unit (Beaverhill Lake Group), and b) the overlying Leduc Formation Golden Spike reef.

$$DFR = \frac{\Delta p}{p_0} \cdot \frac{|\nabla E|}{|\nabla H_0|_h} \quad (7)$$

where the subscript h denotes the horizontal component of the hydraulic gradient.

The hydrodynamic drive in turn has two components, one induced by injection and/or production (if present), and the second corresponding to the flow of formation water. The hydraulic gradient created by injection decreases logarithmically with distance from the well, such that in the vicinity of the well (near field) the hydrodynamic drive induced by injection dominates the flow, while away from the injection well (far field) it becomes negligible. Thus, in the vicinity of the injection well the acid gas will spread laterally (almost radially). In the far field, away from the injection well, the natural flow in the aquifer becomes dominant over the hydrodynamic drive caused by injection. Since the subject of the analysis is the long-term fate of the injected acid gas, the following discussion addresses acid gas migration in the far field, within the local, regional and even basin-scale study areas.

At Watelet the hydraulic gradient is $\nabla H_0 = 0.3\%$ (3 m/km) at 25° NE (Figure 37b), and the slope of the top of aquifer is $\nabla E = 1.6\%$ (16 m/km) at 45° to the northeast. At the regional-scale, the hydraulic gradient is on the order of 0.2% (2 m/km) at 10° to the northwest and the slope of the top of the aquifer is 0.8% (8 m/km) at 52° to the northeast (Figures 22a and 14b, respectively). Considering the density contrast between the injected acid gas and formation water (Table 15), the driving force ratio at the local scale is $DFR=3.3$, which indicates that buoyancy will dominate the flow of the acid gas once the hydrodynamic drive due to injection becomes negligible. This means that the plume of acid gas will migrate generally to the northeast at $\sim 45^\circ$. Outside the local scale study area, the driving force ratio decreases to ~ 2.5 due to changes in slope of the Cooking Lake aquifer, which indicates that buoyancy will continue to be the dominant driving force.

Injection of acid gas at Watelet was approved in October 1997 for an operational lifetime of 15 years. The average injection rate to the end of 2003 is $11,630 \text{ m}^3/\text{day}$ at STP (standard temperature and pressure) conditions (Bachu et al., 2004), which, due to gas compressibility, is equivalent to $45.67 \text{ m}^3/\text{day}$ at in-situ conditions. For a horizontal aquifer, the maximum plume spread at the end of 15 years of injection into an aquifer of same characteristics is estimated to be $\sim 1000 \text{ m}$ from the injection well. This estimate is based on a certain set of simplifying assumptions, such as no mixing and diffusion between the acid gas and aquifer brine, no gas dissolution in the brine, full saturation with either acid gas or brine in their respective domains, no capillary effects, and a sharp interface between the two fluids (Nordbotten et al., 2004a). All these assumptions by and large lead to overestimates of the plume spread because, in reality, some plume mass will be lost through dissolution, diffusion and mixing. Also, saturations less than 100% and capillary effects will retard the gravity override and plume spread. On the other hand, because the Cooking Lake aquifer is dipping at an angle of 16 m/km in the local scale study area, buoyancy will distort the plume, which will advance faster updip and slower downdip. As a result, the plume will become elongated along dip, with the downdip edge of the plume closer to and the updip edge of the plume farther from the injection well than the radial plume for a horizontal aquifer. Thus, based on the interplay between the various factors that control the spread of the acid gas plume, it is reasonable to assume that the maximum distance of the updip edge of the acid gas plume from the injection well at the end of injection would be on the order of 1-1.5 km. After cessation of injection, the plume will migrate driven mainly by buoyancy.

If the hydrodynamic drive in the natural flow of formation water is neglected, equation (6) becomes:

$$q = -\frac{kk_{rag}(\rho_b - \rho_g)g}{\mu_{ag}} \nabla E \quad (8)$$

where ρ_b and ρ_g are the densities of the brine and acid gas, respectively. On the basis of the permeability values for the Cooking Lake aquifer (Table 7) and of acid gas and brine properties (Table 15), an order-of-magnitude analysis shows that, once outside the cone of influence around the injection well, the Darcy velocity of the updip migrating acid gas is on the order of 8 m/year, depending on relative permeability k_{rag} .

During plume migration, acid gas will continuously come in contact with formation water, and the process of dissolution, diffusion and mixing will continue. As acid gas dissolves in formation water, this will become heavier than unsaturated brine, and a process of brine free convection will be set in motion (Lindeberg and Wessel-Berg, 1997). The heavier brine will drop to the bottom of the aquifer and then migrate downdip, while brine not saturated with acid gas will replace it and come in contact with the acid gas plume. This process will continue as the plume migrates, ultimately leading to the total dissolution of the acid gas plume (McPherson and Cole, 2000).

The Wizard Lake reef, located at a distance of 4-4.5 km west of the Watelet acid-gas injection site (Figure 61) is still producing and, as a result, the pressure drawdown likely propagates beyond the reef outline, creating locally a westward hydrodynamic drive towards the reef (Figure 37b). Similarly, production from the Glen Park reef located at some 6.5 km to the northwest of the injection well, and from the Leduc Woodbend reef located at ~12 km to the north induces a drawdown with a hydrodynamic drive toward these reefs. As a result of the interplay between acid gas buoyancy and the hydrodynamic drive towards the producing reefs, the acid gas plume will be deflected to the north from the 45° NE structural dip of the Cooking Lake aquifer. Thus, after cessation of injection, the plume of acid gas will likely migrate in a N-NE direction (Figure 61). However, at velocities on the order of 8 m/year, it will take several hundreds of years for the acid gas to reach any of these reefs, by which time most of the plume will most likely have dissolved.

Assuming that not all the acid gas will dissolve and that it will migrate updip east of the Leduc Woodbend reef, the plume will have to migrate some 150 km to the edge and subcrop of the Cooking Lake aquifer underneath the Lower Mannville aquifer (Figure 13). The estimated timeframe for this migration path is on the order of 20,000 years, by which time the acid gas will completely dissolve in formation water (McPherson and Cole, 2000). Nevertheless, assuming that not all the acid gas will dissolve by the time the plumes reaches the edge of the Cooking Lake aquifer (a completely implausible assumption), and it reaches the subcrop area at the pre-Cretaceous unconformity, the gas will migrate upward into the Lower Mannville aquifer, where the strong overlying Clearwater aquitard will stop any upward migration. The dip of the Mannville Group strata is milder than that of Devonian strata, such that buoyancy will decrease. On the other hand, the gas will likely decompress, becoming lighter than at Watelet, which will increase buoyancy. The remaining gas will flow to the north-northeast, unless caught in stratigraphic and/or structural traps. The flow will be the resultant of updip, northeastward buoyancy and draining to the north-northwest by the Grosmont drain that controls the flow of formation water in Upper Devonian and Lower Mannville strata in northeastern Alberta (Bachu, 1999; Barson et al., 2001). However, all the gas will dissolve, diffuse and disperse along the way, such that no acid gas can/will migrate to shallower strata.

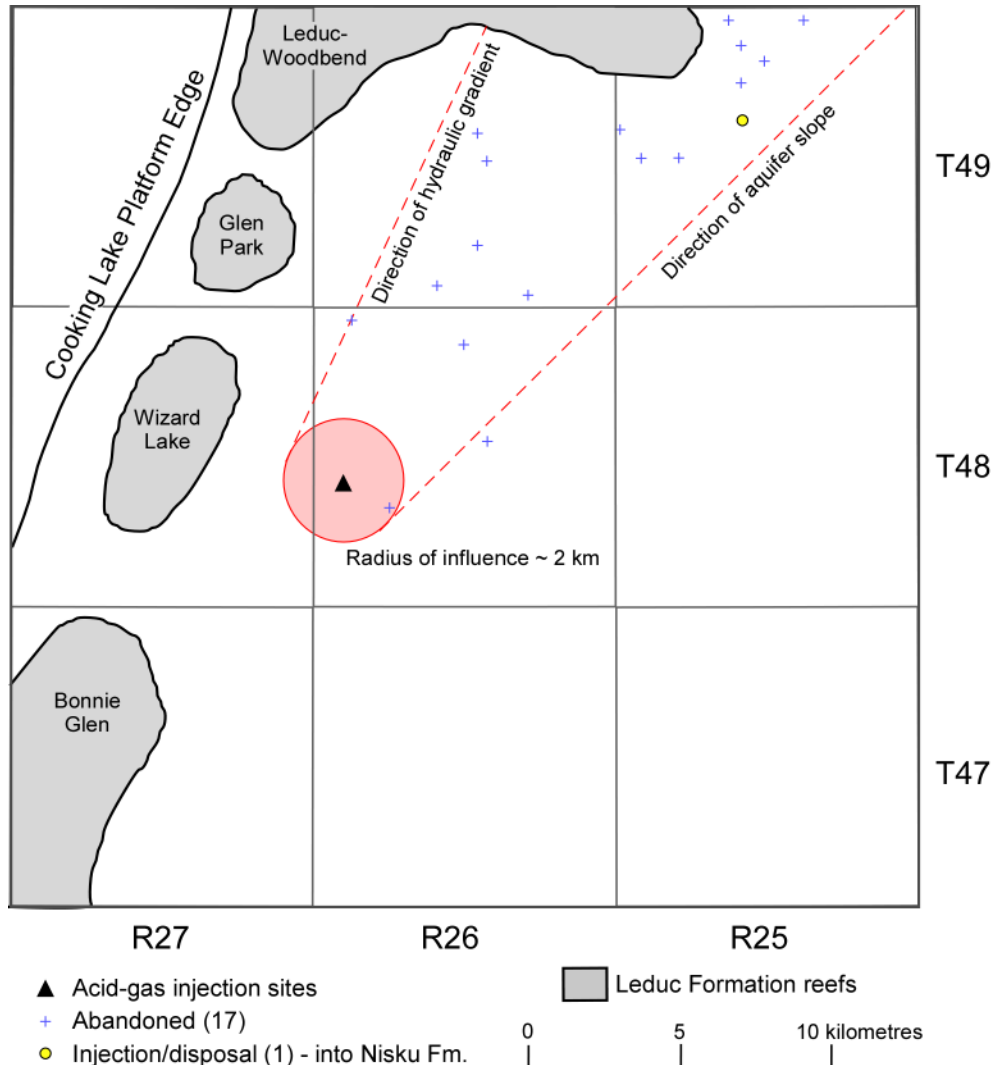


Figure 61. Inferred migration path for a plume of acid gas injected in the Cooking lake aquifer at Watelet, and distribution and status of wells along this path.

In the absence of numerical modeling, the time scale of the flow process along the path described previously can be only estimated to be of the order of thousands to millions of years. It is highly improbable that such a flow path would be ever completed, because the amount of acid gas that will be injected during the lifetime of the operation is much smaller than the volumetric traps that would be encountered along the path. Also, the acid gas will disperse and dissolve in formation water, such that an acid gas plume would disappear along a basin-scale flow path (McPherson and Cole, 2000). Most likely the injected acid gas will be contained within the Woodbend Group on a local scale.

6.2 Acid Gas Leakage

Upward leakage of the acid gas may occur through weak aquitards and natural faults and/or fractures, and through induced fractures and/or improperly completed and/or abandoned wells. There are no known faults and fractures in the Edmonton area that propagate through the sedimentary succession. Leakage through the overlying aquitards is very unlikely, practically impossible to happen, because the Beaverhill Lake, Cooking Lake and Leduc aquifers are capped by the thick, tight and competent shales of

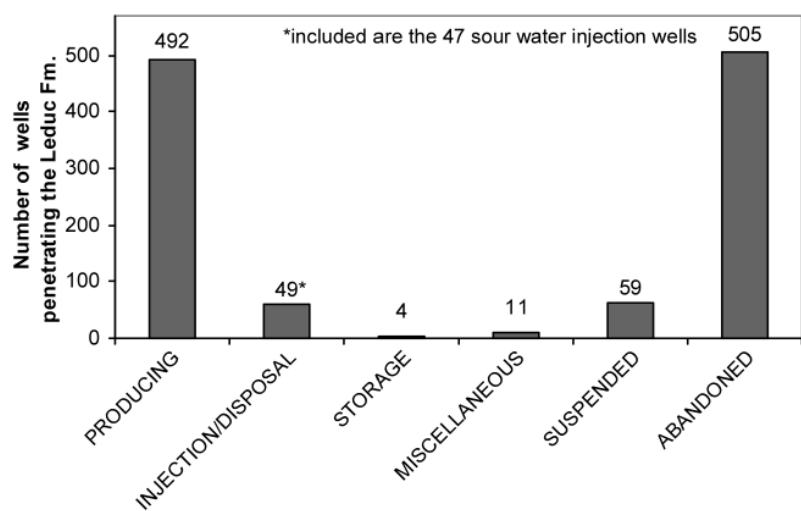
the Ireton aquitard, which have been shown in many regional-scale studies to separate the flow systems in Devonian aquifers from flow systems in overlying strata except where hydraulic communication is established through penetrating reefs or at erosional unconformities (e.g., Bachu, 1995; Rostron and Toth, 1997; Michael et al., 2003). Similarly, the shales of the Clearwater Formation form a strong aquitard that confines the Lower Mannville aquifer and reservoirs contained therein. Further up, the thick shales of the Colorado Group that overlie the Upper Mannville aquifer form another strong aquitard. These barriers to vertical leakage of the acid gas in the natural system exist not only at the site and local scales in the Edmonton area, but also at the regional and even basin scales (Bachu, 1999). Diffusion of gas through the sedimentary succession is an extremely slow process, on the order of hundreds of thousands of years and more, depending on the thickness of the intervening shale layers (Gurevich et al., 1993). Thus, acid gas leakage through the natural system in the Edmonton area is not a practical possibility.

Leakage of the injected acid gas through local fractures induced in the caprock as a result of injection would be possible if the caprock is fractured or weakened by geomechanical and/or geochemical processes. However, even if the immediate caprock layer may have been weakened, the large thickness of the overlying aquitards ensures that no leakage will occur. No leakage further up is possible because of the overlying succession of aquifers and aquitards.

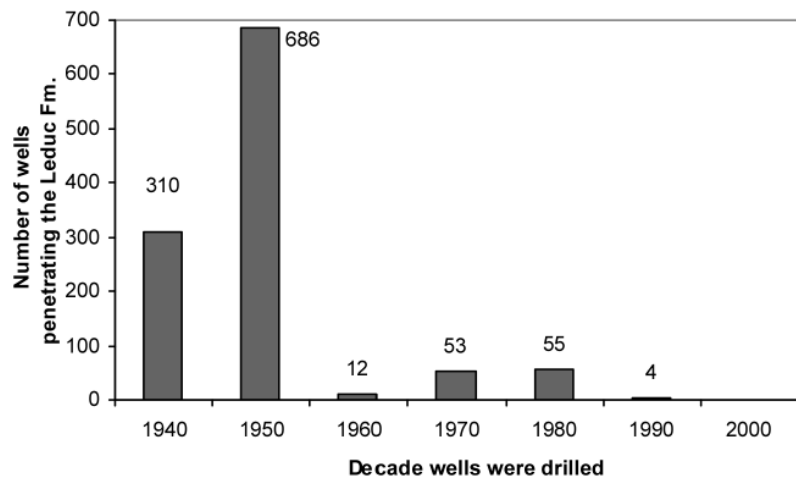
While leakage of acid gas through the natural system is very unlikely to happen, leakage through wells is a very distinct possibility, now or in the future. Again, the situation at Redwater, where sour water is injected through 47 alternating wells in the depleted Leduc Formation Redwater reservoir, is different from the other four cases where dry acid gas is injected. Figure 62 shows the status, time of drilling and time of abandonment for the wells that penetrate the Leduc Formation Redwater reef that is the injection unit. The great majority of wells, including the injection ones, are along the eastern rim of the reef (Figure 58). Close to half of the wells are already abandoned. The producing wells (~44% of the wells) are actually producing from the overlying Cretaceous Mannville Group, not from the Redwater reef. Four wells are used for gas storage in salt caverns in the underlying Lotsberg Formation. Most of the wells were drilled in the late 1940's and in the 1950's (Figure 62b), using the technology and cements available at that time, and conform to regulatory requirements in force then. Many wells were abandoned in the 1950's and 1960's (Figure 62c), but then a large number were abandoned in the 1990's when more stringent regulations addressed well abandonment. In any case, leakage to the surface through abandoned wells at Redwater, now or in the future, should not be a concern, even if some wells are improperly abandoned, for the following reasons:

- 1) The injection reservoir is still underpressured. Thus, the injected water will not have enough pressure drive to reach the surface.
- 2) At Redwater the hydraulic gradient is downwards, from the Mannville Group to the Redwater reef (Figure 45), and any leaked sour water will encounter a downward hydrodynamic drive that will keep it within the Redwater reef.
- 3) The injected weak acidic solution will dilute and disperse through the reservoir.
- 4) Leaky wells affect each other (pressure interference), such that the leakage rate per well is significantly reduced (Nordbotten et al., 2004b)
- 5) The leakage rate is again significantly reduced when a whole succession of aquifers overlies the injection unit (i.e., in this case Winterburn, Wabamun, Lower Mannville, Upper Mannville, Viking) because these aquifers serve as receptors for some of the leaked water (Nordbotten et al., 2004b), by analogy with an “elevator model” whereby many passengers get off successively on intervening floors and very few, if any, reach the top.

a.



b.



c.

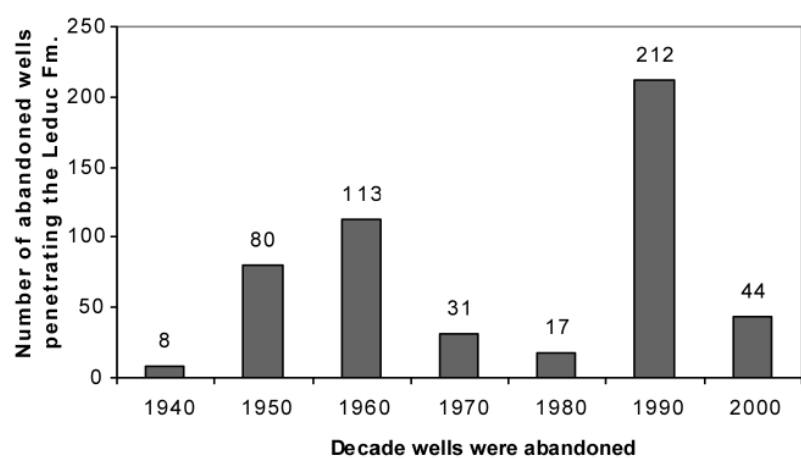


Figure 62. Histograms for wells that penetrate the Leduc Formation Redwater reef showing: a) well status, b) time of drilling, and c) time of abandonment for abandoned wells.

Any water that would leak from the Redwater reef into overlying or underlying aquifers will disperse, diffuse and mix further with the formation water in that aquifer.

At Golden Spike, only three other wells just penetrate the top of the reefal carbonates that are the acid-gas injection target, located at more than 1.5 km to the east of the injection well (Figure 60a). Two of these wells, drilled in 1958 and 1981, were abandoned in 1959 and 1994, respectively. The third well was drilled in 1981 and produces from the overlying Leduc Formation Golden Spike reef. These wells, if improperly abandoned or if degraded, may serve as a conduit for upward leakage of acid gas when the plume will reach them. Although there are five other abandoned wells that penetrate the tight Beaverhill Lake Group argillaceous carbonates updip of the reefal carbonates that are the injection unit (Figure 60a), it is very unlikely that the plume of acid gas will reach them because of the low permeability of the Waterways Formation, except possibly for the well just outside the pool edge. If leakage through one of these wells will occur, driven by acid gas buoyancy and the pressure drive induced by injection, the leaked acid gas most likely will accumulate in the overlying Leduc Formation Golden Spike reef, which is currently penetrated by 106 wells, whose distribution and status are shown in Figures 60b and 63a. A fifth of these wells are abandoned, the others being used for production, gas storage or disposal of produced water. Most of the wells that penetrate the Leduc Formation Golden Spike reef were drilled in the 1950's and 1970's (Figure 63b), and similarly for the abandoned ones (Figure 63c). If leakage occurs, a much smaller, secondary plume of acid gas will likely form at the top of the Leduc Formation Golden Spike reef, whose growth will be controlled by the leakage rate (several orders of magnitude smaller than the injection rate through a disposal well). The leaked acid gas will likely dissolve in reservoir oil and water, or mix with the gas cap at the top of the reservoir, and in any case will be trapped in the reservoir, with no possibility of further leakage except if other leaky wells are in its immediate, very close vicinity.

Open-hole wells are abandoned by plugging every aquifer and producing formation in the succession above perforations, to avoid cross-formational flow, such that further leakage through these wells is unlikely unless cement plugs are completely degraded. In the case of open hole abandoned wells, further leakage of acid gas is stopped by the succession of plugs. Cement degradation takes place in the presence of both formation water and acid gas; if the acid gas forms an isolating layer at the bottom of the plug that stops any contact between cement and formation water, then further degradation will not occur (Scherer et al., 2004). Any leaked acid gas will likely spread into the aquifer that is isolated by that plug, where it will dissolve. The rate of leakage is relatively small (flow through porous media) and likely decreases from one aquifer to another, similarly to the "elevator model" in the case of water leakage. Cased wells are usually abandoned by emplacing a plug just above perforations, and another one close to surface. If acid gas corrodes the casing and leaks inside casing, and then degrades the cement plug, then it will migrate upwards all the way to the top plug. Along the way the acid gas will decompress and reach gaseous phase at the top. Accumulation of acid gas with water present will have a corrosive effect on casing, such that acid gas leakage may subsequently occur directly into shallow groundwater close to the surface. In this case, the well tubing provides an open-flow conduit that bypasses the entire succession of aquifers and aquitards above the injection unit with their retarding effect. From this point of view, leaky cased wells represent a greater risk than open hole abandoned wells.

At Watelet, estimates of the size of the plume of acid gas at the end of 15 years of injection vary between ~1 km using the analytical method presented in Nordbotten et al. (2004a) and <2 km by the operator. Only one abandoned well will be reached by the plume of acid gas at that time (Figure 61). After cessation of injection, the plume will migrate updip (see the previous section) in a north-northeast direction, bracketed likely by the direction of the updip slope and of the gradient of natural flow (Figure 61). Along this path there are 18 wells, of which 17 are abandoned and one is used for injection of produced water in the overlying Winterburn Nisku Formation. Most of these wells were drilled in the

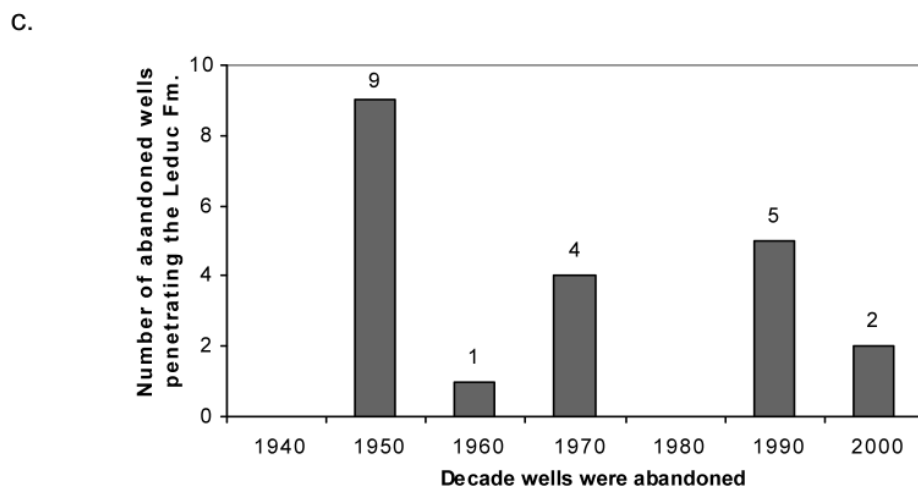
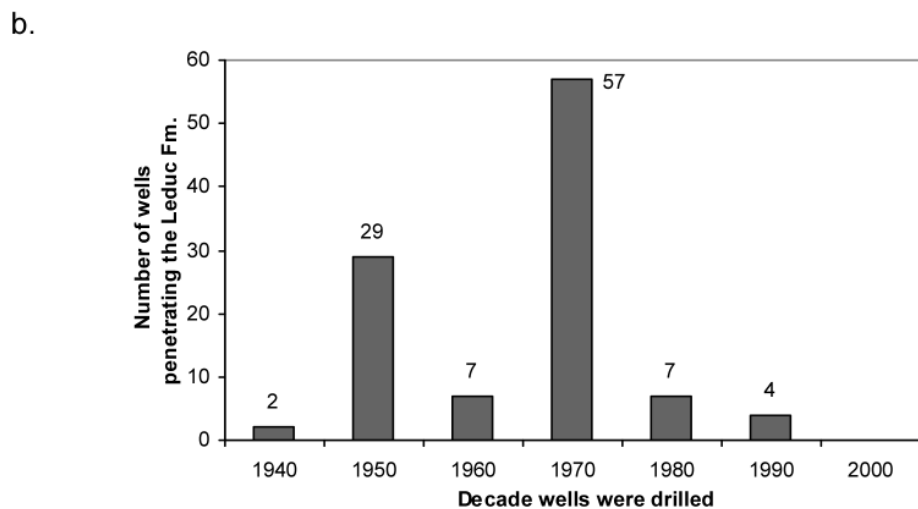
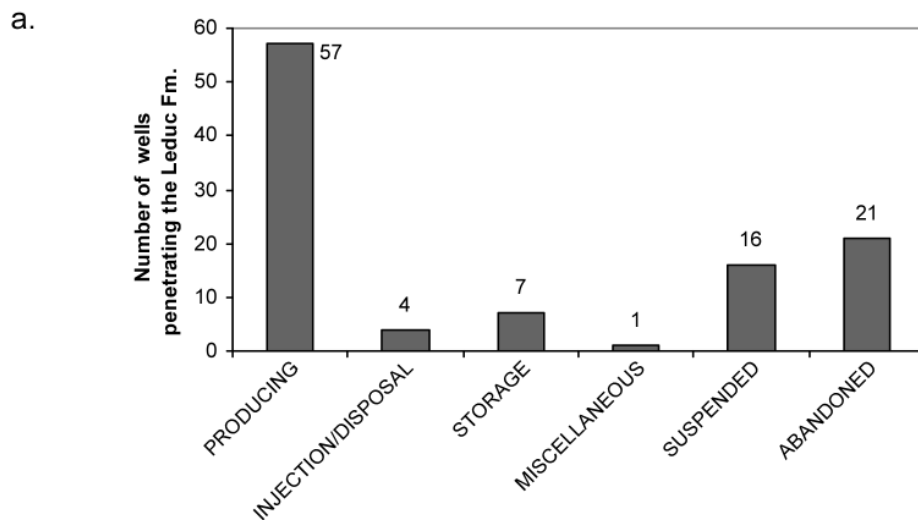


Figure 63. Histograms for wells that penetrate the Leduc Formation Golden Spike reef showing: a) well status, b) time of drilling, and c) time of abandonment for abandoned wells.

1950's and 1960's, and subsequently abandoned since they were dry holes (Figure 64). By the time acid gas reaches these wells, if not dissolved by then in aquifer water, it may leak upwards if these wells are degraded, but most likely it will stop at plugs and/or will disperse in intervening overlying formations.

At Acheson, where injection of acid gas has taken place since 1990 into the St. Albert-Big Lake Ostracod A gas pool (which includes the formerly Acheson Blairmore T pool), there are 12 wells that produce gas from this reservoir, 13 wells within the reservoir that penetrate all the way through the Lower Mannville Group and produce from underlying Devonian reservoirs, one well that actually produces from the overlying Belly River group, 50 abandoned wells, 4 suspended wells, 7 miscellaneous wells and 2 injection/disposal wells, including the acid-gas injection well (Figures 65 and 66a). Most of these wells were drilled in the 1950's, with another spike in the 1990's (Figure 66b). Wells were abandoned almost evenly throughout the entire period (Figure 66c). The injected acid gas has obviously spread in the southern part of the St. Albert-Big Lake Ostracod A reservoir, as indicated by recent CO₂ breakthrough in well 10-22-53-26W4 (Figure 65). If any of these wells was improperly completed or abandoned, then there is potential for acid gas leakage in overlying strata. In the Edmonton region, more porous and permeable formations are the Upper Mannville Group and Viking Formation in the Lower Cretaceous, and Belly River in the Upper Cretaceous, separated by thick shales of the Colorado Group and Lea Park Formation. If acid gas would leak along a well, most likely it will leak into these overlying units where it will disperse and dissolve, unless leakage occurs inside well tubing.

At Strathfield the gas reservoir that is the target of acid gas injection is undefined because of its small size. If the reservoir is undefined, EUB's regulations require examination of wells in the sections adjacent to the section where the injection well is located (a Section is a land survey unit of 1 x 1 sq. mi.). Figure 67 shows the distribution and status of wells that penetrate the Lower Mannville Group in the nine sections around the acid-gas injection well at Strathfield. Of these, the great majority are abandoned, three produce from Lower Mannville Group reservoirs, and four produce from underlying Devonian reservoirs. A few wells are suspended. Most of the wells were drilled in the 1950's and 1960's and abandoned at about the same time (Figure 68).

In all the cases, poor-quality completion in existing or future wells may provide a pathway for upward leakage from the injection reservoir or from any place that an acid gas plume may reach in the future. However, time scale and magnitude of the degradation cannot be assessed with the current data, knowledge and methods.

7 Conclusions

The experience gained since the start of the first acid-gas injection operation in Canada in 1990 shows that, from an engineering point of view, acid gas disposal is a well-established technology. By the end of 2003, close to 2.5 Mt CO₂ and 2 Mt H₂S had been successfully injected into deep hydrocarbon reservoirs and saline aquifers in Alberta and British Columbia. A major issue that has not been addressed is the containment and long-term fate of the injected acid gas.

Injection of acid gas in the Edmonton region takes place at five sites into three different stratigraphic intervals. Acid gas dissolved in water in the Redwater oil field and the resulting weak acidic solution ("sour" water) is injected into the depleted Leduc Formation Redwater reef through 47 alternating wells. Dry acid gas is injected at four other sites. At Golden Spike and Watelet, the acid gas is injected into deep Devonian carbonate aquifers (Beaverhill Lake Group and Cooking Lake Formation, respectively). At Acheson and Strathfield the acid gas is injected into depleted gas reservoirs in the Cretaceous Lower Mannville Group. Acheson, operating since 1990, is actually the oldest acid-gas injection operation in Canada and the world.

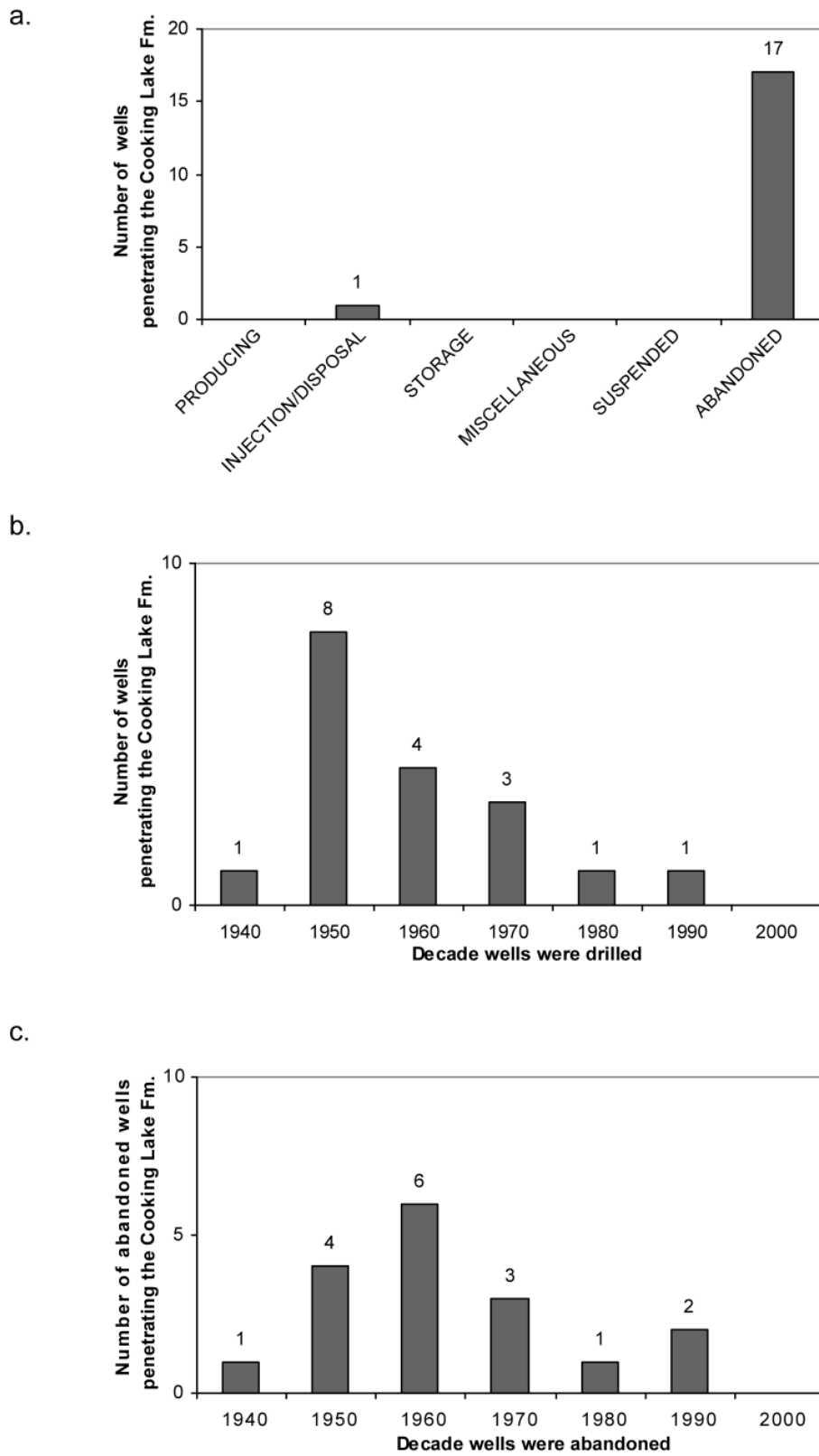


Figure 64. Histograms for wells that penetrate the Cooking Lake Formation at Watelet along a potential migration path of the acid gas plume, showing: a) well status, b) time of drilling, and c) time of abandonment for abandoned wells.

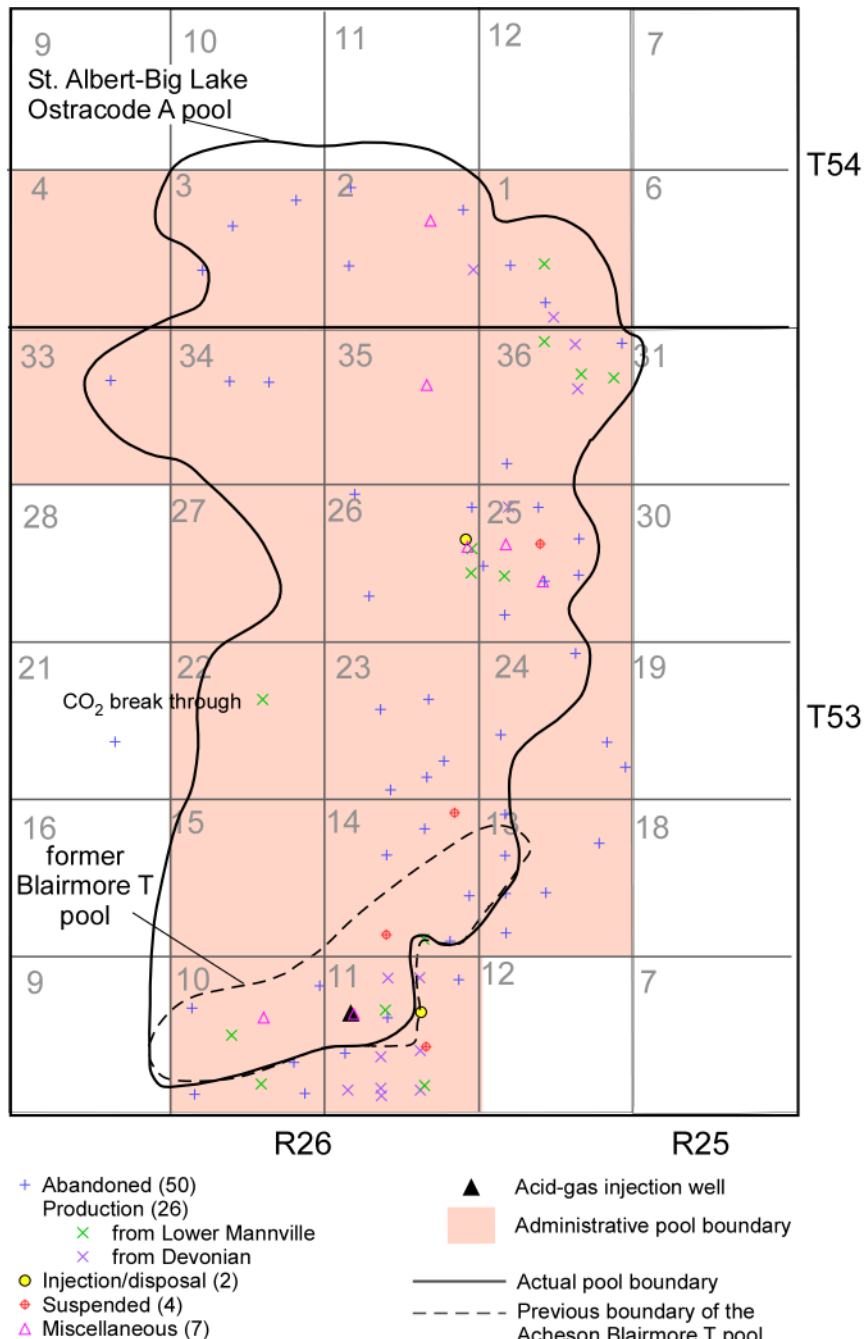
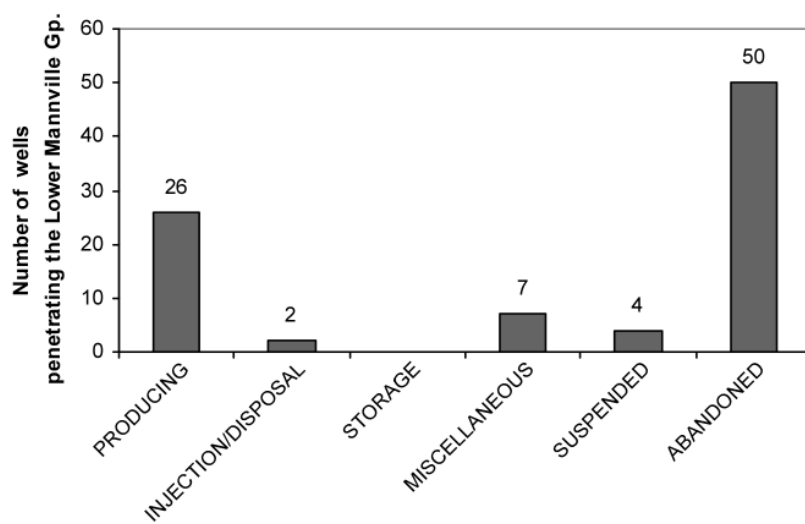


Figure 65. Distribution and status of wells that penetrate the St. Albert-Big Lake Ostracode A gas pool in the Acheson area.

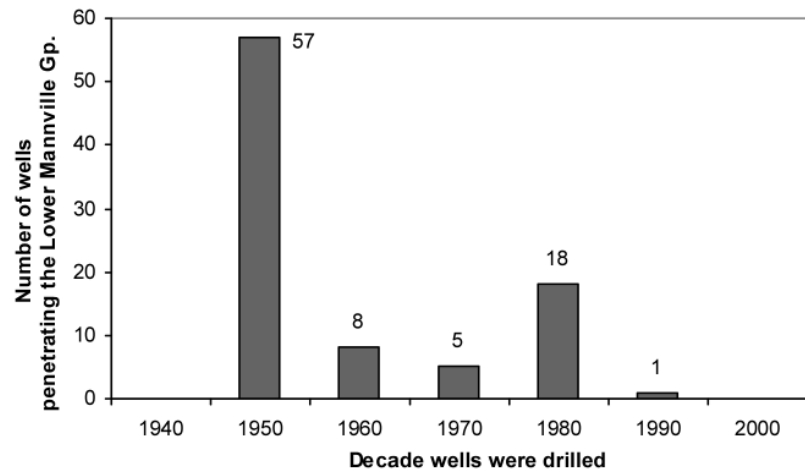
By the end of 2003, more than 200 kt of acid gas have been injected into deep geological formations in the Edmonton region.

If only the natural setting is considered, including geology and flow of formation waters, the basin- and local-scale hydrogeological analyses indicate that injecting acid gas into these deep geological units in the Edmonton region is basically a safe operation with no potential for acid gas migration to shallower strata, potable groundwater and the surface. At Redwater the acid gas is already dissolved in water and it

a.



b.



c.

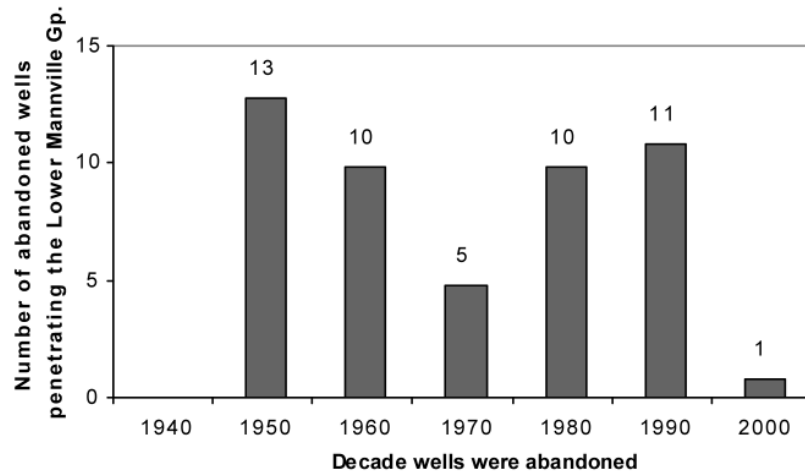


Figure 66. Histograms for wells that penetrate the St. Albert-Big Lake Ostracod A pool in the Acheson area, showing: a) well status, b) time of drilling, and c) time of abandonment for abandoned wells.

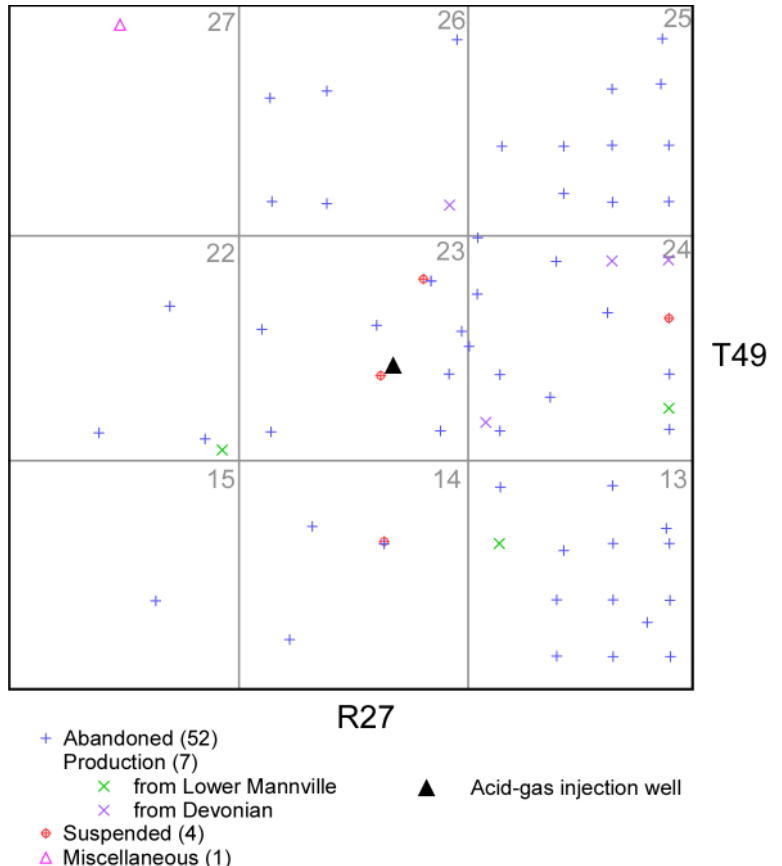


Figure 67. Distribution and status of wells that penetrate the Ellerslie Member in the nine sections around the Strathfield acid-gas injection site.

will dissolve further in the formation water, with no possibility for migration or leakage, being contained in the Redwater reef. At Golden Spike, the acid gas injected into an isolated, confined reefal carbonate in the Beaverhill Lake Group is contained by the surrounding and overlying low-permeability argillaceous limestone at the top of the Beaverhill Lake Group. At Watelet, upward migration is impeded by the overlying thick and tight shales of the Ireton Formation. While the acid gas plume may migrate up dip, it will dissolve in formation water long before it may reach the sub-Cretaceous unconformity. Even there, thick overlying Cretaceous shales will impede any upward migration. At Strathfield and Acheson, the acid gas will be contained within the gas reservoir that is the respective injection target. Upward migration is not possible as a result of thick and tight overlying shales of the Clearwater Formation and its equivalents. Lateral migration within the gas reservoir has been recorded in 2003 at Acheson, where, after 13 years of injection, CO₂ has been detected at an offset producing well at 3,625 m distance in the same gas pool. However, migration within the same unit, particularly in a gas reservoir, is expected and its occurrence should not come as a surprise.

The entire stratigraphic interval from the Beaverhill Lake Group to the Lower Mannville Group is overlain by thick shales of the Colorado Group and Lea Park Formation. There are many barriers to acid gas migration from an injection zone into other strata, and the flow process, if it will ever happen, would take an extremely long time, on a geological time scale. Any acid gas plume would disperse and dissolve in formation water during flow on such large time and spatial scales.

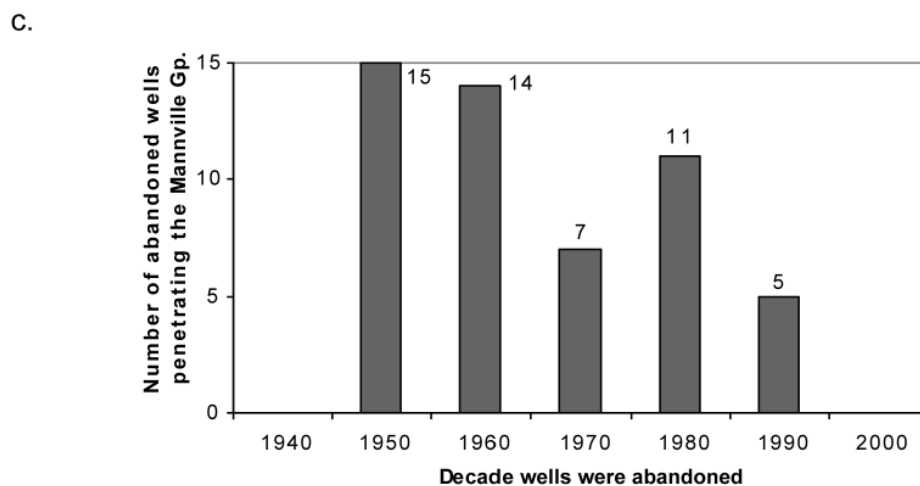
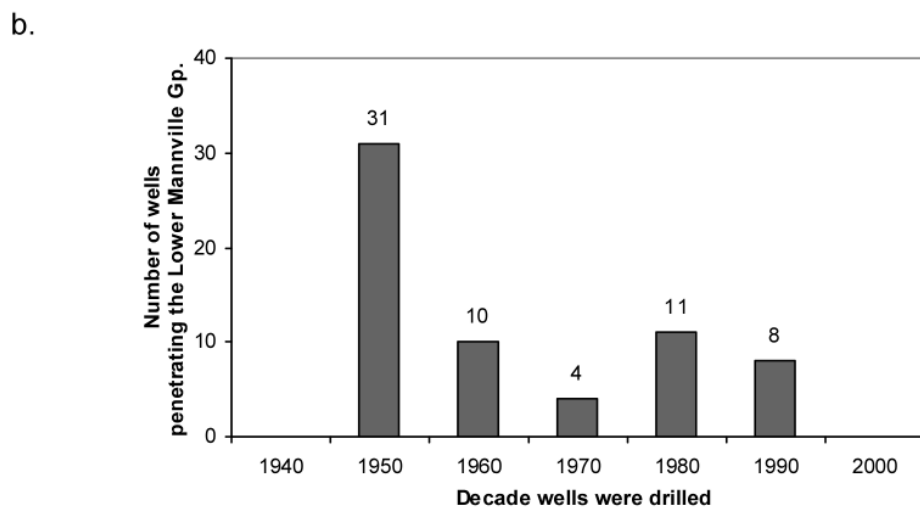
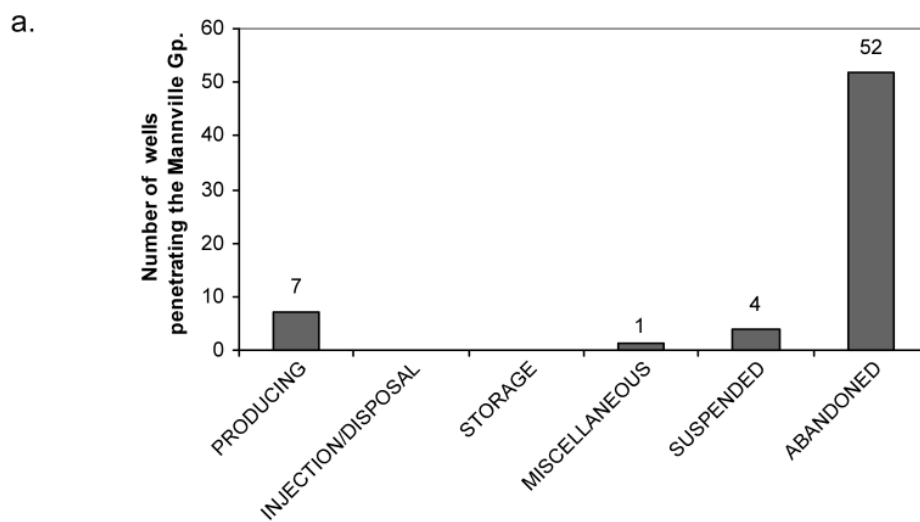


Figure 68. Histograms for wells that penetrate the Ellerslie Member in the nine sections around the Strathfield acid-gas injection site, showing: a) well status, b) time of drilling, and c) time of abandonment for abandoned wells.

Based on available data, it seems that there is no potential for acid gas leakage through fractures. However, the possibility for upward leakage of acid gas exists along wells that were improperly completed and/or abandoned, or along wells whose cement and/or tubing has degraded or may degrade in the future as a result of chemical reactions with formation brine and/or acid gas. A review of the status and age of wells that penetrate the respective injection unit at each site shows that most wells were drilled in the 1950's and 1960's, and that the majority of wells are abandoned. Although no leakage has been detected and reported to date, the potential for this occurring into the future should be considered by both operators and regulatory agencies.

These conclusions are based on a qualitative hydrogeological analysis in the sense that the geological and hydrogeological data were interpreted within the framework of the most current knowledge about the Alberta Basin and its contained fluids. No quantitative analysis based on numerical modeling was performed because, to the best knowledge of the authors, no such models are available. Predictive numerical models of acid gas injection and flow, if not already in existence, should be developed and used to validate the qualitative hydrogeological analysis presented in this report. Geochemical and geomechanical effects on reservoir rock and caprock should be assessed to confirm integrity. The potential for and risk of leakage through existing wells should be better assessed. In addition, a monitoring program would support and provide feedback to the analysis and modeling, and greatly enhance the confidence in the safety of the operation.

Extension of this type of analysis to other current and future disposal sites will lower risk and increase the public trust in the potential and safety of geological sequestration of acid and greenhouse gases. Ideally, a thorough program for predicting the long-term fate of the injected acid gas should contain the following major components:

- a hydrogeological analysis of the injection site at various scales, from site-specific to regional, to provide the context, understanding and necessary data for a qualitative assessment;
- numerical modeling for predicting possible migration and/or leakage paths and corresponding time scales for the injected acid gas;
- monitoring of the acid gas plume, to validate and update the numerical model;
- continuous updating of the hydrogeological and numerical models as new data are acquired.

Currently there are no adequate numerical models that could properly simulate the fate of the acid gas injected in deep geological formations. Also, monitoring programs are expensive, and, in the absence of forward-simulating models, may not provide the necessary information. However, the hydrogeological analysis, the first step for understanding the fate of the acid gas, can be easily implemented for all acid-gas injection sites, particularly in the case of basins with a wealth of data such as the Alberta Basin.

8 References

- Adams, J.J., and Bachu, S. (2002): Equations of state for basin geofluids: algorithm review and inter-comparison for brines. *Geofluids*, 2, p. 257-271.
- EUB (Alberta Energy and Utilities Board) (2000): Guide 65: Resources applications for conventional and gas Reservoirs. Alberta Energy and Utilities Board, Calgary, AB,p. 113-136. DOI eub.gov.ab.ca/bbs/products/guides/g65.pdf.
- Anfort, S.J., Bachu, S., and Bentley, L.R. (2001): Regional-scale hydrogeology of the Upper Devonian-Lower Cretaceous sedimentary succession, south-central Alberta basin, Canada. *American Association of Petroleum Geologists Bulletin*, 85, p. 637-660.
- Bachu, S. (1995): Synthesis and model of formation water flow in the Alberta basin, Canada. *American Association of Petroleum Geologists Bulletin*, 79, p. 1159-1178.
- Bachu, S. (1999): Flow systems in the Alberta Basin: Patterns, types and driving mechanisms. *Bulletin of Canadian Petroleum Geology*, 47, p. 455-474.
- Bachu, S. and Adams, J.J. (2003): Sequestration of CO₂ in geological media in response to climate change: capacity of deep saline aquifers to sequester CO₂ in solution. *Energy Conversion and Management*, 44, p. 3151-3175.
- Bachu, S. and Carroll, J.J. (2004): In-situ phase and thermodynamic properties of resident brine and acid gases (CO₂ and H₂S) injected in geological formations in western Canada; in *Proceedings, 7th International Greenhouse Gas Technologies Conference*, Vancouver, B.C., September 5-9, 2004, in press.
- Bachu, S. and Michael, K. (2002): Flow of variable-density formation water in deep sloping aquifers: minimizing the error in representation and analysis when using hydraulic-head distributions. *Journal of Hydrology*, 259, p. 49-65.
- Bachu, S. and Michael, K. (2003): Hydrogeology and stress regime of the Upper Cretaceous-Tertiary coal-bearing strata in the Alberta basin: toward coalbed methane producibility. *American Association of Petroleum Geologists Bulletin*, 87, p. 1729-1754.
- Bachu, S. and Underschultz, J.R. (1993): Hydrogeology of formation waters, northeastern Alberta basin. *American Association of Petroleum Geologists Bulletin*, 77, p. 1745-1768.
- Bachu, S. and Underschultz, J.R. (1995): Large-scale erosional underpressuring in the Mississippian-Cretaceous succession, southwestern Alberta basin. *American Association of Petroleum Geologists Bulletin*, 79, p. 989-1004.
- Bachu, S., Michael, K. and Buschkuehle, B.E. (2002): The relation between stratigraphic elements, pressure regime, and hydrocarbons in the Alberta deep basin (with emphasis on select Mesozoic units): Discussion. *American Association of Petroleum Geologists Bulletin*, 86, p. 525-528.
- Bachu, S., Buschkuehle, B.E. and Michael, K. (2003a): Subsurface characterization of the Brazeau Nisku Q Pool reservoir for acid gas injection. Alberta Energy and Utilities Board, EUB/AGS, 58 p.

- Bachu, S., Buschkuehle, B.E. and Michael, K. (2003b): Subsurface characterization of the Pembina-Wabamun acid-gas injection area. Alberta Energy and Utilities Board, EUB/AGS, 55 p.
- Bachu, S., Buschkuehle, B.E., Haug., K. and Michael, K. (2004): Characteristics of Acid-Gas Injection Operations in Western Canada, Final Report. Alberta Energy and Utilities Board, EUB/AGS, 32 p. and appendices.
- Barson, D., Bachu, S. and Esslinger, P. (2001): Flow systems in the Mannville Group in the south Athabasca area: implications for steam-assisted gravity drainage (SAGD) operations for in-situ bitumen production. *Bulletin of Canadian Petroleum Geology*, 49, p. 376–392.
- Batzle, M. and Wang, Z. (1992): Seismic properties of pore fluids. *Geophysics*, 57, p. 1396-1408.
- Bell, J. S. (2003): Practical methods for estimating in-situ stresses for borehole stability applications in sedimentary basins. *Journal of Petroleum Science and Engineering*, 38:3-4, p. 111-119.
- Bell, S. J. and Babcock, E. A. (1986): The stress regime of the Western Canada Sedimentary Basin and implications for hydrocarbon production. *Bulletin of Canadian Petroleum Geology*, 34, p. 364-378.
- Bell, S. J. and Bachu, S. (2003): In-situ stress magnitude and orientation estimates for Cretaceous coal-bearing strata beneath the plains area of central and southern Alberta. *Bulletin of Canadian Petroleum Geology*, 51, p. 1-28.
- Bell, S. J., Price, P. R. and McLellan, P. J. (1994): In-situ stress in the Western Canada Sedimentary Basin; in Geological Atlas of the Western Canada Sedimentary Basin (Mossop, G.D. and Shetsen, I., comp.). Canadian Society of Petroleum Geologists and Alberta Research Council, Calgary, p. 439-446.
- Bennion, D.B., Thomas, F.B., Bennion, D.W. and Bietz, R.F. (1996): Formation screening to minimize permeability impairment associated with acid gas or sour gas injection/disposal. CIM Paper 96-93 presented at the 47th Annual Technical Meeting of the CIM Petroleum Society, Calgary, AB, June 10-12, 1996.
- Burrowes, O.G. and Krause, F.F. (1987): Overview of the Devonian System: Subsurface Western Canada Basin; in Devonian lithofacies and reservoir styles in Alberta, (Krause, F.F. and Burrowes, O. G., eds.) 2nd International Symposium of the Devonian System, 13th CSPG Core Conference, p. 1-52.
- Buschkuehle, B.E. and Machel, H.G. (2002): Diagenesis and paleofluid flow in the Devonian Southesk-Cairn carbonate complex in Alberta, Canada. *Marine and Petroleum Geology*, 19, p. 219-227.
- Buschkuehle B.E. and Perkins, E.H. (2004): Mineralogy and geochemical trapping of acid gas in the Edmonton area of central Alberta, Canada; in: Proceedings, 7th International Greenhouse Gas Technologies Conference, Vancouver, B.C., September 5-9, 2004, in press.
- Bustin, R.M. (1991): Organic maturation of the Western Canadian Sedimentary Basin. *International Journal of Coal Geology*, 19, p. 319-358.

- Campbell, C.V. (1992): Beaverhill Lake megasequence; in: Devonian-Early Mississippian carbonates of the Western Canada Sedimentary Basin: a sequence-stratigraphic framework (Wendte, J.C., Stoakes, F.A. and Campbell, C.V., eds.). Society for Sedimentary Geology, Short Course No. 28, p. 163-182.
- Campbell, J. D. (1979): Major cleat trends in Alberta Plains coals. Canadian Institute of Mining Bulletin, 72, p. 69-75.
- Cant, D.J. and Stockmal, G.S. (1989): The Alberta Foreland Basin: relationship between stratigraphy and Cordilleran terrane accretion events. Canadian Journal of Earth Sciences, v.26, p.1964-1975
- Caritat, P. de, Bloch, J. and Hutcheon, I.E. (1994): LPNORM: A linear programming normative analysis code. Computers and Geosciences, 20, p. 313-347.
- Carroll, J. J. (1998a): Phase diagrams reveal acid-gas injection subtleties. Oil and Gas Journal, 96:9, p. 92-96.
- Carroll, J. J. (1998b): Acid-gas injection encounters diverse H₂S, water phase changes. Oil and Gas Journal, 96:10, p. 57-59.
- Carroll, J. J. and Lui, D. W. (1997): Density, phase behavior keys to acid gas injection. Oil and Gas Journal, 95:25, p. 63-72.
- Davison, R. J., Mayder, A., Hladiuk, D. W. and Jarrell, J. (1999): Zama acid gas disposal/miscible flood implementation and results. Journal of Canadian Petroleum Technology, 38:2, p. 45-54.
- Deming, D. and Nunn, J.A. (1991): Numerical simulations of brine migration by topographically driven recharge. Journal of Geophysical Research, 96:B2, p. 2485-2499.
- Desbarats, A. J. and Bachu, S. (1994): Geostatistical analysis of aquifer heterogeneity from the core scale to the basin scale: A case study. Water Resources Research, 30:3, p. 673-684.
- Grasby, S. and Hutcheon, I. (2001): Controls on the distribution of thermal springs in the southern Canadian Cordillera. Canadian Journal of Earth Sciences, 38:3, p. 427-440.
- Geological Staff, Imperial Oil Ltd. Western Division, (1950): Devonian nomenclature in Edmonton area. Bulletin of American Association of Petroleum Geologists, v. 34, p. 1807-1825.
- Gunter, W. D., Perkins, E. H. and Hutcheon, I. (2000): Aquifer disposal of acid gases: modeling of water-rock reactions for trapping acid wastes. Applied Geochemistry, 15 p. 1085-1095.
- Gurevich, A.E., Endres, B.L., Robertson Jr., J.O., and chilingar, G.V. (1993): Gas migration from oil and gas fields and associated hazards. Journal of Petroleum Science and Engineering, vol. 9., p. 223 - 238.
- Haas, C. J. (1989): Static stress-strain relationships; in: Physical properties of rocks and minerals (Touloukian, Y. S., Judd, W. R. and Roy, R. F., eds.), Hemisphere Publishing Corporation, New York, p. 123-176.

- Hayes, B.J.R., Christopher, J.E., Rosenthal, L, Los, G. and McKercher, B. (1994): Cretaceous Mannville Group of the Western Canada Sedimentary Basin; in: Mossop, G.D. and Shetsen, I. (comp.), Geological Atlas of the Western Canada Sedimentary Basin. Canadian Society of Petroleum Geologists and Alberta Research Council, Calgary, p. 317-334.
- Hearn, M.R. and Rostron, B.J. (1997): Hydrogeologic, stratigraphic, and diagenetic controls on petroleum entrapment in Devonian reefs, Bashaw area, Alberta. Core Conference Proceedings, CSPG-SEPM Joint Convention, June 1997, Calgary, AB, p. 89-101.
- Hitchon, B. (1996): Rapid evaluation of the hydrochemistry of a sedimentary basin using only “standard” formation water analyses: example from the Canadian portion of the Williston Basin. *Applied Geochemistry*, 11 p. 789–795.
- Hitchon, B. (1969a): Fluid flow in the Western Canada Sedimentary Basin. 1. Effect of topography. *Water Resources Research*, 5, p. 186-195.
- Hitchon, B. (1969b): Fluid flow in the Western Canada Sedimentary Basin. 2. Effect of geology. *Water Resources Research*, 5, p. 460-469.
- Hitchon, B. and Brulotte, M. (1994): Culling criteria for “standard” formation water analyses: *Applied Geochemistry*, v. 9, p. 637–645.
- Hitchon, B., Bachu, S. and Underschultz, J.R. (1990): Regional subsurface hydrogeology, Peace River arch area, Alberta and British Columbia. *Bulletin of Canadian Petroleum Geology*, 38A, p. 196-217.
- Hitchon, B., Perkins, E. H. and Gunter, W. D. (2001): Recovery of trace metals in formation waters using acid gases from natural gas. *Applied Geochemistry*, 16 p. 1481-1497.
- Hnatiuk, J., and Martinelli, J.W. (1967): The relationship of the Westerose D-3 pool to other pool on the common aquifer. *Journal of Canadian Petroleum Technology*, 16, p. 7-13.
- Jumikis, A.R. (1983): Rock Mechanics (2nd Edition); Trans Tech Publications, Rockport, M.A., 613 p.
- Keushnig, H. (1995): Hydrogen sulphide-if you don’t like it, put it back. *Journal of Canadian Petroleum Technology*, 34:6, p. 18-20.
- Krause, F.F. and Burrowes, O. G. (eds.), (1987): Devonian lithofacies and reservoir styles in Alberta. Manual of the 13th CSPG Core Conference, p. 87-152.
- Lambe, T.W. and Whitman, R.V. (1979): Soil mechanics, SI version. John Wiley and Sons Inc., New York, New York, 553 p.
- Lindeberg, E. and Wessel-Berg, D. (1997): Vertical convection in an aquifer column under a gas cap of CO₂. *Energy Conversion and Management*, 38S, p. 229-234.
- Lock, B. W. (1997): Acid gas disposal-A field perspective; in Proceedings of the Seventy-Sixth Gas Processors Association Annual Convention, San Antonio, TX, March 10-12, 1999, Tulsa, OK, p. 161-170.

Longworth, H. L., Dunn, G. C. and Semchuk, M. (1996): Underground disposal of acid gas in Alberta, Canada: Regulatory concerns and case histories. SPE Paper 35584; in: Proceedings of the Gas Technology Symposium, Calgary, AB, Canada, 28 April-1 May 1996, SPE, p. 181-192.

Machel, H.G., Cavell, P.A. and Patey, K.S. (1996): Isotopic evidence for carbonate cementation and recrystallization, and for tectonic expulsion of fluids into the Western Canada sedimentary basin. Geological Society of America Bulletin, 108, p. 1108-1119.

Masters, J.A. (ed.), (1984): Elmworth: Case study of a deep basin gas field. American Association of Petroleum Geologists Memoir 38, Tulsa, OK, 316 p.

McLennan, J.D., Elbel, J., Mattheis, E. and Lindstrom, L. (1982): A Critical evaluation of the Mechanical Properties Log (MPL) on a Basal Quartz Well in the Caroline Area, Paper 82, p. 33-45, Presented at the Annual Technical Meeting of the Petroleum Society of CIM, Calgary, Alberta.

McPherson, B.J.O.L. and Cole, B.S. (2000): Multiphase CO₂ flow, transport and sequestration in the Powder River basin, Wyoming, USA. Journal of Geochemical Exploration, 69-70, p. 65-69.

Michael, K. and Bachu, S. (2001): Fluids and pressure distributions in the foreland-basin succession in the west-central part of the Alberta basin, Canada: evidence for permeability barriers and hydrocarbon generation and migration. American Association of Petroleum Geologists Bulletin, 85, p. 1231-1252.

Michael, K. and Bachu, S. (2002): Origin, chemistry and flow of formation waters in the Mississippian-Jurassic sedimentary succession in the west-central part of the Alberta Basin, Canada. Marine and Petroleum Geology, 19, p. 289-306.

Michael, K., Machel, H.G. and Bachu, S. (2003): New insights into the origin and migration of brines in deep Devonian aquifers, Alberta, Canada. Journal of Geochemical Exploration, 80:2-3, p. 193-219.

Miller, S.L.M. and Stewart, R.R. (1990): Effects of lithology, porosity, and shaliness on P- and S- wave velocities from sonic logs, Canadian Journal of Exploration Geophysics, 26, p. 94-103.

Mossop, G.D. and Shetsen, I. (comp.) (1994): Geological atlas of the Western Canada Sedimentary Basin. Canadian Society of Petroleum Geologists and Alberta Research Council, Calgary, 510 p.

Nesbitt, B.E. and Muehlenbachs, K. (1993): Synorogenic fluids of the Rockies and their impact on paleohydrogeology and resources of the Western Canada sedimentary basin; in Alberta Basement Transect Workshop (G.M. Ross, ed.), LITHOPROBE Report 31, LITHOPROBE Secretariat, University of British Columbia, p. 60-62.

Ng, H-J., Carroll J. J. and Maddocks, J. R. (1999): Impact of thermophysical properties research on acid-gas injection process design; in Proceedings of the Seventy-Eighth Gas Processors Association Annual Convention, Nashville, TN, March 1-3, 1999, Tulsa, OK, p. 114-120.

Nordbotten, J.M, Celia, M.A. and Bachu, S. (2004a): Injection and storage of CO₂ in deep saline aquifers: analytical solution for CO₂ plume evolution during injection. Transport in Porous Media, in press.

Nordbotten, J.M, Celia, M.A. & Bachu, S. (2004b): Analytical solutions for leakage through abandoned wells. Water Resources Research, 40, W04204, doi:10.1029/2003WR002997, 10p.

Nurkowski, J.R. (1984): Coal quality, coal rank variation and its relation to reconstructed overburden, Upper Cretaceous and Tertiary plains coals, Alberta, Canada. American Association of Petroleum Geologists Bulletin, 68, p. 285-295.

Oldale, H.S. and Munday, R.J. (1994): Devonian Beaverhill Lake Group of the Western Canada Sedimentary Basin; in: Mossop, G.D. and Shetsen, I. (comp.) 1994. Geological Atlas of the Western Canada Sedimentary Basin. Canadian Society of Petroleum Geologists and Alberta Research Council, Calgary, p. 149-163.

Parks, K.P. and Toth, J. (1993): Field evidence for erosion-induced underpressuring in Upper Cretaceous and Tertiary strata, west central Alberta, Canada. Bulletin of Canadian Petroleum Geology, 43, p. 281-292.

Penson, D., Olsen, T. and Gess, B. (1993): Design and evaluation of hydraulic fracture treatments in the Nisku Formation southern Alberta, presented at the Petroleum Society of CIM 1993 Annual Technical Conference, Calgary, May 9-12, 1993.

Perkins, E.H., Buschkuehle, B.E., Durocher, K. and Gunter, W.D. (2004): Geochemistry of the Edmonton-area acid-gas injection operations. Client report.

Pettijohn, F.J. (1975): Sedimentary Rocks. Third edition, Harper and Row, New York. 628p.

Porter, I.W., Price, R.A., and McCrossan, R.G. (1982): The Western Canada Sedimentary Basin. Philosophical Transactions of Royal Society of London, Series A, 305, p. 169-182.

Price, R.A. (1994): Cordilleran tectonics and the evolution of the Western Canada Sedimentary Basin; in: Geologic Atlas of the Western Canada Sedimentary Basin; G.D. Mossop and I. Shetsen (comps.), Canadian Society of Petroleum Geologists and Alberta Research Council, p. 13-24.

Ricketts, B.D. (ed.) (1989): Western Canada sedimentary basin-a case history. Canadian Society of Petroleum Geologists, Calgary, 320 p.

Rostron, B.J., and Toth, J. (1996): Ascending fluid plumes above Devonian pinnacle reefs: numerical modeling and field example from west-central Alberta, Canada; in Hydrocarbon Migration and its Near-Surface Expression (Schumacher, D. and Abrams, M.A., eds.). American Association of Petroleum Geologists Memoir 66, Tulsa, OK, p. 185-201.

Rostron, B.J., and Toth, J. (1997): Cross-formational fluid flow and the generation of a saline plume of formation waters in the Mannville Group, west-central Alberta; in Petroleum Geology of the Cretaceous Mannville Group (Pemberton, S.G. and James, D.P., eds.). Canadian Society of Petroleum Geologists Memoir 18, Calgary, p. 169-190.

Scherer, G.W., Celia, M.A., Prévost, J-H., Bachu, S., Bruant, R., Duguid, A., Fuller, R., Gasda, S.E., Radonjic, M., Vichit-Vadakan, W. (2004): Leakage of CO₂ through abandoned wells: Role of Corrosion of Cement; in: The CO₂ Capture and Storage Project (CCP) for Carbon Dioxide Storage in Deep Geologic Formations For Climate Change Mitigation, Volume II "Geologic Storage of Carbon Dioxide with Monitoring and Verification" (S. M. Benson, ed.), Elsevier, London, U.K., in press.

Smith, D.G. (1994): Paleogeographic evolution of the Western Canada Foreland basin; in Mossop, G.D. and Shetsen, I. (comp.) 1994, Geological Atlas of the Western Canada Sedimentary Basin. Canadian Society of Petroleum Geologists and Alberta Research Council, Calgary, p. 277-296.

Spencer, R.J. (1987): Origin of Ca-Cl brines in Devonian formations, Western Canada Sedimentary Basin. *Applied Geochemistry*, 2, p. 373-384.

Stoakes, F.A. (1992): Winterburn megasequence; in: Devonian-Early Mississippian carbonates of the Western Canada Sedimentary Basin: a sequence-stratigraphic framework (Wendte, J.C., Stoakes F.A. and Campbell, C.V., eds.). Society for Sedimentary Geology, Short Course No. 28, p. 207-224.

Switzer, S.B., Holland, W.G., Christie, P.S., Graf, G.C., Hedinger, A.S., McAnley, R.J., Wierzbicki, R.A., and Packard, J.J. (1994): Devonian Woodbend - Winterburn Strata of the Western Canada Sedimentary Basin; in: G.D. Mossop and I. Shetsen (comps.): Geological Atlas of the Western Canada Sedimentary Basin. Canadian Society of Petroleum Geologists and Alberta Research Council, p. 165-202.

Toth, J. (1978): Gravity-induced cross-formational flow of formation fluids, Red Earth region, Alberta, Canada: analysis, patterns, and evolution. *Water Resources Research*, 14, p. 805-843.

Toth, J. and Corbet, T. (1986): Post-Paleocene evolution of regional groundwater flow-systems and their relation to petroleum accumulations, Taber area, southern Alberta, Canada. *Bulletin of Canadian Petroleum Geology*, 34, p. 339-363.

Walls, R.A., Mountjoy, E.W. and Fritz, P. (1979): Isotopic composition and diagenetic history of carbonate cements in the Devonian Golden Spike reef, Alberta. *Geological Society of America Bulletin* (part 1), v.90, p. 963-982.

Wendte J. (1992): Platform evolution and its control on reef inception and localization; in: J.C. Wendte, F.A. Stoakes and C.V. Campbell (eds.): Devonian-Early Mississippian carbonates of the Western Canada Sedimentary Basin: a sequence-stratigraphic framework. Society for Sedimentary Geology, Short Course No. 28, p. 41-88.

Wendte, J. (1994): Platform evolution and its control on Late Devonian Leduc reef inception and localization, Redwater, Alberta. *Bulletin Canadian Petroleum Geology*, v. 42, p. 499-528.

Whalen M.T., Eberli, G.P., van Buchem, F.S.P., Mountjoy, E.W. and Homewood, P.W. (2000): Bypass margins, basin-restricted wedges, and platform-to-basin correlation, Upper Devonian, Canadian Rocky Mountains: implications for sequence stratigraphy of carbonate platform systems. *Journal of Sedimentary Research*, v. 70, p. 913-936.

Whatley, L. (2000): Acid-gas injection proves economic for west-Texas plant. *Oil and Gas Journal*, 98:21, p. 58-61.

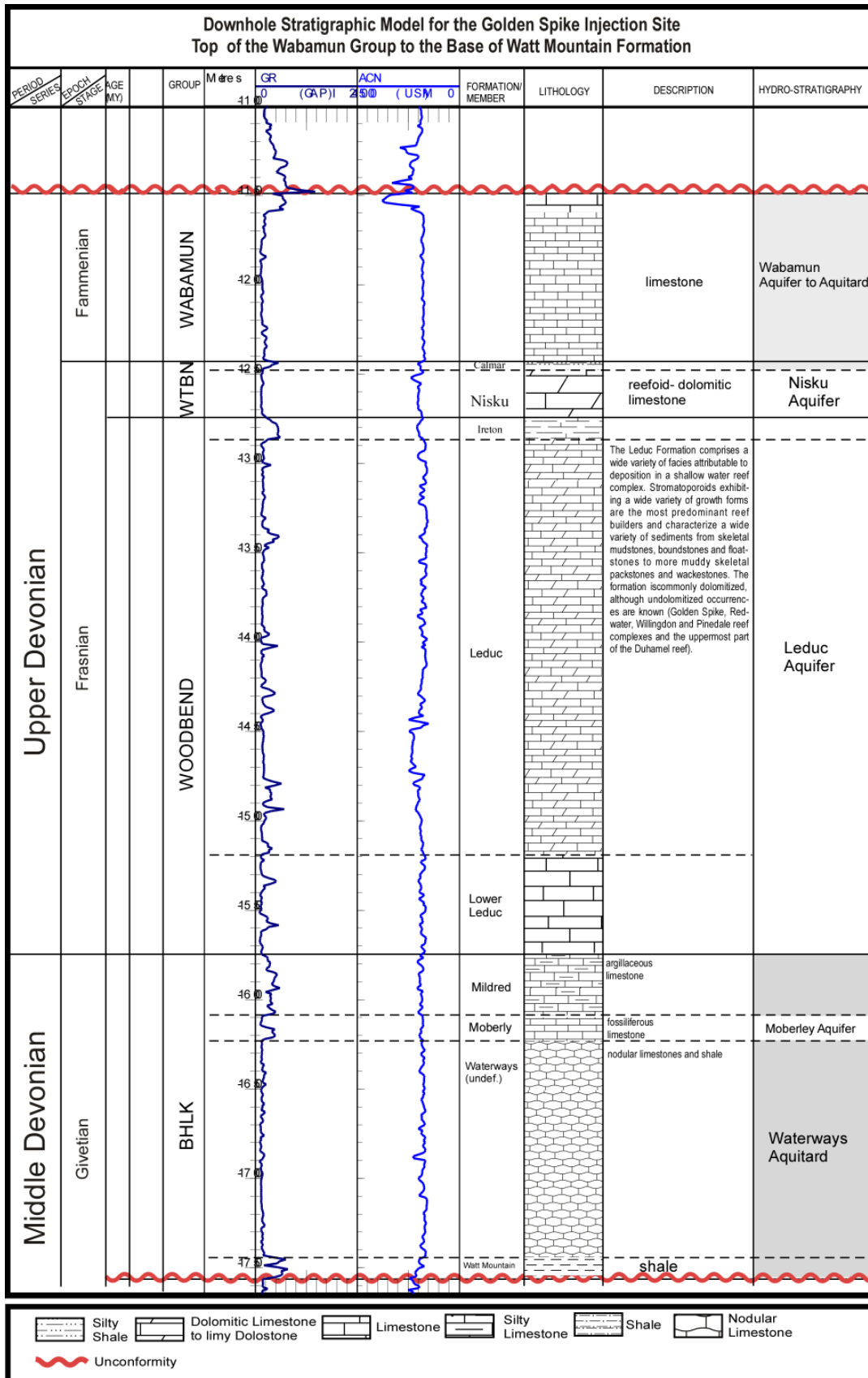
Wichert, E. and Royan, T. (1996): Sulfur disposal by acid gas injection. SPE Paper 35585; in: Proceedings of the Gas Technology Symposium, Calgary, AB, Canada, 28 April-1 May 1996, SPE, p. 193-200.

Wichert, E. and Royan, T. (1997): Acid gas injection eliminates sulfur recovery expense. *Oil and Gas Journal*, 95:17, p. 67-72.

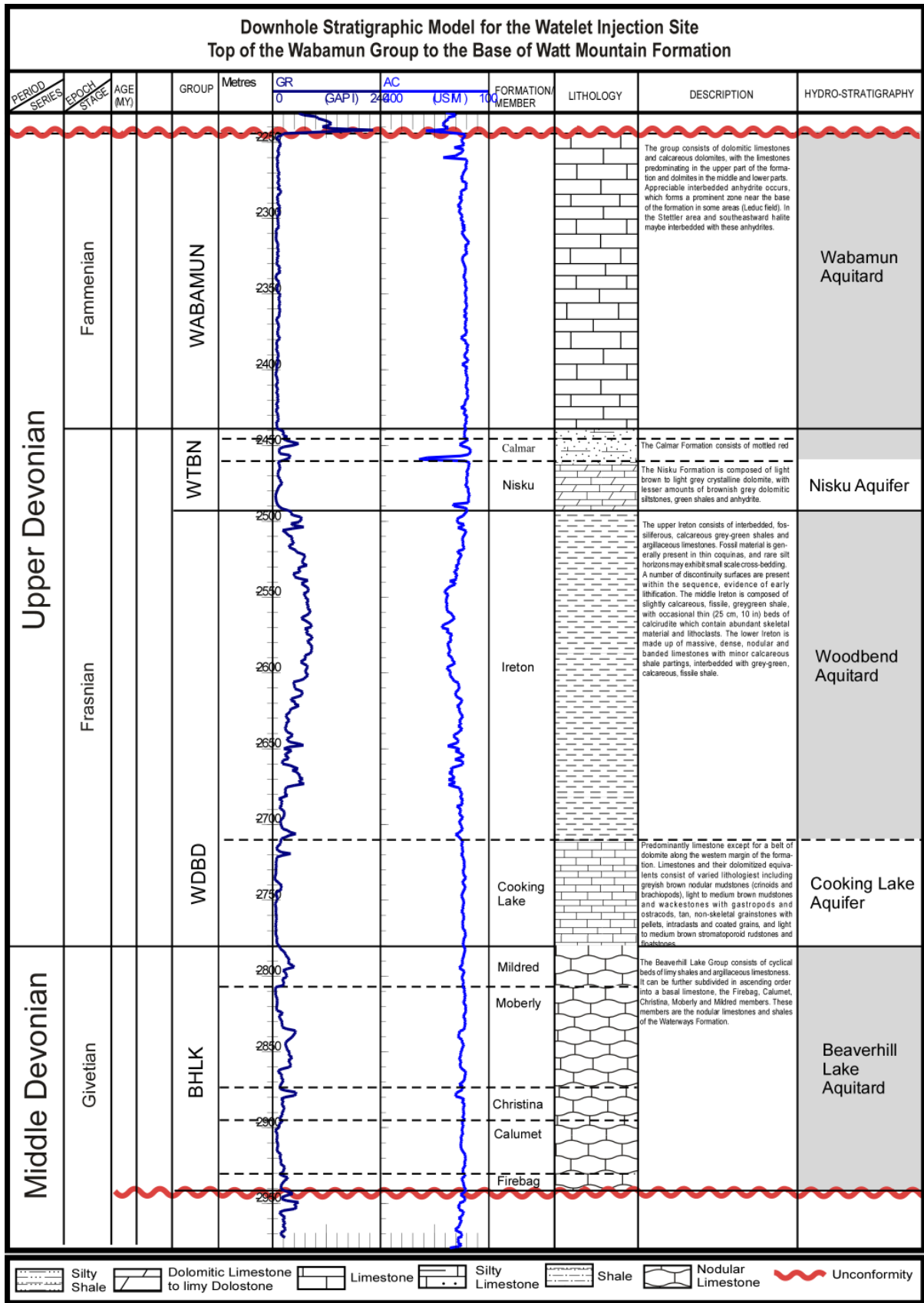
Wilkinson, P.K. (1995): Is fluid flow in Paleozoic formations of west-central Alberta affected by the Rocky Mountain thrust belt? Unpublished M.Sc. Thesis, University of Alberta, Edmonton, 102 p.

Appendix 1

- 1-1 Downhole Stratigraphic Model for the Golden Spike Injection Site**
- 1-2 Downhole Stratigraphic Model for the Watelet Injection Site**
- 1-3 Downhole Stratigraphic Model for the Strathfield and Acheson Injection Sites**

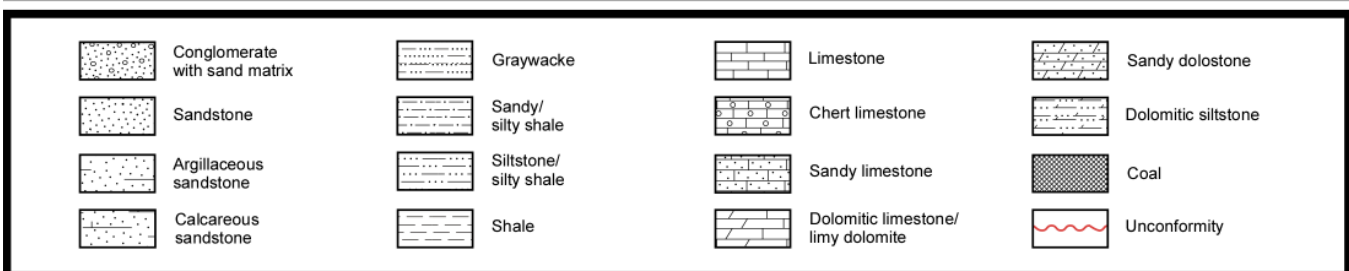
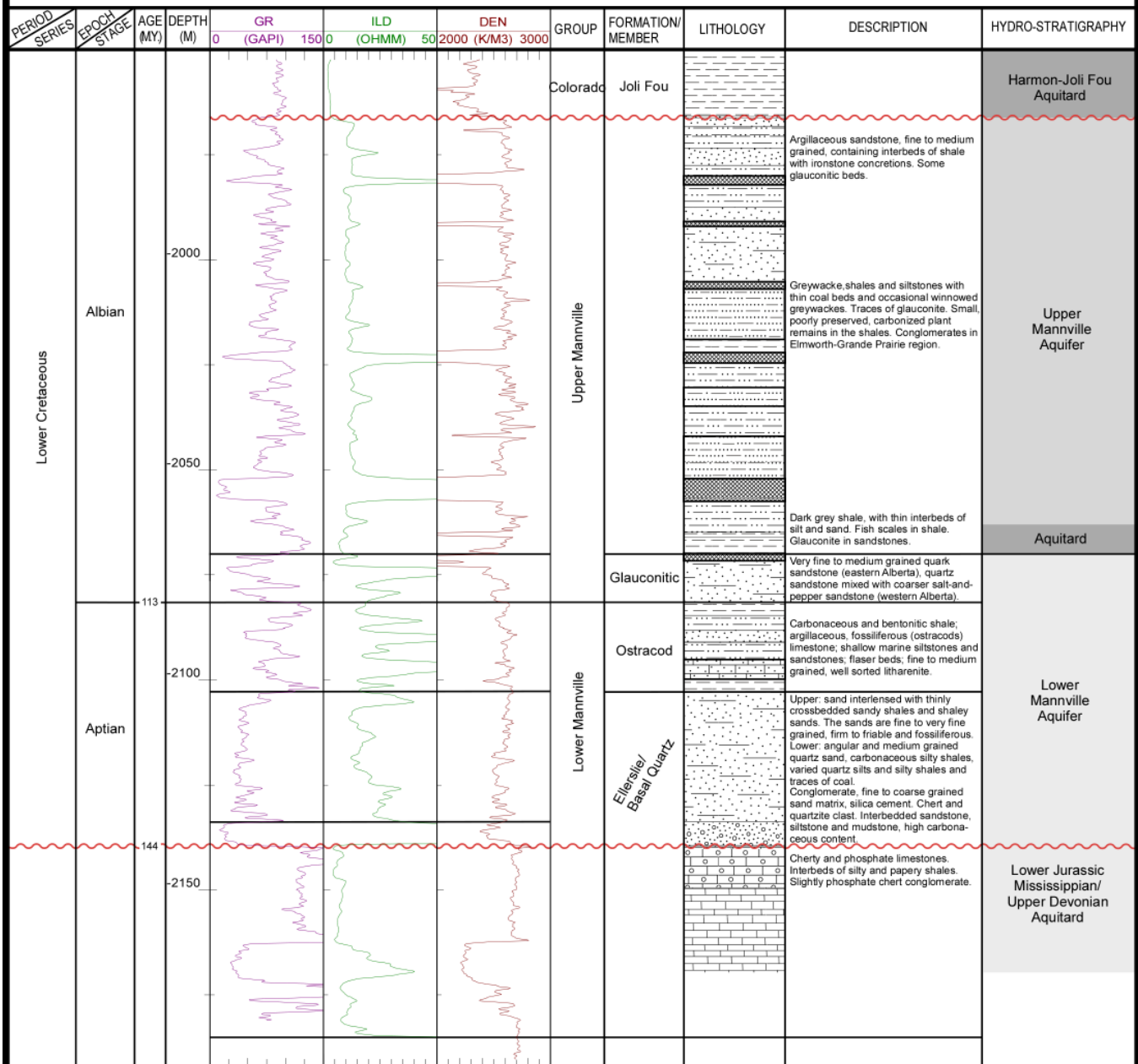


Appendix 1 / 1 of 3



Appendix 1 / 2 of 3

Downhole Stratigraphic Model for the Strathfield and Acheson Injection Sites
Top of the Joli Fou Formation to the Base of Lower Mannville Group



Appendix 1 / 3 of 3 (modified from D. Chen, 2003 unpublished.)

Appendix 2

Table 1. Major ion chemistry of formation waters from the Leduc and Cooking Lake formations in the Redwater area (concentrations in mg/l)

Table 2. Major ion chemistry of formation waters from the Lower Mannville Group in the Acheson area (concentrations in mg/l)

Table 3. Major ion chemistry of formation waters from the Lower Mannville Group in the Strathfield area (concentrations in mg/l)

Appendix 2, Table 1 - Major ion chemistry of formation water from the Leduc and Cooking Lake formations in the Redwater area (concentrations in mg/l).

DLS	Sodium	Potassium	Calcium	Magnesium	Chloride	Sulfate	Bicarbonate	TDS
06-34-55-21W4	28223		3340	1110	52200	45	744	85284
07-21-55-22W4	41184		8280	2140	83500	1000	266	136235
10-33-55-23W4	43008		6635	2049	82870	1257	400	136016
16-08-55-24W4	39530		8140	1960	79800	1170	700	130945
07-10-55-24W4	39928		6850	1695	77400	1180	615	127355
13-24-55-24W4	38769		7523	1464	76540	510	760	125179
06-30-55-24W4	38807		6656	1796	75500	1218	780	124361
13-05-55-25W4	37362		7768	1737	75200	1202	570	123549
05-08-55-25W4	32680		6260	1970	65800	1300	775	108391
05-08-55-25W4	29960	1621	6070	1818	61000	1171	813	100483
05-08-55-25W4	31280	1624	6406	1448	60900	1430	891	101050
11-08-55-25W4	23357		4890	1189	47000	930	770	77745
11-08-55-25W4	23286		5063	1135	47000	1078	650	77882
10-17-55-25W4	31639		10248	2096	71019	1211	746	116580
07-19-55-25W4	33529		7662	1387	68041	1044	801	112057
02-20-55-25W4	34301		7675	1520	68932	1222	597	113944
02-20-55-25W4	32286		10665	1542	71317	1333	7	117147
06-25-55-25W4	32590		7247	2989	73300	1218	917	119703
06-25-55-25W4	32259	1875	5982	1584	64800	1018	649	105962
13-29-55-25W4	28013	1275	6158	1636	61100	1263	798	100921
16-30-55-25W4	34440	2311	6791	1550	68500	1424	958	113480
10-32-55-25W4	32810		6166	1531	66500	1448	567	109988
05-29-56-20W4	33885	1864	5360	1817	64844	2107	460	108239
05-15-56-21W4	31335		4532	1296	58148	1533	693	97185
05-16-56-21W4	28841		5412	1664	57850	386	502	94400
15-16-56-21W4	31829		4358	1430	58762	1798	703	98523
16-16-56-21W4	30531		4359	1238	56695	1943	465	94994
01-17-56-21W4	33770		4443	1456	61682	2255	709	103955
07-17-56-21W4	19200	1525	2790	341	34400	1560	127	58565
01-21-56-21W4	33405		4493	1183	60639	1923	699	101987
11-24-56-21W4	30137		3620	1197	55600	375	840	91342
11-24-56-21W4	30089		3603	1181	55500	369	760	91115
11-24-56-21W4	30398		3707	1129	55900	510	770	92023
11-24-56-21W4	30593		3698	1145	56200	560	760	92570
01-25-56-21W4	32832		3510	980	58600	992	621	97219
01-33-56-21W4	31080		4256	1478	58000	1909	610	97023

10-33-56-21W4	27855		6080	462	54000	13	780	88794
09-11-56-22W4	34297		4724	1359	62944	2449	780	106156
14-12-56-22W4	31269		3332	1428	56800	1400	761	94603
02-22-56-23W4	29215		4186	1176	53200	1903	950	90147
07-28-56-23W4	29841		5300	1430	58300	1345	460	96442
10-10-56-24W4	56159		5668	1708	100352	531	620	164723
10-10-56-24W4	35087		8315	1160	70920	1364	195	116942
10-10-56-24W4	55835		5668	1708	100352	531	620	164399
10-10-56-24W4	34986		8315	1160	70920	1364	195	116841
10-10-56-24W4	39560		7372	1647	77196	1375	1091	127687
10-23-56-24W4	32779		6118	1599	64600	1323	780	106802
11-12-56-25W4	34647		7262	1774	70034	1331	737	115410
10-19-56-25W4	33061		7159	1559	66866	1144	824	110194
01-20-56-25W4	34919		7605	1747	71000	1228	835	116909
06-22-56-25W4	33460	1820	6727	1434	72500	1222	588	119567
09-30-56-25W4	33277	1690	6687	1543	68000	1531	115	112103
16-02-57-20W4	39603		7800	4310	87000	368	279	139219
02-06-57-20W4	33921		4833	1632	63457	1774	689	105956
02-06-57-20W4	33962		4830	1673	64000	1802	794	106657
16-01-57-21W4	30983		4342	1562	58587	1366	715	97191
12-09-57-21W4	32050	607	3996	1264	57500	1761	322	95958
06-12-57-21W4	34318		4156	1898	64228	946	703	105892
08-12-57-21W4	30670		5242	2102	60340	2152	610	100806
09-12-57-21W4	29900		5535	1801	59740	1550	455	98750
04-13-57-21W4	30810		5024	2234	61220	1384	304	100821
09-14-57-21W4	34197		4307	1561	63152	1189	731	104765
11-14-57-21W4	34200	896	4380	1870	63100	880	585	103830
14-17-57-21W4	35570		4030	969	62800	1380	728	105107
11-19-57-21W4	30425		2770	1930	56390	930	631	92755
06-20-57-21W4	31100	842	4260	1582	60000	1280	550	99537
15-22-57-21W4	32558		5350	1465	63000	695	735	103429
02-23-57-21W4	27344		5110	2280	56940	1027	266	92832
12-23-57-21W4	31829		3052	2992	62380	802	398	101250
07-27-57-21W4	31911		4200	2080	62200	426	322	100975
11-27-57-21W4	30592		5382	1935	60870	1119	542	100165
04-31-57-21W4	31297		4682	1085	57617	1716	754	96768
01-32-57-21W4	29888		3930	1310	55490	510	770	91506
01-32-57-21W4	30782		3560	1270	56300	925	832	93246
15-32-57-21W4	33879		3992	1606	62900	897	730	103633

08-33-57-21W4	30761		3988	1592	58223	788	560	95627
04-34-57-21W4	32629		4609	1596	62181	939	425	102163
09-25-57-22W4	29495		4095	1210	55123	1276	325	91359
16-35-57-22W4	27569		3340	1120	51400	23	461	83678
09-36-57-22W4	28039	640	4348	1128	53000	2331	165	89316
11-36-57-22W4	31526		4695	1180	58105	2082	535	97851
16-17-57-23W4	30136		5350	1460	59600	658	181	97293
07-20-57-23W4	29294		5182	1560	57443	1653	385	95321
13-22-57-23W4	35130		6320	1720	68650	1930	500	113995
11-04-57-24W4	27700	1600	4980	1360	56600	1240	654	93762
10-08-57-24W4	28189		5174	1416	56080	742	208	91703
16-08-57-24W4	35356		6078	1614	69000	915	518	113217
13-16-57-24W4	30916		6840	2208	65042	968	780	106357
09-17-57-24W4	31629		5896	1543	63056	658	275	102918
14-21-57-24W4	33317		5984	1484	64987	877	119	106708
07-28-57-24W4	31814		5614	2240	64679	871	341	105386
07-28-57-24W4	31991		5614	2240	64679	871	341	105563
07-28-57-24W4	31831		5652	1842	63296	882	363	103681
03-32-57-24W4	30588		5414	2138	62020	746	702	101251
01-33-57-24W4	32247		6311	1650	64500	890	935	106058
15-33-57-24W4	27335		4893	1249	52715	800	850	87410
04-04-58-21W4	32936		5146	2035	64030	1164	705	105658
04-04-58-21W4	31098		5000	1420	59950	890	570	98638
04-04-58-21W4	30517		5895	1420	60470	880	870	99609
01-05-58-21W4	31473		4380	1390	59210	930	750	97752
08-05-58-21W4	31851		4500	1360	59920	990	670	98950
01-06-58-21W4	28238		3781	1227	52273	1476	770	87374
04-08-58-21W4	33504		4821	1450	62901	844	705	103867
05-08-58-21W4	31953		4514	1764	61260	951	755	100813
04-26-58-21W4	40788		7224	3036	84000	591	156	135716
08-02-58-22W4	29075		4626	2184	58420	729	380	95220
09-02-58-22W4	32696		4738	1348	60854	2414	160	102128
10-02-58-22W4	32873		4973	1167	60256	2341	719	101963
13-02-58-22W4	33815		4937	1454	62600	2122	700	105272
13-02-58-22W4	33102		4823	1507	62000	2133	680	103899
13-02-58-22W4	32699		4527	1430	60600	2104	770	101739
13-02-58-22W4	33111		4484	1305	60800	2127	730	102186
13-02-58-22W4	33463		4937	1454	62600	2122	700	104920
13-02-58-22W4	33008		4744	1464	61566	2303	505	103333

13-02-58-22W4	32273		4996	1352	60428	2296	727	101702
13-02-58-22W4	32446		4987	1336	60626	2304	727	102056
13-02-58-22W4	33463		4937	1454	62600	2122	700	104920
14-02-58-22W4	30741		5978	777	58197	2255	657	98271
15-09-58-22W4	32524		4620	923	59100	1990	769	99535
15-10-58-22W4	31807		4788	1592	60239	2395	260	100948
02-11-58-22W4	30294		4033	1238	55400	2395	500	93606
03-11-58-22W4	31836		4779	1331	59145	2429	840	99933
11-12-58-22W4	34900	1080	5220	1987	66100	1240	515	109061
03-14-58-22W4	26480		3451	1352	49896	1085	315	82419
07-15-58-22W4	32853		4481	1588	62181	1002	510	102356
13-15-58-22W4	34268		5198	1603	64365	1913	771	107726
07-16-58-22W4	31136		4950	1256	58587	2103	500	98277
11-17-58-22W4	32578		4580	890	59200	1830	657	99401
02-19-58-22W4	33027		4567	1566	62030	1290	1016	102979
02-19-58-22W4	29658		6260	1948	61400	1025	569	100571
03-19-58-22W4	30028		6254	1902	61850	976	588	101299
07-19-58-22W4	34845		4760	1760	66410	1120	81	108935
09-19-58-22W4	32939		4272	1566	61600	1136	820	101916
10-19-58-22W4	32874		4410	1573	62000	939	666	102124
05-20-58-22W4	33823		4870	1464	63343	983	841	104897
09-20-58-22W4	32949		4925	1711	63552	993	385	104319
09-20-58-22W4	32190		4970	1739	62559	982	370	102621
13-20-58-22W4	31158		4560	2208	61566	984	445	100695
13-20-58-22W4	31469		4560	2374	62559	990	385	102141
13-20-58-22W4	31984		4469	2484	63552	998	310	103640
14-20-58-22W4	33781		4188	1621	63296	846	525	103990
04-21-58-22W4	32440		4457	1579	61274	984	880	101167
08-21-58-22W4	33378		4714	1593	63300	979	740	104328
08-21-58-22W4	33436		4714	1603	63400	1004	740	104521
11-21-58-22W4	30777		5927	2102	61930	1234	380	102157
12-21-58-22W4	33348		4466	1638	63168	986	350	103778
16-21-58-22W4	33499		4380	1658	63200	1021	490	103999
02-22-58-22W4	32492		4734	1511	61159	984	781	101264
03-22-58-22W4	32492		4734	1511	61159	984	781	101264
04-22-58-22W4	32492		4734	1511	61159	984	781	101264
03-29-58-22W4	31446		4917	1660	60854	954	810	100230
10-22-58-23W4	34962		5682	1514	66800	1654	650	110945
01-24-58-23W4	32706		4118	1591	61230	892	806	100933

06-36-58-23W4	19496		4030	1600	41000	940	281	67204
08-08-58-24W4	30001		4404	2331	60000	410	940	97608
14-08-58-24W4	30680		5397	1442	60225	392	939	98597
14-09-58-24W4	28670	1275	4765	1448	56000	523	1078	92035
08-18-58-24W4	31062		5530	1290	60100	990	1050	99488
12-27-58-24W4	27892		4933	1453	54100	1845	880	90656
10-32-58-24W4	32297		5246	1670	63000	542	950	103222
02-05-58-25W4	32700	1777	6967	1968	71050	1309	800	116978
11-15-58-25W4	38237		2371	1932	67524	1042	855	111527
10-34-58-25W4	31025		5998	1586	62063	863	645	101852
10-34-58-25W4	31353		5998	1586	62063	863	645	102180
04-07-59-20W4	26180		3821	1452	50750	751	100	83003
06-14-59-22W4	44613		8099	3194	92026	398	195	148426
02-09-59-24W4	33083		4404	966	61000	105	935	100017
16-09-56-21W4	31857		4280	1410	59000	1920	670	98797
13-10-56-21W4	34649		3153	1296	60960	2086	493	102387
08-17-56-21W4	29910		3861	2436	58520	1840	304	96717
09-17-56-21W4	32224		3350	2545	61510	1786	360	101593
05-03-56-24W4	32152		10506	1764	71894	1276	809	117990
05-06-57-20W4	31223		4979	1080	59152	858	547	97561
07-04-57-21W4	31648		4099	1388	58351	1771	760	97631
13-31-57-21W4	33944		4805	1652	64000	1646	801	106455
05-36-57-22W4	27470	493	4324	1157	52500	1547	1019	88052
03-04-58-21W4	32433		4000	1620	60800	820	700	100018
10-05-58-21W4	31365		4952	2040	62000	977	607	101633
13-02-58-22W4	31105		4552	1346	57957	2034	830	97402
13-02-58-22W4	31288		4351	1270	57957	1809	610	96975
13-02-58-22W4	31203		4430	1270	57859	1725	900	96930
13-02-58-22W4	31560		4569	1361	58740	2033	820	98667
03-14-58-22W4	30278		4481	1413	57262	1543	575	95259
06-19-58-22W4	32396		4200	1700	61400	960	400	100852
04-28-55-24W4	36971		7940	1936	75383	1241	690	123810
04-27-57-20W4	37586		5839	2743	75825	506	150	122573
10-27-57-21W4	44547		6312	3470	89076	635	740	144403
10-27-57-21W4	45792		6512	3339	90919	849	553	147683
10-27-57-21W4	45608		6336	3387	90529	627	724	146843
01-34-57-22W4	29935		3652	1727	56594	1231	265	93270

Appendix 2, Table 2 - Major ion chemistry of formation water from the Lower Mannville Group in the Acheson area (concentrations in mg/l).

DLS	Sodium	Potas-sium	Calcium	Magne-sium	Chloride	Sulfate	Bicarbon-ate	TDS
06-04-52-25W4	34763		5777	1091	66068	304	284	108143
08-05-52-25W4	33600	1030	6893	1364	69016	260	196	112098
02-11-52-25W4	43190		3890	1010	76000	394	232	124598
13-30-52-25W4	32800	840	4630	1160	66107	224	166	105927
15-31-52-25W4	30690	644	5085	1094	60500	247	354	98684
02-32-52-25W4	34030		5557	1259	65083	352	205	106382
07-01-52-26W4	33733		5760	1119	65042	227	445	106100
16-12-52-26W4	35300	425	4670	922	62800	390	381	102925
14-13-52-26W4	31070	710	5285	1142	65000	496	388	106428
04-17-52-26W4	32115		6150	1590	64800	113	264	104898
14-18-52-26W4	34440	601	5806	1324	65950	167	290	107184
06-23-52-26W4	32748		6320	1050	64200	320	520	104893
14-23-52-26W4	35000	944	5780	1307	67400	215	415	110133
02-25-52-26W4	33427	902	4822	1069	63500	356	461	103945
03-28-52-26W4	33145		5450	1290	64000	296	504	104428
04-31-52-26W4	32501	795	6334	1181	65000	212	602	106005
04-34-52-26W4	39849		5560	1191	74550	33	311	121336
05-34-52-26W4	26697		5692	1260	54018	752	580	88704
06-35-52-26W4	37737		6159	964	70983	217	245	116181
02-36-52-26W4	33072	1662	4917	1006	63600	412	435	104212
04-36-52-26W4	35208	705	5606	1166	67800	280	451	110711
02-01-52-27W4	36429		6725	1349	71172	105	550	116050
04-25-52-27W4	33376		5581	1190	64400	206	442	104971
04-25-52-27W4	37817		2610	594	64400	116	306	105688
11-25-52-27W4	34650		4913	1135	65100	167	391	106170
16-25-52-27W4	33648		6830	1500	73200	668	488	116086
10-04-53-25W4	39298		5160	1020	72200	298	480	118212
05-05-53-25W4	27641		4518	952	52866	364	439	86556
08-05-53-25W4	31300	813	4180	833	62100	366	247	101771
01-06-53-25W4	35001		5739	1372	67211	346	261	109797
12-07-53-25W4	33811	650	5125	1074	64300	461	523	105424
13-07-53-25W4	33650	821	4805	1337	64000	181	415	104234
12-02-53-26W4	33806		5293	1215	64516	262	560	105367
07-03-53-26W4	36964		5970	1128	69913	337	52	114338
07-06-53-26W4	33261		5013	1108	62901	247	522	102786

07-07-53-26W4	33783		4805	1243	63900	194	342	104109
07-11-53-26W4	36387	914	5086	1130	69000	158	234	112429
02-23-53-26W4	33393		5232	1166	63635	308	490	103975
05-25-53-26W4	35184		5300	848	65778	141	378	107437
10-34-53-26W4	36038		5450	764	67000	242	447	109713
09-02-53-27W4	33420		5157	1069	63351	132	560	103405
01-14-54-25W4	32600	762	3360	976	57500	370	650	94537
06-19-54-25W4	32905		4800	1050	62100	123	174	101063
13-24-54-25W4	35503		4204	972	64091	366	270	105269
04-25-54-25W4	41274		4905	1312	75176	414	170	123164
01-26-54-25W4	33984		4084	1106	61996	364	200	101632
04-27-54-25W4	30315		3779	1003	55769	191	115	91114
16-30-54-25W4	29140	1750	3427	880	54500	469	834	89973
11-31-54-25W4	33425		4172	836	61100	175	259	99849
03-32-54-25W4	31810	594	3924	1069	56250	601	397	92432
10-32-54-25W4	27250	588	3812	1238	55900	533	573	91773
06-34-54-25W4	33221		4543	1004	61126	441	509	100586
16-35-54-25W4	32872		5300	1460	63900	392	228	104036
11-05-54-26W4	32298		4595	978	60120	281	785	98658
12-12-54-26W4	29830	537	4404	1312	58500	160	496	95288
07-15-54-26W4	36471		5606	1594	70300	328	450	114521
10-17-54-26W4	32405		4020	1497	60900	273	590	99385
10-19-54-26W4	25241		4033	832	47916	79	159	78179
10-19-54-26W4	32124		4313	1079	59616	271	839	97811
12-20-54-26W4	31070	494	3580	909	59800	317	891	98487
05-24-54-26W4	27731		3750	940	52000	74	140	84564
05-24-54-26W4	30919		4280	957	57700	74	489	94170
05-24-54-26W4	32240		4370	1071	60300	37	412	98220
07-27-54-26W4	29921		3844	1059	55700	173	340	90864
07-30-54-26W4	25980	57	3303	923	49750	286	647	81690
06-31-54-26W4	32404		3692	1115	59250	252	570	97005
11-02-54-27W4	32874		3604	1094	60000	68	390	97845
06-13-54-27W4	32208		3870	937	58500	139	297	95800
07-19-54-27W4	30792		2240	920	51000	39	393	85184
07-19-54-27W4	32303		2800	1040	52000	63	421	88413

Appendix 2, Table 3 - Major ion chemistry of formation water from the Lower Mannville Group in the Strathfield area (concentrations in mg/l).

DLS	Sodium	Potassium	Calcium	Magnesium	Chloride	Sulfate	Bicarbonate	TDS
06-11-48-26W4	33796		6725	1141	66792	271	590	109014
10-34-48-26W4	33778	673	6006	1123	66200	216	442	107950
10-36-48-26W4	32168		5531	962	61932	89	322	100836
16-12-48-27W4	33017		4404	1554	65750	214	275	105074
02-27-48-27W4	32399		6428	1045	63808	325	341	104463
07-27-48-27W4	28735		4360	975	58000	193	686	92600
16-32-48-01W5	31720	257	3363	608	56100	47	439	91895
02-33-48-01W5	30470	375	3211	524	54500	40	641	89761
16-34-48-01W5	33000	520	4377	905	61344	17	934	100512
11-06-49-26W4	32778		5149	1439	63356	227	592	103253
04-01-49-27W4	34171		2848	832	59975	1	180	98067
04-01-49-27W4	35553		3170	773	62357	23	337	102288
01-02-49-27W4	34446	680	2773	1137	60937	45	432	99800
13-16-49-27W4	36076		3700	750	67500	264	717	108643
01-24-49-27W4	34609		4820	1200	65000	117	517	106000
06-24-49-27W4	34634		5465	1081	65700	181	710	107424
07-36-49-27W4	33414		5061	1268	64000	101	210	103962
12-12-49-28W4	31280	802	2090	530	55900	160	996	92473
12-23-49-28W4	34590		4284	1408	66200	53	256	106661
15-36-49-28W4	36022	718	5069	739	66900	21	732	109548
08-04-49-01W5	32230	455	4765	802	61000	25	299	99440
01-20-49-01W5	41094		7800	1010	81500	58	519	131717
01-36-49-01W5	34487		3908	835	64000	150	259	103507
16-15-50-26W4	33127		5830	1210	64460	185	562	105088
01-16-50-26W4	32027		5430	1080	61600	294	555	100703
11-19-50-26W4	34947		5330	455	64430	53	300	105363
13-25-50-26W4	37640		6275	1260	71774	240	454	117412
03-31-50-26W4	41220		6720	1257	75075	80	62	124382
03-31-50-26W4	35035		9753	1806	75696	84	204	122474
07-22-50-27W4	31200	2250	5020	970	61390	15	727	100252
11-14-50-28W4	35791		5846	1074	67800	84	366	110775
11-14-50-28W4	36172		5670	1128	69500	6	138	112861
11-14-50-28W4	36755	513	5670	1128	69500	6	138	113127
09-25-50-01W5	33994		6518	1327	67688	61	147	109661